Distribution Categories:
Magnetic Fusion Energy (UC-20)
MFE—Fusion Systems (UC-20d)
MFE—Environment and Safety
Analysis (UC-20e)

ANL/FPP/TM-163

ANL/FPP/TM--163

DE83 010317

ARGONNE NATIONAL LABORATORY
9700 South Cass Avenue
Argonne, Illinois 60439

MATERIALS RECYCLE AND WASTE MANAGEMENT IN FUSION POWER REACTORS

PROGRESS REPORT FOR 1982

by

S. Vogler, J. Jung, and M. J. Steindler

Fusion Power Program
Argonne National Laboratory

I. Maya, H. E. Levine, D. D. Peterman,
S. Strausburg, and K. R. Schultz

G. A. Technologies
P. O. Box 81608
San Diego, California 92138

NOTICE
PORTIONS OF THIS REPORT ARE ILLEGIBLE.
It has been reproduced from the best available copy to permit the broadest possible availability.

January 1983

DISCLAIMER

This report was prepared as an account of work sponsored by an agency of the United States Government. Neither the United States Government nor any agency thereof, nor any of their employees, makes any warranty, express or implied, or assumes any legal liability or responsibility for the accuracy, completeness, or usefulness of any information, apparatus, product, or process disclosed, or represents that its use would not infringe privately owned rights. Reference herein to any specific commercial product, process, or service by trade name, trademark, manufacturer, or otherwise does not necessarily constitute or imply its endorsement, recommendation, or favoring by the United States Government or any agency thereof. The views and opinions of authors expressed herein do not necessarily state or reflect those of the United States Government or any agency thereof.

DISTRIBUTION OF THIS DOCUMENT IS UNLIMITED

TABLE OF CONTENTS

TABLE OF CONTENTS (Cont'd.)

LIST OF FIGURES

LIST OF TABLES

LIST OF TABLES (Cont'd)

LIST OF TABLES (Cont'd)

ABSTRACT

Several components of a STARFIRE fusion reactor have been studied. The breeding ratios were calculated as a function of lithium enrichment and neutron multiplier for systems containing either Li_2O or $LiAlO_2$. The lithium requirements for a fusion economy were also estimated for those cases and the current U.S. resources were found to be adequate. However, competition with other lithium demands in the future emphasizes the need for recovering and reusing lithium. The radioactivities induced in the breeder and the impurities responsible for their formation were determined. The residual radioactivities of several low-activation structural materials were compared with the radioactivity from the prime candidate alloy (PCA) a titanium modified Type 316 stainless steel used in STARFIRE. The impurities responsible for the radioactivity levels were identified. From these radioactive impurity levels it was determined that V15Cr5Ti could meet the requirements for shallow land burial as specified by the Nuclear Regulatory Commission (10CFR61), whereas PCA would require a more restrictive disposal mode, i.e. in a geologic medium. The costs for each of these disposal modes were then estimated. The V15Cr5Ti residual activity is sufficiently low that adequate removal of the limiting niobium radioactivities might allow recycling of V15Cr5Ti about 80 years after its removal from the reactor. Two techniques for recovering the lithium from the $LiAlO_2$, an aqueous recovery technique and a solid-state reaction, are discussed. Several options were also considered for recovering the toroidal magnet materials at the termination of reactor lifetime: disposal of the materials, recovery of the materials by chemical processing, and recovery of the materials for refabrication of the magnet and dewar assembly. The last method was judged most cost effective.

MATERIALS RECYCLE AND WASTE MANAGEMENT IN FUSION POWER REACTORS

PROGRESS REPORT FOR 1982

1. Introduction (ANL)

The purpose of these studies is to define, examine and evaluate the waste handling and materials recycle problems of fusion reactors. A product of these studies is information on what reactor materials can be reused and how such reuse can be accomplished, what material must be discarded to waste, and what level of confinement is required for the waste, i.e., shallow land burial or geologic media. The scope of the study will include all materials associated with fusion reactors both during routine maintenance, the routine periodic replacement of the first wall and blanket as well as the accumulated material at decommissioning. The handling of the bulk of the tritium formed in lithium during reactor operation was not considered in this initial study.

In this first report, the lithium requirements are calculated for the solid breeders Li_2O and $LiAlO_2$ as a function of lithium enrichment and neutron multiplier. These requirements are then estimated for a fusion economy of 1000 GW(e) and compared with the estimates for the available lithium resources in the U.S. The calculated radionuclide content of the solid breeder materials Li_2O and $LiAlO_2$ after irradiation in a reactor are presented, and the troublesome impurities are identified. Since it appears that conservation of lithium will be necessary, procedures for recovering the lithium from spent $LiAlO_2$ are given. A study was made comparing what is termed "low activation" structural materials, particularly the radioactivity produced in each material and techniques for disposing or recycling of these materials. The superconducting magnet structures exhibit low levels of radioactivity and are candidate materials for recycle. Three options for handling the magnets are considered with reuse (to the extent possible) being the most effective for recycling magnet materials.

Some of the detailed information from this study is included in the appendices, for example a discussion of the conversion of decay gamma source to dose, the detailed summary of the activation analyses for the

first wall/blanket combinations, and the activation for the toroidal field magnets. Discussions are presented of the radioactive waste disposal requirements based on current regulations, including a discussion of the biological hazard potential (BHP), materials recycle requirements and the possibility of isotopic modification of some of the materials of construction. Also included in the appendices are some of the detailed procedures proposed for handling irradiated magnet materials.

This study is focused on the STARFIRE reactor, mainly because the most detailed information on construction, materials and nucleonics are available for this design. The results of the study are, nevertheless, generic because they are generally independent of plasma physics or the details of a particular fusion reactor concept and depend upon the neutron spectrum and the materials of construction. This study will indicate the waste disposal techniques required, the costs of waste disposal, the possibilities for recycle of materials and any incentives for substituting materials with the aim of decreasing the impact of disposal. Low activation materials offer the promise of reduced radioactivity in certain configurations and the possibility of recycle of materials. The impact on waste disposal requirements of low activation materials, and in particular vanadium, is evaluated. The vanadium was selected merely as a representative of a class of "low activation" materials. The use of vanadium structural material will be discussed for a STARFIRE type reactor that was an earlier version in the STARFIRE study and utilizes vanadium in the first wall and blanket, with liquid lithium as the coolant and breeder material.

This interim report focuses on the problems of the structural material for the first-wall/blanket, how long it must be cooled before it can be handled, how it is processed, disposed of, and an estimate of the costs of disposal. Also included is a comparison of a low activation material, vanadium, with the PCA* as a first wall material.

---

*Prime Candidate Alloy, an advanced titanium-modified Type 316 austenitic stainless steel.

1.1 Summary

At present stainless steel is the leading candidate as the structural material for fusion power reactors. However, the large amount of induced radioactivity has encouraged a search for materials with adequate or perhaps even improved physical properties as well as lesser amounts of induced radioactivities. Several candidate low activation materials were examined: Ti6Al4V, Al 6063 and V15Cr5Ti. For all of these materials, the impurity content controlled the final dose rate. The aluminum alloys could not escape the formation of ^{26}Al and thus the radiological dose rate for Ti6Al4V at 100 years after reactor shutdown is approximately 0.9 rem per hour* while for Al 6063 the dose rate is approximately 14 rem per hour. The V15Cr5Ti dose rate after 100 years is approximately 100 mrem mostly due to ^{94}Nb. Thus reduction or elimination of molybdenum and niobium isotopes, from which ^{94}Nb is formed by neutron activation, could result in a lowering of the radiological dose to very low limits. Further reductions in the impurity content, namely of nickel, will be reflected in a lower ^{60}Co content and lower dose rate at shorter time periods.

In a fusion reactor, neutron activation of materials results in a first-wall/blanket structure containing 98% of the total radioactivity and the larger volume of the remainder of the reactor structure containing the remaining radioactivity at a low concentration. An important goal for fusion reactor development is to minimize the formation of large amounts of long-lived activities to permit recycling of structural materials [BAKER].

Over the 30 year lifetime of the reactor, approximately 4500 m^3 of the structure remains at shutdown; approximately 99% would be available for recycle with about 1% destined for disposal in shallow land burial [BAKER]. The periodic removal of the the first-wall/blanket structure yields approximately 2160 m^3 of material. Of this material 1850 m^3 (the multiplier, reflector and breeder) could be disposed of in shallow land burial (after recovery of the tritium). The remainder, 310 m^3 of

*For these analyses the surface dose rate is estimated based on a sphere of 1 meter in diameter.

PCA (5% of the total amount of material) would require some more restrictive disposal option.

Disposal of some of these materials is controlled by the proposed 10 CFR 61 "Licensing Requirements for Land Disposal of Radioactive Wastes." Under these regulations, PCA requires more restrictive confinement than land disposal, e.g., in a geologic medium, mainly because the ^{63}Ni and ^{94}Nb contents of the first wall/blanket materials exceed the limits permitted for shallow land burial by factors of 20 and 65 respectively. The activity in the vanadium alloy is sufficiently low that shallow land burial would be acceptable at any time 1 year after removal from the reactor. However the disposal costs can be reduced substantially if a decay period of 10 years is selected. The activity level of the vanadium alloy is sufficiently low, especially with effective removal of the troublesome impurities, niobium, molybdenum and nickel, that recycling of the vanadium alloy becomes a likely possibility.

Other studies have shown that the use of a neutron multiplier in a fusion system enhances the breeding ratio of a particular system. For the $LiAlO_2$ system with a Zr_5Pb_3 multiplier, the breeding ratio increases slowly with enrichment up to 30% ^6Li, beyond which it becomes insensitive to enrichment.

An analysis of the lithium requirements for a fusion economy of 1000 GWe indicates that approximately 80% of the U.S. resources would be required assuming lithium resources at the level of the present knowledge, and that no lithium is recycled. But since only 3% of the total lithium is consumed during a time equal to sector lifetime, recovery of lithium is necessary to conserve what may be limited supplies of lithium.

The results of the neutron irradiation of breeder materials is dominated by the presence of impurities. The presence of zirconium and molybdenum isotopes in the $LiAlO_2$ yield an assortment of radioisotopes. Based on these results, concentration limits of these impurities can be established so that the resulting induced radioactivity does not inhibit recycle of the breeder material.

For the recycle of the $LiAlO_2$ two techniques are available, a solid state reaction in which the residual material (containing $LiAlO_2$ and $LiAl_5O_8$) is reacted with Li_2CO_3 (of proper ^6Li enrichment) to yield $LiAlO_2$ and an aqueous technique in which the residual oxide is dissolved in an aqueous solution and the lithium isolated for recovery. The solid state method is simple but has the limitation that all radioactivity is carried on to the new product. The aqueous technique has the possibility of achieving a separation of lithium from all extraneous materials, thus permitting hands-on operation for subsequent processing but requires disposal of the aluminum.

Three options for the disposition of irradiated materials from the STARFIRE toroidal field (TF) magnets were examined, namely, (1) disposal of the irradiated magnet material, (2) reprocessing of selected materials and the subsequent manufacturing of a new magnet using these and new materials with standard fabrication techniques, and (3) preparation of the irradiated magnet for the subsequent refabrication of a new magnet using the irradiated materials. The results indicate that refabrication of a magnet using the acceptable components of the irradiated magnet is technologically feasible. The total cost of refabricating the 12 TF magnets was estimated to be $21 million in 1982 dollars. Since this option avoids the purchase of new magnets, which would cost over $170 million, it is the preferred economic choice. In comparison, reprocessing and recycling of the magnet materials yields a net profit of $0.4 million, but requires the purchase of a new set of magnets. In the event that the old magnets are unusable (e.g., as a result of significant advances in magnet design or severe accidental damage), reprocessing of the TF-coil materials can be used to recover the decommissioning costs associated with the STARFIRE magnets. Lastly, the low induced radioactivity levels in the magnets permit their qualification as Class A low level radioactive waste. Simply disposing of the magnets via shallow land burial was estimated to cost $3.5 million, including all the associated costs of dismantling, packaging, shipping, and ultimate disposal.

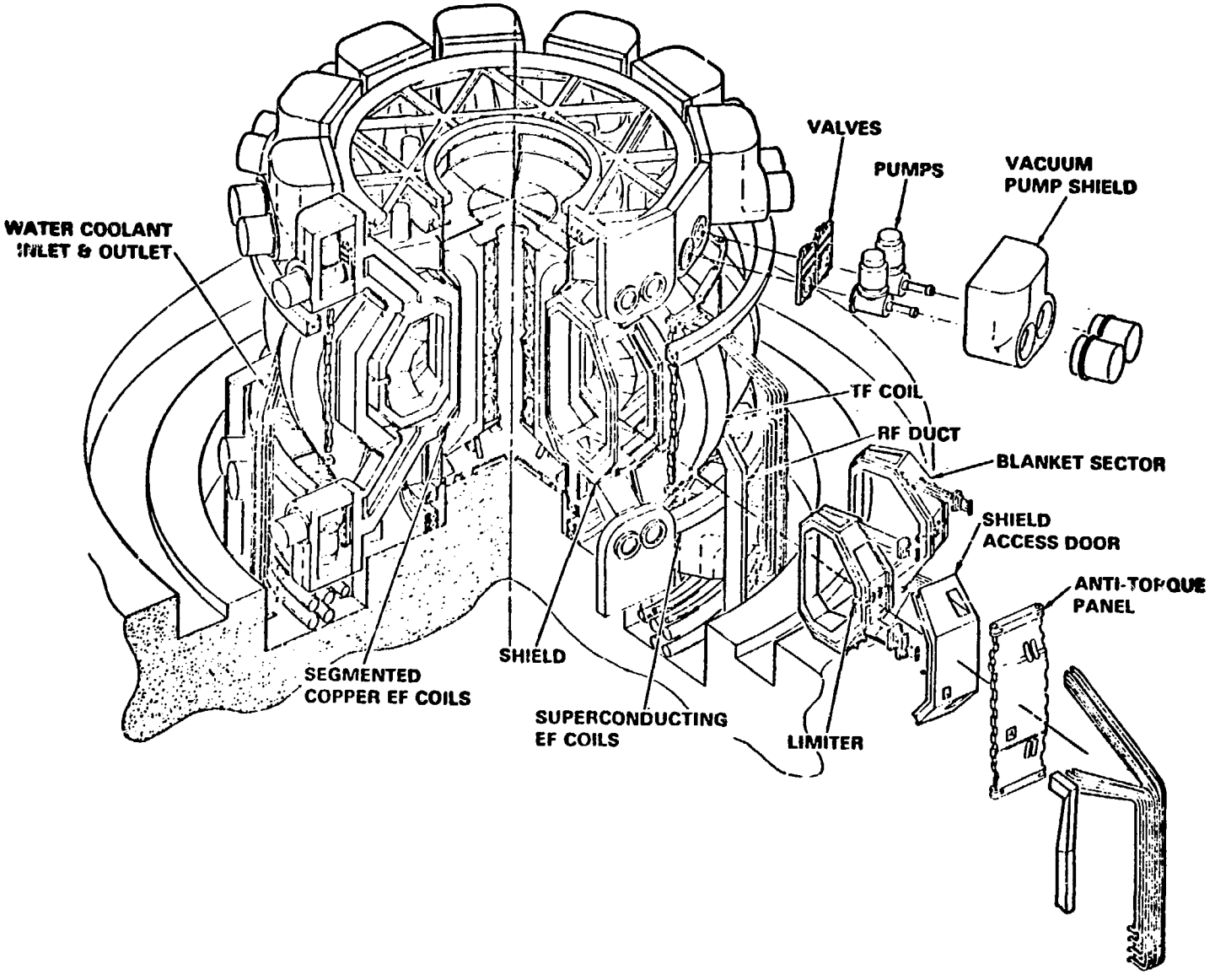

Fig. 1.1. STARFIRE reactor concept.

1.2. STARFIRE Reactor

The STARFIRE reactor is a water-cooled fusion reactor of the tokamak design operating in a continuous plasma burn mode with a thermal power of 4000 MW and a net electrical power of 1200 MW [BAKER]. The fuel for the reactor is deuterium-tritium. An isometric view of the reactor is shown in Fig. 1-1. The reactor configuration involves 12 toroidal field (TF) coils, 12 superconducting poloidal coils (EF and OH) and 4 small, normal conducting control coils (CF). The reactor configuration was developed to permit the superconducting EF coils to be kept external to the superconducting TF coils so that their replacement is possible without fabrication of a new coil on the reactor. The shield consists of twenty-four sectors so that it may be installed between the TF coils. The sectors are joined together by a welded vacuum seal. The vacuum boundary location was selected at the shield interior with access door seals located at the outer surface. The magnet systems and shield are expected to last for the life of the reactor.

The blanket is divided into twenty-four toroidal sectors of two different sector sizes to permit their installation between the TF coils. In the STARFIRE reactor, the twenty-four first wall/blanket sectors are integral units. The basic functions of the first-wall/blanket are to provide the first physical barrier for the plasma, to convert the fusion energy into sensible heat and to provide for the heat removal, to breed tritium and to recover the bred tritium and to provide some shielding for the magnet system. The first wall is modified 316 stainless steel, identified as "prime candidate alloy" or PCA. The first wall must withstand high particle and energy fluxes from the plasma, high thermal and mechanical stresses and elevated temperature operation.

The blanket must breed tritium and since lithium is the only viable tritium-breeding material, lithium must be present in the blanket; in the case of STARFIRE, lithium is present as $LiAlO_2$. With the use of $LiAlO_2$ as the breeder, it is necessary to use lithium enriched in ^6Li and to have a neutron multiplier such as Be or Zr_5Pb_3. A graphite reflector completes the blanket structure. Some of the details of blanket construction are given later in the report. It is anticipated that the blanket sectors will have a six year lifetime.

The primary function of the STARFIRE vacuum system is to remove the helium formed as ash from the fusion reaction. The system must also produce a high vacuum of approximately 1.3×10^{-6} Pa for initial plasma startup, it must regenerate the cryopumps, and interface with the tritium recovery system. To achieve these goals, the system requires roughing and regeneration pumps, 48 cryopumps on 24 vacuum ducts and a gate valve and right-angle valve for each of the cryopumps. Each of the cryopumps contains molecular sieves for pumping non-condensibles. During normal operation, 24 of the cryopumps will be evacuating the system while the other 24 cryopumps are being regenerated on a two hour cycle. The right angle valve (regeneration valve) opens and closes during the operating cycle, while the gate valve (isolation valve) is only closed to isolate the cryopump from the vacuum system when replacement is necessary. It is anticipated that the cryopumps and the right-angle valves will have a two year lifetime and will then be replaced.

The reactor configuration was developed so that each component could be replaced in a time consistent with its anticipated life using remote maintenance techniques. Components have been combined where possible in modular units so that all reactor components can be removed and replaced in a simple manner. Such a "remove and replace" concept permits quick resumption of reactor operation while the more time-consuming activities are carried out in the adjacent hot cell. The maintenance schedule calls for reactor downtime for approximately 28 days per year to permit replacement of four first-wall/blanket sectors including limiters and rf ducts and 24 of the cryopumps with their accompanying right-angle regeneration valves. These tasks will be accomplished by means of remotely controlled special purpose machines.

Low activation materials such as vanadium offer the promise of reduced radioactivity in the structural material and the possibility of recycle of the structural material. In order to optimize the properties of the reactor system with vanadium as the first wall material, liquid lithium was selected as the coolant and breeder material. A consequence of using liquid lithium as the breeder is that no neutron multiplier is required. Also with the V/Li system, lithium can be removed from the

sector before its removal from the reactor and only vanadium and graphite need to be handled during maintenance operations. The use of the V/Li system results in a first-wall lifetime that is expected to be twice that of the PCA in the PCA/$LiAlO_2$ system, thus reducing the frequency of blanket sector replacement [ABDOU].

1.3 Background

This section contains a summary of work by others that serves as background to the present studies. Fusion power reactors use fuel that yields no radioactive byproducts as part of the generation of energy, but the very high neutron flux in fusion reactors produces activation of structural materials to levels that require extensive shielding during operation and careful radioactive waste management. Comparison of the radioactive components of fusion and fission reactors is generally not useful since only fission reactors contain long-lived, highly toxic trans-uranium nuclides and modest-lived ($T_{1/2}$ < 30 y) fission products, while fusion reactors contain activation products only a few of which are long-lived and many of which emit no penetrating radiation. Nevertheless, the experience gained in the management of radioactive wastes from fission reactors can be applied to fusion reactor systems. It has been recognized that some consideration must be given as to how the radioactive wastes from fusion reactors will be handled [BOTTS 1978A, BOTTS 1978B, GORE, WILLENBERG].

An earlier study [STEINER-1972] contains a discussion of the quantities of radioactivity that would be expected from the operation of fusion reactors and the role of this radioactivity in the biological effects of an accident, the radioactive effluents resulting from normal operation, and the management and disposal of radioactive wastes. The fusion reactor chosen as a model was a 1000MW(t) tokamak reactor using D-T fuel in which the released energy is recovered as heat in a lithium blanket. It was anticipated that tritium would be the major source of radioactivity in effluents, but it was estimated that leakage can be controlled to manageable levels, i.e., ~7 Ci/day.

In a discussion of long-lived radioactive wastes, a comparison was made between vanadium and niobium as structural materials and it was pointed out that the use of vanadium yielded much less radioactivity and vanadium could most certainly be processed for reuse. It was also recognized that the radioactivity induced in vanadium would be due to impurities in the vanadium. Steiner concluded that the afterheat removal will be less of a problem in the fusion reactor than in a fission reactor. This study contained a generalized discussion of the wastes that would accumulate from an early model of a fusion reactor using either niobium or vanadium but there was no discussion as to the disposition of these wastes.

Another early appraisal of fusion reactor wastes was mainly concerned with comparing those wastes with fission wastes [YOUNG]. It was pointed out that gaseous and solid radioactive wastes from fusion power plants are expected to be less than the comparable radioactive wastes from fission power plants. The amount of materials required for fusion reactors was estimated to be more than two times that for an LMFBR. Some of this material will certainly become radioactive and will require disposal as radioactive materials.

In another study [BOTTS 1978A], several fusion reactor designs were examined and the radioactive wastes generated were compared with the wastes from fission reactors. The fusion reactors compared were UWMAK-I, UWMAK-III, BNL Minimum Activity Blanket, and the PPPL Fusion Power Plant. The handling of these radwastes was discussed for on-site storage and processing, transportation and disposal, and reactor decommissioning. For the reactors examined, the radioactive waste from fission reactors has a much higher biological hazard potential than does the waste from a fusion reactor and this higher biological hazard becomes more obvious after a decay period of 200 years. It was observed that aluminum is an attractive material of construction, yielding low levels of radioactivity. The use of aluminum as a structural material results in the formation of long-lived ^{26}Al which yields a 1.8 MeV gamma during the decay process. The ^{26}Al can result in a high radiological dose in close proximity to the material. However Botts expected that in disposal, the radioactive

aluminum (^{26}Al) will equilibrate with natural aluminum, thus reducing the activity of ^{26}Al in groundwater to levels orders of magnitude below the radiation protection guide values [10 CFR 20].

A conclusion in this study [BOTTS 1978A] was that most materials considered for fusion reactors could be recycled after a two hundred year decay. Prior to isolation it would probably be necessary to store the material on site for about one year to make shipping easier. During that interval, retrievable isolation by shallow land burial would be acceptable. If recycle were not chosen, provisions for final disposal would be necessary. Waste management evaluations included transportation requirements from plant site to disposal site, cost of transportation, accident rate during transportation, decommissioning of the reactor, and isolation and disposal of the waste material. All evaluations included comparisons with fission reactors.

Recycle of structural materials was considered [BOTTS 1978A] as a means of conserving scarce or valuable materials. Two options were considered for recycle: permitting decay until the amount of radioactivity was trivial or recycling as soon as the radiological dose rate (a function of residual radioactivity) was low enough to permit handling. In evaluating the dose effects it was assumed that the material was in a one meter sphere and that a worker spent varying times in the proximity of the sphere; a protocol was set up in which the operator spent no more than 5-10 percent of his time close (2m) to the sphere [BOTTS 1978A]. Approximately 50 years of decay is adequate to maintain the worker dose level below 5 rem/year. These comments apply to the UWMAK-I using 316 SS as the structural material and to the PPPL with PE-16, a high nickel steel. These standards are much less stringent than the standard postulated in STARFIRE in which it is assumed that the activity is sufficiently low (< 2.5 mrem/hr) so that direct contact with the material for 8 hour work days conforms to the NRC guidelines of less than 1.25 rem/ calendar quarter [BAKER].

In general, fusion reactors are expected to create larger physical amounts of radioactive waste with lower levels and shorter-lived activity than do fission plants.

One of the conclusions [BOTTS 1978A] was that reuse of materials is possible at some finite time (two centuries) and that storage in shallow trenches is acceptable during this decay time. Such trenches were chosen because of ease of retrieval. There is no assurance that such techniques will be acceptable based on current proposed rules for waste disposal [10 CFR 61].

Eight conceptual deuterium-tritium fueled fusion power plant designs, vintage 1975, were evaluated for the wastes to be expected [GORE]. Wastes included radiation damaged structural, moderating, and fertile materials; getter materials for removing corrosion products and other impurities from coolants, absorbents for removing tritium from ventilation air; getter materials for tritium recovery from fertile materials; vacuum pump oil and mercury sludge, failed equipment; decontamination and laundry wastes.

For the designs analyzed, the total annual radwaste volume was estimated to be 150-600 m^3/GWe of which 35-295m^3 is attributable to blanket and failed equipment replacement. The volume of the total wastes may be compared with the 500-1300 m^3/GWe estimated for the LMFBR fuel cycle. The major waste sources from fusion reactors are replaced reactor structures and decontamination wastes.

Another report of materials flow for a fusion reactor discussed three fusion reactor systems, GA Demo, UWMAK-II and the ORNL Demo [WILLENBERG]. In this discussion, the blanket materials were compared, as were the activation product inventories for each fusion reactor. For the GA-Demo (1676 MWt), the isotopes responsible for the activity are detailed and at shutdown a total of $\sim 2 \times 10^9$ Ci are present in the blanket. During the first year, after shutdown, the cobalt isotopes dominate the residual activity. For the UWMAK-II (4000 MWt) blanket, the activity builds up to a level of approximately 3.5×10^9 Ci. In this case, the activity is dominated by ^{55}Fe and the cobalt isotopes. For the ORNL Demo (1615 MWt), the total activity is 2.1×10^9 Ci at the time of blanket replacement. Again the ^{55}Fe and cobalt isotopes are prominent. It is pointed out that remote handling for the blanket materials is

Table 1.1. Radioactivity Content of Fusion Reactor Blanket Materials at Time of Blanket Removal [WILLENBERG]

	GA-DEMO	UWMAK-II	ORNL-DEMO
Thermal Power MW(th)	1676	4000	1615
Primary Structural Material	Inconel 718	316 SS	316 SS
Blanket Replacement Period (y)	4	2	6
Activity (at Blanket Repl.) (Ci)	2.5×10^9	3.6×10^9	2.1×10^9
Radioisotopes	Percent of Total Activity		
^{58}Co	30.2	19.4	15.8
^{28}Al	23.7	-	-
^{57}Co	21.6	11.1	7.9
^{56}Mn	8.6	19.4	29.1
^{51}Cr	4.3	13.9	7.9
^{55}Fe	4.3	25.0	29.1
^{54}Mn	2.2	5.6	6.3
^{60}Co	0.9	-	1.1
^{52}V	2.2	5.6	-
^{203}Pb	2.2	-	-
^{99}Mo	-	-	2.6

required because of the residual activity. An examination of the radioactivities of the blankets of the three reactors indicates that they are similar, differing perhaps by a factor of two to three in most cases (Table 1.1).

One alternative considered [WILLENBERG] was disposal of the blanket material. In the GA-DEMO reactor, the first wall/blanket consists of approximately 2,000 cylindrical modules (0.7 m diam.) mounted on the inside of the inner shield. The blanket module contains SiC, Inconel, Li_7Pb_2, and Li_4SiO_4. It is suggested that four modules be placed in a cylindrical can 0.7 m in diam. by 1 m and four cans are placed in a reusable shipping cask. This would yield 7.4 Mg of blanket material in each cask. For the UWMAK-II, processing would require breaking up the blanket segments and reprocessing some of the metal and all the fertile

material. For the ORNL-DEMO, the first problem is the removal of the liquid lithium before processing. There is also a discussion of the handling and disposition of the secondary or operational wastes.

There were three objectives for the waste handling procedures; a) to recycle blanket materials as much as possible to recover resources, reduce radioactive waste storage and reduce shipping; b) to convert radioactive waste effluents into as dense a form as possible to minimize handling and shipping; and c) to ensure that all steps yield a low biological hazard.

Also included is a discussion of the relative merits of crushing (compacting) versus melting for handling steel components. The major disadvantage to melting is that it requires about a megawatt-day/tonne of stainless steel. One virtue of melting is that the metal ingot will provide a much better path for decay heat flow than with crushed (compacted) metal.

There is also a discussion of the relative merits of liquid (lithium) and solid ($LiAlO_2$) breeder materials, a subject which has been reviewed many times [SMITH-1979]. When liquid lithium is used as the breeder, normal lithium may be used. The use of liquid lithium as the breeder is characterized by in-plant (but external to the fusion reactor) recovery of tritium and recycle of the lithium.

Willenburg suggested that solid compounds are less limiting in terms of corrosive interactions with possible structural materials. More recent information shows that Li_2O is a quite corrosive material [KURASAWA, FINN]. However, for a reaction time of 100 h at about 1000°C, 316 stainless steel in contact with Li_2O in vacuum yielded a scale approximately 100 μm thick. Other work at lower temperatures (600°C) confirmed the appearance of thick reaction scale at the Li_2O/metal interface for HT-9 and 316 SS [FINN]. In the same type of experiment with $LiAlO_2$, the reaction of $LiAlO_2$ with the metal was much less than that with Li_2O. There was no apparent scale in contact with the 316 SS and the $LiAlO_2$ exhibited little change.

It was reported [WILLENBERG] that the lower tritium solubility in the solids (compared with liquid lithium), as well as the requirement that the breeding material be a powder results in a much lower tritium inventory in the blanket than for a liquid lithium breeder. More recent information has shown that tritium levels in liquid lithium can be reduced to less than 1 ppm [WESTON]. Also irradiation experiments with solide breeders have indicated that the fractional rate of removal of formed tritium varies inversely with the fluence [WISWALL]. In these experiments, samples were subjected to a neutron flux at room temperature. The samples were removed from the radiation source and the tritium removed was measured under different experimental conditions. The removal of tritium from solid breeders is still an unresolved issue and is addresssed in the TRIO experiments.

In summary, the previous work consisted of general discussions of the radioactivities to be expected from the blankets of several typical fusion reactors, how these blankets might be handled to recover the valuable materials, and how the wastes might be packaged for ultimate storage.

These early studies examined fusion wastes after removal from the reactor, during on-site storage, packaging for disposal, transportation, and disposal, and final decommissioning of the reactor. Among the conclusions reached are:

1. Fission wastes are more hazardous than fusion wastes based on the biological hazard potential, especially after long decay periods (> 200 years).

2. From the point of view of waste management, aluminum is a potentially attractive material, disposal being possible after several years decay.* Molybdenum is the least attractive. Stainless steel is intermediate but after about 100 years decay recycling or disposal is possible.

*However, the following limitations for aluminum should be noted: temperatures are limited to about 200°C, radiation induced embrittlement may result in reduced component life, and new alloys need to be developed to achieve low activation and adequate strength.

3. Fusion reactor activated material will probably require on-site decay for at least a short period (1-2 y) to permit reasonable size shipments to be made using conventional shipping casks.

4. It is indicated that fusion reactors will generate a greater amount of waste from the replaceable blanket components than do fission reactors as reflected in the amount of spent fuel elements.

5. Transport costs for wastes from fusion reactors appear to be two to six times greater than those for LWR's of comparable electrical output. However, transport costs are small compared to other costs [BOTTS 1978A].

6. The amount and activity of low level liquid and solid waste seems to be comparable for fusion and fission wastes.

7. Tritium is the most significant effluent associated with fusion power plants.

8. It was recognized that materials requirements for deployment of a fusion power economy require recycle of some materials.

These conclusions are generally still valid, but it seems that decay times of 100 years are impractically long.* The present work is aimed at exploring the factors that could reduce the required decay time to more realistic values, e.g., 10-30 years. Techniques for achieving this include reductions in the impurity content of materials of construction

*Long-term materials storage in anticipation of recycle is outside of current experience and practice. In addition, refurbishing of equipment stored for long periods encounters problems of traceability, QA/QC, and impact of design modifications. There are, consequently, a number of reasons other than cost that result in the need for caution when analyzing on a realistic basis the recycle of fusion reactor materials.

and the use of remote control techniques for processing material too radioactive to be directly handled. Another technique discussed here is isotopic tailoring, i.e., removing deleterious isotopes from those materials composed of several isotopes. In this manner, the physical and chemical properties are maintained but the activation properties are favorably altered. Such a technique, if achievable at reasonable cost, could lead to reductions in activity of the materials of construction. The costs of geologic disposal waste is compared with the costs of recycling material to identify some of the economic incentives and hence allowable costs for recycling operations.

2. Materials Recycle and Waste Management (ANL)

2.1 Introduction

The use in fusion reactors of materials of construction that are only slightly subject to activation by neutrons has been considered advantageous for the reduction of the hazards from and the expense of handling radioactive wastes [KUMMER]. In order to identify the specific advantages for waste management of such low activation materials, the waste management activities for handling the structural materials from two different tokamak reactor concepts are described. The PCA/$LiAlO_2$ combination of first wall/blanket structural material and breeder material is from the STARFIRE reactor [BAKER] which is described as a commercial tokamak fusion reactor in a mature fusion reactor economy. The V/Li case is from one of the earlier but similar designs in which liquid lithium is the coolant and breeding material [SMITH-1979].

STARFIRE

The STARFIRE is a tokamak fusion reactor with a 7.0 m major radius and operates at an average neutron loading of the first wall of 3.6 MW/m^2. The reactor configuration is given in Fig. 1.1. The reactor itself is composed of 24 sectors, so that four sectors will require replacement every year. The sectors are not all identical, but differ slightly to permit removal between the TF coils. The larger sectors subtend an angle

of 16.2° and each weighs approximately 65 Mg; the smaller sectors subtend an angle of 13.8° and each weighs approximately 60 Mg. Each of the blanket sectors can be separated into nine separate tritium breeding modules arranged poloidally around the sector. Primary structural support for each sector is provided by large frames at the sector sides; each module is individually connected to the frame.

The water-cooled blanket sectors are 68-cm thick and consist of a 1-cm thick first wall, a 5-cm thick neutron multiplier Zr_5Pb_3, a 1-cm thick second wall, a 46-cm thick breeding zone of $LiAlO_2$ and a 15-cm thick graphite reflector zone that contains the blanket support structure and the manifold lines. The modules are 2-3 m wide by ∿3 m high depending upon location within the reactor. The module walls and all support structures in the high-radiation zone are fabricated from an advanced low-swelling austenitic stainless steel. A diagram for a typical sector is shown in Fig. 2.1.

Lithium-Cooled Blanket

The primary incentive for use of lithium as a coolant in a commercial fusion reactor is the fact that it also is used as the tritium-breeding medium. With liquid lithium as the coolant and stainless steel as the structural material, the maximum operating temperature is restricted to 500°C with a predicted lifetime of 3.1 MW-yr/m^2 (without a divertor). With vanadium as the structural material the maximum operating temperature is calculated to be 650°C and the predicted lifetime is 34 MW-yr/m^2 (without a diverter and ignoring fatigue effects) [ABDOU]. The data base for vanadium and its alloys is limited, and the projections given here are only rough estimates.

The general design of the reactor using liquid lithium is the same as for the STARFIRE with 24 removable sectors forming the torus. Each of the sectors in turn is composed of smaller modules for ease of handling. The construction of the lithium-cooled fusion reactor can be more easily appreciated by examination of Fig. 2.2.

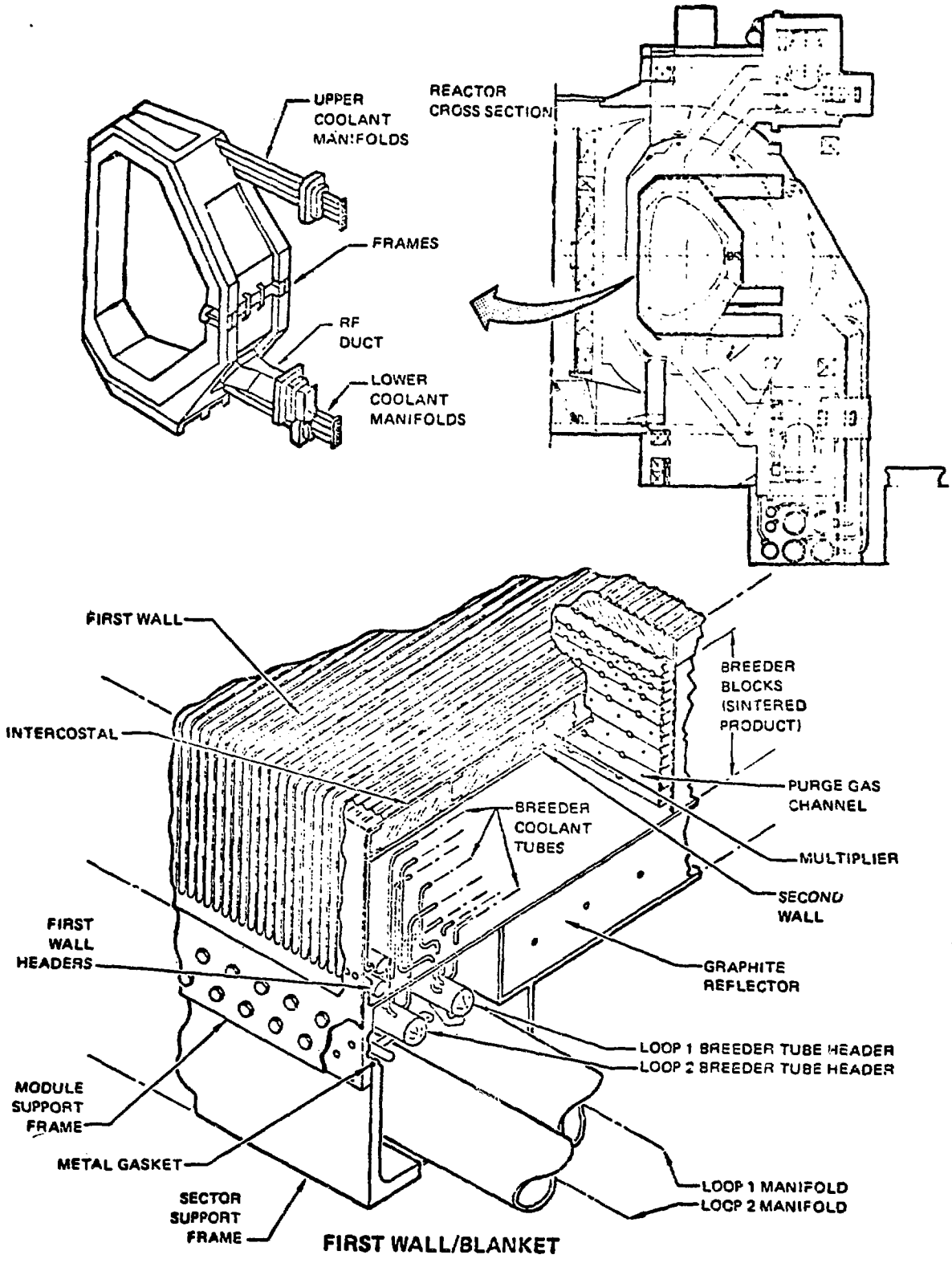

Fig. 2.1. STARFIRE blanket concept [BAKER].

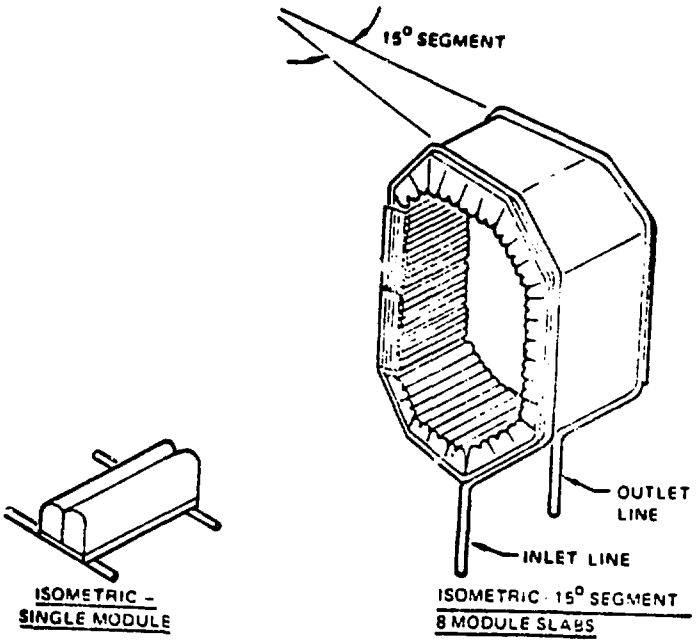

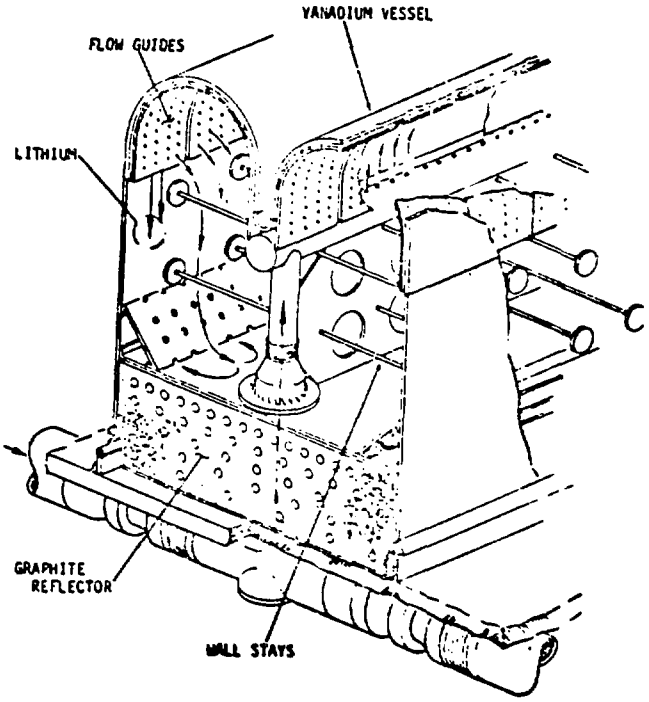

Fig. 2.2. Vanadium alloy blanket module [ABDOU].

2.2 Nuclear Analysis

2.2.1 Introduction

The present study is devoted to the analysis of the neutron-induced activation of fusion reactor components. The most serious concern with regard to the activation of components, as envisioned for commercial fusion reactors, is the production of radioisotopes with very long half-lives in relatively large volumes of construction materials. This has an obvious environmental consequence, i.e., a requirement of long-term storage of radioactive waste. An important strategy for fusion reactor development, therefore, is to minimize the generation of large inventories of high-level, long-term activation. This can be accomplished by careful choices of material and design along with a waste management scheme that includes material recycling as a key element. It should be particularly emphasized that in a mature fusion power economy, the continued use of materials without recycle (due to a high-level activation) could result in a serious depletion of some resource-limited materials such as niobium [MCP-10] and chromium [MCP-1]. Selection of reactor materials that are less resource-limited and/or intrinsically little activated, complements the potential of material recyling and results in fusion power reactors that are less constrained by environmental impacts.

In general, fusion reactor activation can be classified into two distinct categories. Approximately 90% of the total radioactivity is confined to the first-wall/blanket system which is a small portion of the total system volume. The remaining 10% radioactivity is spread out at a low concentration in a much larger volume of reactor components external to the first-wall blanket. In the case of STARFIRE [BAKER], the volume of these external components (bulk shield, penetration shield, and superconducting magnets) amounts to ~3600 m^3, compared to ~350 m^3 in the first-wall and blanket regions. As a result, from a viewpoint of volumetric activation, these external components are also of great importance in the management of radioactive wastes. In fact, this has been one of the motivations for exploring the possibility of recycling the bulk of shield and magnet materials in the STARFIRE study [JUNG-1981, JUNG-1980]. On the other hand, the concern about the first-wall/blanket radwastes is centered on the high-level of radioactivity due to activation.

activation. In addition, the lifetime of these components is shorter, than the plant lifetime, and hence they require replacement on a regular basis. In STARFIRE, which requires a replacement of each first-wall/blanket module every six years, the total accumulation of regularly discharged materials amounts to ~1850 m^3 over the 40-y plant lifetime (at a plant availability of 75%). The management of these discharged materials also yields radioactive wastes which must be handled.

Two major components of the first-wall/blanket system must be considered. They are structural materials and lithium-bearing tritium breeders. In many of the earlier works [STEINER-1970, STEINER-1974, DUDZIAK, VOGELSANG, POWELL-1973, GROUBER, CONN-1974] on the activation of fusion reactor materials, the importance of breeder activation has been less emphasized than the structural material activation. In most cases the structure activation dominates the first-wall/blanket radwastes in terms of the radioactivity level but a careful assessment of breeder activation is also necessary because of its relatively large volume. In the case of STARFIRE, for instance, of the ~60 m^3 wastes discharged annually, approximately one-half the volume is the $LiAlO_2$ breeder [BAKER]. A large portion of the remaining radwaste volume is the graphite reflector (~17 m^3). The total PCA in the first-wall/blanket waste results in only ~9 m^3 on an annual basis. The analysis of breeder activation is helpful in designing a process for recovering and recycling the lithium breeder. Analysis of blanket designs could lead to the most effective lithium utilization for breeding of tritium.

In Section 2.2.2 the scope of the present analysis and the computational method used for the analysis are described. Section 2.2.3 is devoted to the analysis of breeder activation in the context of the solid-breeder blanket concept of STARFIRE. Section 2.2.4 presents a brief overview on potential low-activation structural materials, which is followed in Section 2.2.5 by a comparative analysis of the structural material activation. Appendix A describes a conversion technique from decay gamma source strength to contact biological dose using slab and spherical models. Summary tables of the activation analyses for the first-wall/blanket system and toroidal-field superconducting magnets are presented in Appendices B and C respectively.

2.2.2 Scope of Activation Analysis and Computational Method

Among the purposes of this analysis are to develop quantitative information on the activation of breeder materials and to evaluate the overall lithium requirements for a fusion economy compared with the available resources. The reactor model used for the analysis is based on the STARFIRE design concept (see Tables 2.1 and 2.2.) The activation analysis has been conducted using this reactor model for two primary material categories: (1) solid tritium breeders; and (2) first-wall/blanket structural materials. The solid breeders studied include alpha-phase $LiAlO_2$ and Li_2O as representative cases of ternary and binary ceramics, respectively. The importance of breeder activation is examined in terms of: (a) ^6Li enrichment of the breeder; (b) use of a neutron multiplier; and (c) impurity contents in primary breeder constituents.

With regard to the structural material activation, three low-activation candidates, V15Cr5Ti, Ti6Al4V, and Al-6063 alloys are analyzed. The results are compared to the reference case that uses modified austenetic stainless steel, PCA (prime candidate alloy). In this analysis several combinations of breeder, structure, and coolant materials are selected as follows:

Case	Structure	Breeder/Coolant	
1	PCA	α-$LiAlO_2/H_2O$	(STARFIRE)
2	PCA	Li	
3	V15Cr5Ti	Li	
4	Ti6Al4V	Li	
5	Al-6063	Li	

Comparisons of Cases 1 and 2 will serve to identify the impact of design selection regarding the tritium breeder and coolant materials, i.e., the design impact of solid and liquid blanket concepts on the activation. Analyses of Cases 2 through 5 will provide information on the activation characteristics of each candidate alloy, leading to an intercomparison among the potential low-activation candidates. Although a certain class of alloys may not be compatible with the liquid lithium breeder/coolant from a materials viewpoint, the study of these material combinations is expected to afford a consistent comparison by singling out the essential effect of the structural material choice. The potential of structural material recycling for each blanket

Table 2.1. The Dimensions and Material Compositions of the STARFIRE Outboard Blanket/Shield Design Used in the One-Dimensional Analysis

Component	Outer Radius (m)	Thickness (m)	Composition
1. Plasma	2.53	2.53	Vacuum
2. Scrape-off	2.73	0.20	Vacuum
3. First wall	2.74[a]	0.01	50% PCA + 27% H_2O
4. Multiplier	2.79	0.05	100% Zr_5Pb_3
5. Second wall	2.80	0.01	35% PCA + 17% H_2O
6. Blanket	3.26	0.46	6.55% PCA + 3.26% H_2O + 52.16% $LiAlO_2$[b] + 3.26% He
7. Reflector	3.41	0.15	5% PCA + 5% H_2O + 90% C
8. Blanket jacket	3.43	0.02	100% PCA
9. Coolant header	3.63	0.20	2.5% PCA + 18% H_2O
10. Plenum	4.13	0.50	Vacuum
11. Shield jacket	4.15	0.02	100% Fe-1422[c]
12. HFS shield	4.65	0.50	5% Ti6Al4V + 65% TiH_2 + 15% H_2O + 15% B_4C
13. MFS shield	5.05	0.40	70% Fe-1422 + 15% B_4C + 15% H_2O
14. LFS shield	5.33	0.28	100% Fe-1422 (anti-torque panel)
15. CO_2	5.83	0.50	CO_2
16. Magnet dewar	5.86	0.03	100% Fe-1422
17. Thermal insulator	5.91	0.05	Liquid N_2
18. Helium vessel	5.98	0.07	100% 304 SS
19. Magnet 1	6.51	0.53	4% Nb_3Sn + 35% Cu + 30% 304 SS + 4% insulator + 27% He
20. Magnet 2	6.86	0.35	2% NbTi + 32% Cu + 38% 304 SS + 4% insulator + 24% He

[a] Based on the first wall area of 755.8 m^2 and the major radius of 7 m.

[b] 60% ^6Li enrichment.

[c] Fe14Mn2Ni2Cr.

Table 2.2. The Dimensions and Material Compositions of the STARFIRE Inboard Blanket/Shield Design Used in the One-Dimensional Analysis

Component	Outer Radius (m)	Thickness (m)	Composition
1. Plasma	2.53	2.53	Vacuum
2. Scrape-off	2.73	0.20	Vacuum
3. First wall	2.74[a]	0.01	50% PCA + 27% H_2O
4. Multiplier	2.79	0.05	100% Zr_5Pb_3
5. Second wall	2.80	0.01	35% PCA + 17% H_2O
6. Blanket	3.08	0.28	6.55% PCA + 3.26% H_2O + 52.16% $LiAlO_2$[b] + 3.26% He
7. Blanket jacket	3.10	0.02	100% PCA
8. Plenum	3.12	0.02	Vacuum
9. Shield jacket	3.14	0.02	100% Fe-1422[c]
10. Shield 1	3.29	0.15	Tungsten-base shield, W*[d]
11. Shield 2	3.365	0.075	Boron carbide base shield, B_4C*[e]
12. Shield 3	3.515	0.15	W*[d]
13. Shield	3.59	0.075	B_4C*[e]
14. Shield 5	3.665	0.075	W*[d]
15. Shield 6	3.74	0.075	B_4C*[e]
16. Shield jacket	3.76	0.02	100% Fe-1422
17. Gap	3.78	0.02	Vacuum
18. Magnet dewar	3.80	0.02	100% Fe-1422
19. Thermal insulator	3.85	0.05	Liquid N_2
20. Helium vessel	3.92	0.07	100% 304 SS
21. Magnet 1	4.45	0.53	4% Nb_3Sn + 35% Cu + 30% 304 SS + 4% insulator + 27% He
22. Magnet 2	5.15	0.70	2% NbTi + 32% Cu + 38% 304 SS + 4% insulator + 24% He
23. Helium vessel	5.22	0.07	100% 304 SS

[a] Based on the first-wall area of 755.8 m^2 and the major radius of 7 m.

[b] 60% ^6Li enrichment.

[c] Fe14Mn2Ni2Cr.

[d] W*: 80% W (@ 95% TD) + 10% Fe-1422 + 10% H_2O.

[e] B_4C*: 80% B_4C (@ 95% TD) + 10% Fe-1422 + 10% H_2O.

material combination is deduced based on two measures: (1) evaluation of the volumetric radioactivity (Ci/m^3); and (2) evaluation of the contact biological dose (rem/h) due to decay gamma emission (see Appendix A).

The neutron transport calculation that is required prior to the activation analysis has been carried out by one-dimensional discrete-ordinate code, ANISN, [ANISN-ORNL] with the S_8P_3 approximation. The associated transport cross sections were obtained from the VITAMIN-C [ROUSSIN] library that is based on the ENDF/B-IV [GARKEN] data files. The original 171 neutron groups of VITAMIN-C were converted to a 46-neutron-group structure. The activation analysis has been performed by making use of the RACC code [JUNG-1979] along with the associated decay and cross-section data libraries [RACCXLIB]. The computational technique of RACC is based on Gear's stiff matrix method [GEAR].

2.2.3 Solid-Breeder Performance and Its Impact Upon Materials Recycling

In this section the tritium breeding performance is evaluated as a function of lithium enrichment and from these results the lithium requirements for a fusion economy are calculated and compared with the available lithium resources. Finally, the effects of impurities upon breeder activation are evaluated.

2.2.3.1 Tritium Breeding Potential

In order to assess the impact of tritium breeding performance upon the lithium resource requirement, a breeding evaluation has been made for several blanket systems. As shown below, the STARFIRE $LiAlO_2$ (α-phase) blanket has been selected as the reference case. It is compared with several alternate designs including Li_2O blankets.

System	Breeder	Multiplier	Comments
A0	$LiAlO_2$	None	Maximum BR < 1
A1	$LiAlO_2$	Zr_5Pb_3	STARFIRE - reference case
A2	$LiAlO_2$	Be	
B0	Li_2O	None	Sufficient for BR > 1
B1	Li_2O	Zr_5Pb_3	
B2	Li_2O	Be	

The breeding performance is investigated in terms of: (1) intrinsic breeding capability without additional neutron multiplication; (2) breeding enhancement by use of a multiplier; and (3) breeding variation with ^6Li enrichment.

Figure 2.3 compares the tritium breeding ratios (BR's)* as a function of ^6Li enrichment. Several important observations can be made. The effect of a multiplier is very substantial and the breeding enhancement can amount to ~0.5/D-T source. In fact, the $LiAlO_2$ system results in a BR of only ~0.88 without multiplier even for the full breeding coverage case.** The breeding amplification by beryllium is ~0.2/D-T greater than that by Zr_5Pb_3 for the Li_2O systems, and slightly less than 0.2/D-T for the $LiAlO_2$ systems. Although the use of the beryllium multiplier may involve a beryllium resource problem and an additional design complexity, such a design could lead to an appreciable reduction in the lithium resource requirement.

The breeding characteristics of Li_2O with ^6Li enrichment are quite different from those of $LiAlO_2$. The Li_2O systems, for instance, exhibit almost monotonic breeding decreases as ^6Li is enriched. This trend is particularly enhanced when no multiplier is used. On the other hand, the $LiAlO_2$ BR shows a significant increase with enrichment up to ~30%, beyond which the BR becomes quite insensitive to the enrichment. For example, the STARFIRE design which employs the $LiAlO_2$ breeder with a ^6Li enrichment of 60% along with the Zr_5Pb_3 multiplier results in a decrease in BR of only ~0.01 when the enrichment is lowered to 30%. The penalty for such a marginal breeding gain is not trivial, from the standpoint of resource requirements, as will be shown shortly. It is important, however, to note that the ^6Li enrichment must be high enough not to allow potential breeding deterioration and/or stoicheometric breeder compound instability due to possible high ^6Li burnup.

---

*Breeding ratio (BR) is defined as the number of tritium atoms formed per fusion reaction.

**The case in which all sections of the torus considered contain breeding material and do not include any major penetrations such as limiters.

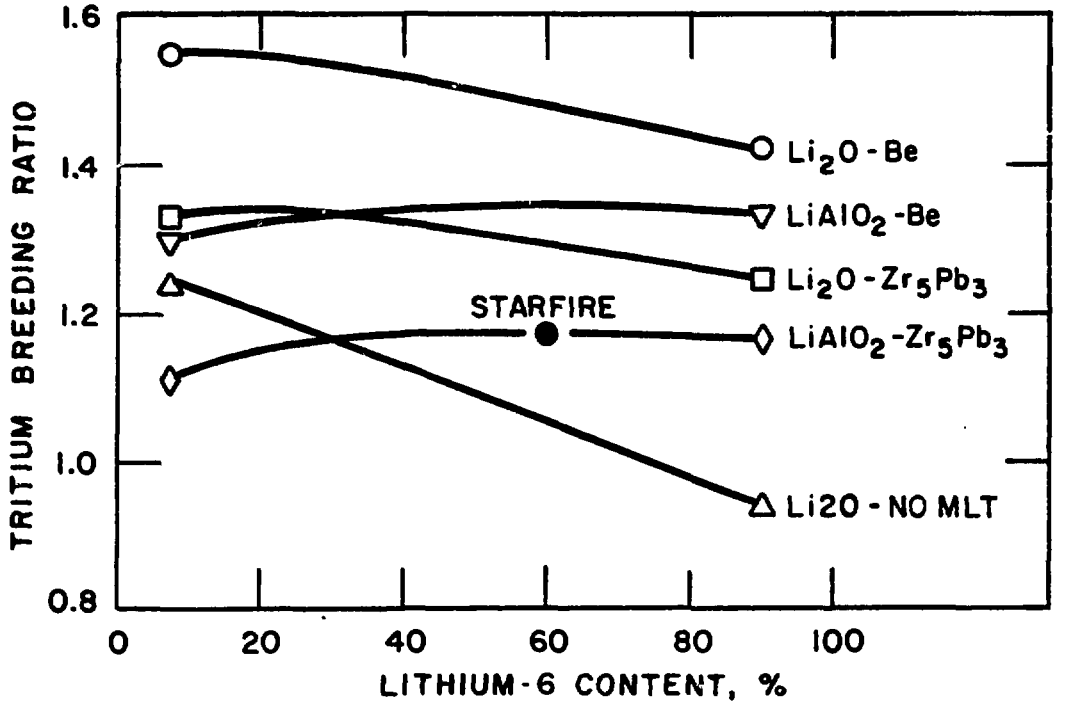

Fig. 2.3. Effect of ^6Li enrichment on tritium breeding ratio. ("No MLT" designates no multiplier.)

2.2.3.2 Lithium Resource Requirement and Availability

Figure 2.4 illustrates the impact of the selection of breeder material and its ^6Li enrichment on the lithium resource requirement. Plotted in the figure is the total (natural) lithium requirements for the 1000-GWe fusion economy (corresponding to ~833 STARFIRE plants) over 40 y (at a plant availability factor of 0.75) without any breeder material recycling. Note that STARFIRE is designed to generate a thermal power of 4000 MW and an electric power of 1200 MW. In addition, it is assumed that one-sixth of the blanket sectors is scheduled to be removed annually from the reactor for replacement. The lithium requirements shown in Fig. 2.4, thus, are for the lithium supplies necessary for a 30,000-GWe-y power generation (or equivalently 100,000 GWth-y) based on the STARFIRE model under the assumption of no breeder recycling.

The availability of natural lithium is somewhat uncertain at present since there exist significantly large differences in the assessments made by several lithium specialists. Rhinehammer [RHINEHAMMER] notes that the major differences in resource projections appear to result from assumption variables and the manner of handling data (e.g., criteria used in categorization of lithium, optimism in evaluating lithium deposits, etc.). The values for the U.S. reserves and U.S. resources presented in Fig. 2.4 are based on the findings by the NRC Lithium Subpanel [EVANS]. The lithium reserves in the U.S. include two lithium categories: Class A - reserves proved by systematic exploration; and Class B - reserves indicated by limited exposures and/or exploration. On the other hand, the U.S. lithium resources consist of: Class C - resources inferred on geological evidence; and Class D - quantities largely known but economic extraction probably dependent upon marketing of co-products. The U.S. reserves and U.S. resources of lithium thus estimated amount to ~4.2×10^5 Mg and 3.1×10^6 Mg respectively. It is noted that the projected lithium resources (3.1×10^6 Mg) should be considered conservative since the estimates do not take into account undeveloped or unproven sources of lithium. The demand and pricing for lithium have not encouraged exploration and development. There is disagreement with resource figures and one specialist [KUNASZ] insists that the Lithium Subpanel numbers must be multiplied by a large factor to reach a correct understanding of future availability of lithium.

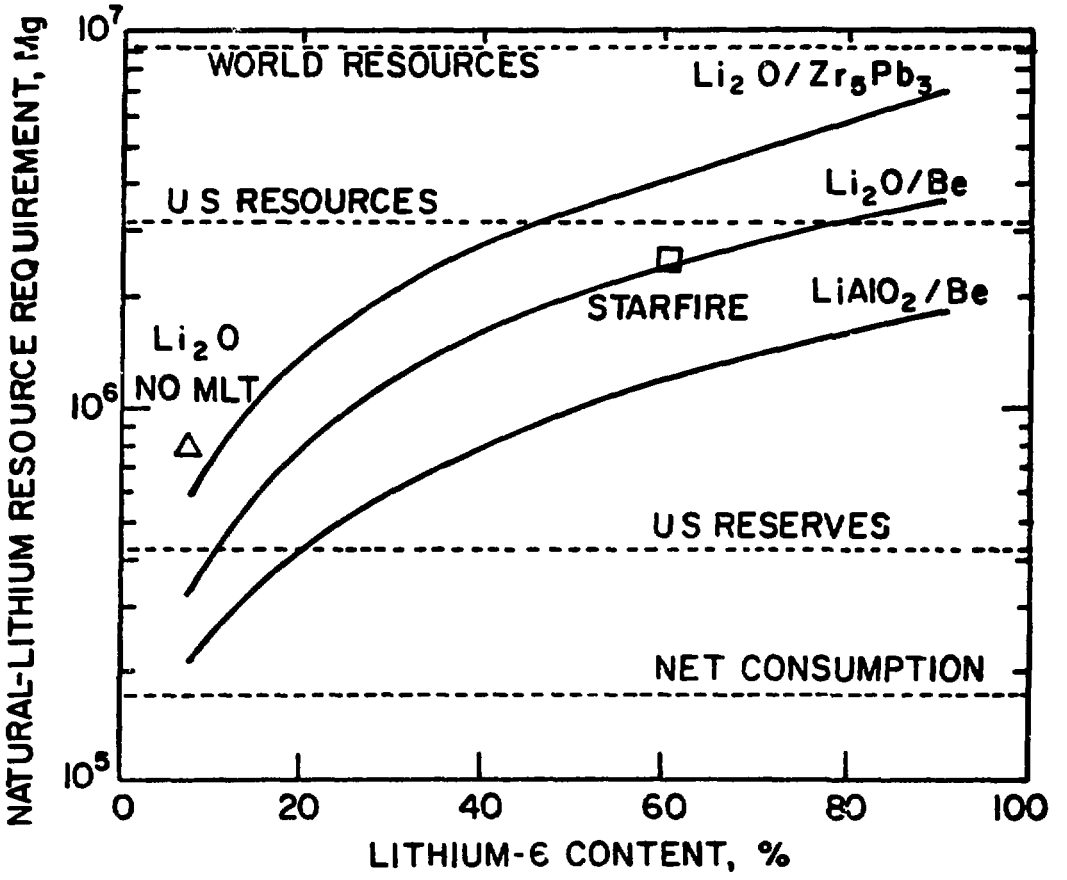

Fig. 2.4. Impact of selection of solid breeder and its ^6Li enrichment on lithium resource requirement.

Little is known about lithium resources worldwide (particularly the eastern hemisphere). However, according to Rhinehammer large undetermined deposits of lithium are forecasted for Canada and Chile. For example, it has been estimated that one salt basin of the Salar de Atacama in Chile may equal the known recoverable resources in the U.S. as estimated by the NRC Lithium Subpanel. In the present study, the value of worldwide resources is taken from the STARFIRE study, i.e. ~9.2×10^6 Mg. This value compares favorably with Norton's evaluation [NORTON] of ~1.4×10^7 Mg and is ~30% higher than the total western world reserves of ~7.1×10^6 Mg reported by Rhinehammer [RHINEHAMMER].

It is reported that the oceans contain 2.5×10^{14} kg of lithium [RHINEHAMMER]. The nominal lithium concentration is 0.2 ppm and economic recovery from such low concentrations may not be achievable. Preliminary production cost estimates have indicated a cost of lithium extraction from sea water of at least twice the current lithium selling price.

As shown in Fig. 2.4 most of the fusion systems investigated require more lithium than the U.S. reserves and depend upon the availability of the U.S. resources, provided that none of the breeder materials used are recycled. For example, using the reference STARFIRE system in a 1000-GWe economy (corresponding to ~833 STARFIRE reactors) will require ~80% of the total U.S. resources or about six times the total U.S. reserves. Even the Li_2O breeder blanket design without multiplier (which employs natural lithium) requires a lithium supply of ~8.1×10^5 Mg which is a factor of approximately two greater than the U.S. reserves.

The use of a neutron multiplier can substantially decrease the lithium resource requirement for both Li_2O and $LiAlO_2$ systems. The natural lithium Li_2O system with the beryllium multiplier, for instance, requires an amount of lithium which is only 40% of that without a multiplier and 50% of that with the Zr_5Pb_3 multiplier. From the lithium resource requirement, therefore, there appears to be an incentive to employ a neutron multiplier (most preferably beryllium) along with the Li_2O breeder, even if the Li_2O system can yield enough tritium without multiplier aid. It is worthwhile to note that the Li_2O systems contain more lithium than the $LiAlO_2$ systems in spite of the higher breeding capability in the Li_2O systems. This

is simply because of the substantially higher lithium density in Li_2O (ρ_{Li} = 0.94 g/cc) than in $LiAlO_2$ (ρ_{Li} = 0.36 g/cc).

The burnup rate of lithium atoms that is required to sustain a given fusion power production is, in general, insensitive to the blanket performance, and hence to the blanket design concept. Many fusion blanket design studies [JUNG-1980B], show a total energy yield of ~21 MeV (including the 3.5 MeV alpha energy) per D-T fusion event. Therefore, the energy production of 10^5 GWth-y (or 3×10^4 GWe-y) studied in Fig. 2.4 requires a total lithium burnup of $\sim 10^{33}$ atoms. When all of the tritium production is assumed to be undertaken by the $^6Li(n,\alpha)t$ reaction, the above lithium burnup corresponds to a natural-lithium requirement of $\sim 1.6 \times 10^5$ Mg. This value is shown in Fig. 2.4 under the "Net Consumption" label. The result of Fig. 2.4 clearly indicates that a large quantity of lithium resources is wasted compared to what is actually required if the breeder material recycling is not undertaken. Such a penalty appears to rapidly increase with ^6Li enrichment which is likely to be an absolute necessity for the viability of any ternary ceramic breeder concept using a neutron multiplier.

It should be noted that cumulative lithium demands of both conventional and battery uses are estimated to amount to ~30% of the U.S. domestic resources by 2010 and ~70% by the year 2040 [RHINEHAMMER]. In consequence, it is expected that by 2050 the lithium requirements for fusion reactors may become strongly competitive with these other energy uses for lithium. Although the ^7Li tails from isotopic enrichment plants for some fusion reactors can be utilized for the conventional and battery energy uses, the continual construction of such fusion reactors will eventually use up all ^6Li resources available in the U.S. (which is only $\sim 2.0 \times 10^5$ Mg) and will strongly impact the competitive lithium market.

The previous discussion only emphasizes the need for recovering and reusing the lithium from the fusion reactor blankets. The net consumption of ^6Li in the 1000 GWe fusion power economy is approximately 12 Mg per reactor over the reactor lifetime of 40 y at 75% availability or $\sim 10^4$ Mg of ^6Li for the 833 reactors, only about 5% of the currently identified lithium resources in the United States.

2.2.3.3 Breeder Activation

As shown in Fig. 2.4, the demand for the lithium inventory requirement might be unacceptably high if the breeder material could not be recycled. The ease of recycling or reprocessing depends largely on the level of residual activation in the breeder material. Figure 2.5 compares the breeder activations with and without inclusion of the respective trace elements shown in Table 2.3. The result clearly indicates the importance of impurity activation in considerations of post-irradiation breeder handling. In fact, the Li_2O activation shown in Fig. 2-5 is due solely to trace elements, since the activation associated with Li_2O itself decays completely within a few minutes after discharge from the reactor. Even for $LiAlO_2$, in which the primary constituent, aluminum, becomes a major activation source, inclusion of the trace elements increases the radioactivity level by two to three orders of magnitude relative to the pure $LiAlO_2$ radioactivity, over the entire time span relevant for the waste management. It is noted that the activation levels indicated in Fig. 2.5 are not as high as those of structural material activation (as will be shown later), but are sufficiently high to require care during any reprocessing.

As shown in Figs. 2.6 and 2.7 three trace elements, potassium, iron, and nickel, are the most important in such reprocessing considerations. In addition, copper in Li_2O, and molybdenum and aluminum itself in $LiAlO_2$ are the important elements to be taken into consideration.

Tables 2.4 and 2.5 show the isotopic breakdown of radioactivity concentration for Li_2O and α-$LiAlO_2$, respectively. The isotopes listed are limited to those which have a radioactivity concentration greater than 10^{-10} Ci/cc at 1 y after shutdown. For the sake of comparison, the maximum permissible concentration (MPC) value is also listed for each isotope. The MPC values that are taken from Column 1, Table II of Appendix B in NRC-10CFR20 [10CFR20], indicate the highest MPC values among those shown in the Appendix and correspond to the maximum allowable concentration in air.

It is noticed that there exist several activation trends common to the two breeder materials examined. The highest activation (other than those of the primary constituents) is contributed by ^{39}Ar ($T_{1/2}$ = 269 y,

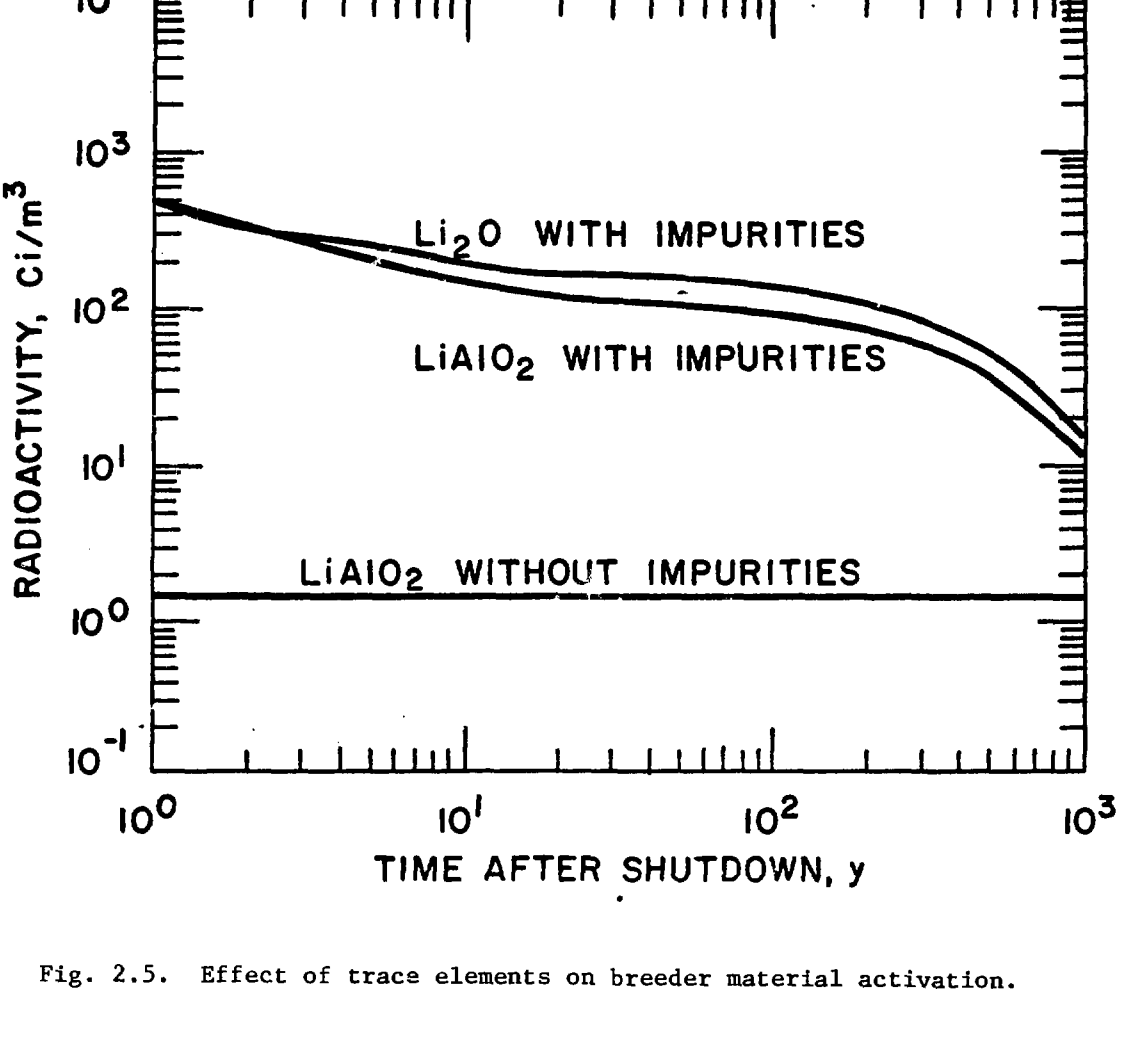

Fig. 2.5. Effect of trace elements on breeder material activation.

Table 2.3. Trace Element Composition of Breeder Materials

Trace Element	Li_2O[a]		α-$LiAlO_2$[b]	
	wt %	atom/b-cm[c]	wt %	atom/b-cm[c]
Be			0.001	2.27(-6)
B			0.001	1.89(-6)
Na	0.066	3.48(-5)	0.005	4.46(-6)
Al	0.002	8.99(-7)		
Si	0.001	4.32(-7)		
P			0.05	3.31(-5)
K	0.111	3.44(-5)	0.05	2.62(-5)
Ca	0.029	8.76(-6)	0.003	1.53(-6)
Ti			0.003	1.28(-6)
V			0.003	1.21(-6)
Cr			0.003	1.18(-6)
Mn	0.002	4.42(-7)	0.001	3.73(-7)
Fe	0.006	1.30(-6)	0.003	1.10(-6)
Co			0.003	1.04(-6)
Ni	0.002	4.13(-7)	0.002	6.98(-7)
Cu	0.0006	1.15(-7)		
Zn			0.05	1.57(-5)
As			0.05	1.37(-5)
Sr			0.10	2.34(-5)
Zr			0.01	2.25(-6)
Mo			0.003	6.41(-7)
Ag			0.001	1.90(-7)
Cd			0.01	1.82(-6)
Sn			0.003	5.18(-7)
Sb			0.01	1.68(-6)
Ba			0.01	1.49(-6)
Pb	0.008	4.68(-7)	0.001	9.89(-8)
Bi			0.001	9.80(-8)
Density (g/cc)	2.01		3.40	

[a] Ref. 37 [TAKAHASHI].

[b] Ref. 38 [CLEMMER].

[c] atom/b-cm = 10^{24} × atom/cc.

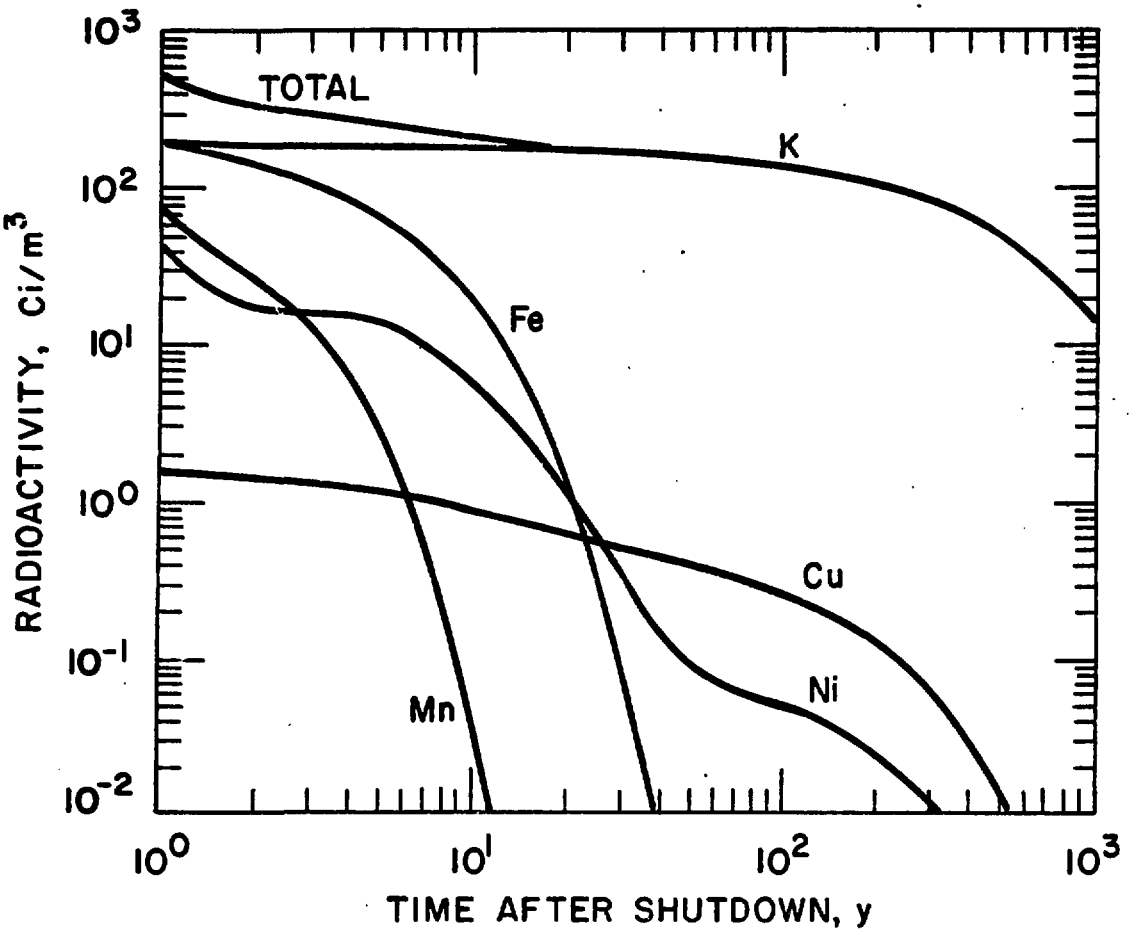

Fig. 2.6. The elemental impurity contribution to the Li_2O activation.

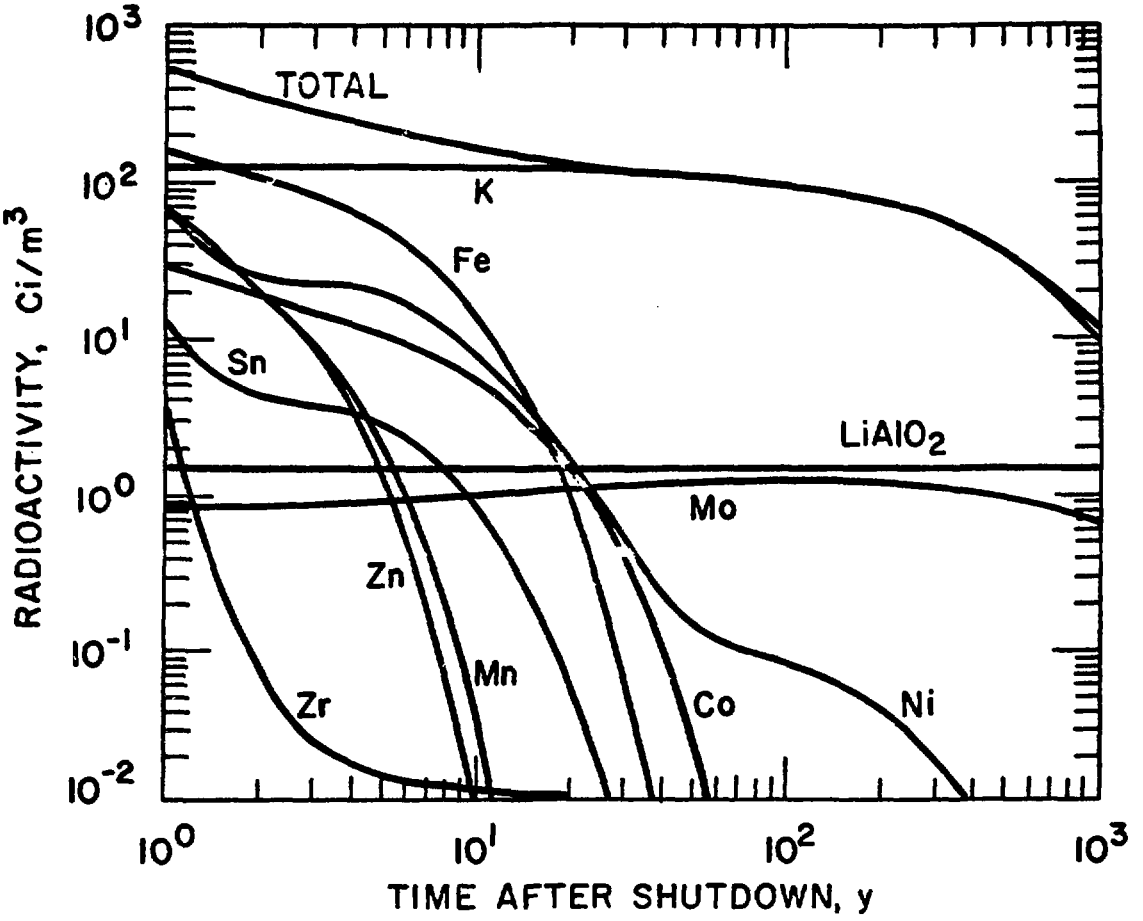

Fig. 2.7. The elemental contribution to the $LiAlO_2$ activation.

Table 2-4. Isotopic Contribution of Li_2O Breeder Activation Radioactivity Concentration (Ci/cc)

Isotope	Primary Parent	Time After Shutdown (y)					MPC[a]
		0	1	10	100	1000	
^{36}Cl	K	8.6(-8)[b]	8.6(-8)	8.6(-8)	8.6(-8)	8.6(-8)	8.0(-16)
^{39}Ar	K	1.9(-4)	1.9(-4)	1.8(-4)	1.4(-4)	1.4(-5)	(c)
^{54}Mn	Mn/Fe	2.2(-4)	9.5(-5)	4.8(-8)	(d)	---	1.0(-15)
^{55}Fe	Fe	2.7(-4)	2.1(-4)	1.9(-5)	---	---	3.0(-14)
^{57}Co	Ni	3.0(-5)	1.2(-5)	2.5(-9)	---	---	6.0(-15)
^{58}Co	Ni	1.2(-4)	3.4(-6)	---	---	---	2.0(-15)
^{60}Co	Ni	1.4(-5)	1.2(-5)	3.7(-6)	2.5(-11)	---	3.0(-16)
^{59}Ni	Ni	1.2(-10)	1.2(-10)	1.2(-10)	1.2(-10)	1.2(-10)	2.0(-14)
^{63}Ni	Ni/Cu	7.0(-7)	7.0(-7)	6.5(-7)	3.3(-7)	3.7(-10)	2.0(-8)
^{203}Hg	Pb	8.4(-8)	3.7(-10)	---	---	---	2.0(-15)
^{204}Tl	Pb	4.4(-9)	3.7(-9)	8.1(-10)	---	---	9.0(-16)

(a) The lower of the soluble or unsoluble values.

(b) Read as 8.6×10^{-8}.

(c) 1×10^{-16} Ci/cc.

(d) Less than MPC.

Table 2.5. Isotopic Contribution of α-$LiAlO_2$ Breeder Activation Radioactivity Concentration (Ci/cc)

Isotope	Primary Parent	Time After Shutdown (y)					MPC[a]
		0	1	10	100	1000	
^{26}Al	Al	1.5(-6)[b]	1.5(-6)	1.5(-6)	1.5(-6)	1.5(-6)	(c)
^{36}Cl	K	6.0(-8)	6.0(-8)	6.0(-8)	6.0(-8)	6.0(-8)	8.0(-16)
^{39}Ar	K	1.2(-4)	1.2(-4)	1.2(-4)	9.5(-5)	9.4(-6)	(c)
^{45}Ca	Ca/Ti	1.5(-5)	3.2(-6)	3.4(-12)	(d)	---	1.0(-15)
^{46}Sc	Ti	2.6(-5)	1.3(-6)	---	---	---	8.0(-16)
^{49}V	V/Cr	5.0(-6)	2.3(-6)	2.3(-9)	---	---	(c)
^{54}Mn	Mn/Fe	1.6(-4)	7.1(-5)	3.6(-8)	---	---	1.0(-15)
^{55}Fe	Fe	2.2(-4)	1.7(-4)	1.6(-5)	---	---	3.0(-14)
^{60}Co	Co/Ni	4.0(-5)	3.5(-5)	1.1(-5)	7.3(-11)	---	3.0(-16)
^{59}Ni	Ni	2.0(-10)	2.0(-10)	2.0(-10)	2.0(-10)	2.0(-10)	2.0(-14)
^{63}Ni	Ni	2.0(-7)	1.9(-7)	1.8(-7)	9.2 (-8)	1.0(-10)	2.0(-15)
^{65}Zn	Zn	1.9(-4)	6.6(-5)	6.1(-9)	---	---	2.0(-15)
^{89}Sr	Zr	2.4(-6)	2.0(-8)	---	---	---	3.0(-16)
^{90}Sr	Zr	7.9(-9)	7.7(-9)	6.2(-9)	6.6(-10)	---	3.0(-17)
^{90}Y	Zr	2.4(-5)	7.7(-9)	6.2(-9)	6.6(-10)	---	3.0(-15)
^{88}Zr	Mo	4.0(-8)	2.0(-9)	---	---	---	(c)
^{93}Zr	Zr/Mo	8.3(-10)	8.3(-10)	8.3(-10)	8.3(-10)	8.3(-10)	4.0(-15)
^{93m}Nb	Mo	7.2(-8)	9.9(-8)	2.9(-7)	5.8(-7)	3.1(-7)	4.0(-15)
^{94}Nb	Mo/Nb	3.1(-10)	3.1(-10)	3.1(-10)	3.1(-10)	3.0(-10)	(c)
^{93}Mo	Mo	7.2(-7)	7.2(-7)	7.1(-7)	6.7(-7)	3.6(-7)	(c)
^{99}Tc	Mo	3.1(-9)	3.2(-9)	3.2(-9)	3.2(-9)	3.1(-9)	2.0(-15)
^{113}Sn	Sn	2.7(-6)	3.0(-7)	---	---	---	2.0(-15)
^{123}Sn	Sn	3.8(-5)	5.0(-6)	6.1(-14)	---	---	(c)
^{125}Sb	Sn	1.0(-5)	8.0(-6)	8.0(-6)	---	---	9.0(-16)
^{204}Tl	Pb	8.7(-10)	7.4(-10)	1.6(-10)	---	---	9.0(-16)

[a] The lower of the soluble or insoluble values.

[b] Read as 1.5×10^{-6}.

[c] 1×10^{-16} Ci/cc.

[d] Less than MPC.

β-decay with no γ emission) induced from the potassium impurity. The radioactivity of this isotope is extremely high when compared to its MPC values and shows an insignificant decay even at 1000 y after reactor shutdown. Two nickel radioisotopes, ^{63}Ni (100 y, β^-/no γ) and ^{59}Ni (7.5×10^4 y, EC, β^+/no γ) are also commonly induced from the nickel impurity. Note that the ^{63}Ni activation is to some extent contributed by the copper impurity in the case of Li_2O.

One of the more serious breeder activations is observed in $LiAlO_2$ due to the presence of the zirconium and molybdenum impurities. These two elements yield the following nuclides:

^{89}Sr (51 d, β^-/γ [0.91 MeV])

^{90}Sr (29 y, β^-/no γ)

^{90}Y (64 h, β^-/γ[2.2 MeV])

^{93}Zr (1.5×10^6 y, β^-/no γ)

^{93m}Nb (17 y, IT/γ [30 keV])

^{94}Nb (2.0×10^4 y, β^-/γ [0.70 MeV, 0.87 MeV])

^{93}Mo (3.5×10^3 y, EC/no γ)

^{99}Tc (2.1×10^5 y, β^-/γ [90 keV])

The total radioactivity of these isotopes amounts to ~4.9 kCi at reactor shutdown or a specific radioactivity of ~2.7×10^{-5} Ci/cm^3 (~1.2 μCi/Wth). The radioactivity at shutdown due to these mid-Z number isotopes is dominated by the ^{90}Y contributing ~90% (~1.1 μCi/Wth) of the total activation of these isotopes. The high ^{90}Y concentration is a result of the direct formation of ^{90}Y. In about one month the ^{90}Y activity has diminished by a factor of ~1000 so that ^{90}Y is no longer a major activity. At longer decay times, ^{93m}Nb and ^{93}Mo become most important among these mid-Z isotopes. The subsequent slow reduction of the ^{90}Y radioactivity despite its short half-life (64 h) stems from the presence of ^{90}Sr ($T_{1/2}$ = 29 y) decaying to ^{90}Y. Strontium-90 is one of the most toxic radioisotopes (as reflected by its very low MPC value listed in Table 2-5) and the radioactivity level amounts to ~1.7×10^{-8} Ci/cm^3 (~7.0×10^{-4} μCi/Wth) at shutdown. It is desirable that special caution is exercised for the elimination or significant reduction of

the two trace elements, zirconium and molybdenum, upon fabrication of the $LiAlO_2$ breeder in order to minimize the radioactivity content at shutdown. Particular emphasis should be placed on the fact that many of these mid-Z number radioisotopes emit gamma rays with energies ranging from ~30 keV to ~2.2 MeV. In fact, these gamma rays are the primary source contributing to the biological dose, other than the main gamma ray of ~1.8 MeV which is emitted from the primary constituent radioisotope, ^{26}Al in $LiAlO_2$.

Table 2.6 shows the importance of four key impurity elements, potassium, nickel, zirconium, and molybdenum, to the long-term radioisotope generation in terms of a unit content (atomic parts per million, appm) of each element. It is observed that the importance of potassium and nickel is more or less identical in the two breeder materials. Although the Li_2O breeder examined in the present study does not include zirconium nor molybdenum, it is conceivable that these elements could be introduced in Li_2O during its manufacture. Table 2.6 provides useful information related to the allowed levels of impurity in order for the breeder activation to remain tolerable.

Table 2.6. Radioactive Content[a] of Important Long-Term Radioisotopes in Solid Breeders, (Ci/cc)/appm of Impurity

Radioisotope	Primary Parent Impurity	Li_2O	α-$LiAlO_2$	MPC
^{36}Cl	K	3.0(-10)[b]	2.9(-10)	8.0(-16)
^{39}Ar	K	5.0(-8)	4.5(-8)	(c)
^{59}Ni	Ni	3.5(-11)	3.6(-11)	2.0(-14)
^{63}Ni	Ni(Cu)	8.5(-11)	1.8(-11)	2.0(-15)
^{93}Zr	Zr,Mo	---	3.6(-11)	4.0(-15)
^{93m}Nb	Mo	---	6.0(-8)	4.0(-15)
^{94}Nb	Mo,Zr	---	1.3(-11)	(c)
^{93}Mo	Mo	---	7.0(-8)	(c)
^{99}Tc	Mo	---	6.0(-10)	2.0(-15)

(a) Radioactivity concentration at 1000 y after shutdown.

(b) Read as 3.0×10^{-10}.

(c) 1×10^{-16} Ci/cc.

The elemental contribution in terms of different activation measures, such as biological dose and biological hazard potential, still remains to be studied. Such a study will be essential for the development of optimum waste management because the activation shown in Figs. 2.6 and 2.7 consists of quite different decay modes. In fact, some of the high activation, such as that induced by potassium, possesses only beta-decay activation.

2.2.4 Potential Low-Actication Structural Materials

2.2.4.1 General Remarks

The austenitic stainless steels, which have been one of the most widely studied structural materials for fusion reactor applications [BAKER], possess several salient advantages in comparison with other candidate structural materials. The austenitic stainless steels have been used extensively in fission reactor application and therefore a substantial technology base has been generated. Fabrication procedures have been well developed and the ease of fabrication and welding should lead to increased reliability of structural components. One of the unfavorable characteristics of austenitic stainless steels, however, relates to their high neutron-induced activation. The fact that primary structural materials represent the major radioactive source of fusion reactors provides the incentive for exploring reactor designs based on the use of inherently low-activation structural materials other than austenitic stainless steels. It should be noted, however, that the selection of structural materials depends upon many other design considerations and cannot be derived solely from the activation standpoint. The selection of structural materials as well as the remaining blanket/shield materials must evolve from an overall design tradeoff involving various considerations for reactor performance, engineering feasibility, material development, material compatibility, plasma-wall interaction, etc. In particular, the requirement of self-sufficient tritium fuel production in fusion reactor blankets strongly influences the choice of reactor materials depending upon the chemical and physical properties of breeder materials selected. Use of a liquid metal or liquid compound breeder, for instance, limits the selection of structural materials to a class of alloys such as austenitic stainless steels, niobium-base alloys, and vanadium-base alloys because of the need for corrosion resistance against the breeder under the anticipated operating conditions. In addition, the

choice of coolant materials, which is also affected to a large extent, by the breeder selection, further narrows the choice of candidate structural materials to those that are compatible with the coolant. The situation observed here clearly indicates that the selection of low-activation structural materials must be coordinated with the complex matrix of possible combinations of first-wall/blanket materials.

Another important design consideration in connection with the choice of low-activation primary structural materials is the nuclear performance of the radiation shielding design [JUNG-1981]. The importance of the shielding design is two-fold, in that (1) the reactor power depends substantially on the inboard shield design for toroidal reactors; and (2) the reactor accessibility (at short post-shutdown times) depends on the outboard shield design. The importance of the outboard shielding design is further emphasized by the fact that more than 90% of the radioactive material inventory is present in the outboard shield and reactor components external to the shield, such as TF magnets and penetration shields [JUNG-1980A]. An important strategy for the low-activation fusion reactor development is, therefore, to select the structural material that assures the overall design credibility and conforms with various design aspects of the relevant technical areas.

2.2.4.2 Proposed Low-Activation Structural Materials

An in-depth study [SMITH-1979] has been carried out for a blanket/shield design in which a vanadium-base alloy is employed along with a liquid lithium breeder/coolant. The results indicate that there is substantial potential for minimization of long-term activation induced in a fusion power reactor. Vanadium-base alloys are among the most radiation-damage resistant alloys known. They maintain good strength properties to relatively high reactor operating temperatures. The major concerns regarding the use of vanadium alloys are the lack of information on fabricability, particularly welding, and on the effects of atmospheric environment during fabrication and operation. A second-generation research alloy, V15Cr5Ti, is expected to alleviate the swelling and fabricability problems and to improve the elevated temperature creep properties because of the increased chromium and titanium contents.

The NUWMAK [BADGER] design explores the possible use titanium-base alloy structural material along with the lithium-lead eutectic (62% Li + 38% Pb) as the tritium breeding and heat transfer material. Titanium-base alloys, which have been used extensively in the aircraft industry because of their relatively light weight and high strength at moderate temperatures have several favorable properties for fusion reactor applications, such as good fabricability, high strength, long fatigue life, good corrosion resistance against water coolant, etc. The major concerns regarding the use of titanium alloys for fusion reactor applications are the lack of data on radiation effects with respect to swelling and mechanical properties, the potential for hydrogen embrittlement, and the strength deterioration at elevated operating temperatures. Although the titanium alloys can be regarded as intrinsically low-activation structural materials, it is worthwhile to note that most of the high-strength commercial alloys contain molybdenum or other alloying elements that have been shown in previous discussions to produce long-lived radioactive products.

Another class of possible low-activation structural materials is represented by low atomic number materials such as silicon carbide, carbon materials, and aluminum-base alloys. A first-wall/blanket design concept based on silicon carbide has been proposed [HOPKINS-1974] and is currently being investigated by GA Technologies [HOPKINS-1981]. The use of silicon carbide as the first-wall/blanket material is clearly motivated by the associated low long-lived activation, and potentially small temperature rise caused by the decay heat. Although silicon carbide possesses some other favorable properties such as the excellent thermal shock resistance, good thermal fatigue resistance, and inherently low X-ray attenuation coefficient, it must be recognized, as Hopkins states, that the primary problem associated with the application of low-Z ceramic materials for structural purposes is their almost complete lack of ductility. The design and fabrication of relatively large-size components, that can withstand tensile loads, requires relatively detailed stress analysis, careful control of fabrication processes, and extensive quality tests under conditions closely approximating expected operating conditions.

Powell and his colleagues [POWELL-1974] proposed the use of aluminum structures in fusion reactor blankets. The tritium breeding

materials are restricted to solid lithium compounds such as LiAl and $LiAlO_2$ from the material compatibility standpoint. A detailed analysis of the potential problems for the aluminum structures has been conducted in a recent U.S.-INTOR design study [STACEY] in the context of a comparison with stainless steel first-wall design. The study shows that the primary concern regarding the use of aluminum structures, in particular in their first-wall application, is associated with the limited temperature capabilities of these alloys due to the strength limitations at elevated temperatures. The study also reveals that there is almost no data base for aluminum alloys irradiated at temperatures above ~60°C.

2.2.4.3 Comparative Study of Potential Low-Activation Structural Materials

This section presents a comparison of neutron-induced activation for several proposed low-activation structural materials for use in fusion reactor designs. The primary objective is to identify the generic characteristics of each candidate and thereby provide a comparison of low-activation reactor designs. Three first-wall/blanket structural materials, a vanadium-base alloy (V15Cr5Ti), a titanium-base alloy (Ti6Al4V) and an aluminum-base alloy (Al-6063) are analyzed and compared with a PCA stainless steel case, based on a geometrical model of the STARFIRE design. All of these four designs use liquid lithium as the coolant as well as the tritium breeding medium. The reference STARFIRE design in which the α-$LiAlO_2$ breeder, light-water coolant and PCA structure are employed is also added to the comparative study. The material compositions of the four alloys used for the analysis are presented in Table 2.7.

It is noted that certain class of alloys may not be compatible with the liquid-lithium breeder/coolant concept from a materials point of view. It is expected, however, that those material combinations described above afford a consistent intercomparison of the low activation characteristics by identifying the essential effect of the structural material choice. It is also noted that in the liquid-lithium systems studied, the material compositions of some of the STARFIRE components have been replaced as follows:

Table 2.7. Structural Material Compositions

Element	PCA Stainless Steel		V15Cr5Ti		Ti6Al4V		Al-6063	
	wt %	atom/b-cm	wt %	atom/b-cm	wt %	atom/b-cm	wt-%	atom/b-cm
B	0.005	2.188(-5)						
C	0.05	1.971(-4)	0.02	6.118(-5)	0.01	2.267(-5)		
N	0.01	3.380(-5)	0.05	1.311(-4)	0.008	1.555(-5)		
O			0.05	1.148(-4)	0.065	1.106(-4)		
Mg							0.68	4.548(-4)
Al	0.03	5.264(-5)	0.004	5.447(-6)	6.0	6.056(-3)	98.07	5.913(-2)
Si	0.5	8.427(-4)	0.03	3.924(-5)	0.01	9.695(-6)	0.40	2.316(-4)
P	0.01	1.528(-5)	0.01	1.186(-5)				
S	0.005	7.382(-6)						
Ti	0.30	2.965(-4)	5.00	2.835(-3)	89.84	5.108(-2)	0.10	3.396(-5)
V	0.10	9.292(-5)	79.794	5.754(-2)	4.0	2.138(-3)		
Cr	14.0	1.274(-2)	15.00	1.060(-2)	0.01	5.236(-6)	0.10	3.128(-5)
Mn	2.0	1.723(-3)			0.0025	1.239(-6)	0.10	2.961(-5)
Fe	64.88	5.499(-2)	0.01	6.578(-6)	0.02	9.752(-6)	0.35	1.019(-4)
Co	0.03	2.410(-5)						
Ni	16.0	1.290(-2)	0.001	6.258(-7)	0.005	2.319(-6)		
Cu	0.02	1.490(-5)			0.01	4.286(-6)	0.10	2.560(-5)
Zn							0.10	2.488(-5)
Ga			0.01	5.270(-6)				
As	0.02	1.264(-5)						
Nb	0.03	1.529(-5)	0.0025	4.996(-7)				
Mo	2.0	9.868(-10)	0.008	3.164(-6)	0.005	1.419(-6)		
Sn					0.01	2.294(-6)		
Ta	0.01	5.453(-10)	0.003	1.149(-6)				
W			0.0075	1.523(-7)				
Density (g/cc)	7.86		6.10		4.52		2.70	

- First wall: 27% Li + 50% structure
- Multiplier, Second wall, Blanket: 93.45% Li + 6.55% structure
- Reflector: 5% Li + 5% structure + 90% C
- Coolant header: 18% Li + 2.5% structure

The geometrical dimensions have been kept unchanged. In consequence, the tritium breeding performance exhibits a significant variation from one system to another as shown in Table 2.8, indicating that the liquid-lithium designs studied here are not necessarily optimized in terms of tritium production. In general, the tritium breeding capability of the liquid-lithium systems is appreciably larger than that of the solid breeder system (i.e., the STARFIRE design). Therefore, the actual requirement of breeding blanket zone thicknesses for the liquid-lithium systems is expected to be much smaller than that used in the present analysis (52 cm). The blanket optimization for each alloy design and the following activation analysis for the optimized system remain to be further investigated.

Table 2.8. A Comparison of Tritium Breeding Ratios[a]

Case	Structure	Breeder	Coolant	TBR
1 (Ref.)	PCA	α-$LiAlO_2$	H_2O	1.17
2	PCA	Li	Li	1.45
3	V15Cr5Ti	Li	Li	1.55
4	Ti6Al4V	Li	Li	1.56
5	Al-6063	Li	Li	1.50

[a]Based on 100% breeding coverage by the outboard blanket.

The discussion presented in this section is limited to the ouboard breeding blanket region where most of the activation is expected to exist in terms of the blanket volume and the level of activation. The activation is examined with regard to two radioactivity measures: (1) volumetric radioactivity (Ci/cc); and (2) contact biological dose (rem/h) due to decay gamma emission (see Appendix A).

2.2.4.4 Comparison Based on Radioactivity Concentration

Figure 2-8 shows a comparison of the candidate structural materials in terms of radioactivity concentration (Ci/cc) as a function of time after reactor shutdown following a six-year reactor operation at a plant availability of 75% (i.e., equivalent to an integral neutron wall load of 18 MW-y/m^2). This integral wall load corresponds to the maximum neutron fluence expected before the regular replacement of each first-wall/blanket module. Due to the large amount of ^{55}Fe isotope ($T_{1/2}$ = 2.7 y, EC decay/no gamma emission), the PCA systems (STARFIRE and Li/PCA) exhibit much higher radioactivity levels than the other cases. The activation decay rates in these PCA systems become lower beyond ~50 y after shutdown, reflecting the contribution from ^{63}Ni (100 y, β^-/no γ) induced by the $^{62}Ni(n,\gamma)$ and $^{64}Ni(n,2n)$ reactions. The difference between the STARFIRE and Li/PCA systems is due largely to the fact that the average blanket radioactivity of the latter system includes contributions from the second-wall and multiplier zones in STARFIRE, which are exposed to much higher neutron fluxes. Normally, the soft neutron spectrum system characteristic of STARFIRE strongly enhances the neutron capture reactions such as $^{54}Fe(n,\gamma)$ and $^{62}Ni(n,\gamma)$ in comparison with the hard neutron-spectrum system represented by the Li/PCA design. In fact, as shown in Table 2.9, the first-wall radioactivity of Li/PCA is not higher but instead lower than that of STARFIRE. The difference is magnified particularly at long post-shutdown times when the ^{63}Ni activation becomes dominant.

Table 2.9. A Comparison of First-Wall Radioactivity (Ci/cc)

Case	System	Time After Shutdown (y)					
		0	1	10	100	500	1000
1	STARFIRE	3.82(2)[a]	1.39(2)	1.24(1)	1.37(-1)	1.72(-2)	8.16(-3)
2	Li/PCA	3.52(2)	1.38(2)	1.20(1)	2.85(-2)	8.87(-3)	5.69(-3)
3	Li/V15Cr5Ti	1.03(2)	4.29(0)	5.59(-3)	8.16(-5)	7.37(-5)	6.71(-5)
4	Li/Ti6Al4V	8.51(1)	2.93(0)	2.67(-3)	1.14(-4)	2.84(-5)	2.05(-5)
5	Li/Al-6063	1.25(2)	3.03(-1)	2.06(-2)	5.34(-4)	7.35(-5)	5.03(-5)

[a]Read as 3.82 × 10^2.

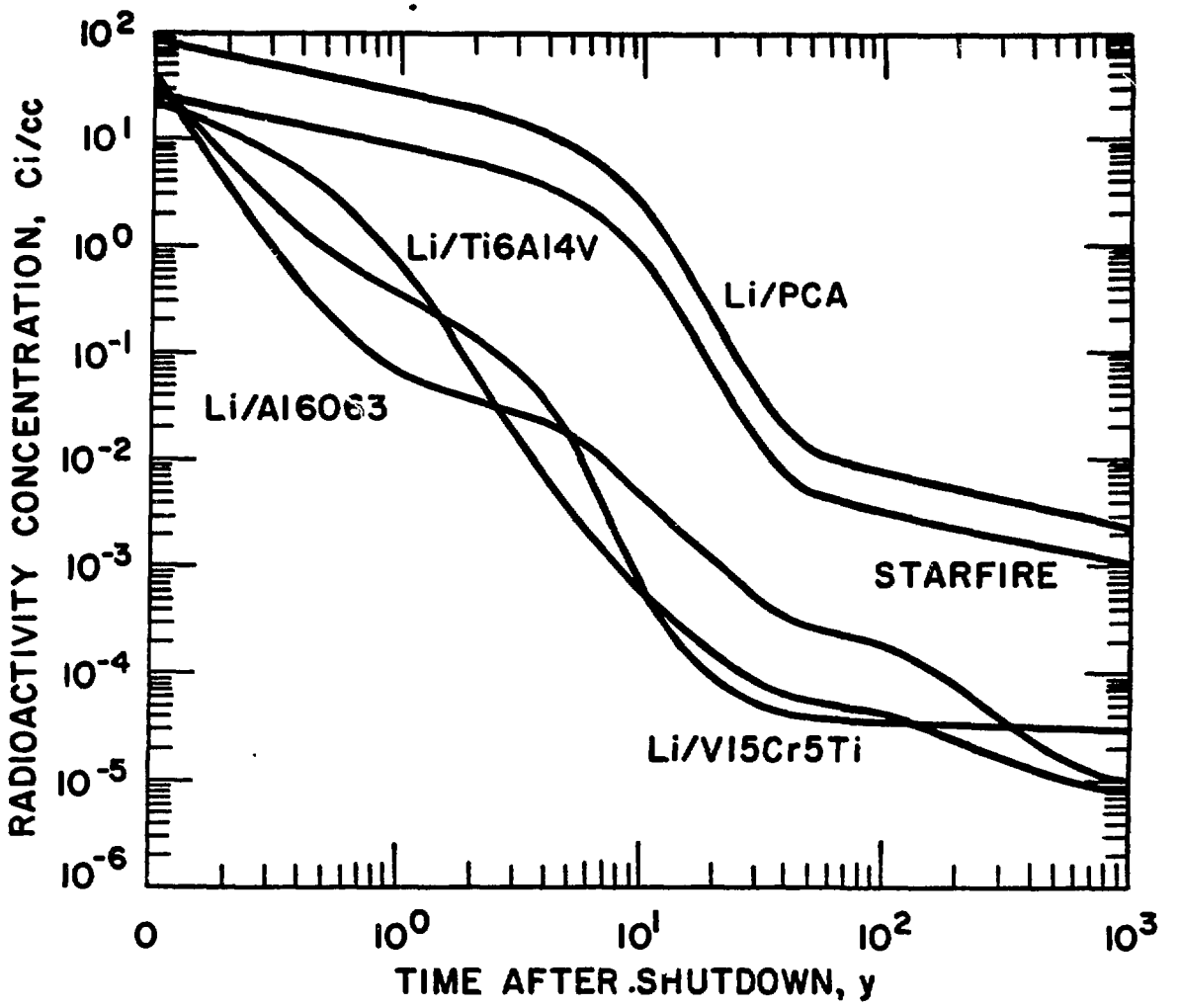

Fig. 2.8. Impact of structural material selection upon STARFIRE/blanket activation. Total exposure: 18 MW-y/m^2, 6-y operation.

The V15Cr5Ti system activation exhibits a continually sharp decrease as short-lived isotopes such as ^{45}Ca (165 d, β^-/γ), ^{49}V (330 d, EC/no γ), and ^{51}Cr (27.7 d, EC/γ) decay until the ^{93m}Nb (13.6 y, IT/γ) isotope becomes significant at ~10 y after shutdown. At times greater than ~10 y, ^{14}C (5700 y, β^-/no γ) is the most dominant radioactive isotope and its concentration is only on the order of $10Ci/m^3$. The primary gamma emission from the V15Cr5Ti system after ~100 y, is mostly associated with the ^{93m}Nb isotope produced from an impurity activation of ^{93}Mo (3500 y, EC/no γ). It is noted, however, that as will be shown later, the associated biological dose in V15Cr5Ti is controlled by the ^{94}Nb content at times greater than 100 y.

The Ti6Al4V activation steeply decreases 10 y after shutdown due primarily to the fast decay of ^{24}Na (15 h, β^-/γ), ^{45}Ca, ^{46}Sc (84 d, β^-/γ), and ^{48}Sc (44 h, β^-/γ). After 10 y, the radioactivity in this alloy is dictated by the impurity activation products such as ^{63}Ni, ^{93m}Nb, ^{93}Mo, and ^{14}C. Because of the similarity of the isotope contents in Ti6Al4V and V15Cr5Ti alloys, the general trend of activation variation in both systems is almost identical, keeping about a factor of 2-3 difference at most in their absolute magnitudes over the entire time span under consideration.

The high purity aluminum alloy Al-6063 [ALUMINUM ASSOCIATION] contains alloying elements, magnesium (~0.7 wt %) and silicon (~0.4 wt %), and impurities iron (3-4 wppm), copper (~0.1 wppm), manganese (~0.1 wppm), and zinc (~0.1 wppm). This aluminum alloy shows a rapid activity decrease as the primary short-lived isotopes ^{24}Na, ^{27}Mg (9.5 m, β^-/γ), and ^{28}Al (2.2 m, β^-/γ) decay. The major contribution up to ~30 y after shutdown comes from ^{54}Mn (312 d, EC/γ), and ^{55}Fe. Beyond ~30 y the dominant isotopes are ^{63}Ni, which in this case is produced mainly by the $^{63}Cu(n,p)$ reaction, and the constituent-element activation of ^{26}Al (7.2×10^5y, β^+/EC/γ). Note that the aluminum activation level in the neighborhood of 10-100 y after reactor shutdown is somewhat dependent upon the specific alloy chosen. Many of the wrought aluminum alloys ranging from 2000 to 7000 [SONDERS] series, for instance, include manganese by 0.2-1.2 wt %, compared to ~0.1 wppm used in Al-6063. Copper also is a typical constituent element found in most of the aluminum alloys except for the 5000 series. For example, the activation level of a 2000-series aluminum alloy, Al-2024, is within only an order of magnitude of the PCA activation level in the neighborhood of the time interval under question.

The result of Fig. 2.8 indicates a substantial advantage inherent in fusion reactor designs based on low-activation alloys such as V15Cr5Ti, Ti6Al4V, and Al-6063 from the standpoint of the radioactivity concentration measure (Ci/cc). The difference in the radioactivity between such an alloy system and an austenitic stainless steel system is anticipated to amount to a factor of 1000 or more during the post-shutdown interval relevant for radwaste management (5-20 y after shutdown).

2.2.4.5 Comparison Based on Contact Biological Dose and Material Recycling Considerations

In general, radioactive waste can be defined by different waste categories, and various categories have been proposed. For radwaste management a suitable waste classification would be: (1) materials adequate for shallow land burial as specified in 10CFR61; and (2) materials requiring a more stringent confinement (e.g., deep geologic medium). On the other hand, for recycling considerations, the biological dose that reflects the human interaction with radiation would be a more pertinent measure.

The contact biological dose as calculated here appears to be a convenient basis for comparing the relative radiation doses that might be expected from these materials.

This section presents an assessment of the contact biological dose for the five first-wall/blanket designs studied in the previous section. The assessment method is, as described in Appendix A, based on a spherical model of 1-m diameter. The contact biological dose is defined as the maximum dose equivalent for normally incident gamma rays on a slab of tissue 30 cm thick [PROF10], which contacts to the 1-m diameter sphere. This gamma flux to dose-equivalent conversion is based on the Clairborne and Truby method [CLAIRBORNE] for dose evaluation in a slab phantom. In the present analysis, it is assumed that the decay gamma source is uniformly distributed in the test piece of the 1-m diameter sphere.

Figure 2.9 compares the biological dose as a function of post-shutdown time. It is noticed that all of the systems studied show dose rates substantially higher than 2.5 mrem/h and, in fact, level off in the vicinity of 100 y after shutdown. Up to 100 y, the PCA systems (Li/PCA and

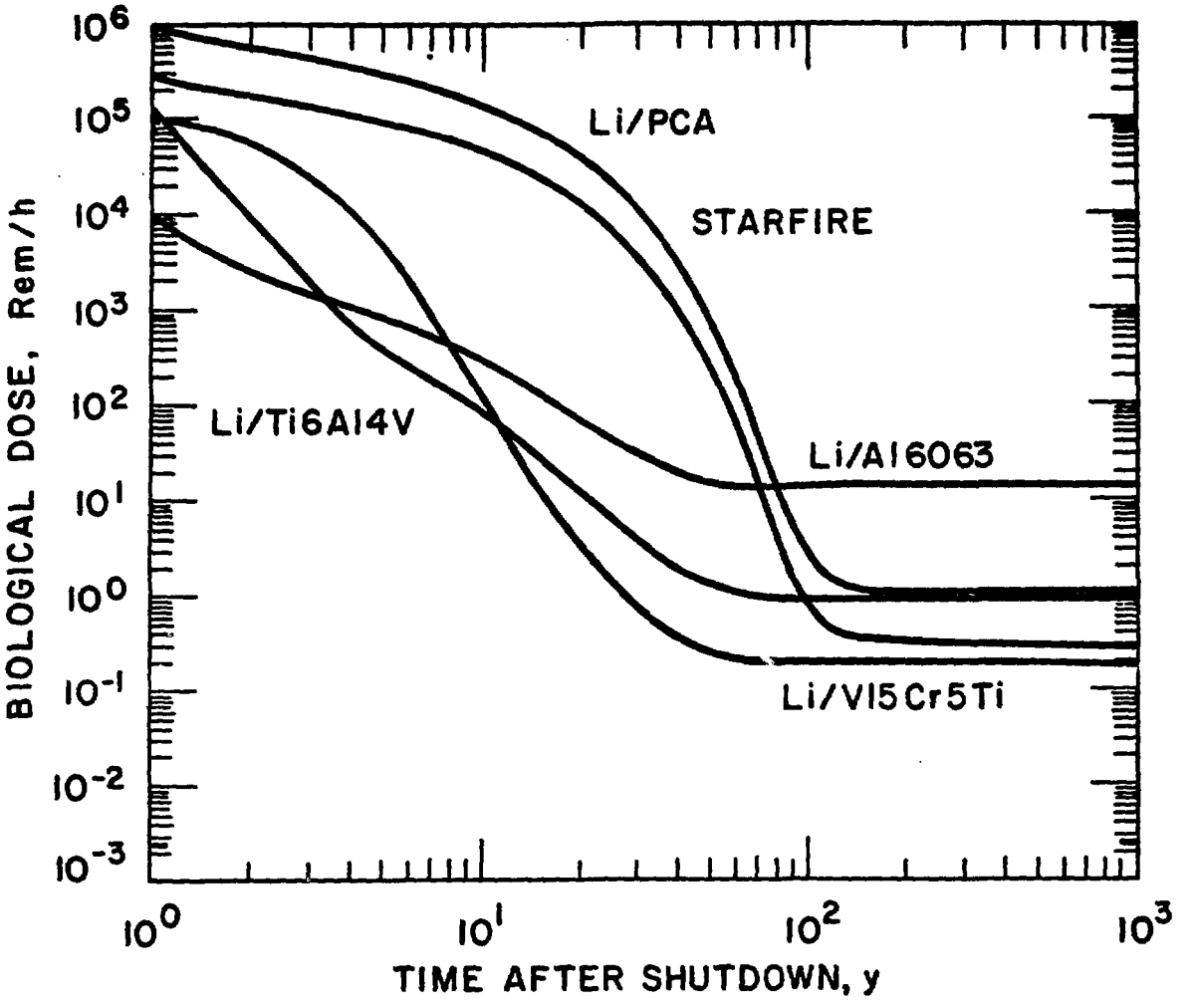

Fig. 2.9. Impact of structural materials selection upon STARFIRE/blanket biological dose.

STARFIRE) exhibit again the highest biological dose, maintaining a substantial difference from the other structure doses. This result is more or less identical with what was shown in Fig. 2.8 regarding the radioactivity concentration. Beyond ~100 y after shutdown the result of Fig. 2.9 shows a vivid contrast to that of Fig. 2.8. As shown in Fig. 2.10 approximately 90% of the PCA dose (in Li/PCA) after 100-y decay is contributed by the two major gamma rays, ~0.703 MeV and ~0.871 MeV of ^{94}Nb. Another major gamma emitter at the post-shutdown times under question is ^{93m}Nb which undergoes the internal transition to the ground-state ^{93}Nb, emitting a gamma ray of ~30 keV. Elimination of ^{94}Nb and ^{93m}Nb from the PCA activation leads to a dose reduction by almost three orders of magnitude, resulting in a dose rate of only ~4 mrem/h. The PCA activation in terms of curies can be drastically decreased by eliminating only ^{93m}Nb or the molybdenum impurity which induces ^{93m}Nb through the ^{94}Mo(n,2n)^{93}Mo and ^{92}Mo(n,γ)^{93}Mo reactions leading in turn, to ^{93m}Nb via the beta decay. However, from the dose standpoint, the importance of ^{93m}Nb is less appreciable because of its relatively soft gamma-ray emission associated with ^{93m}Nb. The ^{94}Nb dose is almost equally contributed by the niobium [e.g., via ^{93}Nb(n,γ)] and molybdenum [e.g., via ^{94}Mo(n,p) and ^{95}(n,d)] impurities. Thus, from the dose standpoint the elimination (or drastic reduction) of these elements is crucial to the minimization of the long-term PCA activation. In fact, the PCA dose becomes completely negligible at long post-shutdown times, after these elements are removed because the residual dose (shown by the curve labeled "No ^{94}Nb+ ^{93m}Nb in Fig. 2.10 consists solely of ^{92}Nb (~0.560 MeV and 0.934 MeV gamma emission) that is also generated by niobium and molybdenum.

As shown in Figs. 2.11 and 2.12 the activations of the Ti6Al4V and Al-6063 alloys are both dominated by the primary constituent activation, ^{26}Al itself. The most dominant gamma-ray energy of ~1.81 MeV emitted from ^{26}Al renders these alloy doses very high. The ^{26}Al dose in Ti6Al4V is ~0.9 rem/h after 100-y decay whereas the ^{26}Al dose in Al-6063 amounts to as much as ~14 rem/h. The relatively high dose in Al-6063 reflects the larger aluminum content in Al-6063 and the less-effective self-shielding of this "light" alloy. It should be noted that the Al-6063 activation observed here is more or less representative of all series of wrought aluminum alloys.

Figure 2.13 shows the importance of ^{94}Nb activation to the long-term dose of the V15Cr5Ti alloy. The long-term activation trend in

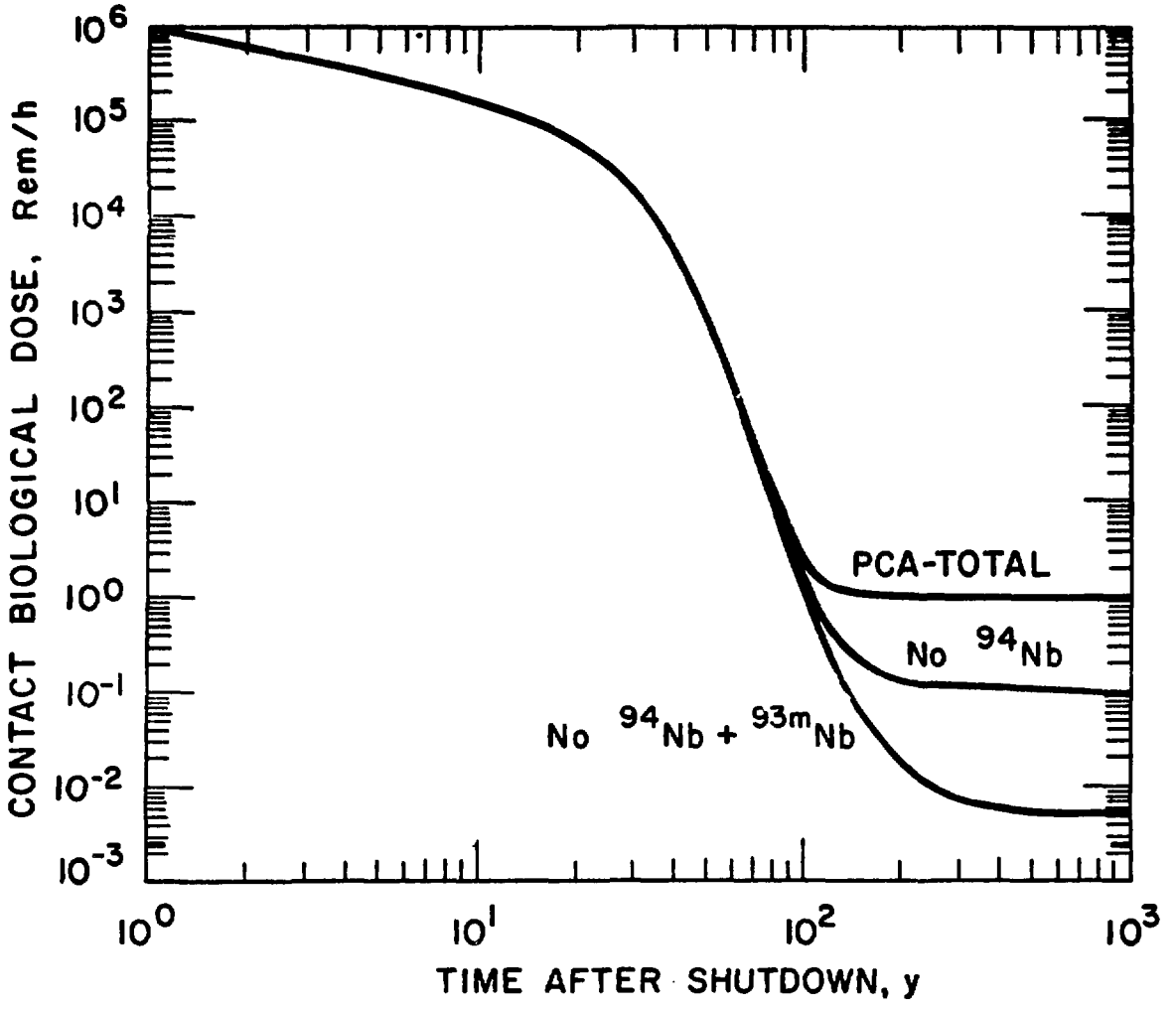

Fig. 2.10. PCA structure dose.

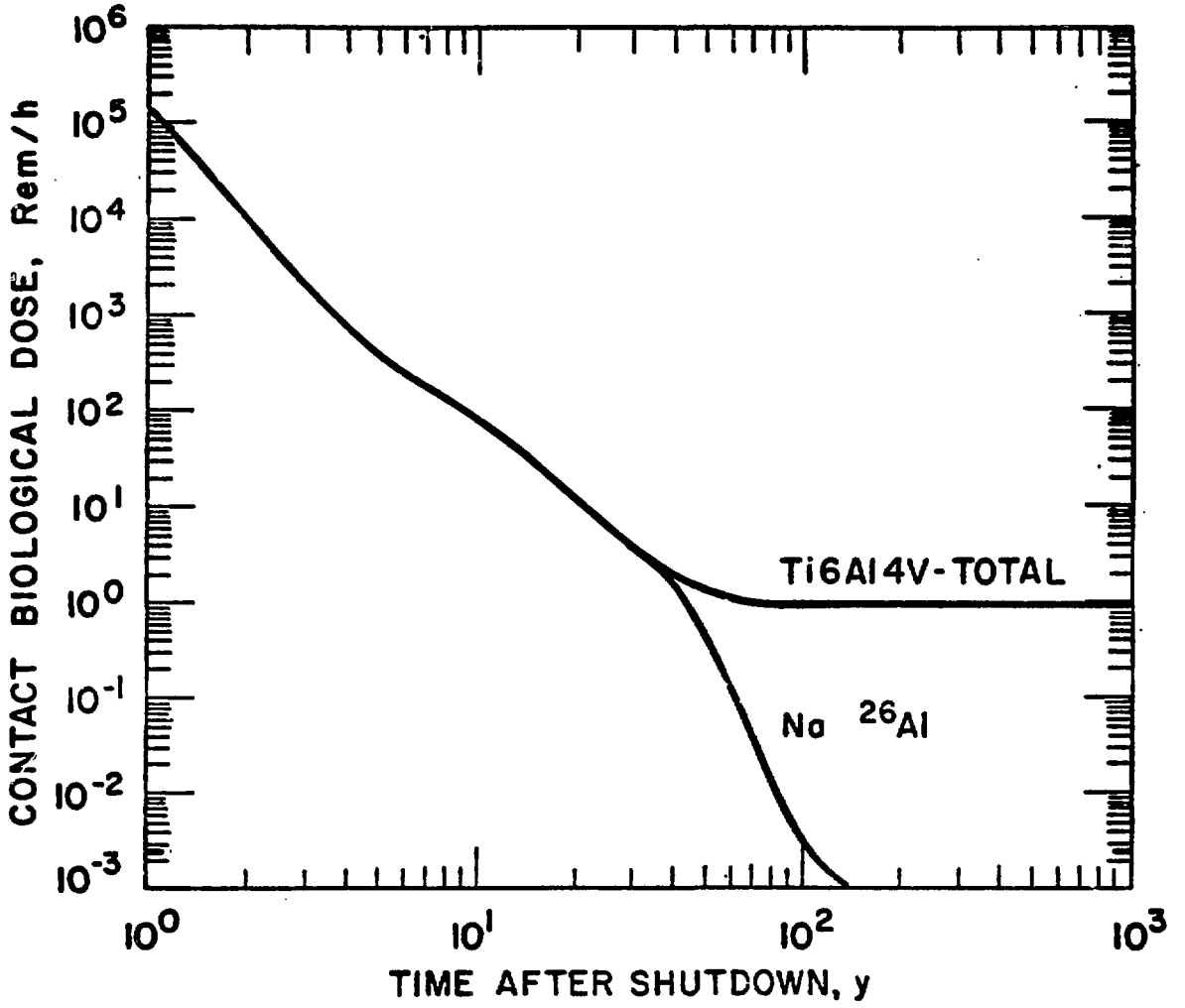

Fig. 2.11. T16A14V structure dose.

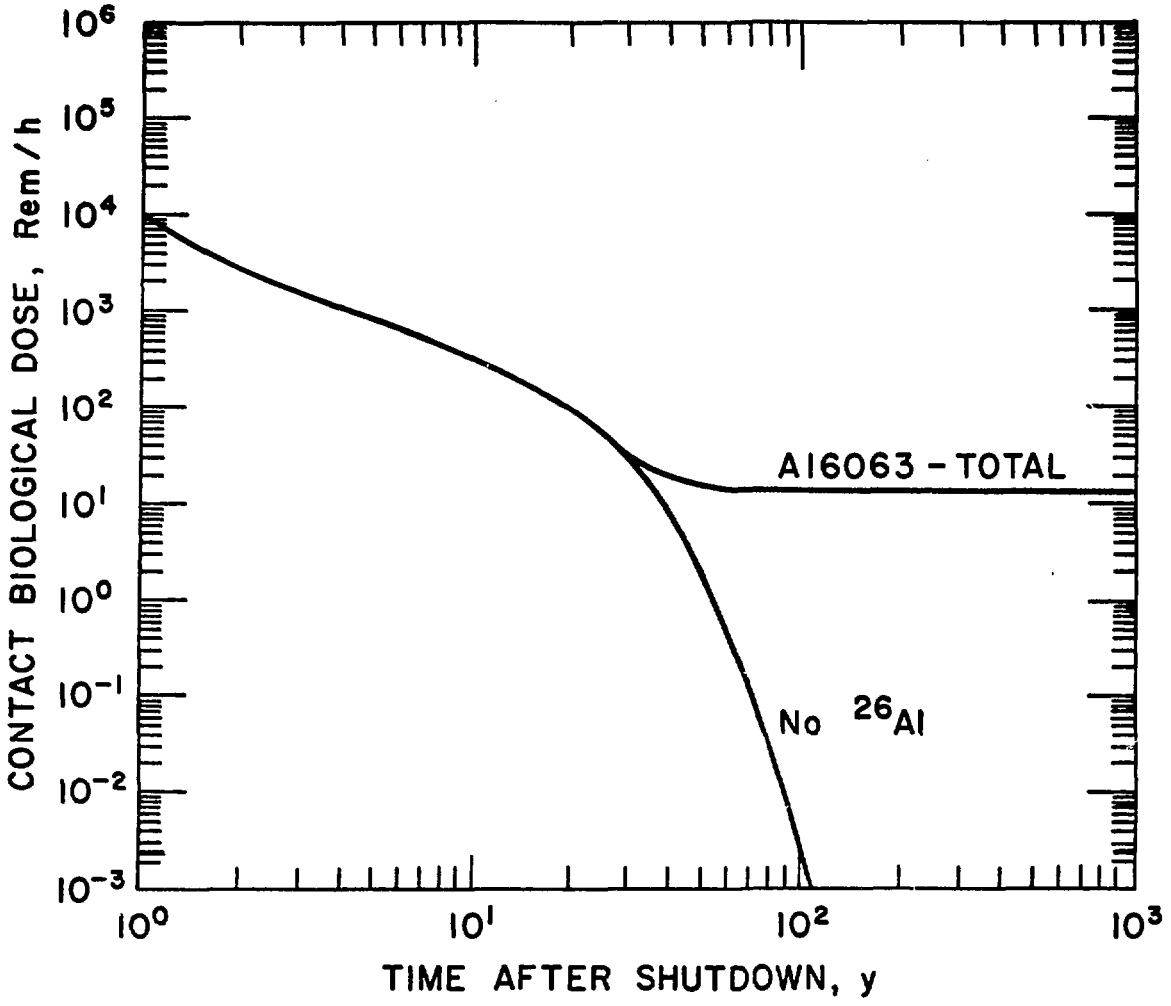

Fig. 2.12. Al-6063 structure dose.

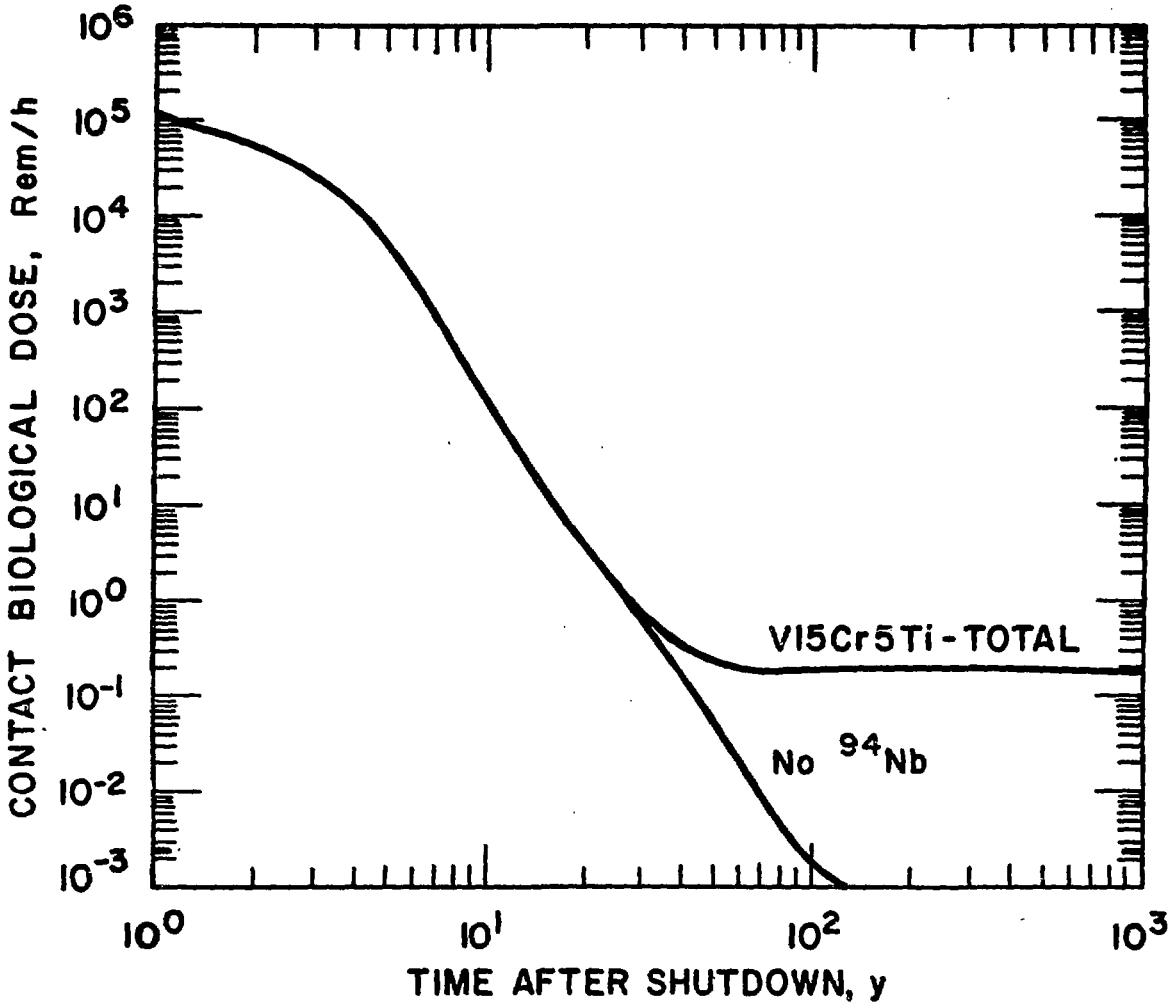

Fig. 2.13. V]5Cr5Ti structure dose for a 1-m sphere.

this alloy is very similar to that already described for the PCA alloy. In order to reduce the V15Cr5Ti dose to less than 2.5 mrem/h within ~100 y after shutdown, the elimination (or drastic curtailment) of both niobium (25 wppm in the present analysis) and molybdenum (80 wppm) is essential.

In summary, the V15Cr5Ti alloy and the PCA stainless steel are the only alloys for which one could realize a significant dose reduction possibly by some alloy purification. Elimination of the molybdenum and niobium impurities from these alloys before irradiation will render them very promising and attractive for fusion reactor applications from the standpoint of the minimization of long-term structural-material activation. On the other hand, the Al-6063 alloy (and all wrought aluminum alloys, in general) and Ti6Al4V alloy exhibit a very high dose rate even beyond ~100 y after shutdown, and are less attractive in terms of long-term radwaste management.

2.3 Comparison of Materials Handling for PCA and Vanadium Structural Materials

In making this comparison the STARFIRE reactor is the model for water-cooled reactors using stainless steel as a structural material. The handling of the PCA is compared with vanadium, a representative of the class of low activation alloys. In order to exploit the properties of vanadium, liquid lithium metal is used as the breeder and coolant for the fusion reactor. A brief description of these fusion reactors is given in Section 2.1.

In this discussion the activation of the PCA and vanadium structural materials and the disposal of these materials will be compared. For the low activation material vanadium, recycle of the material is also considered.

2.3.1 Assumptions

The basis for the discussion is the routine maintenance or periodic replacement of the torus sectors for both fusion reactors. First the disposition of the metallic structural materials including the first wall is considered and then a brief discussion is given of techniques for reprocessing the $LiAlO_2$ from the STARFIRE blanket.

Three options for handling the blanket structural materials are immediately apparent.

1. Recycle or reuse of the material,
2. Disposal and burial in shallow land burial, and
3. Disposal and burial under greater confinement.

Disposal of any radioactive material should take into consideration existing and proposed regulations. Regulations applied to shallow land burial are broadly applicable and are outlined in the 10 CFR 61, "Licensing Requirements for Land Disposal of Radioactive Wastes" [10 CFR 61]. The proposed 10 CFR 61 has been reviewed and comments have led to revision in the proposed table of limits. The most

recent values for limits applicable to shallow land burial are listed in Tables 2.10 and 2.11. It is emphasized that reference to regulations concerning the disposal of radioactive material serves only as a guide. While it is likely that these or similar regulations will be in force and applicable when the need to dispose of fusion reactor wastes arises, neither the magnitudes nor the scope implicit in these current regulations can be ensured to be applicable. It will be assumed as a working rule that procedures that are in accord with current regulations would probably be satisfactory at some future time, and waste streams not now in accord with current regulations will also be outside this domain at a future time.

There are three classes of wastes that are defined in 10 CFR 61, section 61.55. They are labeled Class A, B, and C and in general the packaging requirements are more stringent for the B and C wastes than for class A wastes. The radioactive content of the wastes from a fusion reactor plant will determine their subsequent disposition. If the radionuclide content is below the limits shown in Tables 2.10 and 2.11, the waste can be placed in shallow land burial. Material with a radioactive content that exceeds those limits is not generally acceptable for near-surface disposal.*

These are the only specified nuclides. If the radioactive wastes do not contain any of the radionuclides listed in Table 2.10, classification is determined based on the radionuclides in Table 2.11. If a nuclide is not listed in Table 2.11, it does not need to be considered in determining the waste class. If radioactive waste does not contain any nuclides listed in either Table 2.10 and 2.11, the waste is Class A.**

---

*NRC apparently has no plans to establish a "de minimis" category for radioactive wastes. Rather, it is the policy to grant exemptions from 10 CFR 61 on a specific waste stream basis [NUREG].

**There is one caution. In preparing these tables, the NRC reviewed the wastes that are currently available, primarily the fission products, activation products and transuranic elements derived from fission reactors. Some fusion activation products are undoubtedly covered in this list. But there may be one or two radionuclides that were not considered, in particular ^{26}Ar.

Table 2.10. Concentrations of Long-Lived Radionuclides for Establishing Waste Classification*

Radionuclide	Concentration Curies/cubic meter
C-14	8
C-14 in activated metal	80
Ni-59 in activated metal	220
Nb-94 in activated metal	0.2

*If the waste contains less than 0.1 the indicated concentration, the material is Class A. If the concentration exceeds 0.1 the indicated concentration, the material is Class C.

Table 2.11. Concentrations of Short-Lived Radionuclides for Establishing Waste Classification

Radionuclide	Concentration Curies/cubic meter		
	Column 1*	Column 2*	Column 3*
Total of all nuclides with less than 5 year half-life	700	**	**
H-3	40	**	**
Co-60	700	**	**
Ni-63	3.5	70	700
Ni-63 in activated metal	35	700	7000
Sr-90	0.04	150	7000

*Class A waste, if nuclide concentration in Column 1 is not exceeded.
Class B waste, if nuclide concentration is greater than value in Column 1, but less than that in Column 2.
Class C waste, if nuclide concentration is greater than value in Column 2, but less than that in Column 3.

**There are no limits established for these radionuclides in Class B or C wastes. Practical considerations such as the effects of external radiation and internal heat generation on transportation, handling, and disposal will limit the concentrations for these wastes. These wastes shall be Class B unless the concentrations of other nuclides in Table III-2 determine the waste to the Class C independent of these nuclides.

The classification of waste that contains a mixture of nuclides from both Table 2.10 and 2.11 is determined as follows. If the concentration of a nuclide listed in Table 2.10 is less than 0.1 times the value listed, the class shall be determined by the concentration of nuclides listed in Table 2.11. If the concentration of a nuclide listed in Table 2.10 exceeds 0.1 times the value listed, the waste shall be class C provided the concentrations of nuclides listed in Table 2.11 do not exceed the values shown in column 3 of Table 2.11.

For determining classification for waste that contains a mixture of radionuclides from one table, it is necessary to determine the sum of fractions by dividing each nuclide's concentration by the appropriate limit and adding the resulting values. The appropriate limits must all be taken from the same column of the same table. The sum of the fractions for the column must be less than 1.0 if the waste class is to be determined by that column. Example: A metallic waste contains ^{90}Sr in a concentration of 50 Ci/m^3 and ^{63}Ni in a concentration of 100 Ci/m^3. Since the concentrations both exceed the values in Column 1, Table 2.11, they must be compared to Column 2 values. The ^{90}Sr fraction is 50/150 = 0.33; the ^{63}Ni fraction is 100/700 = 0.14; the sum of the fractions = 0.47. Since the sum is less than 1.0, the waste is Class B.

It has been suggested [BAKER] that material is suited for reuse if the contact radiological dose rate is less than 2.5 mrem/hr in conformity with the applicable Federal Standards [10 CFR 20]. It should be clear, however, that reuse (or recycle) of materials is not limited to materials with radioactivity levels satisfactory for direct contact. There exists a large body of technology applicable to the handling and application of radioactive components where surface dose rates are significantly in excess of 2.5 mrem/h.

In evaluating the radioactive dose of a material, one measure used in the fusion reactor community has been the dose rate from a one meter sphere of metal containing the radioactivity [BOTTS-1978A]. The choice of a one-meter sphere for calculating dose rates appeared to be a matter of calculational convenience. Later calculations showed that

for PCA the surface dose rate for 1.5-2.0 MeV gamma radiation quickly saturated as a function of specimen diameter (Appendix A). In this case greater than 90% saturation was observed with a 0.5 m diameter specimen. The use of a one-meter sphere for calculating dose rates permits the calculation of an upper bound estimate without reference to the many geometries of the pieces to be recycled. Other calculations on geometry effects showed that for an infinite slab, saturation occurred at a slab thickness of 10 cm. For a 2 cm slab, the dose was approximately half the saturation value. The slab saturation dose rate was esentially the same as that for a one-meter sphere. The consequences of these results are that a) 1 m dia. sphere calculations yield saturated dose rates applicable to smaller spheres, b) substantial slab thickness geometries are also approximated by the 1 m dia. sphere data, and c) thin slab geometries that may be closest to practical fabrication and handling situations will probably show surface dose rates lower by modest factors (e.g., two) compared to the 1 m sphere data.

2.3.2 Source Terms

2.3.2.1 PCA/$LiAlO_2$

At yearly intervals, four sectors of the STARFIRE torus are removed and replaced with fresh sectors. The amount of material removed is given in Table 2.12. In the present evaluation only the disposition of the metals PCA and vanadium is considered. The elemental compositions of the metals PCA and the vanadium alloy are shown in Table 2.3. The elemental compositions of these materials control their radioactivity content after irradiation.

At the time of the annual routine maintenance, it is planned to remove the four sectors remotely, transfer them to a hot processing cell, and replace them with four new sectors. In the hot processing cell the sectors will be disassembled and various materials sorted and combined for storage, reprocessing or disposal. In this context it is useful to examine the radioactivity level of the PCA used in the

Table 2.12. Amounts of Material Removed from a STARFIRE Reactor Annually

Material	Amount Mg	Volume (m^3)
PCA (first wall)	4.8	0.6
PCA (second wall)	3.4	0.43
PCA (remainder)	66.9	8.53
Zr_5Pb_3	54.7	6.1
$LiAlO_2$	101.1	29.7
Graphite	27.3	17.0

structure of the sectors shown in Table 2.13. It is apparent that approximately 70% of the radioactivity is contained in the first and second walls with 11% of the mass of material. The specific nuclides responsible for the radioactivity are given as a function of time in Table 2.14.

Also of importance is the radioactive decay heat of the structural materials at time of removal from the reactor and as a function of time thereafter. These are important values because they help determine the handling that is required, i.e., whether active heat removal is required and how densely the material may be packed. The decay heat values for PCA are given in Table 2.15.

2.3.2.2 V15Cr5Ti

The design for the reactor using liquid metal as the coolant and breeder is similar to that of the STARFIRE with 24 removable sectors (Fig. 2.2). The basic system components consist of integral first-wall/breeder modules and shield segments. The reactor blanket/shield is divided into 24 wedge-shaped sectors that form the torus. Each sector is composed of 32 blanket modules (Fig. 2.2), a limiter and an RF grille section. Tritium is bred in the blanket modules filled and cooled with liquid lithium. The bred tritium is removed on-line by a low-capacity process operating on the circulating lithium. The reactor

Table 2.13. Radioactivity of PCA as a Function of Position in the Sector

Position	Amount		Radioactivity (Ci/cm^3)		Total Radioactivity (Ci) Discharged Annually	% of Total Ci
	Mg	m^3	0	1 y	at time 0	
1st wall	4.8	0.6	380	140	2.3×10^8	56
2nd wall	3.4	0.43	140	50	6.2×10^7	15
Inner blanket	3.3	0.42	41	14	1.7×10^7	4.2
Outer blanket	25.8	3.3	26	9	8.6×10^7	21
Reflector	7.5	0.95	3.4	0.6	3.2×10^6	0.8
Inner blk jacket	4.6	0.58	7.3	2.2	4.2×10^6	1.0
Outer blk jacket	20.3	2.6	2.1	0.4	5.5×10^6	1.3
Header	5.4	0.68	2.2	0.4	1.5×10^5	0.4
TOTAL	75.1	9.5			4.1×10^8	

Table 2.14. Radioactivity of First Wall for a Fusion Reactor Blanket Design with PCA/$LiAlO_2$

	Activity in PCA (Ci/cm^3)						
Time (y)	1	5	10	20	30	50	100
Total Activity (Ci/cm^3)	140	44	12	1.4	0.37	0.20	0.14
^{14}C 5400 y (no γ)	7.5×10^{-5}	7.5×10^{-5}	7.5×10^{-5}	7.5×10^{-5}	7.5×10^{-5}	7.4×10^{-5}	7.4×10^{-5}
^{26}Al 8×10^{5} y (1.83 MeV γ)	4.4×10^{-8}	4.4×10^{-8}	4.4×10^{-8}	4.4×10^{-8}	4.4×10^{-8}	4.4×10^{-8}	4.4×10^{-8}
^{45}Ca 150 d (no γ)	0.01	2.4×10^{-5}	1.1×10^{-8}	—	—	—	—
^{49}V 330 d (no γ)	0.3	0.01	2.6×10^{-4}	—	—	—	—
^{54}Mn 209 d (860 keV γ)	9.8	0.34	0.004	1.1×10^{-6}	2.4×10^{-10}	—	—
^{55}Fe 2.6 y (no γ)	120	41	11	0.75	0.05	2.5×10^{-4}	4.1×10^{-10}
^{57}Co 270 d (136, 122 keV γ)	4.7	0.11	0.001	—	—	—	—
^{58}Co 71 d (800 keV γ)	0.9	6×10^{-7}	—	—	—	—	—
^{60}Co 5.2 y (1.17, 1.33 MeV γ)	4.6	2.7	1.4	0.37	0.099	0.007	9.4×10^{-5}
^{63}Ni 100 y (no γ)	0.26	0.25	0.24	0.22	0.21	0.17	0.12
^{94}Nb 1.8×10^{4} y (875, 650 keV γ)	1.3×10^{-5}	1.3×10^{-5}	1.3×10^{-5}	1.3×10^{-5}	1.3×10^{-5}	1.3×10^{-5}	1.3×10^{-5}
^{93m}Nb 12 y (30 keV γ)	2.1×10^{-3}	3.0×10^{-3}	3.9×10^{-3}	5.2×10^{-3}	5.9×10^{-3}	6.5×10^{-3}	6.7×10^{-3}
^{93}Mo 3500 y (no γ)	8.3×10^{-3}	8.2×10^{-3}	8.2×10^{-3}	8.2×10^{-3}	8.1×10^{-3}	8.0×10^{-3}	7.8×10^{-3}

Table 2.15. Decay Heat as a Function of Time for the PCA from the STARFIRE (kW/m^3)

	Time After Reactor Shutdown (y)							
	0	1	5	10	20	30	50	100
First wall	811	73	24	10	2.4	0.63	5.3×10^{-2}	2.0×10^{-3}
Second wall	320	27	8.8	3.8	0.9	0.23	1.9×10^{-2}	8.6×10^{-4}
Inner blanket	90	8	2.6	1.1	0.26	6.7×10^{-2}	5.0×10^{-3}	1.5×10^{-4}
Outer blanket	57	5	1.6	0.7	0.16	4.2×10^{-2}	3.1×10^{-3}	9.6×10^{-5}
Reflector	10	0.2	6.7×10^{-2}	2.6×10^{-2}	6×10^{-3}	2.1×10^{-3}	7.8×10^{-4}	1.2×10^{-4}
Inner blk jacket	19	1.3	0.4	0.17	3.9×10^{-2}	1.0×10^{-2}	7.9×10^{-4}	4.6×10^{-5}
Outer blk jacket	6	0.1	3.4×10^{-2}	1.3×10^{-2}	2.8×10^{-3}	1.1×10^{-3}	5.3×10^{-4}	8.5×10^{-5}
Header	6	9.6×10^{-2}	3.1×10^{-2}	1.1×10^{-2}	2.4×10^{-3}	1.1×10^{-3}	6.3×10^{-4}	1.0×10^{-4}

contains 563 tonnes of vanadium in the first wall, blanket and reflector and 260 tonnes of a graphite reflector. The 332 tonnes of lithium are removed before sector disassembly. A significant difference between the use of PCA and V15Cr5Ti is that first wall lifetime is increased with the use of vanadium [ABDOU]. At present the most efficient way of capitalizing on the longer life time for vanadium is not clear, i.e., removing two sectors every year or removing four sectors at a time but at two year intervals. In the alternate years, only the cryogenic pumps would require maintenance. Aside from the mechanics of maintenance, an average of two sectors would require replacement annually. Since a multiplier is not required with a liquid lithium breeder and because the molten breeder can be removed before the sectors are removed, fewer materials are handled together. The amount of material handled annually is given in Table 2.16. A typical impurity content of the V15Cr5Ti alloy is given in Table 2.3.

At the time of removal for maintenance, the radioactivity of the structural material is given in Table 2.17. The decay of radioactivity in V15Cr5Ti is compared with that in PCA in Fig. 2.14. A more detailed description of the radioactivities is given in Table 2.18 which lists the specific radionuclides contributing to the radioactivity.

Table 2.16. Annual Amounts of Material Removed from a Lithium-Cooled Tokamak Reactor [STEVENS]

Material	Amount Mg	Volume (m^3)
Vanadium (first wall)	1.9	0.32
Vanadium (blanket)	35.0	5.83
Graphite (reflector)	22	13.7
Vanadium (reflector)	10	1.67
Vanadium (total)	46.9	7.82

Table 2.17. Specific Radioactivity of Structural Materials from Lithium-Cooled Tokamak Reactor

Time (y)	Activity (Ci/cm^3) 0	1	5	10	50	100
First wall	$1.0x10^{2}$	4.3	$2x10^{-1}$	$5.6x10^{-3}$	$9.3x10^{-5}$	$8.2x10^{-5}$
Blanket	$3.6x10^{1}$	$3.4x10^{-1}$	$1.5x10^{-2}$	$6.5x10^{-4}$	$4.0x10^{-5}$	$3.4x10^{-5}$
Reflector	$3.6x10^{1}$	$2.6x10^{-2}$	$6.7x10^{-4}$	$6.0x10^{-5}$	$1.8x10^{-5}$	$1.7x10^{-5}$

For the vanadium alloy, the radioactive decay heat is much less than that of the PCA. In this instance only the decay heat from the first wall is tabulated. The decay heat from material farther removed from the plasma will be less. These results are listed in Table 2.19.

2.3.3 Disposal Processes for PCA

2.3.3.1 Procedure

When the blanket sectors are removed from the torus during routine maintenance there is sufficient radioactive decay heat remaining (Table 2.15) so that forced cooling is required. At 12 hours after shutdown 2 MW of afterheat is being produced in each blanket sector. Thus, before any disassembly is undertaken the blanket sectors are cooled for 30 days until the afterheat can be readily handled by the hot cell system. After the cooling period, the sectors are separated into the segments. It may be advantageous to delay processing for about one year while heat and radioactivity releases decay.

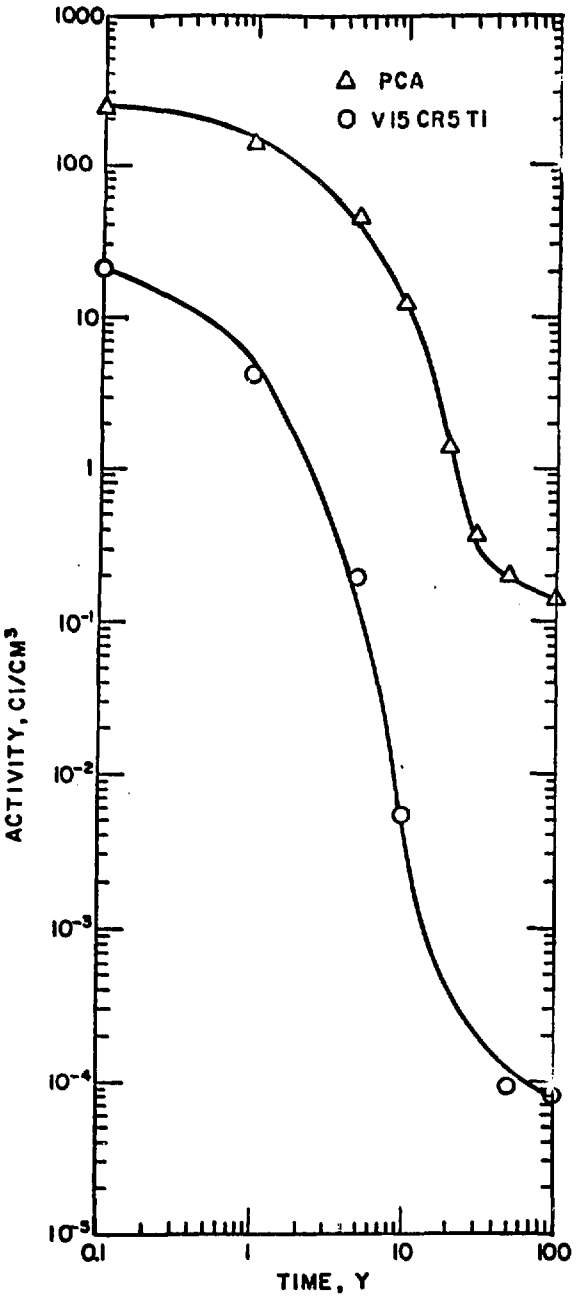

Fig. 2.14. Decay of radioactivity in the first wall as a function of time.

Table 2.18. Radioactivity of First Wall for a Fusion Reactor Blanket Design with V15Cr5Ti/Li

Time (Y)	Activity in V (Ci/cm^3)						
	1	5	10	20	30	50	100
Total Activity (Ci/cm^3)	4.3	0.20	5.6×10^{-3}	2.3×10^{-4}	1.2×10^{-4}	9.3×10^{-5}	8.2×10^{-5}
^{14}C 5300 y (no γ)	6.7×10^{-5}	6.7×10^{-5}	6.7×10^{-5}	6.7×10^{-5}	6.7×10^{-5}	6.7×10^{-5}	6.7×10^{-5}
^{26}Al 8×10^{5} y (1.83 MeV γ)	4.6×10^{-9}	4.6×10^{-9}	4.5×10^{-9}	4.5×10^{-9}	4.5×10^{-9}	4.5×10^{-9}	4.5×10^{-9}
^{45}Ca 150 d (no γ)	0.11	2.5×10^{-4}	1.2×10^{-7}	2.2×10^{-14}	--	--	--
^{49}V 330 d (no γ)	4.11	0.19	4.1×01^{-3}	1.9×10^{-6}	9.0×10^{-10}	--	--
^{63}Ni 100 y (no γ)	1.8×10^{-6}	1.8×10^{-6}	1.7×10^{-6}	1.6×10^{-6}	1.5×10^{-6}	1.3×10^{-6}	8.7×10^{-7}
^{55}Fe 2.6 y (no γ)	0.014	4.7×10^{-3}	1.2×10^{-3}	8.5×10^{-5}	5.9×10^{-6}	2.9×10^{-8}	4.6×10^{-14}
^{60}Co 5.2 y (1.17, 1.33 MeV γ)	2.3×10^{-4}	1.4×10^{-4}	7.0×10^{-5}	1.9×10^{-5}	5.0×10^{-6}	3.5×10^{-7}	4.8×10^{-10}
^{94}Nb 1.8×10^{4} y (875, 650 keV γ)	6.8×10^{-7}	6.8×10^{-7}	6.8×10^{-7}	6.8×10^{-7}	6.8×10^{-7}	6.8×10^{-7}	6.8×10^{-7}
^{93m}Nb 13.6 y (30 keV γ)	1.4×10^{-4}	1.1×10^{-4}	8.6×10^{-5}	5.4×10^{-5}	3.5×10^{-5}	1.7×10^{-5}	6.7×10^{-6}
^{93}Mo 3500 y (no γ)	7.3×10^{-6}	7.3×10^{-6}	7.3×10^{-6}	7.2×10^{-6}	7.2×10^{-6}	7.1×10^{-6}	6.8×10^{-6}

Table 2.19. Radioactive Decay Heat of the First Wall for V-15Cr-5Ti as a Function of Decay Time

Time (years)	Radioactive Decay Heat (kW/m^3)
0	840
1	5
5	0.21
10	6×10^{-3}
20	3.6×10^{-4}
30	1.1×10^{-4}
50	3.6×10^{-5}
100	2.8×10^{-5}
500	2.6×10^{-5}
1000	2.5×10^{-5}

Even after one year cooling, the first and second wall PCA are extremely radioactive (Table 2.13). The radioactivity of the other materials are listed below (Table 2.20). The economic values of Zr_5Pb_3 and graphite are low enough that these materials might be discarded as radioactive waste. The $LiAlO_2$ containing enriched ^6Li will be valuable, both economically and as a unique resource because the lithium is the sole material for breeding tritium and thus will be recovered.

The segments will be disassembled and the different materials segregated. The PCA will be cut, compacted and placed in canisters 0.61 m dia. x 3.05 m tall (2 ft diam by 10 feet tall).* With 9.5 m^3 of PCA available annually and assuming that compaction to 25% of theoretical density is attainable, approximately 44 canisters would be required annually. Examination of the decay heat values (Table 2.15)

*This geometry was arbitrarily selected to duplicate the containers of high level waste from the fission reactor fuel cycle. A systems analysis is desirable to define optimum geometries applicable to the fusion waste disposal process.

Table 2.20. Radioactivity of Blanket Materials as Function of Cooling Time

Time	Activity, Ci/cm^3			
	1 y	5 y	10 y	30 y
Zr_5Pb_3	3.5×10^{-1}	1.6×10^{-3}	1.2×10^{-3}	6.4×10^{-4}
Graphite	2.3×10^{-8}	2.3×10^{-8}	2.3×10^{-8}	2.3×10^{-8}
$LiAlO_2$	2.4×10^{-6}	2.4×10^{-6}	2.4×10^{-6}	2.4×10^{-6}

suggests that the first wall itself has sufficient decay heat after one year that it might offer problems if packaged by itself. However by blending all the PCA and thereby diluting the most active first wall, the lower average decay heat can be accommodated since under these conditions each canister would emit about 1.8 kW of decay heat at one year after removal from the reactor. Such a canister could be sent off-site for disposal without encountering significant heat-removal problems. If further reductions in the heat load were desired before transporting the waste to disposal sites, the canister could be stored on-site for another four years, thereby reducing the decay heat to 0.6 kW per canister. Thus processing of the blanket sectors could start some time after one year following removal from the reactor.

2.3.2.2 Disposition of PCA

The PCA would have a radioactivity content as shown in Tables 2.13 and 2.14. Thus after 50 years decay the first wall PCA would contain the radionuclides shown in Table 2.21. In the last column are the maximum permitted concentrations for shallow land burial [amended 10 CFR 61]. Comparison of the two columns shows that the PCA first wall material exceeds the allowed concentrations for ^{63}Ni and ^{94}Nb. The ^{94}Nb requirement is too high by a factor of 65. The ^{63}Ni concentration in the PCA is greater than 20 times the allowable limit.

Table 2.21. Radioactivity in PCA First Wall After 50 Years Decay, Compared to Current Regulations for Shallow Land Burial.

Nuclide	$\mu Ci/cm^3$	Amended 10 CFR 61 $\mu Ci/cm^3$*
Total	2×10^5	
^{14}C	74	80
^{26}Al	0.04	**
^{55}Fe	2.5×10^2	†
^{60}Co	7.0×10^3	††
^{63}Ni	1.7×10^5	7000
^{94}Nb	13	0.2
^{93m}Nb	6.5×10^3	†
^{93}Mo	8.0×10^3	†

*Allowable concentrations for shallow land burial.

**^{26}Al was not considered in the preparation of 10 CFR 61. Considerations of ^{26}Al must be handled cautiously.

†Not listed in 10 CFR 61.

††There are no concentration limits for this radionuclide in Class B or C wastes. Practical considerations such as effects of radiation, the does rates upon employees handling the material will limit the concentrations for these nuclides.

Since the first and second walls (11% of the PCA) contain 70% of the radioactivity, one plan for waste management considers placement of the first and second wall PCA into, for example, geologic storage and the remainder of the PCA in shallow land burial. However since even the least radioactive PCA would contain $\sim$1 x 10^5Ci per canister at 1 year after discharge decreasing by a factor of ten after ten years, such high levels might pose a handling problem for the burial site based on license restrictions [CRASE]. Consequently, it is probable that all PCA removed from a STARFIRE reactor will require disposal by a

greater confinement method than shallow land burial, e.g., in a geologic medium. The 9.5 m^3 of PCA removed annually when packaged at a density of 0.22 m^3 PCA/canister will require approximately 44 canisters per year but any increase in the packing density of the PCA will be reflected in a decrease in the number of canisters requiring disposal.

2.3.3.3 Hazard Index

The total Curie level, i.e., disintegration rate, of a radioactive source is an inadequate measure of the impact of that source upon man. Efforts have been made to devise a measure that will more closely reflect the impact of a given isotope. Some of these measures are discussed in Appendix D. The biological consequences of the individual nuclides are recognized by utilizing the maximum permissible concentration in water or air (MPC) which takes into account the radiation energy level, the decay rate of the nuclide, and its biological impact and lifetime. These values are established by the NRC and are published in 10 CFR 20.

Combining the Curie content with the MPC can yield a hazards index termed the biological hazard potential (BHP) [STEINER-1972]. This measure is defined as the total Curies of a radionuclide divided by the MPC in Ci/m^3 for that radionuclide. Such an index gives the volume of air or water needed to dilute the contained nuclide to the MPC concentration for ambient air or water. This index does not reflect release rates to the environment nor the movement of radionuclides through the environment. It is clear that hazards indices have to be used with great caution, that the proper hazards index must be used for each situation, and that the indexes are at best only useful in comparing materials.

One of the important deficiencies in the use of the BHP is the absence of dispersion mechanisms or potential for dispersion in the "index." The transition of radioactivity, even if "normalized" by the MPC listed in 10 CFR 20, from a metallic form to a solution to be ingested or an aerosol to be inhaled clearly involves processes that are a) scenario-dependent, b) materials-dependent, and c) probably selective

for the various radioelements in the activated components. Hence in the important step of conveying the radioactive material to man, the BHP fails to address any parts of the process and the BHP cannot recognize differences among materials. This deficiency makes use of the index highly questionable.

Application to waste disposal is also difficult to envision. The criteria for shallow burial are specific for isotopes and already include consideration of some of the factors that are included in the MPC. Similarly, disposal as high level waste involves material (waste) attributes that are specific to the waste form, an issue that causes BHP to be inapplicable.

In summary, the use of BHP is not meaningful in any context that can be used in a realistic and technically rational analysis. Comparisons using the BHP, even in the context of time needed to decay to levels comparable with natural products can be responsibly done only with great caution and many debilitating assumptions.

2.3.3.4 Comparison with Fission Reactor Wastes

The amount of radioactivity from the PCA of a STARFIRE reactor is compared with the amount of radioactivity generated by fission reactors in Table 2.22. The fission reactors are 1250 MW(e) reactors compared with the 1200 MWe output of the STARFIRE [CROFF]. These data show that the fusion reactor yields about three times the radioactivity of fission reactors. However, because the volume of fusion waste is somewhat greater than the fission wastes, the concentration in each of the wastes is approximately the same. It is recognized that this comparison involves structural materials for the fusion system and fuel (i.e., fission products) from the fission reactor. Nevertheless, this comparison is useful since it involves the largest part of the radioactivity from each power system. For the fission reactors it is assumed that reprocessing occurs and that the waste solution is calcined and formed into a glass.

Table 2.22. Comparison of the STARFIRE PCA Radioactivity with that of Fission Reactors at One Year After Removal from the Reactor

	Vol HLW* (m^3)	Ci in HLW per MTIHM**	MTIHM/y	Total Ci	Ci/m^3
STARFIRE	9.5	---	----	1.5×10^8	1.6×10^7
PWR	2.4	1.7×10^6	33.7	5.7×10^7	2.4×10^7
BWR	2.8	1.3×10^6	40.4	5.3×10^7	1.9×10^7
LMFBR	1.2	2.7×10^6	16.9	4.6×10^7	3.8×10^7

*High Level Waste.
**Metric tonnes initial heavy metals.

A comparison of fusion and fission wastes involves a comparison of relative short-lived activation products with higher MPC values with much longer-lived actinides and fission products with lower MPC values. The fission wastes will contain radionuclides with longer half-lives and lower MPC values than will fusion wastes and thus the fission wastes are potentially more hazardous.

2.3.3.5 Cost of Disposal of PCA

It was estimated that 44 canisters would be required annually to remove the PCA from the reactor site for disposal. The cost of such disposal is composed of three elements, the cost of packaging, transportation costs to the disposal site, the cost of emplacing the waste.

a. Cost of packaging

The canisters selected for packaging the highly radioactive waste are 0.61 m x 3.05 m. Such a size for waste containers has been selected for the high level waste (HLW) package for defense waste so as to yield a tolerable center-line heat load for glass. Currently some fuel element destined for movement are packaged in 0.35 m diameter (1' x 10') canisters that are placed in shielded shipping casks. The use

of a canister 0.35 m in diameter would require comminution of metallic waste pieces to that size. Increasing the canister diameter to 0.6 m would accommodate larger pieces and make disassembly of the fusion reactor sectors easier. The use of the larger diameter canister results in a volume increase in the payload for the shipping cask containing the canisters. Currently, shipping casks are being designed that will accommodate such canisters [ALLEN, RHOADS]. These canisters are of a relatively simple design and should be fabricable for approximately $7500 [SMITH-1978], corrected for inflation. The cost of comminuting the PCA and packaging it into the canisters is difficult to estimate, but should not significantly affect the total waste disposal costs.

b. Transportation

Transportation of the material destined for geologic storage is assumed to be by rail. The cost for a round-trip for a total distance of 4828 km (3000 miles) is about $25,000 for a rail car carrying a GE IF-300 cask [SMITH-1978]. These are data for 1978 and should be multiplied by a factor of 1.5 to yield a cost of $37,500, to make the data current (1982) assuming an inflation factor of 10% per year.

c. Storage

Estimates for the costs for deep geologic storage have been obtained from a recent study (1981) of mined geologic repositories for the disposal of nuclear waste [CLARK]. The geologic repository was designed to accommodate approximately 300,000 spent fuel assemblies. Several techniques for storing the wastes were considered and evaluated including the simplest, namely a single PWR element in its own canister. The emplacement cost for each such element was calculated to be $43,000 using the average of the calculated costs for each of the media studies, i.e., salt, granite, basalt, and tuff. The canisters containing fusion wastes are approximately twice the volume of the fuel element canisters and assuming that the unit costs are directly related to volume occupied yields a cost of approximately $90,000 corrected for current dollars.

The annual costs for geologic disposal are summarized in Table 2.23 and are also normalized to 1 GWe-y.

2.3.3.6 Modifications to Materials to Reduce the Induced Radioactivity

For PCA there is little that needs to be done about improving the impurity content of the metal since the bulk of activity after 30-50 years decay is due primarily to the activation of molybdenum and nickel which are basic constituents of the alloy. Analysis of the radioactivity of the waste indicates the responsible nuclides are ^{63}Ni and ^{93m}Nb. However, the ^{93m}Nb, while present at lower levels, yields a significant radiological dose rate (see Section 2.2.4.5). Thus, if these isotopes could be eliminated, the radioactivity after a 50-year decay would be reduced by > 90%. It has been suggested that molybdenum be tailored to 100% ^{97}Mo (9.6% in the natural abundance) since this isotope is least likely to be a source of radioactivity among the stable molybdenum isotopes [CONN-1978]. In a similar vein, Conn also suggests that nickel be tailored to 100% ^{61}Ni (1.25% in the natural abundance).

Thus, if the PCA were fabricated of these specific isotopes, ^{97}Mo and ^{61}Ni the macroproperties of the PCA would be maintained while yielding a reduction in the radionuclides ^{93m}Nb and

Table 2.23. Estimate of Annual Disposal Costs for PCA (44 Canisters)*

	Total Cost	Cost/GWe-y
Containers, 44 @ $7500 =	$330,000	$275,000
Shipment, 15 RT @ $37,500/RT =	$563,000	469,000
Emplacement 44 canisters @ $90,000/canister =	$3,960,000	3,300,000
TOTAL =	$4.9 million	$4.0 million

*It should be noted that for geologic disposal, costs associated with final emplacement are about 80% of the total.

^{63}Ni. Such a technique might be particularly useful for Mo since the content is only 2%.

Preliminary experiments on laser isotope separation with MoF_6 [FREUND] had demonstrated the proof-of-principle even though the selectivity was small. These were small scale laboratory experiments and larger scale experiments with improved selectivity are necessary. Still to be examined carefully is whether the isotopic separation by any process can be accomplished on a large-scale and at bearable costs.

2.3.4 Disposal Process for V15Cr5Ti

2.3.4.1 Introduction

Removal and disassembly of the blanket sectors of the vanadium alloy should be carried out in an analogous manner to that for the PCA. Examination of Figures 2.1 and 2.2 shows the similarity of the sectors derived from the PCA/$LiAlO_2$ and V/Li systems. The PCA/$LiAlO_2$ sector contains a solid neutron multiplier and a solid breeder; both contain a solid graphite reflector. The liquid lithium is removed before a sector from the V/Li system is removed. The activity of the metallic structural material is given in Table 2.17. The comparison of activities of the metallic first walls are summarized in Table 2.24. The data show that the vanadium alloy has much less residual activity than does the PCA, by a factor of 35 at one year and a factor of 2000 at 50 years. It also appears that the radioactivity content in the vanadium alloy is approaching an asymptote attributable to five nuclides that are listed in Table 2.25.

These data indicate that the asymtote being approached is that of the sum of ^{14}C, ^{63}Ni, ^{93}Mo, ^{93m}Nb, and ^{94}Nb activities. Since ^{14}C, ^{63}Ni, and ^{93}Mo emit only beta radiation, they have little effect upon the dose rate from the vanadium alloy. A plot of the constant biological dose from a 1 m diameter sphere of vanadium alloy as a function of time is given in Fig. 2.14. It is apparent that with the removal of the ^{94}Nb radioactivity, the residual contact dose rate after about 90 years

Table 2.24. Comparison of First Wall Activities for PCA and V15Cr5Ti

Time (y)	Activity (Ci/cm^3)	
	PCA	V15Cr5Ti
0	380	100
0.083 (30 d)	233	21
1	140	4.3
5	44	0.2
10	12	5.6×10^{-3}
30	0.37	1.2×10^{-4}
50	0.20	9.3×10^{-5}
100	0.14	8.2×10^{-5}

Table 2.25. Major Activities Present in Vanadium Alloy After 50 Years Cooling

	Ci/cm^3 in V alloy at 50 years	
Total	9.3×10^{-5}	
^{14}C (5730 y)	6.7×10^{-5}	(72%)
^{63}Ni (100 y)	1.3×10^{-6}	(1.4)
^{93}Mo (3500 y)	7.1×10^{-6}	(7.6)
^{93m}Nb (13.6 y)	1.7×10^{-5}	(18.0)
^{94}Nb (1.8×10^4 y)	6.8×10^{-7}	(0.7)

decay becomes sufficiently low that handling of a 1 m diameter sphere will not result in a dose in excess of the limits in 10 CFR 20. Another way of looking at dose rates is that when dose rates are in the order of 1-10 rem/quarter equivalent (2-20 mrem/hr) hands-on manipulat ı becomes a reasonable possibility for extended work. As the dose rate increases, the time for contact decreases until at perhaps 50-100 mrem/hr, contact times get to be too short for (unshielded) productive work. Such an analysis of contact dose rates needs to be refined by taking into account the dose rates encountered in realistic operating geometries.

The ^{94}Nb is formed by an (n,γ) reaction on ^{93}Nb, the sole stable isotope of niobium and by the ^{94}Mo (n,p) and the ^{95}Mo (n,d) reactions (Section 2.2.4.5). The niobium content of the vanadium alloy studied was 0.0025 wt. % or 25 ppm and molybdenum content was 80 ppm. Thus, any reductions in these impurities will result in a reduction of the ^{94}Nb radionuclide.

2.3.4.2 Recycle of Vanadium Alloys

The data in the previous section show that if the ^{94}Nb content of the vanadium can be reduced, then after approximately 90 years, the material could be directly handled for recycle without a worker exceeding the dose limits established in 10 CFR 20.

However, a 90 year hold-up time is probably unrealistic. Examination of the radionuclide content of the vanadium alloy (Table 2.18) indicates that after 20 years the bulk of the dose is attributable to the hard gammas from ^{60}Co. The ^{60}Co concentration in the first wall is 1.9×10^{-5} Ci/cm^3, the blanket contains approximately 1/10 that concentration. The bulk of the ^{60}Co is a result of the (n,p) reaction on ^{60}Ni. Thus, any reduction of the nickel impurity of the vanadium will yield a corresponding reduction in the ^{60}Co yield.

Based on the information now available, the dose from a sphere one meter in diameter would be approximately one rem/hr after 30 years decay. Thus to process after 30 year decay would require remote techniques. Such techniques are probably available for recovering the

vanadium. Remote techniques would also be necessary for refabricating the blanket sectors and an analysis of refabrication is needed to define the extent to which remote techniques for such a process are available.

Another alternative involves processing the vanadium structures using pyrochemical techniques and remote operations to isolate the vanadium from the bulk of the radioactive impurities. The vanadium alloy could then be cast into ingots and stored for an additional period of time until hands-on operation for subsequent refabrication becomes attractive.

These data show that hands-on manipulation of the vanadium becomes a possibility at 90 years after removal from the reactor when the molybdenum and niobium impurity content are reduced by a factor of ten. If the nickel impurity in the vanadium alloy (the source of ^{60}Co) is also reduced, then hands-on manipulation of the vanadium alloy becomes possible at even shorter time periods, and recycling of vanadium alloys becomes attractive.

2.3.4.3 Disposal of Vanadium Alloys

If disposal were the fate of the vanadium alloy, it could be packaged into 55 gal drums for placement in shallow land burial. Storage for about one year would be required to permit the radioactive decay heat to decrease to a manageable level, 5 kW/m^3.* Each 55 gal drum has a volume of $\sim$0.2 m^3. If the same packing fraction (25%) is chosen as for the PCA, then each drum will contain 0.05 m^3 of metallic waste emitting a maximum of 0.25 kW/drum. The amount of vanadium requiring handling annually is 7.82 m^3 which will require 160 drums annually for disposal.

*Subsequent discussions under disposal costs suggest that an additional decay period beyond one year may be desirable to reduce the disposal costs dramatically; cooling as long as ten years may be desirable.

a. Packaging

The material will be packaged at the plant site into 55 gal drums. By blending all the vanadium, each of the 55 gal drums will contain 2.2×10^4 Ci/drum after 1 year cooling. After a five year cooling period, each drum will contain 10^3 Ci. For shipment of such wastes a shielded container would be necessary, i.e., CNS-195-H, which can contain 14-55 gal drums.

b. Transportation

Approximately 12 shipments per year would be necessary to handle the 160 drums. Assuming a 1600 km (1000 mi)* trip from reactor to disposal site, an oversized load and with two drivers, the cost per shipment would be $2600 and for 12 shipments $31,200 (1978), or $47,000 corrected for inflation (assuming a 10% annual inflation factor) [SMITH-1978].

c. Disposal Costs

The costs of disposal in shallow land burial are based on the volume of waste to be buried and the activity level [BARNWELL]. Thus for 1 year decay with 2.2×10^4 Ci/drum, the cost would be approximately $5830 per drum or $932,000 per year. If disposal were delayed until five years after removal, the cost would be $622 per drum or $99,600 per year. However, if cooling were continued for 10 years, the activity level would be 35 Ci/drum and all Curie surcharges would be removed. The basic rate would apply; $90 per drum or $14,400 per year.

*It is assumed that there will be more shallow land burial sites than geologic disposal sites and so the distance to a shallow land burial site is somewhat less than to a geologic site.

d. Summary of Disposal Costs

Assuming that it would be advantageous to cool the vanadium on-site for 10 years, the annual disposal costs may be summarized.

Packaging - The cost of 55 gal drums is insignificant compared to other costs

Transportation - $47,000/yr.

Disposal - $14,400/yr.

Total - $60,000/yr.

2.4 Processing and Recovery of Spent $LiAlO_2$

2.4.1 Background

The blanket of a STARFIRE fusion reactor contains 6×10^5 kg of $LiAlO_2$ containing 6×10^4 kg lithium enriched to 60% ^6Li [BAKER]. The torus is made up of 24 sectors containing the blanket, four of which are removed and replaced annually. For calculational purposes it is assumed that each sector has been in the reactor for six years. Calculations indicate that under design conditions 306.6 kg of ^6Li are burned per year, or 51.1 kg per 4 sectors and after 6 years the four sectors are depleted by 306.6 kg of ^6Li. As the lithium in $LiAlO_2$ is consumed, the compound $LiAl_5O_8$ is formed [BAKER]. The equation below is a stoichiometric representation of the formation.

$$5LiAlO_2 \rightarrow Li5Al_5O_8 + 4Li \text{ (burned)} + O_2.$$

After six years exposure, 3440 kg of $LiAl_5O_8$ is calculated to be present in the four sectors removed. The four sectors contain 9.88×10^3 kg lithium less the amount of lithium burned, 0.31×10^3 kg of lithium. The lithium content of the four sectors is summarized below.

Lithium Balance in Four Sectors After Six Years Exposure in a STARFIRE Reactor

	As $LiAlO_2$	As Lithium
Content at start (kg)	101×10^3	9.88×10^3
Lithium reacted to form tritium (kg)	3.2×10^3	0.31×10^3 (3.14%)
Lithium required for $LiAl_5O_8$ (kg)*	0.79×10^3	0.077×10^3
$LiAlO_2$ remaining (kg)	96.98×10^3	9.49×10^3
Total oxide	100.73×10^3	

*Yielding 3.44×10^3 kg of $LiAl_5O_8$.

The earlier discussion (Section 2.3.3.2) had indicated that disposal of the breeder materials without recovery of the lithium would put a severe strain on the world lithium resources. The information in the previous paragraph indicates that the bulk of the original lithium remains unreacted and could be recovered.

2.4.2 Evaluation of Lithium Processing

2.4.2.1 Need for Reprocessing

There are several factors that affect the decision as to whether to reprocess the blanket. These are the possibility of resource depletion, the cost or reprocessing compared with the cost of replacement of material, and disposal costs of the associated wastes.

a. Resource Depletion

The problems of resource depletion were discussed in Section 2.2.3.2 from which it can concluded that recycle of lithium may be required.

b. Cost of Lithium

Lithium in some forms is rather inexpensive, e.g., about 1¢/g for lithium carbonate [LITHCOA]. The cost of lithium for the reactor will be dominated by the cost of enrichment. The classic method for enriching lithium by equilibration between an aqueous solution of LiOH and lithium amalgam yields a product of up to 95% ^{6}Li at a cost of approximately $1.25/g according to the recent price quoted by the Oak Ridge isotopes sales office. More recently, Eagle-Picher has completed the design of a plant to enrich ^{7}Li, but is awaiting for approval and funding to proceed with building a plant. They estimate that it would cost $5-6/g to isolate ^{7}Li [EAGLE-PICHER]. Since ^{6}Li is only 7.5% of the lithium content, the cost for high purity ^{6}Li is not expected to be any cheaper. On the other hand, Wilkes at Mound Laboratory [WILKES] has estimated that ^{6}Li can be isolated at a cost of approximately 50¢ a gram with a plant capacity of 100 Mg using solvent extraction techniques with new solvents called "Crown Ethers" [JEPSON]. These are new extractants and only laboratory tests are available. At present these materials are being studied for calcium isotope separation since certain calcium isotopes after irradiation have a medical application. Other methods have been considered for isotope separation such as laser techniques but no candidates are currently being developed.

Under the most optimistic situations, the $LiAlO_2$ removed will be worth approximately $5 million assuming a lithium content of 9.5×10^3 kg in the removed sectors and a lithium cost of 50¢/g (due to isotope enrichment). This cost does not include fabrication costs since it is assumed fabrication will be necessary in any case. As indicated in Fig. 2.4, a fusion economy based on the STARFIRE reactor will require 80% of the lithium resources (3.1×10^6 Mg) assuming no lithium recovery. When blanket sectors are removed from the reactor at the end-of-life, only about 3% of the lithium will have reacted to form tritium. As long as processing can be achieved at a cost of less than the value of the $LiAlO_2$, processing would be economically justifiable and the resource conservation would be an added benefit.

2.4.3 Reprocessing of the $LiAlO_2$ Blanket

When reprocessing of the lithium aluminate becomes necessary, there are at least two procedures that appear useful. One is a solid-state reaction that may maintain the compound integrity, but carries along the induced ^{26}Al radioactivity into the new breeder assembly. The second is an aqueous technique in which the breeder is dissolved, and the aluminum precipitated as $Al_2O_3 \cdot 3H_2O$ and discarded as a waste. In this procedure, the $LiAlO_2$ is destroyed, but the lithium is separated from the radioactive ^{26}Al and if the separation is adequate, the lithium may be refabricated without shielding. A solid, e.g., Li_2CO_3, must be derived from the lithium in solution and reacted with Al_2O_3 to form fresh $LiAlO_2$.

2.4.3.1 Solid State Reaction

When $LiAlO_2$ is used as the breeder material, reaction of the lithium to form tritium leads to a decrease in the lithium-aluminum ratio in the solid with the formation of $LiAl_5O_8$. It is probable that $LiAlO_2$ can be regenerated by reaction with Li_2CO_3 (enriched in ^6Li) in a manner analogous to the original preparation of $LiAlO_2$.

$$LiAl_5O_8 + 2\ Li_2CO_3 \rightarrow 5\ LiAlO_2 + 2\ CO_2$$

In the preparation of $LiAlO_2$ [ARONS] very fine alumina (< 10 nm) was ballmilled with Li_2CO_3. Sintering in air at 923 K yielded phase-pure $\alpha LiAlO_2$ with a grain size of ~100 mm. Agglomerates were crushed, sized, cold pressed at 345 MPa and fired in air for one hour at 1223-1473 K. At the highest temperature, 95% dense pellets of γ-$LiAlO_2$ were obtained, with minor $LiAl_5O_8$ impurity.

Neutron activation of the aluminum proceeds by the reaction $^{27}Al(n,2n)^{26}Al$. After one month of cooling, the residual activity due to the ^{26}Al is 1.46 Ci/m^3 (1.46 $\mu Ci/cm^3$). When the solid state reaction is used to regenerate the $LiAlO_2$, the radioactive ^{26}Al is carried along and becomes an integral part of the breeder, requiring an awareness of radiation dose levels when handling the material.

The solid state reaction mentioned above will need to be carried out using remote techniques so as to minimize personnel exposure. Then, having the reformed lithium aluminate, it will be necessary to evaluate the capability of loading a blanket sector using remote operations. Laboratory-scale experiments to demonstrate this reaction should be straight forward and, hence, should be carried out as part of the near-term program. An evaluation should also be made of the personnel dose rate from bare residual ^{26}Al and of the shielding requirements for reducing the dose to acceptable limits.

2.4.3.2 Aqueous Flowsheet

Another method for recovering the breeder material is by the use of aqueous reprocessing techniques. It has been reported [LEJUS] that γ-$LiAlO_2$ reacts with water in a few hours via a two-step process. α-$LiAlO_2$ does not react with water under the same conditions as the γ-$LiAlO_2$ [LEJUS]. However α-$LiAlO_2$ can be converted to γ-$LiAlO_2$ by heating in air to about 1200 K [ACKERMAN]. The first step is the rapid formation of an intermediate "H" phase; the second step is much slower and produces $Al_2O_3 \cdot 3H_2O$. If such reactions do occur it should be possible to separate the $Al_2O_3 \cdot 3H_2O$ and discard it to waste. The lithium can then be recovered from the aqueous solution. If the aluminum separation factor is sufficiently high, then the recovered lithium should not require shielding for handling.

A flowsheet for this separation technique should be devised and tested both for $LiAlO_2$ and $LiAl_5O_8$. Preliminary studies would involve the reactions of $LiAlO_2$ and $LiAl_5O_8$ with water.

2.4.3.3 Disposal Costs of the Associated Wastes

Formation of ^{26}Al yields a radioactive content of the breeder solid of 1.46 $\mu Ci/cm^3$, thus yielding a material that could be placed in shallow land burial. If no lithium recovery were undertaken, then 38.5 m^3 of $LiAlO_2$ would require disposal annually, or a

total volume of 1348 m^3 over the 30 year lifetime of the reactor. If reprocessing of $LiAlO_2$ were carried out, the use of the aqueous technique would yield 120.5 Mg ($\sim$50 m^3) of $Al_2O_3 \cdot 3H_2O$ annually. This material also would be suitable for shallow land burial. If the solid state technique of reforming $LiAlO_2$ is selected, no waste will be directly formed. Instead, the radioactive ^{26}Al will remain with the regenerated $LiAlO_2$. The cost of burial of low level radioactive wastes is \$12/ft^3 [BARNWELL] and a 55 gal drum is considered to contain 7.5 ft^3, for a total of \$90/drum. The radioactivity content due to the presence of ^{26}Al is 1.46 Ci/m^3, so that there are no radioactivity surcharges. Assuming processing, the disposal rate is 50 m^3/yr. Based on a fill rate of 90%, approximately 265 drums would be required at a total cost of \$23,850. This is the burial cost; the cost of shipment from the plant site to burial site would have to be included.

3. Assessment of the Disposition Options for Irradiated Magnet Materials (GA Technologies)

3.1 Introduction and Evaluation Criteria

3.1.1 General

An important aspect of fusion waste management is the recovery of valuable and scarce material resources. The superconducting magnets of fusion reactors are large and expensive and may, therefore, have an important impact on resource considerations of waste management issues. The options for the disposition of irradiated materials from the STARFIRE superconducting toroidal field magnets have been examined and the relative costs of each option have been assessed. The three options considered are:

1. Disposal. The irradiated magnet material is prepared for burial, packaged, and shipped to a disposal site; and a new magnet is fabricated from new material.

2. Material Recovery and Purification (Reprocessing). The irradiated magnet material is prepared for a purification process, chemically reprocessed to remove or reduce radioactivity, and a new magnet is fabricated from the reprocessed material. The radioactive wastes are packaged and shipped to a disposal site.

3. Material Recovery for Refabrication. The irradiated magnet material is prepared for fabrication and a new magnet is refabricated from the radioactive material. Unused radioactive materials are packaged and shipped to a disposal site.

3.1.2 Description of STARFIRE Toroidal Field (TF) Magnets

The STARFIRE TF coil/helium vessel assembly consists of 12 large magnets which project radially outward from the reactor centerpost to form a D-shaped torus. The placement of the magnets and some of the related reactor elements are shown in Fig. 1.1. The total weight of the

magnet materials is 6.3×10^6 kg of which 1.8×10^6 kg represents the superconducting alloys and copper. A more detailed description of the TF magnet structure is given in Appendix G.

3.1.3 Radioactivity, Biological Hazard Potential (BHP), Contact Dose, and Afterheat Rates

The nucleonics data required to perform this assessment is given as a function of position and time for all locations within the magnets (Appendix C). The TF coil/helium vessel assembly was divided into the 16 sections shown in Fig. 3.1. This figure also presents the nomenclature used in subsequent discussions. This division permits accounting for the spatial gradients across the magnet components, especially the superconductor regions. The top, bottom, and outboard magnet portions are all categorized into the "OUTBOARD" designation and distinguished from the "INBOARD" magnet section.

The nucleonics data provided includes the radioactivity, BHP in water and in air, contact dose rate, and decay afterheat rate throughout the magnet. The tantalum barrier contribution to the data was not included as it is expected to be small. The decay afterheat calculation assumes that both beta and gamma energies are locally deposited at the source point.

The nucleonics data were analyzed to determine the recommended waiting period before initiating dismantling, refabrication, reprocessing, and disposal operations. The results indicate that the major decrease in the contact dose occurs during the first month after shutdown. The rate of decrease after one month is very low and does not merit delaying the dismantling procedures. In actuality, it is expected that disassembly of related reactor components to provide access to the magnets will not proceed in less than one year's time. However, this report assumes that dismantling of the TF magnets begins one month after shutdown.

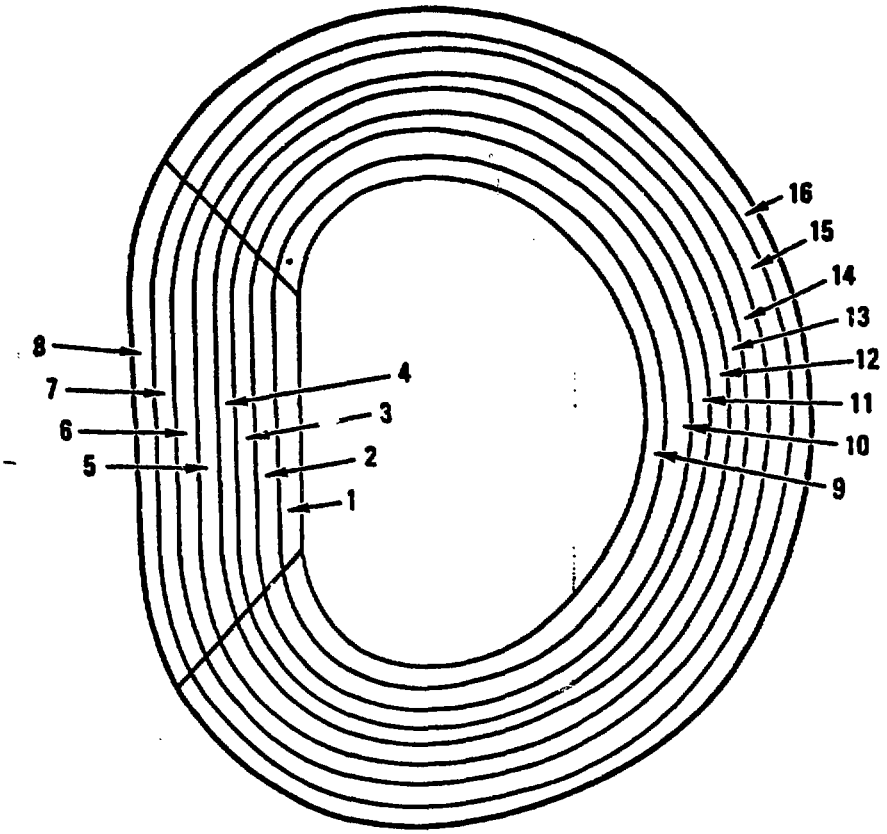

Section Number	Computer Abbreviation	Section Name	Thickness (cm)
1	I-DEWAR1	inner vacuum vessel one	8.0 (5 cm ℓN_2 insulation)
2	I-HEVSL1	inner helium vessel one	7.0
3	I-HFMAG1	inner high field magnet one	26.5
4	I-HMFAG2	inner high field magnet two	26.5
5	I-LFMAG1	inner low field magnet one	35.0
6	I-LFMAG2	inner low field magnet two	35.0
7	I-HEVSL2	inner helium vessel two	7.0
8	I-DEWAR2	inner vacuum vessel two	8.0 (5 cm ℓN_2 insulation)
9	O-DEWAR2	outer vacuum vessel two	8.0 (5 cm ℓN_2 insulation)
10	O-HEVSL1	outer helium vessel one	7.0
11	O-HFMAG1	outer high field magnet one	26.5
12	O-HFMAG2	outer high field magnet two	26.5
13	O-LFMAG1	outer low field magnet one	35.0
14	O-LFMAG2	outer low field magnet two	35.0
15	O-HEVSL2	outer helium vessel two	7.0
16	O-DEWAR2	outer vacuum vessel two	8.0 (5 cm ℓN_2 insulation)

Fig. 3.1 TF coil/helium assembly division and nomenclature.

3.1.4 Evaluation Criteria and Results

From the information obtained during this investigation, it was determined that cost was the most practical basis for comparing the three alternative options. Other factors, such as radiation exposure to occupational workers, materials recycling (resource recovery), and elimination of wastes, would be reflected in costs.

The processes evaluated include all costs associated with dismantling of the irradiated coils, packaging, shipping and disposal of all unused material, and delivery of a set of 12 TF magnets to the original reactor site. A summary of the costs incurred by the three alternatives is presented in Table 3.1, which shows the refabrication option as having a significant economic advantage. This is a result of the high cost of purchasing a new set of TF coils. Since the refabrication and reprocessing options both initially remove the high activity portions of the magnets, they result in no significant increase in occupational radiation exposure over the disposal option. These two options also result in the conservation of valuable resources, and thus are also preferred on this basis. As the value of these resources increases (due to depletion or increased demand), the economic advantage will also increase. These two options result in increased volumes of waste requiring burial due to dismantling operations, whereas the disposal option maintains the magnet in its most compact form. The impact of this is relatively minor as the cost of burial is modest in comparison with the other costs shown in Table 3.1.

3.2 Superconducting Magnet Refabrication

3.2.1 Introduction

This section presents the refabrication option which outlines the preparation for and refabrication of a STARFIRE toroidal field (TF) coil/helium vessel assembly [BAKER] which has reached the end of its design life. A fabrication plan is presented which provides for the replacement of the electrically or mechanically degraded materials while attempting to minimize the number of tasks that must be performed remotely.

Table 3.1. Summary of Costs of Alternative Magnet Disposition Options (All costs in millions of 1982 dollars)

Disposal of All Materials	
Dismantling	$ 0.90
Packaging (including containers)	0.84
Shipping	0.36
Burial at Disposal Site	1.33
Subtotal	$ 3.43
New TF Magnets (escalated from [BAKER] at 10% for 2 years)	176.04
Total	$179.47
Reprocessing and Materials Recovery[a]	
Dismantling	$ 0.90
Packaging of High-Activity Waste	0.03
Shipping of High-Activity Waste	0.01
Burial of High-Activity Waste	0.04
Packaging and Shipping to Reprocessing Site	0.45
Reprocessing Plant Cost	2.64
Reprocessing Plant Revenue	(5.20)
Packaging, Shipping, and Burial of Reprocessing Plant Waste	0.78
Subtotal (overall reprocessing profit)	$ (0.35)
New TF Magnets	176.04
Total	$175.69

(Cont'd)

Table 3.1 (Cont'd)

Magnet Refabrication	
Dismantling	$ 0.90
Packaging of High-Activity Waste	0.03
Shipping of High-Activity Waste	0.01
Burial of High Activity Waste	0.04
Refabrication[b]	19.00
Packaging, Shipping and Burial of Unused Materials	0.77
Total	$ 20.75

[a]Normalized to one reactor.

[b]Includes cost of purchasing new material as required.

The life-limiting properties of each material and component are presented, thus prescribing the suitability of each item for reuse. The strategy is then mapped out for refabrication of the magnet using the acceptable materials. The approach adopted attempts to reuse as much of the superconductor and conductor stabilizer as possible. As discussed below, although certain portions of these materials such as the centerpost's irradiated Nb_3Sn superconductor could be reused if after refabrication they were positioned in the outboard (low neutron fluence) portion of the assembly, the increased cost which would be incurred owing to the totally remote refabrication that would be required justified the disposal of the high activity portions of these materials. However, the stainless steel from the helium vessel and vacuum vessel can be reused to refabricate these components. Unused radioactive materials are packaged and shipped to a disposal site.

Section 3.2.2 discusses the effect of 40 years of STARFIRE operation on the TF coil materials, and presents the basis for determining the acceptability of each material for reuse in a refabricated magnet. It is followed by the cooling, storage and packaging requirements before transportation to the magnet refabrication area or disposal site, as appropriate. Section 3.2.4 discusses the dismantling operations, and the refabrication plan is presented in Section 3.2.5. An estimate of the total cost of the superconducting magnet refabrication option is presented in Section 3.2.6.

3.2.2 Materials Selection

The harsh environment presented by fusion reactors will have a degenerative effect on some of the materials used in the TF coil/helium vessel assembly. The primary cause of the material degradation is neutron irradiation; other causes such as exposure to cryogenic temperatures play only a minor role. The materials which will be adversely affected by irradiation include the superconductor (especially the high-field Nb_3Sn superconductor), the copper stabilizer, the epoxy fiberglass laminate electrical insulation and support material, and aluminized Mylar thermal insulation. The stainless steel conductor

support strips, 316 LN and 14Mn2Ni2Cr austenitic stainless steel helium vessel and dewar, and aluminum thermal radiation shield will not be significantly structurally degraded by irradiation. However, to allow hands-on refabrication, these materials will be replaced in areas where they have accumulated unacceptably high levels of radiation.

3.2.2.1 Superconductor

The STARFIRE high-field superconductor is Nb_3Sn and the low-field superconductor is NbTi. Figure 3.2 [INTOR] presents the effect of neutron irradiation on the critical current-carrying capacity of NbTi and Nb_3Sn. It shows that the NbTi is relatively unaffected by irradiation and should, therefore, be usable for refabrication. However, the critical current density of the Nb_3Sn is severely degraded above a fluence of 3×10^{18} n/cm^2 (E > 1.0 MeV) owing to radiation induced disorder [INTOR].

The total fluence to the STARFIRE TF coil/helium vessel assembly centerpost was calculated to be 1×10^{18} n/cm^2. If the centerpost superconductor were reused in the refabrication of a new assembly, the total fluence would double to 2×10^{18} n/cm^2. Although this is still below the level at which Nb_3Sn experiences severe degradation, Fig. 3.2 shows that some degradation will have occurred. But more importantly, reuse of the Nb_3Sn from the centerpost might result in coil failure owing to localized areas of higher fluences, slight impurities, and structural defects caused by being exposed to large loads over a long time. As a result, the Nb_3Sn will not be reused for refabrication.

3.2.2.2 Stabilizer

The copper conductor stabilizer used in STARFIRE will exhibit an increase in resistivity owing to fast neutron irradiation. Although the resistivity can be decreased significantly during the periodic 10-year, room-temperature anneal cycles (including decommissioning), reuse of copper stabilizer from the centerpost region will result in a neutron fluence degradation factor greater than 3.8. The

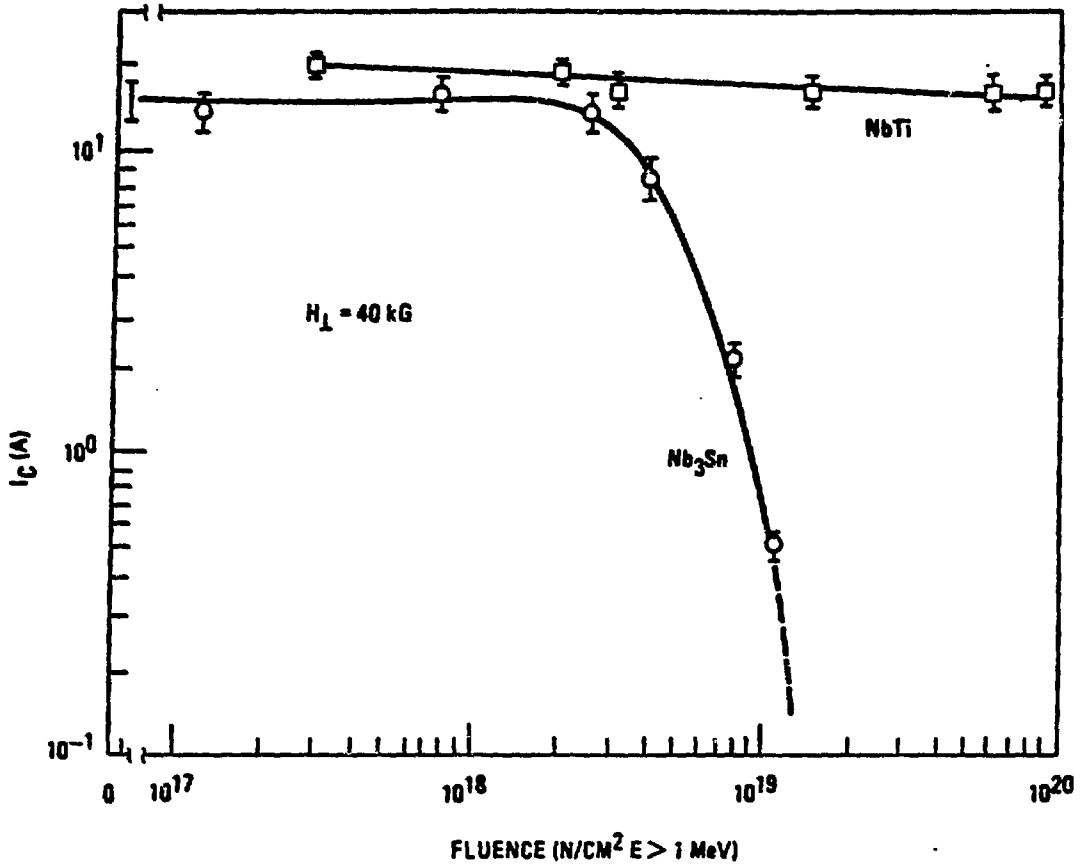

Fig. 3.2. Effect of neutron irradiation on the critical current in Nb-Ti and Nb_3Sn.

conductor was designed using this as the maximum degradation factor, therefore, reuse of the centerpost region copper will not allow the copper to achieve its required current density. Therefore, only the copper from the centerpost region, which is exposed to the highest neutron fluences, will not be reused for refabrication.

3.2.2.3 Electrical Insulation and Support Material

Epoxy fiberglass laminate (G-10CR) is used for the TF coil/helium vessel assembly ground, interturn, and interlayer insulation material as well as the tiebar structures supporting the helium vessel with the vacuum vessel. The mechanical properties of

G-10CR are significantly degraded when exposed to the levels of radiation that will be produced everywhere in the STARFIRE TF magnets. Experiments have shown this degradation in both flexure and compressive strength tests [KERNOHAN]. Therefore, all G-10CR electrical insulation and support material will be replaced for the refabrication of the assembly.

3.2.2.4 Thermal Insulation

Multilayer aluminized Mylar insulation is wrapped around the helium vessel and thermal radiation shield. Experiments have shown aluminized Mylar to be severely embrittled when irradiated [KERNOHAN]. Therefore, the Mylar will all be replaced during refabrication. Either Mylar or Dexter paper (glass paper layered with aluminum foil) would be suitable thermal insulation.

3.2.3 Cooling, Storage, and Transportation Requirements

To minimize the radiation exposure to workers during dismantling operations, the biological contact dose of the materials within the TF magnet was examined to evaluate the required cooling period. The nucleonics data (Table C-3) show that the contact radiation dose decreases with time, with decreases still significant at one year. In order to avoid delaying magnet dismantling procedures, a one-month cooling time was selected. This section thus assumes one month as the in-situ cooling and storage time before dismantling operations begin, and uses the radioactivity data at one month for all analyses. In fact, if the integrity of the TF magnets is to be preserved to the fullest practical extent in order to facilitate refabrication, many related reactor elements must first be removed to provide access to the magnets. The activity in these other components may determine the time before the overall reactor dismantling operations can proceed. Even if this time is greater than one month after shutdown, the entire dismantling procedure described here is still applicable.

This report assumes that all dismantling and refabrication tasks will be performed at the reactor site by an outside contractor who will supply the specialized equipment required for many of the tasks.

Although the standardized design of STARFIRE would allow for economy of scale savings if the magnets from many STARFIRE reactors were shipped to a separate facility for dismantling and refabrication, the extreme difficulty and expense associated with overland movement of such large and massive magnets makes thia approach undesirable [MOORE]. Some of the added expenses associated with overland movement include reinforcing bridges or providing barge bridges, repairing or building new roads, and enlarging bridges and tunnels. Transportation would be greatly simplified if the reactor were located next to water. Since it cannot be assumed that all STARFIRE reactors will be located near water, considerable overland movement may be required. The specialized equipment that will have to be shipped to the reactor site does not present a transportation problem because it can be designed to be modular and, therefore, will not be very large or massive.

It is further assumed that the refabricated magnets will be used to reconstruct another STARFIRE reactor at the original reactor site. If, however, the magnets are to be used for a reactor at a new site, dismantling and refabricating the magnets at the original site will still eliminate shipping to a dismantling and refabricating facility (although the refabricated magnets will still have to shipped to new sites). In any case, it is expected that there will be considerable improvements in overland movement by the time of STARFIRE decommissioning.

In transporting the high-activity portion of the assembly to a waste storage site, the high-activity pieces will have to be packaged properly to provide radiation protection, and comply with existing regulations governing the transport of radioactive materials. Typical wastes expected from the remote fabrication option are summarized in Table 3.2. As indicated below, the components to be disposed of as waste are the more highly radioactive sections, i.e., parts of the vacuum vessel, the helium vessel, and the high-field conductors.

To meet the cargo requirement (discussed in more detail in Section 3.4.4) of less than 22,680 kg (50,000 lb) per carrier, there will be seven truck shipments, as indicated below:

Table 3.2. Radioactive Waste From Remote Fabrication Option

Component	Discarded Weight (Tonnes) Total/ Each Coil	Per Coil Dimensions (m)	Data-Cut Pieces Weight (kg)	Data-Cut Pieces Dimension (m)	Total Magnet Radioactivity (Curies)	Total Magnet Weight (Tonnes)	Total Magnet Millicuries Per gm
Vacuum Vessel	23.3/1.94	0.03x2.16x8.04	485	0.03x2.16x2.01	3.54×10^{2}	69.9	5.06×10^{-3}
		Load 24 pcs/box = 11,648 kg (25,680 lb); box ∿1.22 m x 2.47 m x 2.32 m Requires 2 boxes @ 7.0 m^3/box					
Helium Vessel	48.8/4.07	0.07x1.76x8.04	1016	0.07x1.76x2.01	2.1×10^{2}	119.0	1.77×10^{-3}
		Load 10 pcs/box = 10,160 kg (22,410 lb); box ∿1.22 m x 2.06 m x 2.32 m Requires 4 boxes @ 5.8 m^3/box and 1 box (8 pcs) + 5.0 m^3 box					
High Field Conductors	58.6/4.88	0.53x1.60x8.04	1221	0.53x1.60x2.01	12.55	110.0	1.14×10^{-4}
		Load 4 pcs/box = 4884 kg (10,768 lb); box ∿2.56 m x 1.91 m x 2.32 m Requires 12 boxes @ 11.3 m^3/box					
Other		∿2720 kg (6000 lbs) of waste metal shavings Requiring ∿nine 0.2 m^3 (55 gal) drums					

1. Two shipments each containing a dewer package.
2. One shipment containing two crates of helium vessel components.
3. One shipment containing a lighter box of helium vessel components and two of the high-field conductor packages.
4. Two carriers, each with four boxes of the high-field conductor parts.
5. A lightly loaded shipment containing only two boxes with 9,800 kg (22,000 lb) of the high-field conductor pieces.

The nine, 0.2 m^3 (55 gal) drums, containing about 2720 kg (6000 lb) of waste metal shavings can easily be accommodated by some of the lighter-loaded vehicles.

Most of this material (vacuum and helium vessel sections) will require light shielding in the boxes due to their radioactivity levels. This can easily be accomplished by the use of thin metal sheets attached to the inside of the boxes (see Section 3.4.4.2).

The dewar and metal shavings will qualify for shallow land burial as Class A waste. The Nb_3Sn conductor will be categorized as Class B waste. Reference is made to Section 3.4.4.3 for additional discussion of the shallow land disposal of radioactive waste.

3.2.4 Dismantling and Preparation for Refabrication

STARFIRE was designed as a totally remote facility with the flexibility to allow access to properly suited personnel within 24 h after reactor shutdown. Because dismantling of the magnets will not begin until one month after reactor shutdown, remote operations should be simplified. The remote handling equipment described in the STARFIRE report was assumed available for dismantling of the magnets. Only current state-of-the-art technology and procedures are assumed herein, though, as the STARFIRE report points out, in the STARFIRE timeframe, remote industrial robot technology will likely allow visual recognition

of objects, grasping, feeling, hearing, and connecting basic operations and movements to perform complex operations with a minimum of human supervision. The details of the remote dismantling are given in Appendix G.

3.2.5 Refabrication

The most important difference between the procedure to refabricate the TF coil/helium vessel magnets and the original fabrication is that during refabrication, many of the components will be welded in areas dictated by the required dismantling tasks, whereas originally these components will have been fabricated as monolithic structures or welded in areas which enable the component to be fabricated with minimal difficulty. The refabrication task will be more difficult because some of the components will undoubtedly be bent or dented during dismantling.

To start the refabrication, a new three-level, uninsulated, unsoldered high-field conductor is fabricated using new Nb_3Sn and copper. The low-field NbTi and copper conductor is refabricated by simply replacing the G-10CR Mylar strip. The new conductors are soldered to the old using a lap-jointed configuration. The refabrication steps are sequentially pictured in Fig. 3.3 which shows an outboard region cross-section of the magnet.

While the conductor is being fabricated, a new section of 316 LN austenitic stainless steel is welded to the inner section of the helium vessel to replace the high-activity centerpost section that was removed. Then the central radial spine is lifted with a crane and welded completely around the inner helium vessel forming a T-shaped structure. This new structure forms the helium vessel inner weldment or bobbin [Fig. 3.3(A)]. The lower and upper sets of conductors, which are sandwiched between two pretensioned stainless steel strips and flanked by two bearing load support strips, are then simultaneously pancake wound around the bobbin using new G-10CR epoxy fiberglass laminate as ground, interturn, and interlayer insulation [Fig. 3.3(B)]. The outer sections

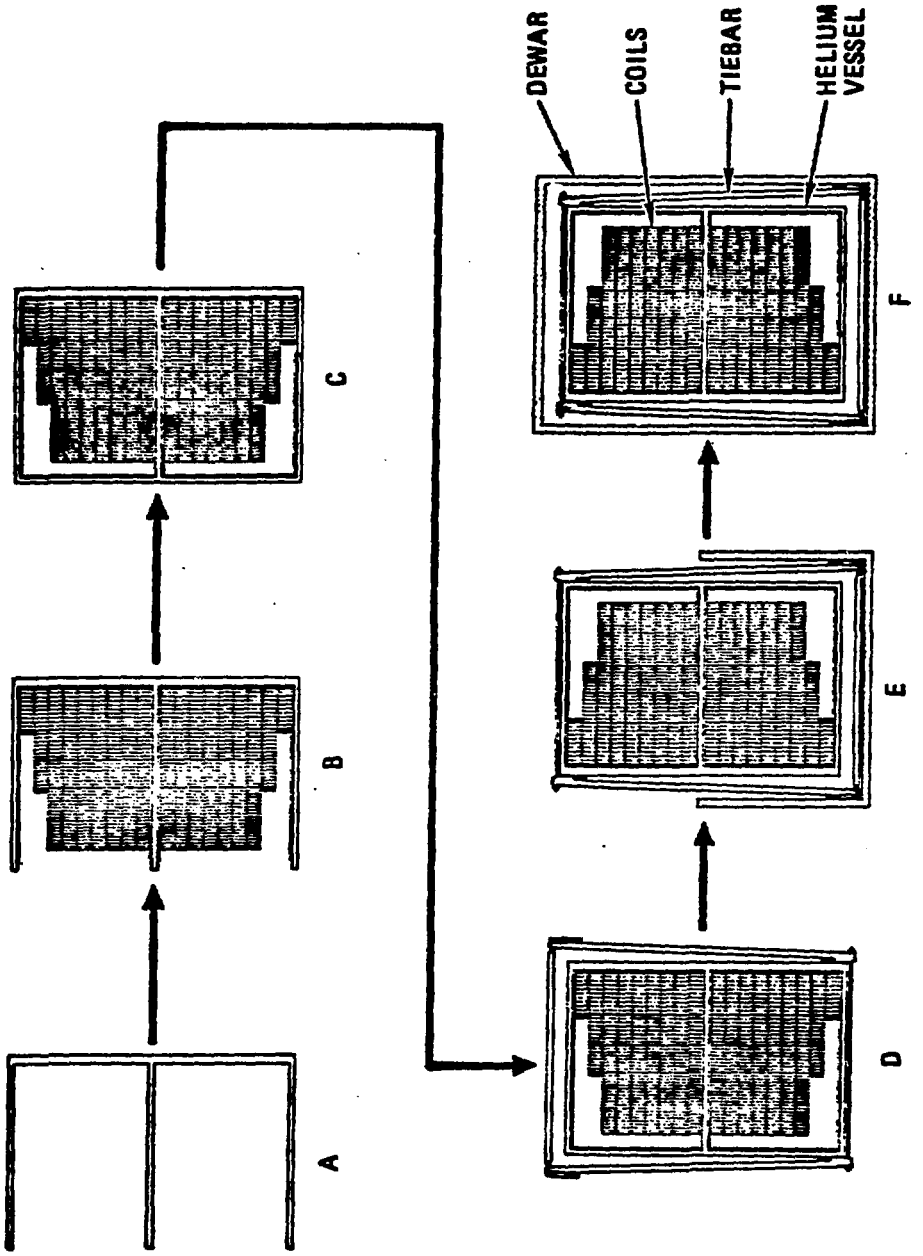

Fig. 3.3. Refabrication steps in magnet outboard region.

of the helium vessel are then lifted with a crane and positioned against the bobbin. The two outer sections are welded shut at both ends and at the central radial spine. This completes the refabrication of the conductor and helium vessel [Fig. 3.3(C)].

Next, the locally-stiffened sheet aluminum thermal radiation shield is welded together and then wrapped, along with the helium vessel, with aluminized Mylar thermal insulation. The thermal radiation shield is positioned outside the helium vessel in both the centerpost and outboard regions and the G-10 tiebars are bolted to the vacuum vessel and readied to support the helium vessel [Fig. 3.3(D)].

Before placing the helium vessel inside the vacuum vessel, new circular pieces of 14Mn-2Ni-2Cr austenitic stainless steel are fitted and welded into the holes that were previously drilled into the lower portion of the vacuum vessel. The helium vessel and conductor are lifted with a crane, inverted, and placed inside the lower section of the vacuum vessel [Fig. 3.3(E)]. Next, the upper section of the vacuum vessel is placed on top of the lower section (using a crane) and welded shut and a new section of 316 LN austenitic stainless steel is positioned and welded to the centerpost portion of the vacuum vessel where the high-activity section was removed earlier [Fig. 3.3(F)].

Because the common inner dewar, section I-DEWAR2, is attached to the reactor's centerpost, the TF coil/helium vessel assembly is not complete until the individual magnets are attached. They will be attached as described in the STARFIRE Reactor Construction plan [BAKER].

Before attaching each magnet, a number of verification tests will be performed to ensure that the assembly meets all of its performance requirements. These include mapping the field in both the axial and radial directions, measuring the boil off from the helium vessel with the coils energized and de-energized, verifying the vacuum integrity of the system, and quenching the magnet to ensure that the coil will withstand quench conditions [ALCORN].

In order to perform these tests, a temporary vacuum barrier will be bolted to the dewar to replace the missing centerpost section. In addition to this, a strongback support plate will be bolted to the vacuum barrier to protect against hoop stresses during charging.

3.2.6 Cost Estimate

Table 3.3 presents a rough order-of-magnitude (ROM) estimate of the cost to perform the remote refabrication option. The STARFIRE TF coil/helium vessel assembly refabrication option is estimated to cost $20.7 million. All costs are in 1982 dollars. The basis for this ROM estimate is consistent with the conceptual nature of the STARFIRE design and refabrication plan. A better estimate will be possible as the STARFIRE design and refabrication plan become more well-defined.

The refabrication cost includes a 100% contingency for indeterminates in all labor costs. This large contingency is reasonable owing to the high uncertainty attributed to successfully completing each refabrication task. For example, it is assumed that all sections to be welded will fit smoothly together and that no major difficulties in the welding process will occur. However, in actuality, the large components to be welded will be bent, dented, and missing fragments lost during the cutting tasks. As a result, welding operations will be quite difficult. As another example, when removing the high-activity portions of the magnets and preparing the low-activity portions for dismantling, the degraded G-10CR tiebars may not be strong enough to support the helium vessel. Therefore, the helium vessel may collapse, deforming all the components within the magnet. The detailed estimates of the man-hours required for the refabrication tasks are given in Appendix H.

3.3 Material Recovery Via Chemical Reprocessing

3.3.1 Introduction and Reprocessing Philosophy

The large amount of materials involved in building a fusion economy of 1.2×10^5 MW(e) presents potential resource problems for the U.S. should these materials continue to be withdrawn from the economy.

Table 3.3. ROM Costs of Refabrication Option

Cost Category	Cost ($K)
Labor	4,440
Materials	12,780
Refabrication Equipment	2,700
Shipping*	400
Disposal*	400
	$20,720

*The ROM estiamte of the cost for shipping and disposal of the high-activity portion and degraded materials is $800,000, based upon the analysis described in Section 3.4.

Previous reports [BAKER, CONN-1976] have identified this as a key problem in the development of a fusion economy.

This section discusses the processing of the materials from the STARFIRE toroidal field (TF) magnets and returning as much of the materials as possible to the fusion system. Based on reasonable projections of construction capability/load demand, the buildup of a fusion economy was assumed to take place over a period of approximately forty years and as the plant lifetimes come to an end, it was assumed that four reactors per year would have to be decommissioned. These assumptions are used only to size the typical reprocessing equipment and plant requirements. Though the present results are not highly sensitive to the assumptions, the assumptions are important from a plant utilization/capital cost recovery perspective. Table 3.4 presents the amounts of major materials involved in the processing of the TF coils from four fusion reactors per year and how these quantities relate to the United States' annual production of these materials. Table 3.5 presents the total quantities involved in relation to the U.S. resource base. It must be pointed out that the quantities presented in Tables 3.4 and 3.5 are probably low by at least a factor of two if the total plant inventory of materials were considered, i.e., including the nonfusion portion of the plant.

Table 3.4. Comparison of Annual Metals Recovery from the TF Magnets of Four STARFIRE Reactors with U.S. Production and Consumption. (Units of 1000 tonnes per year.)

	STARFIRE Economy	U.S. Annual Consumption	U.S. Annual Production from Ore and Scrap	U.S. Total Production	STARFIRE Economy as a Percent of Total Production
Cu	6.389	2,250	1,780	1,785	0.36
Fe	6.38	79,800	52,000	79,000	---
Mo	0.013	30	60	60	0.02
Cr	0.886	534	43	54	2.1
Ti	0.078	17	N/A	15	0.52
Mn	0.60	1,280	$\sim$0	110	0.55
Ni	0.48	210	47	79	0.61
Sn	0.06	247	$\sim$0	23	0.27
Nb	0.3	3	0	3	10

Table 3.5. Materials Requirements and Estimates of Reserves(a) (Reproduced from [BAKER])

(Units of 1000 Tonnes)

Element	STARFIRE Maximum Requirement,[b] 100 Reactors	U.S. Production		U.S. Consumption	World Production (1976)	Reserves at Present Prices		Reserves at 3 Times Present Prices[c]		Principal Present Sources
		From Domestic Ores & Scrap	Total Production			U.S.	World	U.S.	World	
Al	46	960	4,350	5,380	13,860	8,500	5,450,000	~5,000,000	Very Large	Australia, Guinea, Jamaica
B	66	207	207	118	390	~28,500	~124,000	Very Large		U.S.A., Turkey
C	167									
Cr	124	43[e]	43[e]	~534	3,180	None	11,000,000	7,300	20,000,000	S. Africa, U.S.S.R., Albania
Nb	10	0	3	3	11	None	10,000[d]	~60	>20,000	Brazil, Canada, Malaysia
Cu	219	1,780	1,785	2,250	7,620	107,000	~500,000	No data	No data	U.S.A. Chile, Zambia, Zaire
Fe	1,590	52,000	79,000	79,800	485,600	>10,000,000	100,000,000	>20,000,000	Very Large	(Iron Ore) U.S.A., Canada, Venezuela
Pb	38	1,026	1,090	1,440	3,506	26,000	157,000	>40,000	>500,000	Canada, Mexico, Peru
Li	187	~6	~6	3.9	NA	450-600	2,000	2,500	>10,000	U.S.A.
Ti	185	NA	15	17	46	17,700	235,000	Large	Very Large	Australia
Mn	190	Small	110	1,280	10,190	None	>14,000,000	>30,000	>20,000,000	Gabon, Brazil, S. Africa, Australia, U.S.S.R.
Sn	2	Small	23	49[f]	247	740	10,000	No data	720,000	S. E. Asia, Malaysia, U.S.A.
Mg	0	~100	~100	~100	140	Inexhaustible				
V	1	5.3	5.3	7.2	32	113	10,000	600	20,000	U.S.A., S. Africa, U.S.S.R.
Ni	127	47	79	210	588	180	54,000	12,700	136,000	Canada, New Caledonia, U.S.SR.
Zr	28	NA	NA	<3	<6	3,550	18,000	No data	Very Large	U.S.A., Australia
U	84	4.1	10.2	9.3	43.0	125	1,990	No data	No data	China, U.S.A., Bolivia, Thailand
Mo	9	60	60.0	30.0	98.0	4,500	9,300	27,000	No data	U.S.A., Canada, Chile
Co	0	0.3	0.3	8.5	30.8	None	72,600	No data	No data	Zaire, New Caledonia, Australia
Be	1	<0.1	<0.2	<0.1	<0.3	28	380	55	No data	U.S.A., Brazil, S. Africa

[a] Information on U.S. and World production and consumption are from the U.S. Bureau of Mines. Information on reserves is partly from the U.S. Bureau of Mines, partly from Brobst and Pratt, and partly from other miscellaneous sources.

[b] Reactor only.

[c] Includes reserves at present prices.

[d] Reserves in non-Communist countries only.

[e] From stainless steel scrap.

[f] Primary

From the activity levels of the toroidal field (TF) magnet materials, it was determined that the majority of the materials present in STARFIRE could be recycled for reuse if they were blended with normal (nonradioactive) scrap and virgin material. Based on the biological hazard potential (BHP) information given in Table C-2, it was assumed that if the BHP were less than about 10, that it would be possible to blend this material with normal material to produce an acceptable product.* At the present time there is no mechanism for returning radioactive materials to normal commerce forcing all recycling activities to be carried out in controlled facilities. These calculations are detailed in Appendix I and indicate that over 90% of the magnet materials can be recovered except for the Nb_3Sn. For the Nb_3Sn, recovery of 89% of the material can be accomplished either by accepting a high dilution or relaxing the BHP requirements.

With the stricture against returning radioactive materials into normal commerce currently in place, dilution of the radioactive material with non-radioactive material increases the amount of material to be processed and in inventory. As the fusion economy matures there is a potential place for this material in additional reactors. But in a mature fusion economy, such an increase in the amount of magnet material will yield a surplus of magnet materials. What is necessary then is to establish techniques for reprocessing and recycling magnet materials without dilution.

3.3.2 Dismantling and Preparation for Chemical Processing

3.3.2.1 Disassembly at Reactor Site

As was the case for the Remote Refabrication option, the dismantling and preparation for chemical processing task attempts to minimize the number of steps that must be performed remotely, thereby reducing the amount of labor and associated cost. Because it is extremely difficult and expensive to transport the intact TF coil/helium vessel magnets owing to their large size and mass [MOORE], each will be partially dismantled inside the reactor building before being shipped to the processing facility.

*This acceptable product is defined as one whose radioactivity concentration (Ci/cm^3) is below the standards established in 10 CFR 20.

The TF coil/helium vessel assembly is separated from the reactor and the high-activity inboard portion of each magnet is removed following the same procedures outlined previously under Section 3.2.4. Though the materials are potentially recyclable, this separation is performed to minimize dose levels to personnel. While inside the reactor building, each magnet is placed by a crane onto a large, specially-designed lay-down fixture. This fixture, shown in Fig. 3.4, has 46* thin discontinuities through which the magnet can be cut into smaller pieces with a traveling band saw.

The traveling band saw moves from discontinuity to discontinuity on tracks that are just outside of the lay-down fixture. The saw features automated, numerical controls to specify the depth and speed of the cut. It is not possible to use oxygen cutting for this application owing to the large air gaps in the magnet which would cause torch pop-out [GRAHAM].

The traveling band saw cuts the magnets into 46 pieces that are approximately 0.89 m x 2.16 m x 1.6 m and have a mass of 10,910 kg each. Because the strength of the G-10CR conductor interturn and interlayer insultion will be reduced from radiation exposure, the conductor support modules and individual windings will not be strongly constrained. Furthermore, there is no mechanical attachment between the conductor, support strips, and side strips. Therefore, to prevent the internal magnet components from falling out during shipping, temporary end caps will be tack welded onto the ends of each magnet piece and onto the sides of the low-activity pieces.

The pieces will be shipped to the processing facility in the same containers and using the same methods described in Section 3.4.4, Packaging, Transportation, and Disposal.

*The number of magnet sections is determined from packaging and shipping considerations as discussed in Section 3.4.4.

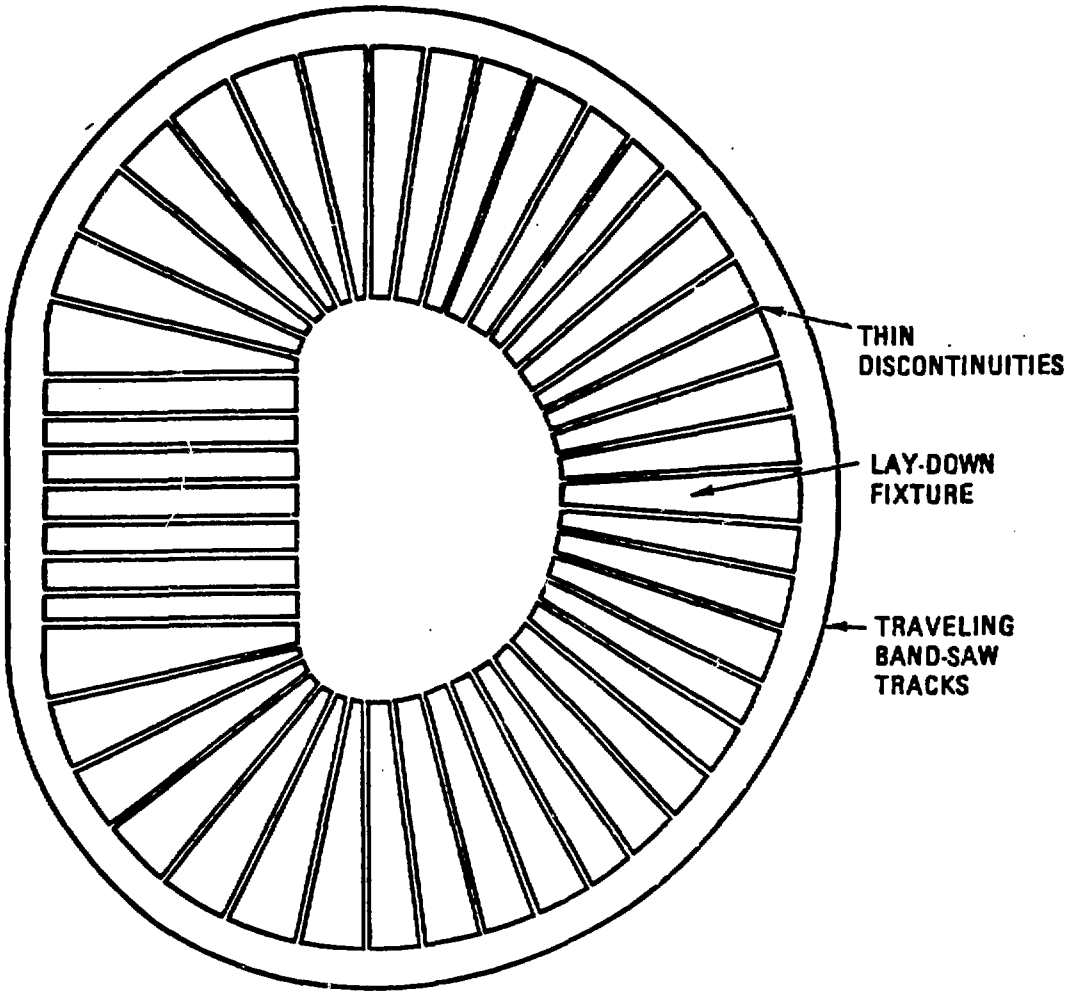

Fig. 3.4. Lay-down fixture with thin discontinuities.

3.3.2.2 Disassembly at Reprocessing Site

Upon receipt of the container at the processing facility, the magnet pieces will be removed from the container using handling lugs permanently attached to the end caps. The magnet pieces are placed by a crane onto a handling jig and secured. The end caps are removed with a plasma torch and returned to a new reactor plant for reuse.

The handling jig is hydraulically angled toward a moving conveyor belt. By restraining the dewar and helium tank, the internal magnet components can be pushed onto a conveyor belt where they are arranged in a linear manner and sorted by width. As can be seen from Figs. 9-5 through 9-7 in [BAKER], each of the four types of conductor used is unique in its dimensions, making sorting of the four conductor types and the stainless steel a relatively simple task to automate.

Following ejection of the internal components from the helium tank, the Fe 1422 dewar will be separated from the stainless steel helium tank by cutting through the dewar and the tiebar tensioning rods on both sides with a plasma cutting torch. At this point the vacuum tank and the helium vessel are separated with a crane, the G-10CR tiebars are unbolted from the dewar, and the G-10CR insulation is separated from the dewar and the helium vessel. All the G-10CR is sent to a waste disposal site.

After separation, the Fe 1422 vacuum tank is crushed and bundled with other Fe 1422 portions and placed in a container for shipping. The helium tank portion is also crushed and bundled with the conductor interlayer support strips and side supports of stainless steel and placed in a container for shipping.

It is expected that there will be at least 82 lead-tin soldered joints in each of the 12 magnets. These joint zones will be approximately twice the height of the normal cable, making them easy to identify. It may be necessary to do this sorting by eye because the exact location of the joints will not be known. Furthermore, thickness change will not be abrupt, but change slowly over about 300 mm and in addition, the solder may run into areas where the conductor has the normal thickness.

3.3.3 Cooling and Storage Requirements

As described in Section 3.1, it is anticipated that the decommissioning of the fusion reactor will not commence earlier than one month following shutdown. An inspection of Table C-3 indicates that having removed the high contact dose sections of the TF magnets shown in Fig. G-1, there is little change in the contact dose of the remaining sections for times even up to 10 years. There is, therefore, no reason to delay shipping and processing while waiting for radioactive decay to lower the contact dose. From a practical standpoint, it is not expected that the processing will occur before one year after shutdown. Therefore, the BHP at one year shown in Table C-2 was used to compute dilution factors.

The decay afterheat of the various zones of the TF magnets are shown in Table C-4. Even the highest afterheat source, the inner dewar (which is removed prior to processing), is less than 0.1 W/m^3 (at times longer than one month). Therefore, no special storage or heat removal is necessary as normal room ventilation will easily accomplish the necessary cooling.

3.3.4 Chemical Processing

3.3.4.1 General

It is assumed that the NbTi-containing wire in the conductor contains the NbTi in filaments approximately 10 μm in diameter in a copper matrix. The Nb_3Sn-containing wire is assumed to have been formed in place after the winding of the subcables by diffusion of Sn from a bronze matrix to yield the brittle Nb_3Sn. The Nb_3Sn is thus in a tin depleted bronze matrix. The bronze matrix is coated with tantalum and the entire tantalum-coated multifilamentary Nb_3Sn is in a copper matrix [GREGORY]. This inclusion of tantalum significantly complicates the reprocessing scheme. The tantalum serves as a barrier to prevent the continuous diffusion of tin from the bronze matrix into the surrounding copper, as this would eventually deplete the Nb of its Sn. Thus, a manufacturing or design technique which would remove the Ta barrier requirement would result in simplifications of the reprocessing.

3.3.4.2 Chemical Processing

The conductor cables will be divided into three groups by mechanical sorting, (1) conductor cables containing NbTi, (2) conductor cables containing Nb_3Sn, and (3) soft lead-tin soldered joints. The processing of each of these groups is discussed separately. For reference, the elemental compositions of the NbTi and Nb_3Sn conductors are shown in Tables 3.6 and 3.7.

Table 3.6. NbTi Cable Composition

Element	Tesla Region (wt. %)			Composite All Regions	
	7 to 9	5 to 7	0 to 5	wt. %	Mg
Cu	88.5	92.5	96.5	93.5	1023.8
Nb	6.2	4.0	1.8	3.4	37.2
Ti	5.3	3.5	1.7	3.1	214.0
Total	100.0	100.0	100.0	100.0	1275.0

Table 3.7. Composition of Superconducting Nb_3Sn

Element	Wire (wt. %)	Cable (wt. %)
Cu	73.3	80.4
Ta	7.3	5.4
Sn	4.4	3.2
Nb	15.0	11.0
Total	100.0	100.0

Processing NbTi Conductor. The processing of the NbTi conductor follows the basic practice used currently in electrorefining of copper. The conductor will be placed in a titanium anode basket [JACOBI] and then placed in an electrolytic cell.* The copper in the anode basket is dissolved in acidic copper sulfate electrolyte and the copper is plated onto a pure copper cathode sheet.

The cells normally operate between 175 to 230 A/m^2 at 0.2 to as high as 0.39 volts dc, with copper concentrations of 30 to 50 g/L at 55° to 65°C [KIRK-OTHMER-1979]. The electrolyte is circulated and purified to control the concentration of copper and impurities by electrowinning in cells similar to normal electrorefining cells. In electrowinning operations, the copper is deposited at the cathode and sulfuric acid is produced at a lead anode.

The NbTi filaments will thus remain behind in the anode basket or in the slimes in the electrolytic cells and it will simply be flushed from the cells, filtered, washed, and dried. At this point, the NbTi alloy should be suitable for recycling.

Processing of Nb_3Sn Conductor. The Nb_3Sn cable will undergo the same initial step as the NbTi cable, that is the electrolysis of the copper material. This step will continue until the tantalum coating on the bronze matrix containing the Nb_3Sn has been exposed.

At this point, the remaining material must be treated to remove the inert tantalum coating. Following a standard step in the preparation of pure tantalum [KIRK-OTHMER-1965], the tantalum will be hydrided in a hydriding furnace to convert the tantalum into the very brittle tantalum hydride. The material on leaving the furnace will be cooled, then tumbled to ensure that all the tantalum is cracked off the bronze substrate and washed to remove the hydride. The tantalum hydride may be used to obtain metallic tantalum. The washing water will be filtered and recycled.

*Alternatively, the copper containing NbTi could be vacuum melted and cast into anodes. This would increase the efficiency of the cells and could allow for some preliminary refining.

The Nb_3Sn in the bronze matrix will then proceed to another electrolysis cell to have the remaining copper removed. The electrolysis cell will remove the tin from the bronze, but not from the Nb_3Sn, depositing the tin in the cell slimes in the bottom of the cell. The Nb_3Sn and any pure Nb will then be sent for removal of Nb as in standard metallurgical practice [KIRK-OTHMER-1979].

Processing of Soldered Joints. The soldered joints will be sorted into three types, those between NbTi cabling, those between Nb_3Sn cabling, and those between NbTi and Nb_3Sn cabling. Joints whose type is not clearly identifiable, such as joints which have been partially destroyed during the magnet cutting operation, will be combined with the Nb_3Sn joints.

Joints in NbTi cabling will be placed in a container and sent to a desoldering furnace which is held above the melting point of the lead-tin solder, about 260°C. The solder will flow from the container containing the cabling and into a recovery vessel within the furnace. The solder will be withdrawn as required and cast into ingots to be recycled for fabricating other magnets. After this step, the NbTi cabling can be processed in the same manner as the other NbTi cable.

Joints between NbTi and Nb_3Sn cable, unidentified joints, and Nb_3Sn joints, will be desoldered as above. The cable from this step will then be batch-processed in an electrolysis bath in the same manner as the Nb_3Sn cable. The resulting scrap can be sent to a niobium refining step operating in a controlled environment along with the material from the recovery of Nb_3Sn cable.

3.3.5 Cost Estimates

3.3.5.1 General

The processing plant, as envisaged, operates as a scrap-sorting plant and as a plant directly electrorefining copper from scrap. Because of the need to dilute the scrap iron-based product and the copper with scrap from normal sources, it may be desirable to locate

the plant close to facilities that normally process materials such as stainless steel and Fe 1422 scrap. The processing plant would be operated by and could also be located adjacent to a producer of copper wirebar produced from scrap and electrolytic copper. The preliminary indications from this work are that the product produced by the plant processing STARFIRE magnet material could be equal or better than conventional electrolytic copper. The proposed plant would produce about 6400 T/yr of copper, or about one-tenth the amount of a primary copper-producing plant. This amount would represent about 0.4% of the copper produced currently in the United States and about 3% of the scrap processed. Therefore, this plant would not have a large effect on the copper market.

3.3.5.2 Capital Cost Estimate

An overall cost estimate was developed for processing the TF magnet material from four STARFIRE reactors per year using a 90% stream factor for the plant. The development of the building area for the plant facilities is shown in Table 3.8.

As can be seen from Table 3.8, approximately 51% of the plant area, less warehouse, is devoted to shipping, receiving, and container handling. Approximately 13 trucks per shift, containing two magnet sections per truck, are unloaded. The containers are opened, unloaded, refurbished if necessary, and returned to the reactor on the trucks.

The other major plant area, electrolysis and electrolyte control, was based upon 40 cells operating, 44 cells installed and producing 160 x 10^3 kg/yr each. Each cell occupies a floor area 4.16 m x 1.09 m and is approximately 1.2 m deep; an additional 11% of the cell area was added for bus bars. The overall cell area for electrolysis was then doubled to allow for anode and cathode handling. It was assumed that the area for electrolyte control would be approximately equal to that for electrolysis.

The process equipment costs are presented in Table 3.9 and are about 28% greater than the building cost.

Table 3.8. Space Requirements and Cost

Operation (Dimensions)	Area (m^2)
Truck Receiving Bays (16 at 6.11 x 12.2 m)	1,200
Truck Wash Down (2 at 6.11 x 12.2 m)	150
Container Opening Area (7.64 x 97.9 m)	750
Container Repair Area (7.64 x 18.3 m)	140
Magnet Cutting Area (10 x 10 m)	100
Sorting Area (6.11 x 18.3 m)	110
Electrolysis Cells and Electrode Stamping (44 cells x 5.05 m^2/cell x 2)[a]	450
Electrolyte Control	450
Desoldering Furnace	60
Crushing and Bundling	280
Shipping	600
Air Conditioning and Filtering	400
Change Rooms	400
Administrative	400
Warehouse	1,600
TOTAL AREA	7,090[b]
Cost at \$1065/m^2	7.55 x 106

[a]KIRK-OTHMER-1965.

[b](75,800 ft^2).

Table 3.9. Processing Equipment Costs[a]

Equipment	Cost ($ x 10^6, 1982)
Electrolysis Cells (44 at $100,000/cell)	4.4
Electrolyte Control	1.5
Desoldering Furnace	0.4
Crushing and Hydriding	0.5
Container Handling (16 x $100,000/station)	1.6
Cutting and Sorting	1
Power Supply (162 kW at 0.2 V dc)	0.3
TOTAL COST	9.7

[a]Includes installation.

3.3.5.3 Operating Costs

It was estimated that approximately 25 people per shift would be required to operate the plant on a three shift per day, seven day per week basis. This labor cost is almost 50% of the plant operating cost presented in Table 3.10. A factor of 0.2 was used to recover capital costs and pay for taxes and insurance. An administrative cost of 10% of labor cost was used.

Other costs such as dismantling and disposal costs are presented in Table 3.10. These are costs which should be considered in performing an overall economic evaluation. The assignment of these costs to various operating centers is open to question. In evaluating the economics of material processing, the only one debited to the processing plant however, and this possibly should be debited to reactor operation, is the shipping of processing plant waste to disposal and its disposal. The majority of this waste, as shown in Table 3.11, is associated with material from the magnet which has no recycling value, such as the mylar insulation, G-10 cable insulation, and G-10 tie bars. The majority of this cost could be debited to the reactor. However, in evaluating the overall economics of the processing option, this cost, as well as that of reactor dismantling and shipping, must be included, as shown in Table 3.10.

Table 3.10. Production Cost for Processing Four STARFIRE Reactor Magnets Per Year (in 1982 Dollars)

	10^6 $/yr
Facility Cost (0.2 x Capital Cost)	1.51
Equipment Cost (0.2 x Capital Cost)	1.94
Labor (25 people/shift, $30/hour)	6.00
Administration	0.60
Utilities, Chemicals and Supplies	0.50
Waste Shipment to Disposal Site and Disposal[a]	3.10
TOTAL	13.65

Reactor Dismantling and Shipping to Processing
(Not Charged to Production)

Dismantling Cost	3.60
Shipping and Disposal of High-Activity Material	0.32
Shipping (Reactor to Reprocessing)	1.44
Containers[b] (Reactor to Reprocessing)	0.37
TOTAL	5.73

[a]Facility is assumed to be near users of product; therefore, no shipping costs to their respective sites are included.

[b]Assumes containers last for 12 round trips.

Table 3.11. Waste Shipping from Reprocessing Facility (Four Reactors Per Year)

Mylar Insulation	$ 247,500
G-10 Insulation	250,500
G-10 Tie Bars	1,092,000
Process Plant Waste	25,000
Truck Trips	128,600
Burial Cost	1,358,000
TOTAL	$3,101,600

3.3.5.4 Operating Revenue

Table 3.12 presents the expected revenue compared to the annual cost given in Table 3.10. The expected net profit from this operation is $7.2 million per year. A conservative approach has been taken in estimating the annual revenue. The annual revenue from the copper sold could be $2.74 million higher annually, if the copper product can be sold at cathode plate price. The prices quoted for NbTi and Nb_3Sn are only approximations at this time. The net profit for the dismantling option is $1.4 million for the four reactors. Thus, reprocessing of the STARFIRE TF coil materials can essentially be used to cover the decommissioning costs associated with the magnets.

3.4 Disposal

3.4.1 Introduction and Disposal Philosophy

This section presents the issues and requirements associated with the disposal of the irradiated, superconducting TF coil magnets from a STARFIRE fusion plant [BAKER]. The aim is to carry out the disposal in the most practical and economical manner, while complying with all existing or anticipated regulations relating to radioactive waste packaging, shipping, and land burial. In evaluating the disposal

Table 3.12. Summary Cost and Revenue Sheet Processing Four STARFIRE Reactor Magnets Annually

Annual Cost (Table 3.10, $ x 10^6, 1982)				-13.65
	Potential Annual Revenue ($10^6/yr)			
	Annual Product Rate (kg)	Recovery Factor	Selling Price ($/kg)	Revenue ($10^6/y)
Copper	6,386,400	0.982	1.155[a]	7.243
304 SS	13,713,600	0.976	0.594[b]	7.960
Fe 1422	4,175,600	0.930	0.154[c]	0.597
NbTi	228,160	1.000	12.21[d]	2.786
Nb_3Sn	204,040	0.890	12.21[d]	2.217
TOTAL				20.803
NET PROFIT from Reprocessing Operations Only				7.15
Additional costs associated with magnet dismantling and shipping to reprocessing site				5.73
NET PROFIT of Reprocessing Option				1.42

[a]Price for refiners' copper scrap could be as high as cathode full plate price, $1.584/kg.

[b]Consumer buying price for 18-8 bundles, solids.

[c]Consumer buying price for 410 bundles, solids.

[d]Estimated to be equal to Ti sponge.

NOTE: Price source is American Metal Market/Metalworking News, issue of August 2, 1982.

option, it is assumed that all the materials from the TF coils are to be discarded. The desirability of selectively recycling some of the materials is described in Section 3.3.

The approach adopted achieves the goals of simplicity, ease of operation, and cost minimization. The magnet coils are first cut across their trapezoidal cross-section into nominally 46 pieces, each with dimensions of 0.89 x 1.6 x 2.16 meters, and weighing about 10,900 kg (∿12 tons). Details of the dismantling operations are provided in Section 3.4.2. Each of the cut sections, containing the inner and outer helium vessels, and the inner and outer high and low field magnets, is then packaged as one unit in a structurally-adequate wooden container, suitable for shipment. Two packaged units are shipped on one truck, in a sole-use carrier. The items classify as low specific activity (LSA) materials for shipping purposes [49 CFR 173]. The waste packages, in their wooden shipping containers, are categorized as Class A waste and are buried in accordance with proposed 10 CFR 61 regulations. Further details of the packaging, transportation and waste disposal operations are provided in Section 3.4.4.

3.4.2 Dismantling and Preparation for Disposal

To simplify and thus reduce the cost of the task of dismantling and preparation for disposal, the high-activity and low-activity portions of the TF coil/helium vessel magnets will not be separated as in the previous two options. Instead, the magnets will be cut into pieces across their trapezoidal cross-sectional width. This approach is possible owing to the overall low activity level of the magnets.

The TF coil/helium vessel assembly is separated from the rest of the reactor by the same procedure outlined in Subsection 3.2.4.1, Remote Dismantling. Once the magnets are removed from the centerpost, they are placed by crane onto a large, specially-designed lay-down fixture with 46 thin discontinuities. This fixture is described in more detail in Section 3.3.2, Dismantling and Preparation for Chemical Reprocessing, and shown in Fig. 3.3.

As in the dismantling step for the reprocessing option, each magnet is cut with a traveling band saw into 46 pieces of approximately 0.89 m (2.9 ft) x 2.16 m (7.1 ft) x 1.6 m (5.3 ft)* and having a mass of 10,900 kg (~12 tons). The band saw moves from discontinuity to discontinuity on tracks that are just outside of the lay-down fixture. This task is more difficult than in the reprocessing option because it must be done entirely remotely.

After cutting up the main magnet, the common inner dewar that was initially removed from the centerpost is cut into 0.89 m long pieces with a plasma torch attached to the Reactor Overhead Electro-Mechanical Manipulator. The pieces cut by the band saw and plasma torch are then moved using the 60-Tonne Reactor Building Bridge Crane.

3.4.3 Cooling and Storage Requirements

A minimum cooling/decay time of one year is adequate prior to packaging, shipping, and waste burial. As discussed in Section 3.1, most of the short, half-life radioactivity will have decayed in this time, with further activity reductions not being very time effective. In addition, considering the approvals, authorizations, etc., which are required, the removal of external hardware to gain access to the magnets, and the setup of special equipment for their dismantling, cooling times much less than one year after plant shutdown are not foreseen.

From a practical standpoint, decay cooling of the TF coils during decommissioning will occur in-situ for most of the time and in a storage area, after dismantling from the reactor, for a relatively shorter period of time. Storage of the large magnet sections will be carried out in the maintenance area of the building.

Assuming 12 x 46 = 552 TF coil sections and an estimated eight comparable packages from miscellaneous magnet metal portions

*Approximately mid-coil, cut section length, as scaled from the coil/helium vessel dimensions of Fig. 9-2 [BAKER]. Height of piece determined from weight limitations on packaging and shipping as discussed in Section 3.4.4. This results in 46 sections per TF coil.

(e.g., bottom vacuum tank section, as indicated in Figs. 2-3 and 9-1 in [BAKER]), it is estimated that two areas totaling about 262 m^2 (~2820 ft^2), could satisfy the storage requirements. These areas could accommodate about one week's storage for each of the packaged and unpackaged TF coil sections. No consideration was given toward crushing the sections for volume reduction purposes, though this could lead to further economies (e.g., for waste burial).

Assuming a conservative 0.86 m (2.5 ft) space between the nominally 1.60 m (5.3 ft) x 0.89 m (2.9 ft) magnet pieces, about 126 m^2 (1358 ft^2) are needed for one week's shipping supply of 28 TF coil sections waiting to be packaged.

The second storage area, also accommodating about one week's shipping supply (28 magnet sections), is available for the packaged TF coil sections. This area, about 136 m^2 (1463 ft^2), is somewhat larger than that needed for the items which have not yet been packaged, due to the addition of the wooden box portions. In addition to the large bulk magnet pieces there will be a relatively large quantity of metal shavings generated during the dismantling operation. This material will be packaged in 0.2 m^3 (55 gal) drums and can be stored on a pallet within an area of about 6 m^2 (64 ft^2). The storage area for the packaged crates and the 0.2 m^3 (55 gal) drums should preferably be located close to the loading dock of the building.

The extremely low decay afterheats will present no cooling problems during either storage or shipping, and therefore no special insulation or cooling will be necessary. Normal room ventilation will easily accommodate the removal of this very low afterheat (i.e., about 0.6 mW, or 0.002 BTU/h, per 12 ton magnet piece).

3.4.4 Packaging, Transportation, and Disposal

3.4.4.1 Packaging

The packaging operation begins in the maintenance area where up to two weeks' supply of magnet sections (up to 56 "pieces") are stored, following dismantling and transfer from the reactor location.

There is no need for crushing operations, no disassembly operations, no segregation process, etc. Thus, a large compact piece would be available for packaging. This will minimize the amount of hand-contact or expensive remote-operating equipment which might be necessary to handle the magnet sections of low activity. The general philosophy is to package the magnet sections in containers suitable for both shipping and waste burial.

Table 3.13 presents the radioactivity concentrations, the contact biological doses and the decay afterheats of the magnet components. These data provide the bases for categorizing these items as low specific activity (LSA) materials [49 CFR 173] for shipping purposes and Class A materials [10 CFR 61] for waste burial purposes. In other words, the magnet components are of low enough radioactivity to be classified in the least restrictive category for shipping and for waste burial. This is discussed in more detail in Subsections 3.4.4.2 and 3.4.4.3. It should be noted that data in the table are associated with a full magnet; since the magnet is cut into 560 pieces, the data for each shipping/burial package is scaled accordingly.

It is likely that the services of an outside contractor can be used for the packaging task. This company would have special expertise in rigging, strapping, boxing, etc., and would provide all needed (box) materials. Personnel would be familiar with all labeling, packaging, shipping and waste burial regulations. A significant portion of the crate could be prefabricated. Packaging operations, for a single magnet section, could be accomplished in a floor area of about 14 m^2 (150 ft^2). An estimate of $1500 (1982 dollars) has been assumed to package one magnet section, including the cost for raw materials and labor for box-prefabrication, labeling, final crating and loading, radioactivity monitoring, and securing on the truck for shipment.

The radioactivity levels per magnet section are low and no remote handling operations are deemed necessary. However, close hands-on operations over extended periods of time will be avoided to minimize dose levels to operating personnel.

Table 3.13. Radioactivity, Contact Biological Doses, and Afterheats of TF Magnet Components, One Year After Reactor Shutdown[a]

Reactor Component	Volume (m^3)	Weight (tonne)	Radioactivity		Contact Biological Dose (rem/hr)	Decay Afterheats		
			curies ($\times 10^6$)	Ci/m^3 ($\times 10^6$)		(MW/m^3)	(MW)	(Btu/hr)
IMAG-DWR Fe 1422	8.80E+00	6.99E+01	3.54E-04	4.02E-05	1.59E+00	2.70E-08	2.38E-07	8.12E-01
OMAG-DWR-Fe 1422	1.23E+02	9.74E+02	1.62E-07	1.32E-09	3.18E-05	6.25E-13	7.69E-11	2.63E-04
IMAG-HET 304 SS	1.51E+01	1.19E+02	2.10E-04	1.39E-05	3.72E-01	6.89E-09	1.04E-07	3.55E-01
OMAG-HET 304 SS	1.28E+02	1.00E+03	1.22E-07	9.57E-10	1.23E-05	3.06E-13	3.92E-11	1.34E-04
IMAGNET1 Copper	6.55E+00	5.86E+01	1.23E-06	1.88E-07	4.39E-02	6.18E-10	4.05E-09	1.38E-02
304 SS	5.65E+00	4.45E+01	9.81E-06	1.74E-06	3.12E-02	6.70E-10	3.79E-09	1.29E-02
Nb_3Sn	6.83E-01	5.41E+00	1.51E-06	2.21E-06	1.88E-03	3.77E-11	2.57E-11	8.77E-05
G-10	6.26E-01	1.18E+00	1.81E-14	2.89E-14	0.0	3.22E-18	2.02E-18	6.90E-12
IMAGNET2 304 SS	2.54E+01	2.00E+02	2.84E-07	1.12E-08	5.20E-05	2.46E-12	6.25E-11	2.13E-04
Copper	1.24E+01	1.11E+02	3.35E-09	2.71E-10	6.38E-05	8.99E-13	1.11E-11	3.79E-05
NbTi	9.37E-01	6.04E+00	2.40E-09	2.57E-09	9.62E-06	2.52E-13	2.36E-13	8.06E-07
G-10	2.82E+00	5.31E+00	1.20E-15	4.27E-16	0.0	4.75E-20	1.34E-19	4.57E-13
OMAGNET1 304 SS	4.76E+01	3.75E+02	1.88E-08	3.95E-10	1.19E-06	7.87E-14	3.75E-12	1.28E-05
Copper	5.53E+01	4.94E+02	2.70E-10	4.88E-12	1.09E-06	1.54E-14	8.52E-13	2.91E-06
Nb_3Sn	5.76E+00	4.56E+01	5.95E-09	1.03E-09	8.95E-07	1.70E-14	9.79E-14	3.34E-07
G-10	5.27E+00	9.92E+00	8.86E-17	1.68E-17	0.0	1.87E-21	9.85E-21	3.36E-14
OMAGNET2 Copper	1.04E+02	9.33E+02	1.40E-12	1.34E-14	3.12E-09	4.39E-17	4.57E-15	1.56E-08
304 SS	2.14E+02	1.69E+03	9.63E-10	4.49E-12	4.88E-09	7.87E-16	1.68E-13	5.74E-07
NbTi	7.90E+00	5.10E+01	4.99E-12	6.31E-13	3.72E-09	9.50E-17	1.70E-16	5.80E-10
G-10	2.38E+01	4.48E+01	4.65E-18	1.95E-19	0.0	2.18E-23	5.19E-22	1.77E-15
Total	9.30E+03	6.24E+03	5.77E-04	--	2.04E+00	--	3..50E-07	1.19E+00

Average radioactivity level = $[5.77 \times 10^{-4})(10^6)(10^3)]/(6.24 \times 10^9)$
= 9 × 10-5 millicuries/gram .

[a] Data are for entire magnet, 12 TF coils, of STARFIRE reactor.

For each magnet section, the shipping crate with appropriate supports is estimated at 2.5 m (8.1 ft) x 1.9 m (6.3 ft) x 1.2 m (3.9 ft), with a volume of about 5.6 m^3 (200 ft^2). The metal shavings generated during the dismantling operations and weighing approximately 4540 kg (10,000 lb) will require fifteen, 0.2 m^3 (55 gal) drums, assuming a settled material density of about 1602 kg/m^3 (100 lb/ft^3) and allowing about 10% freeboard volume in each drum. These metal shavings would not present any pyrophoricity problems.

3.4.4.2 Shipping

The following guidelines have been used as obtained from industry sources [TRUCK-TRAILER] and GA specialists [BURGOYNE] familiar with radioactive shipments:

1. A practical cargo weight of 22,680 kg (50,000 lb), including the weight of the container. This is based on a maximum gross vehicle weight of 36,300 kg (80,000 lb)* with a practical gross vehicle weight of 35,400 kg (78.000 lb).* In the current study, up to 454 kg (1000 lb) has been allocated per package for the weight of the wooden container and accessories needed to secure the box to the trailer bed.

2. Truck shipments must be no greater than 2.6 m (8.5 ft) high x 2.4 m (8 ft) wide x 10.7 m (35 ft) long. Though this provides considerable flexibility, the two waste packages would be positioned in such a manner as to obtain a uniform loading on the truck/trailer bed.

These guidelines and the relatively low radioactivity levels of the magnet components (see Table 3.13) permit them to be categorized as low specific activity (LSA) materials and allow them to be

*In Missouri and Illinois the maximum gross vehicle weight is 33,200 kg (73,000 lb), with a practical gross vehicle weight of 32,300 kg (71,300 lb).

packaged very modestly, e.g., in relatively inexpensive wooden containers [49 CFR 173]. Some of the important requirements for the LSA categorization and minimal packaging requirements include the following:

1. A (sole) exclusive use, closed vehicle will be used for transport.

2. There will be no loose, removable surface contamination.

3. The average radioactivity concentration must be less than 0.001 millicuries/g; as indicated in Table 3.13, the magnet's average radioactivity is less than 1/10 this value. Also, although not applicable to the STARFIRE magnets, the contribution from Group I (actinides) materials must be less than 1% of the total radioactivity.

4. The dose levels must be less than:

   a. 1000 mrem/hr, at 0.9 m (3 ft) from the external surface of the package,
   b. 200 mrem/hr, at any point on the external surface of the vehicle,
   c. 10 mrem/hr, at any point 2 meters (six feet) from the vertical planes projected by the outer lateral surface of the vehicle, and
   d. 2 mrem/hr, in any normal occupied position in the vehicle.

Thus, in theory, packaging is not required for shipping; however, it is required for land burial [10 CFR 61].

The above criteria established the size of the TF coil (magnet) sections to be used for shipping and land burial, and dictate the size of the pieces to be handled during storage. Though half the number of pieces (i.e., 24 tons each, twice the specified weight)

might have been handled, this approach was rejected in favor of the lower, more conventional, weight; this could provide better balance on the truck, more convenient handling at the reactor and the land burial site, etc.

Most of the activity present in the STARFIRE magnet components, i.e., the specific isotopic radioactivity (Ci/cc) for the various magnet components, are of the soft beta type whose energies can readily be stopped by thin aluminum sheets (less than 1/8 in.). Such aluminum sheeting could be incorporated in the packing crates with no significant increase of the cost estimates; however, such measures will not be necessary for the direct disposal option. However, for the disposal of high-activity portions of the magnet required in the previous two options, thin metal shielding may be necessary. It is pointed out that no shielding analyses were carried out in this regard, especially to examine the decay chains for the existence of more penetrating gamma radiation. Estimates by a shielding specialist [SU] at GA suggest that the contact dose of the magnet sections should be reduced by a factor of 2 to 5 for distances of 0.9 m (3 ft) from their surfaces. Radiation attenuation by distance should permit attainment of regulatory dose limits.

For the nominal 560 packages to be shipped to the waste burial location, there would be two trucks loaded daily, each containing two magnet packages. Thus, four packages would be shipped daily (28 per 7 day week), so that about 20 weeks would be needed for the shipment of magnet waste to the burial site. An additional, single truck shipment would be needed to accommodate transport of the fifteen, 0.2 m^3 (55 gal) drums, containing the estimated 4540 kg (10,000 lb) of waste metal shavings. Commensurate with studies carried out for land disposal of radioactive waste [NUREG], it is assumed that the disposal site is 400 miles away and the radioactive waste is processed at the site on a first-come, first-served basis. It is further assumed that the waste is removed from the truck in less than one day, i.e., unloaded directly into a waste trench after temporarily waiting (hours) or unloaded at a temporary storage area for later trench loading. For 24-hour travel, at an

average 35 miles/hour, a round trip would take less than 2 days, so that about 4 trucks would be in use, at any one time. Two drivers are used per truck, incurring an added shipping cost, to permit vehicle travel for 24 hours/day.

Conceptually, two magnet sections are packaged each morning and two magnet sections are packaged each afternoon, but any of the four shipments can be initiated at any time of the day whenever a truck is available. The one week's storage, operating on a 7 day/week schedule, is included to accommodate temporary operational problems (up to several days).

3.4.4.3 Disposal

Waste materials from the STARFIRE magnets will be buried accordingly to the proposed criteria specified by [10 CFR 61], under detailed procedures described in [NUREG].

The amount of waste to be generated is about 5.6 m^3 (200 ft^3) per package or about 3,136 m^3 (110,750 ft^3) from the entire magnet. Additionally, less than 4 m^3 waste volume will be disposed of as metal shavings from the dismantling operations. Waste packages from the TF coil, buried over about a 20 week period, represent a little more than 6% of the annual volumetric capacity of a typical, land waste disposal facility intended to operate for 20 years [NUREG]. The typical trench size, expected to be about 180 m (591 ft) long, 30 m (100 ft) wide, and 8 m (26 ft) deep, will easily accommodate the expected waste shipments from the STARFIRE magnet. The density of the magnet waste packages may justify special handling procedures by the operator at the waste disposal facility, e.g., to load them at the bottom of the trenches to preclude damage to other waste disposal containers.

Radioactivity concentrations of each isotope in each magnet components, as defined by ANL [BAKER], were examined and compared with allowable radioactivity concentrations [10 CFR 61] to determine its waste disposal category. As defined in the proposed regulation, for a mixture of radionuclides, the sum of the fractions

obtained by dividing each nuclides concentration by the appropriate limit must not exceed 1.0, to permit the waste to fall into that specific classification (see Section 2.3.1). The isotope distribution of the radioactivity concentration in the TF magnet components is given in Table 3.14. The table shows that if the components were buried separately, they will all qualify for Class A shallow land burial. It is worthwhile pointing out that the "B" classification imposes no penalties (economic or otherwise) on its waste burial, other than a reuqirement for greater stability (than Class A waste), and this criterion is easily met by the characteristics of the magnet waste.

As mentioned previously, one day has conservatively been assumed for the waste to be handled at the disposal site. This can occur either by direct transfer of the magnet waste from the truck to the trench after a temporary waiting period (hours) or by waste unloading and storage at the burial site in the event of a large backlog of other customers, maintenance, or other problems at the site.

The waste, including its container, is buried at one of the site's trenches with complete location identification, records, etc., as required by the regulations [10 CFR 61].

3.4.5 Cost Estimate

Table 3.15 summarizes the costs associated with the waste disposal alternative for the irradiated TF coils from a STARFIRE fusion reactor after decommissioning. The total cost of this option is $3.43 million, in 1982 dollars. This is equivalent to about $1100/m^3 ($31.00/ ft^3) of waste.

Shipping container costs are estimated at $1400 ($1800 for a box with aluminum shielding) for each large magnet section. The cost for the 0.2 m^3 (55 gal) (lined) containers is about $26 [RAPPAPORT] each and one man-hour ($\sim$$50) is assumed to load and secure each drum onto a shipping carrier.

Table 3.14. Isotopic Distribution of the Radioactivity Concentration in the Magnet Components (Ci/m^3)

Nuclide	Magnet Component						Proposed 10CFR61 Maximum Radioactivity Concentrations[a]		
	Vacuum Vessel	Helium Vessel	Nb_3Sn Coil	NbTi Coil	Copper Stabilizer	G-10CR Insulation	Class A	Class B	Class C
C-14	9.3×10^{-4}	7.9×10^{-4}	--	--	--	4.9×10^{-8}	80	80	80
Ca-45	--	6.1×10^{-5}	--	1.5×10^{-5}	--	--	--	--	--
Sc-46	--	2.3×10^{-5}	--	3.0×10^{-6}	--	--	--	--	--
V-49	4.3×10^{-3}	8.4×10^{-2}	--	--	--	--	--	--	--
Cr-51	1.1×10^{-3}	4.1×10^{-3}	--	--	--	--	--	--	--
Mn-53	1.1×10^{-6}	2.1×10^{-7}	--	--	--	--	--	--	--
Mn-54	6.5	0.46	--	--	--	--	--	--	--
Fe-55	33.5	127.0	--	--	--	--	--	--	--
Fe-59	3.7×10^{-3}	--	--	--	--	--	--	--	--
Co-57	9.4×10^{-2}	--	--	--	--	--	--	--	--
Co-58	4.2×10^{-2}	--	--	--	--	--	--	--	--
Co-60	0.076	0.2	--	--	0.19	--	700	(b)	(b)
Ni-59	9.1×10^{-5}	2.6×10^{-4}	--	--	--	--	220	220	220
Ni-63	0.12	0.35	--	--	0.19	--	35.0	700	7000
Zr-93	--	--	3.69×10^{-7}	--	--	--	--	--	--
Zr-95	--	3.9×10^{-6}	--	--	--	--	--	--	--
Nb-93m	--	4.5×10^{-3}	0.65	5.0×10^{-3}	--	--	--	--	--
Nb-94	--	5.4×10^{-8}	0.0145	1.8×10^{-4}	--	--	0.2	0.2	0.2
Nb-95	--	8.8×10^{-4}	--	--	--	--	--	--	--
Mo-93	--	0.19	--	--	--	--	--	--	--
Tc-99	--	8.8×10^{-5}	--	--	--	--	3.0	3.0	3.0
Sn-123	--	--	0.11	--	--	--	--	--	--
Sb-125	--	--	0.32	--	--	--	--	--	--

(a) Activities without values do not have to be considered in assigning waste class. Such nuclides are Class A wastes.

(b) There are no limits for these nuclides in Class B or C wastes.

Table 3.15. Costs Associated with Handling the Waste From a Fusion Reactor's Superconducting Magnets for Ultimate Burial

Item	Costs per Reactor [$ × 10^6 (1982)] Direct Waste Disposal
Reactor Dismantling[a]	0.90
Cooling and Storage[b]	0.0
Shipping Containers[c]	0.84
Shipping[d]	0.36
Burial[d]	1.33
TOTAL	3.48

[a]Includes costs for cutting and removing magnet sections from the reactor and transferring them to the storage area.

[b]No cooling or storage costs; requirements assumed available in maintenance building.

[c]Includes cost for crate fabrication, waste packaging at the reactor or handling facility, and loading and securing the large magnet waste packages and 55-gal drums containing metal shavings onto the shipping vehicle.

[d]From [BARNWELL].

The shipping costs [NUREG], based on $1.14/round trip mile, are suitable for any one way distance between 400 and 1000 miles. There is an additional cost of $0.15/mile for a second driver as well as a fuel surcharge of 15% of the basic charge; an average fuel consumption rate of 6 miles/gallon is used in their calculations. It is assumed that truck weights are kept within legal limits so that overweight charges or overweight permit fees are not required.

Waste burial costs are a one time charge and currently are $12/ft^3 or $424/m^3 [BARNWELL].

The summary in Table 3.15 shows that a large portion (25%) of the disposal costs is related to the shipping containers. This cost also includes packaging, loading, and securing the waste onto the vehicle at the reactor site. This estimate deserves a more detailed analysis; this, in turn, requires a more definitive shipping container design.

APPENDIX A

Conversion of Decay Gamma Source to Dose

Determination of biological dose for each piece of reactor components is extremely difficult because of the varieties of the component sizes and shapes. An attempt is, therefore, made to provide a standardized technique of dose evaluation which is possibly independent of size and shape of test piece handled during radwaste management.

Figure A.1 shows the surface dose dependence of the four candidate alloys as a function of source size based on a one-dimensional spherical model. The transport calculation was performed by ANISN using a unit strength of 1 photon/cm^3-s for the uniformly distributed source. The dose conversion from the resulting surface flux is done based on the Clairborne and Trubey method [CLAIRBORNE] for photons normally incident on a 30-cm thick slab phantom. It is seen that all of the alloys examined exhibit a more or less identical trend on the surface dose variation, showing a quick dose saturation with test-piece volume. In fact, the contact biological dose for soft gamma-ray source does not show any appreciable variation with test-piece volume as clearly illustrated in Fig. A.2. Such a trend toward small variation with volume stems from the well-known characteristic of the self-shielding of gamma rays by the source materials themselves. The self-shield effect is particularly strong in high-Z materials as shown in Fig. A.1.

The results presented in Figs. A.1 and A.2 indicate that the biological surface dose is not overly sensitive to the size of the piece to be handled. In addition, the fact that the dose level tends to saturate for a reasonably large volume suggests a possibility of deriving an upper-bound dose estimate without going into details of the geometry of pieces to be handled.

The impact of gamma-ray source volume upon the surface dose is also examined by using a one-dimensional slab model and the result is shown in Fig. A.3. It appears that the trend of dose saturation is much more rapid than that of the spherical model previously studied, due to the presence of an infinite amount of test-piece materials in the present slab model. Also shown in Fig. A.3 is the case of 1-m diameter sphere for the sake of comparison. It is found that there is no appreciable difference in the saturated dose (for a reasonably large test piece) between the two geometrical models.

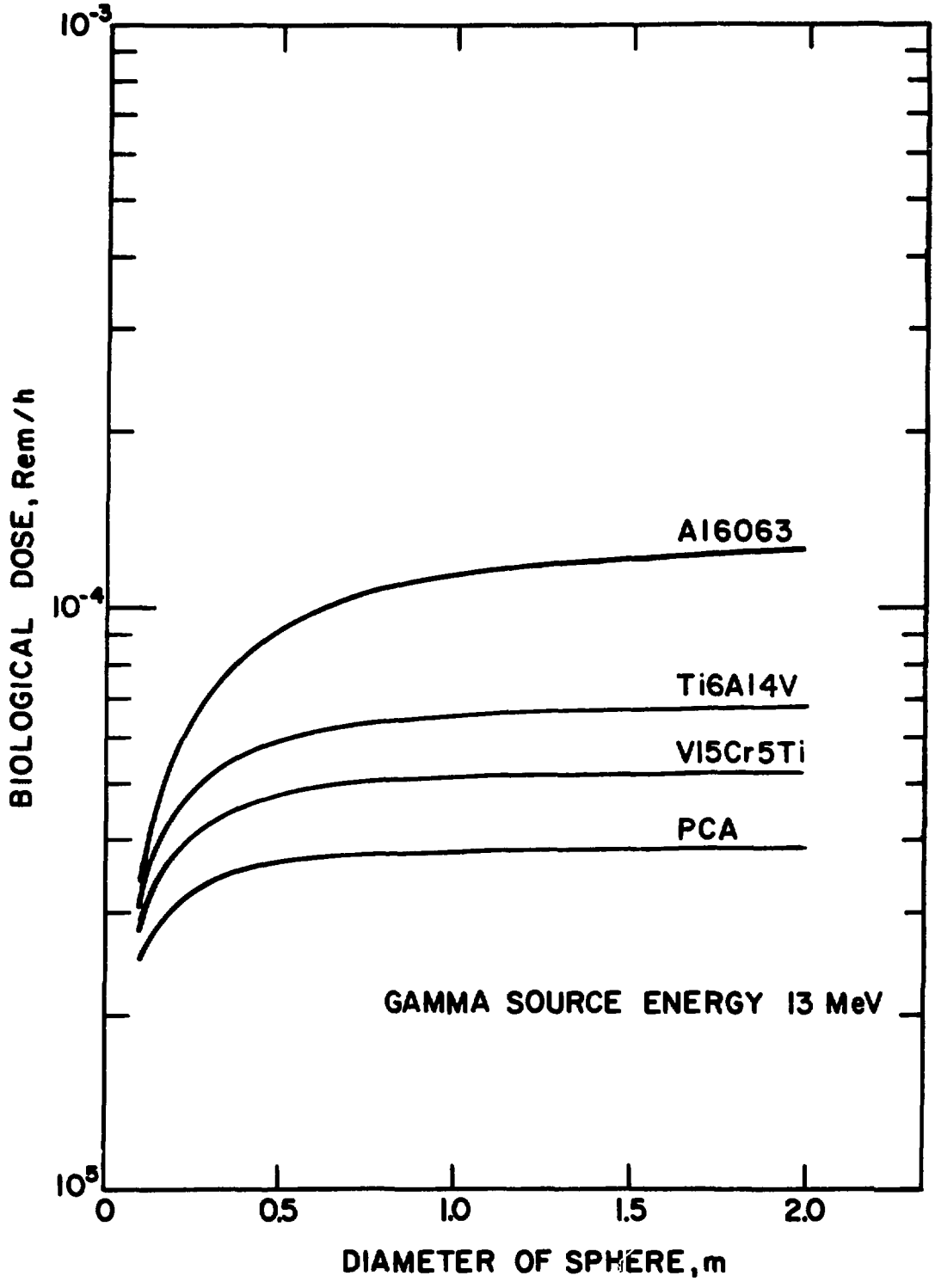

Fig. A.1. Effect of gamma source size upon surface biological dose. (Source strength: 1 photon/cm^3-s.)

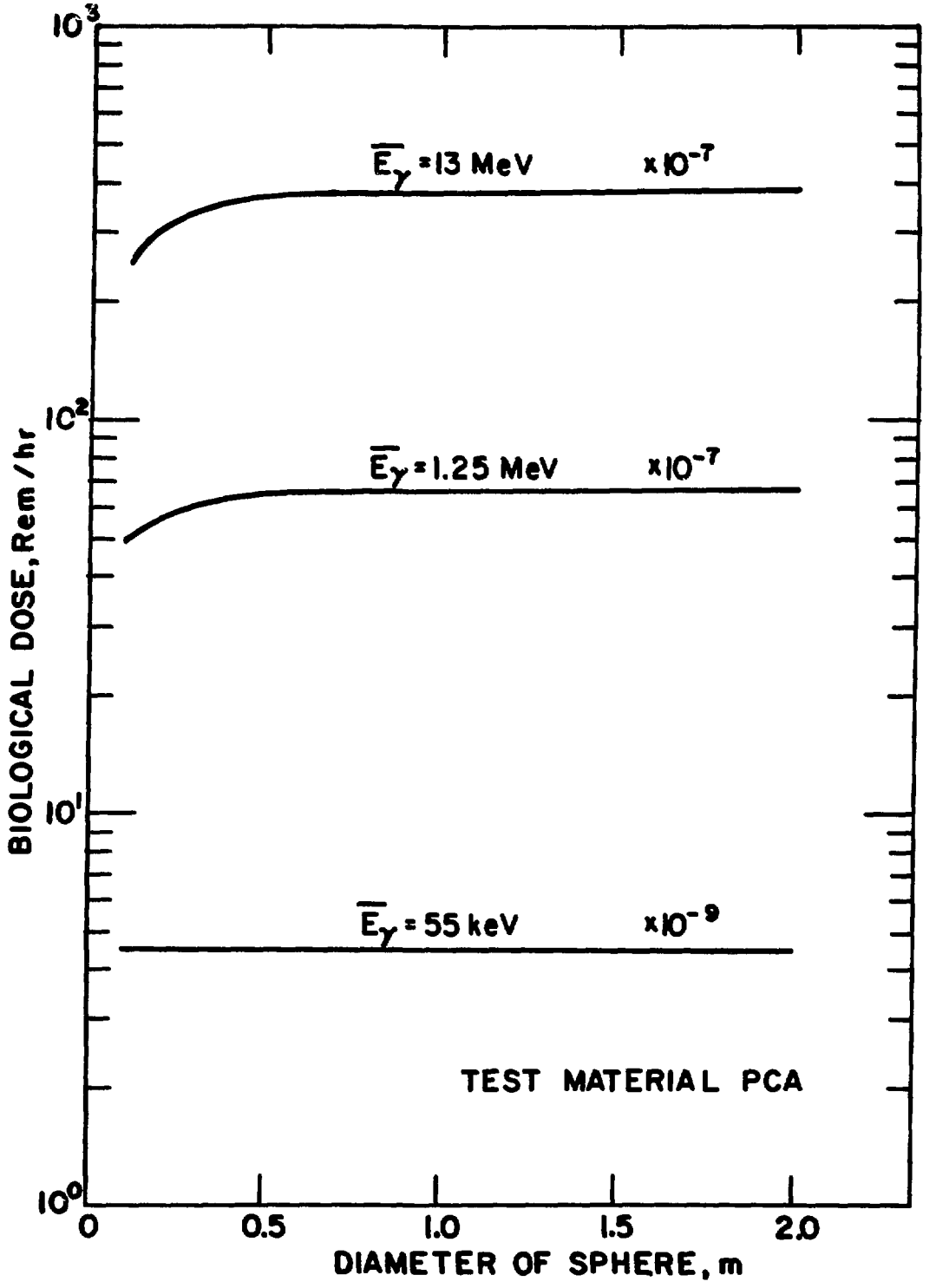

Fig. A.2. Effect of gamma source energy and size upon surface biological dose. (Source strength: 1 photon/cm^3-s).

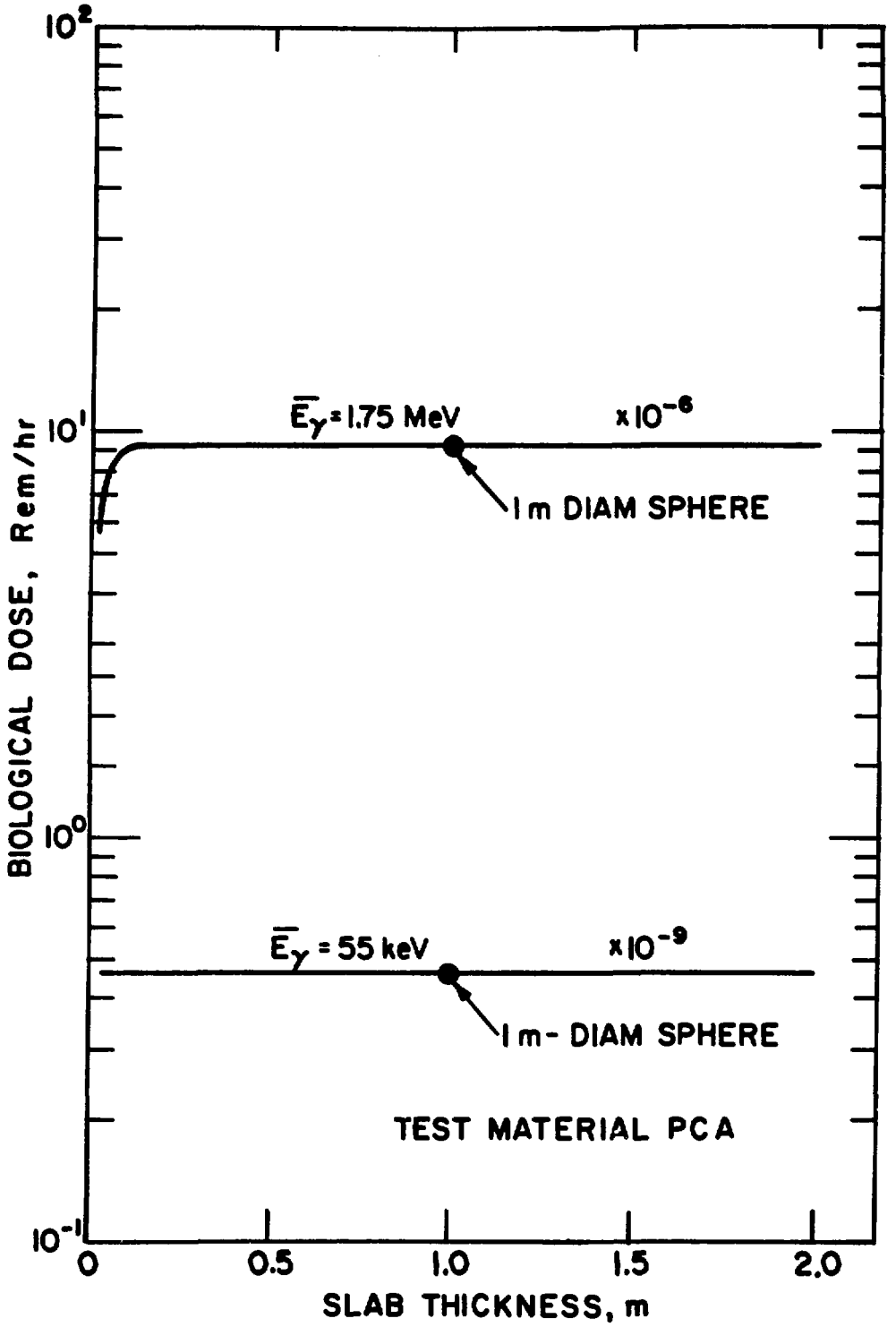

Fig. A.3. Effect of gamma source volume in slab geometry upon surface biological dose. (Source strength: 1 photon/cm^3-s.)

Table A.1 lists the factors to be used for converting the gamma-ray source strength to the surface dose for typical fusion reactor materials. The factors have been derived based on a 1-m diameter sphere, and correspond to conversions from 1 photon/cm^3-s to rem/h. The upper energy boundaries of the six groups are (starting from Group 1) 2 MeV, 1.5 MeV, 1 MeV, 0.4 MeV, 0.2 MeV, and 0.1 MeV. The lower bound of Group 6 is 0.01 MeV.

Table A.1. Gamma Source to Dose Conversion Factors
(g/cc-s → rem/h)

		Group 1	Group 2	Group 3	Group 4	Group 5	Group 6
1	PCA ----	9.17000E-06	6.66000E-06	3.85000E-06	1.26000E-06	3.25000E-07	4.56000E-09
2	S316 ----	9.13000E-06	6.64000E-06	3.83000E-06	1.25000E-06	3.20000E-07	4.58000E-09
3	S304 ----	9.21000E-06	6.70000E-06	3.89000E-06	1.30000E-06	3.45000E-07	4.70000E-09
4	FE22 ----	9.06000E-06	6.60000E-06	3.83000E-06	1.28000E-06	3.39000E-07	4.61000E-09
5	TI64 ----	1.46000E-05	1.07000E-05	6.28000E-06	2.26000E-06	7.21000E-07	1.32000E-08
6	LIAL ----	1.82000E-05	1.35000E-05	8.22000E-06	3.48000E-06	1.57000E-06	1.39000E-07
7	C ----	3.17000E-05	2.37000E-05	1.47000E-05	6.61000E-06	3.44000E-06	1.30000E-06
8	PB ----	5.24000E-06	3.41000E-06	1.27000E-06	1.49000E-07	1.50000E-08	1.45000E-09
9	BE ----	3.20000E-05	2.41000E-05	1.55000E-05	7.23000E-06	4.92000E-06	3.47000E-06
10	CU ----	8.23000E-06	5.97000E-06	3.40000E-06	1.06000E-06	2.44000E-07	3.08000E-09
11	B4C ----	2.41000E-05	1.80000E-05	1.12000E-05	5.17000E-06	2.85000E-06	1.36000E-06
12	H2O ----	3.93000E-05	3.00000E-05	1.87000E-05	8.21000E-06	4.00000E-06	9.31000E-07
13	NBTI ----	5.95000E-06	4.26000E-06	2.33000E-06	6.07000E-07	1.01000E-07	2.61000E-09
14	EPXY ----	4.06000E-05	3.07000E-05	1.92000E-05	8.62000E-06	4.42000E-06	1.55000E-06
15	W ----	3.62000E-06	2.40000E-06	9.61000E-07	1.17000E-07	1.12000E-08	8.07000E-10
16	CNCT ----	2.23000E-05	1.64000E-05	9.84000E-06	3.87000E-06	1.51000E-06	5.29000E-08
17	ZRPB ----	6.89000E-06	4.60000E-06	1.92000E-06	2.70000E-07	2.93000E-08	2.23000E-09
18	NBSN ----	8.76000E-06	6.19000E-06	3.22000E-06	7.15000E-07	1.01000E-07	3.43000E-09
19	TIH2 ----	1.59000E-05	1.16000E-05	6.84000E-06	2.47000E-06	7.96000E-07	1.52000E-08
20	V155 ----	1.16000E-05	8.49000E-06	4.97000E-06	1.75000E-06	5.24000E-07	8.68000E-09
21	AL24 ----	2.21000E-05	1.63000E-05	9.92000E-06	4.10000E-06	1.76000E-06	9.51000E-08

PCA: Prime candidate alloy
S316: Type 316 stainless steel
S304: Type 304 stainless steel
FE22: Fe14Mn2Cr2Ni
TI64: Ti6Al4V
LIAL: $LiAlO_2$
C: Carbon
PB: Lead
BE: Beryllium
CU: Copper
B4C: B_4C

H2Ø: H_2O
NBTI: NbTi
EPXY: Epoxy
W: Tungsten
CNCT: Normal concrete
ZRPB: Zr_5Pb_3
NBSN: Nb_3Sn
TIH2: TiH_2
V155: V15Cr5Ti
AL24: Al-2024/Al-6063

Group 1: 1.5-2.0 MeV
Group 2: 1.0-1.5 MeV
Group 3: 0.4-1.0 MeV
Group 4: 0.2-0.4 MeV
Group 5: 0.1-0.2 MeV
Group 6: 0.01-0.1 MeV

APPENDIX B

Summary of Activation Analyses for First-Wall/Blanket Designs

(Tables B-1 through

Table B.1. Radwaste Analysis for the Lithium/PCA Blanket Design

Radioactivity Concentration of Blanket Components (MCi/m3)

Blanket Component	Time After Reactor Shutdown									
	0	1 d	1 mo	1 y	5 y	10 y	50 y	100 y	500 y	1000 y
1ST WALL PCA --	3.52E+02	2.68E+02	2.32E+02	1.38E+02	4.33E+01	1.20E+01	4.43E-02	2.85E-02	8.87E-03	5.69E-03
IBLANKET PCA --	1.13E+02	8.24E+01	7.10E+01	4.06E+01	1.26E+01	3.51E+00	1.67E-02	1.17E-02	4.70E-03	3.13E-03
OBLANKET PCA --	8.00E+01	5.76E+01	4.95E+01	2.81E+01	8.72E+00	2.43E+00	1.22E-02	8.62E-03	3.50E-03	2.34E-03
REFLECTR PCA --	1.45E+01	5.64E+00	4.37E+00	2.21E+00	6.79E-01	1.98E-01	1.19E-02	8.54E-03	1.46E-03	7.97E-04
GRAPHITE--	2.50E-08	2.50E-08	2.50E-08	2.50E-08	2.49E-08	2.49E-08	2.48E-08	2.47E-08	2.35E-08	2.21E-08
IBLK-JKT PCA --	2.94E+01	1.93E+01	1.63E+01	8.90E+00	2.73E+00	7.62E-01	6.86E-03	5.56E-03	3.03E-03	2.09E-03
OBLK-JKT PCA --	7.10E+00	2.42E+00	1.85E+00	9.35E-01	2.89E-01	8.52E-02	5.96E-03	4.26E-03	6.77E-04	3.60E-04
HEADER PCA --	4.03E+00	1.55E+00	1.21E+00	6.08E-01	1.84E-01	5.25E-02	1.82E-03	1.36E-03	3.73E-04	2.33E-04

1ST WALL: First wall
OBLANKET: Outboard blanket
IBLK-JKT: Inboard blanket jacket
HEADER: Coolant manifold header
IBLANKET: Inboard blanket
REFLECTR: Neutron reflector
OBLK-JKT: Outboard blanket jacket

Table B.2. Radwaste Analysis for the Li/Ti6Al4V Blanket Design

Radioactivity Concentration of Blanket Components (MCi/m3)

Blanket Component	Time After Reactor Shutdown									
	0	1 d	1 mo	1 y	5 y	10 y	50 y	100 y	500 y	1000 y
1ST WALL TI6AL4V --	8.51E+01	5.82E+01	1.98E+01	2.93E+00	1.99E-02	2.67E-03	1.55E-04	1.14E-04	2.84E-05	2.05E-05
IBLANKET TI6AL4V --	3.14E+01	2.07E+01	6.99E+00	9.66E-01	5.02E-03	8.45E-04	7.21E-05	5.35E-05	1.42E-05	1.01E-05
OBLANKET TI6AL4V --	2.27E+01	1.48E+01	5.00E+00	6.82E-01	3.38E-03	5.93E-04	5.44E-05	4.03E-05	1.06E-05	7.58E-06
REFLECTR TI6AL4V --	3.86E+00	1.61E+00	5.47E-01	6.66E-02	2.77E-04	5.93E-05	1.22E-05	9.61E-06	3.68E-06	2.81E-06
GRAPHITE--	1.96E-08	1.96E-08	1.96E-08	1.96E-08	1.96E-08	1.96E-08	1.95E-08	1.94E-08	1.85E-08	1.74E-08
IBLK-JKT TI6AL4V --	9.76E+00	5.90E+00	1.99E+00	2.63E-01	1.18E-03	2.22E-04	2.90E-05	2.25E-05	7.95E-06	5.79E-06
OBLK-JKT TI6AL4V --	1.82E+00	7.25E-01	2.46E-01	2.98E-02	1.23E-04	2.68E-05	5.79E-06	4.54E-06	1.73E-06	1.31E-06
HEADER TI6AL4V --	1.29E+00	5.56E-01	1.88E-01	2.29E-02	9.31E-05	1.98E-05	4.07E-06	3.18E-06	1.17E-06	8.70E-07

1ST WALL: First wall
OBLANKET: Outboard blanket
IBLK-JKT: Inboard blanket jacket
HEADER: Coolant manifold header
IBLANKET: Inboard blanket
REFLECTR: Neutron reflector
OBLK-JKT: Outboard blanket jacket

Table B.3. Radwaste Analysis for the Li/V15Cr5Ti Blanket Design

Radioactivity Concentration of Blanket Components (MCi/m3)

Blanket Component	Time After Reactor Shutdown									
	0	1 d	1 mo	1 y	5 y	10 y	50 y	100 y	500 y	1000 y
1ST WALL V15CR5TI--	1.03E+02	4.18E+01	2.06E+01	4.29E+00	1.96E-01	5.59E-03	9.28E-05	8.16E-05	7.37E-05	6.71E-05
IBLANKET V15CR5TI--	4.70E+01	1.08E+01	4.67E+00	5.94E-01	2.65E-02	1.03E-03	5.28E-05	4.49E-05	4.06E-05	3.70E-05
OBLANKET V15CR5TI--	3.64E+01	7.38E+00	3.10E+00	3.43E-01	1.51E-02	6.50E-04	4.00E-05	3.41E-05	3.08E-05	2.81E-05
REFLECTR V15CR5TI--	3.58E+01	9.68E-01	4.45E-01	2.53E-02	6.71E-04	5.97E-05	1.81E-05	1.67E-05	1.52E-05	1.40E-05
GRAPHITE--	2.17E-08	2.17E-08	2.17E-08	2.17E-08	2.17E-08	2.17E-08	2.16E-08	2.14E-08	2.04E-08	1.92E-08
IBLK-JKT V15CR5TI--	2.69E+01	2.50E+00	1.02E+00	8.57E-02	3.57E-03	2.23E-04	3.00E-05	2.47E-05	2.21E-05	2.00E-05
OBLK-JKT V15CR5TI--	1.81E+01	4.42E-01	2.11E-01	1.34E-02	2.76E-04	2.62E-05	8.26E-06	7.59E-06	6.91E-06	6.36E-06
HEADER V15CR5TI--	9.69E+00	2.82E-01	1.31E-01	8.78E-03	2.02E-04	1.77E-05	4.60E-06	4.11E-06	3.73E-06	3.41E-06

1ST WALL: First wall
OBLANKET: Outboard blanket
IBLK-JKT: Inboard blanket jacket
HEADER: Coolant manifold header
IBLANKET: Inboard blanket
REFLECTR: Neutron reflector
OBLK-JKT: Outboard blanket jacket

Table B.4. Radwaste Analysis for the Li/Al-6063 Blanket Design Radioactivity

Radioactivity Concentration of Blanket Components (MCi/m^3)

Blanket Component	Time After Reactor Shutdown									
	0	1 d	1 mo	1 y	5 y	10 y	50 y	100 y	500 y	1000 y
1ST WALL AL6063 --	1.25E+02	2.34E+01	5.15E-01	3.03E-01	7.68E-02	2.06E-02	7.60E-04	5.34E-04	7.35E-05	5.03E-05
IBLANKET AL6063 --	5.10E+01	8.73E+00	1.66E-01	9.69E-02	2.42E-02	6.63E-03	3.53E-04	2.45E-04	2.50E-05	1.40E-05
OBLANKET AL6063 --	3.74E+01	6.29E+00	1.16E-01	6.78E-02	1.69E-02	4.65E-03	2.69E-04	1.86E-04	1.80E-05	9.58E-06
REFLECTR AL6063 --	6.48E+00	7.13E-01	1.07E-02	5.91E-03	1.45E-03	4.20E-04	4.37E-05	3.00E-05	2.00E-06	5.92E-07
GRAPHITE--	1.66E-08	1.66E-08	1.66E-08	1.66E-08	1.66E-08	1.66E-08	1.65E-08	1.64E-08	1.56E-08	1.47E-08
IBLK-JKT AL6063 --	1.77E+01	2.63E+00	4.34E-02	2.50E-02	6.14E-03	1.72E-03	1.29E-04	8.91E-05	7.13E-06	3.01E-06
OBLK-JKT AL6063 --	2.99E+00	3.23E-01	4.88E-03	2.67E-03	6.56E-04	1.93E-04	2.20E-05	1.51E-05	9.76E-07	2.64E-07
HEADER AL6063 --	2.32E+00	2.55E-01	3.76E-03	2.06E-03	5.04E-04	1.49E-04	1.73E-05	1.19E-05	7.66E-07	2.08E-07

1ST WALL: First wall
OBLANKET: Outboard blanket
IBLK-JKT: Inboard blanket jacket
HEADER: Coolant manifold header
IBLANKET: Inboard blanket
REFLECTR: Neutron reflector
OBLK-JKT: Outboard blanket jacket

Table B.5. Radwaste Analysis for the Li/PCA Blanket Design

Contact Biological Dose of Blanket Components for 1-m diameter sphere (rem/h)

Blanket Component	Time After Reactor Shutdown									
	0	1 d	1 mo	1 y	5 y	10 y	50 y	100 y	500 y	1000 y
1ST WALL PCA --	4.15E+07	1.48E+07	1.18E+07	4.21E+06	1.43E+06	7.09E+05	3.58E+03	8.49E+00	3.46E+00	3.23E+00
IBLANKET PCA --	1.44E+07	5.11E+06	4.07E+06	1.31E+06	4.32E+05	2.14E+05	1.08E+03	3.38E+00	1.81E+00	1.68E+00
OBLANKET PCA --	1.04E+07	3.65E+06	2.90E+06	9.21E+05	3.01E+05	1.49E+05	7.51E+02	2.47E+00	1.37E+00	1.28E+00
REFLECTR PCA --	2.90E+06	3.83E+05	2.94E+05	7.79E+04	2.25E+04	1.10E+04	5.59E+01	6.07E-01	5.00E-01	4.68E-01
GRAPHITE--	0.0	0.0	0.0	0.0	0.0	0.0	0.0	0.0	0.0	0.0
IBLK-JKT PCA --	4.25E+06	1.31E+06	1.03E+06	3.07E+05	9.54E+04	4.70E+04	2.38E+02	1.49E+00	1.09E+00	1.00E+00
OBLK-JKT PCA --	1.50E+06	1.60E+05	1.22E+05	3.21E+04	9.20E+03	4.50E+03	2.29E+01	2.75E-01	2.30E-01	2.15E-01
HEADER PCA --	8.24E+05	1.12E+05	8.62E+04	2.29E+04	6.60E+03	3.23E+03	1.64E+01	1.73E-01	1.42E-01	1.33E-01

1ST WALL: First wall
OBLANKET: Outboard blanket
IBLK-JKT: Inboard blanket jacket
HEADER: Coolant manifold header
IBLANKET: Inboard blanket
REFLECTR: Neutron reflector
OBLK-JKT: Outboard blanket jacket

Table B.6. Radwaste Analysis for the Li/V15Cr5Ti Blanket Design

Contact Biological Dose of Blanket Components for 1-m diameter sphere (rem/h)

Blanket Component	Time After Reactor Shutdown									
	0	1 d	1 mo	1 y	5 y	10 y	50 y	100 y	500 y	1000 y
1ST WALL V15CR5TI--	2.40E+07	9.31E+06	3.34E+06	1.48E+06	6.81E+04	1.51E+03	4.81E-01	2.55E-01	2.51E-01	2.46E-01
IBLANKET V15CR5TI--	1.19E+07	2.42E+06	5.23E+05	1.99E+05	8.87E+03	2.05E+02	3.08E-01	2.36E-01	2.32E-01	2.28E-01
OBLANKET V15CR5TI--	9.39E+06	1.65E+06	3.18E+05	1.13E+05	4.99E+03	1.17E+02	2.39E-01	1.89E-01	1.86E-01	1.82E-01
REFLECTR V15CR5TI--	1.09E+07	1.61E+05	4.27E+04	7.94E+03	2.00E+02	5.15E+00	1.06E-01	1.01E-01	9.99E-02	9.81E-02
GRAPHITE--	0.0	0.0	0.0	0.0	0.0	0.0	0.0	0.0	0.0	0.0
IBLK-JKT V15CR5TI--	7.69E+06	5.66E+05	9.29E+04	2.73E+04	1.12E+03	2.76E+01	2.12E-01	1.94E-01	1.91E-01	1.88E-01
OBLK-JKT V15CR5TI--	5.55E+06	7.56E+04	2.41E+04	4.10E+03	8.13E+01	2.10E+00	4.65E-02	4.46E-02	4.39E-02	4.32E-02
HEADER V15CR5TI--	2.95E+06	5.31E+04	1.52E+04	2.70E+03	6.03E+01	1.56E+00	2.67E-02	2.53E-02	2.50E-02	2.45E-02

1ST WALL: First wall
OBLANKET: Outboard blanket
IBLK-JKT: Inboard blanket jacket
HEADER: Coolant manifold header
IBLANKET: Inboard blanket
REFLECTR: Neutron reflector
OBLK-JKT: Outboard blanket jacket

Table B.7. Radwaste Analysis for the Li/Ti6Al4V Blanket Design

Contact Biological Dose of Blanket Components for 1-m diameter sphere (rem/h)

Blanket Component	Time After Reactor Shutdown									
	0	1 d	1 mo	1 y	5 y	10 y	50 y	100 y	500 y	1000 y
1ST WALL TI6AL4V --	4.85E+07	3.16E+07	7.20E+06	5.31E+05	3.79E+03	3.90E+02	6.48E+00	4.88E+00	4.88E+00	4.87E+00
IBLANKET TI6AL4V --	1.85E+07	1.18E+07	2.68E+06	1.83E+05	6.25E+02	1.20E+02	1.87E+00	1.32E+00	1.32E+00	1.32E+00
OBLANKET TI6AL4V --	1.34E+07	8.55E+06	1.94E+06	1.31E+05	3.80E+02	8.38E+01	1.30E+00	9.02E-01	9.01E-01	9.00E-01
REFLECTR TI6AL4V --	2.09E+06	9.86E+05	2.37E+05	1.57E+04	2.39E+01	7.90E+00	9.09E-02	5.23E-02	5.22E-02	5.20E-02
GRAPHITE--	0.0	0.0	0.0	0.0	0.0	0.0	0.0	0.0	0.0	0.0
IBLK-JKT TI6AL4V --	5.76E+06	3.50E+06	7.95E+05	5.30E+04	1.11E+02	3.12E+01	4.26E-01	2.76E-01	2.75E-01	2.74E-01
OBLK-JKT TI6AL4V --	9.70E+05	4.42E+05	1.07E+05	7.08E+03	1.04E+01	3.52E+00	4.02E-02	2.30E-02	2.29E-02	2.28E-02
HEADER TI6AL4V --	6.99E+05	3.39E+05	8.14E+04	5.38E+03	8.01E+00	2.71E+00	3.10E-02	1.77E-02	1.76E-02	1.76E-02

1ST WALL: First wall
OBLANKET: Outboard blanket
IBLK-JKT: Inboard blanket jacket
HEADER: Coolant manifold header
IBLANKET: Inboard blanket
REFLECTR: Neutron reflector
OBLK-JKT: Outboard blanket jacket

Table B.8. Radwaste Analysis for the Li/Al-6063 Blanket Design

Contact Biological Dose of Blanket Components for 1-m diameter sphere (rem/h)

Blanket Component	Time After Reactor Shutdown									
	0	1 d	1 mo	1 y	5 y	10 y	50 y	100 y	500 y	1000 y
1ST WALL AL6063 --	1.27E+08	3.24E+07	8.32E+04	3.68E+04	3.10E+03	1.06E+03	7.79E+01	7.30E+01	7.30E+01	7.30E+01
IBLANKET AL6063 --	5.01E+07	1.21E+07	2.85E+04	1.26E+04	1.15E+03	4.13E+02	2.21E+01	2.01E+01	2.01E+01	2.01E+01
OBLANKET AL6063 --	3.64E+07	8.75E+06	2.03E+04	8.94E+03	8.32E+02	3.00E+02	1.52E+01	1.38E+01	1.37E+01	1.37E+01
REFLECTR AL6063 --	5.73E+06	9.85E+05	1.99E+03	8.63E+02	9.26E+01	3.56E+01	9.92E-01	8.19E-01	8.19E-01	8.18E-01
GRAPHITE--	0.0	0.0	0.0	0.0	0.0	0.0	0.0	0.0	0.0	0.0
IBLK-JKT AL6063 --	1.67E+07	3.66E+06	7.99E+03	3.52E+03	3.45E+02	1.27E+02	4.88E+00	4.27E+00	4.27E+00	4.27E+00
OBLK-JKT AL6063 --	2.62E+06	4.45E+05	9.12E+02	3.94E+02	4.21E+01	1.61E+01	4.42E-01	3.63E-01	3.63E-01	3.63E-01
HEADER AL6063 --	2.04E+06	3.52E+05	7.16E+02	3.10E+02	3.33E+01	1.28E+01	3.47E-01	2.85E-01	2.85E-01	2.85E-01

1ST WALL: First wall
OBLANKET: Outboard blanket
IBLK-JKT: Inboard blanket jacket
HEADER: Coolant manifold header
IBLANKET: Inboard blanket
REFLECTR: Neutron reflector
OBLK-JKT: Outboard blanket jacket

Table B.8. Radwaste Analysis for the Li/Al-6063 Blanket Design

Contact Biological Dose of Blanket Components for 1-m diameter sphere (rem/h)

Blanket Component	Time After Reactor Shutdown									
	0	1 d	1 mo	1 y	5 y	10 y	50 y	100 y	500 y	1000 y
1ST WALL AL6063 --	1.27E+08	3.24E+07	8.32E+04	3.68E+04	3.10E+03	1.06E+03	7.79E+01	7.30E+01	7.30E+01	7.30E+01
IBLANKET AL6063 --	5.01E+07	1.21E+07	2.85E+04	1.26E+04	1.15E+03	4.13E+02	2.21E+01	2.01E+01	2.01E+01	2.01E+01
OBLANKET AL6063 --	3.64E+07	8.75E+06	2.03E+04	8.94E+03	8.32E+02	3.00E+02	1.52E+01	1.38E+01	1.37E+01	1.37E+01
REFLECTR AL6063 --	5.73E+06	9.85E+05	1.99E+03	8.63E+02	9.26E+01	3.56E+01	9.92E-01	8.19E-01	8.19E-01	8.18E-01
GRAPHITE--	0.0	0.0	0.0	0.0	0.0	0.0	0.0	0.0	0.0	0.0
IBLK-JKT AL6063 --	1.67E+07	3.66E+06	7.99E+03	3.52E+03	3.45E+02	1.27E+02	4.88E+00	4.27E+00	4.27E+00	4.27E+00
OBLK-JKT AL6063 --	2.62E+06	4.45E+05	9.12E+02	3.94E+02	4.21E+01	1.61E+01	4.42E-01	3.63E-01	3.63E-01	3.63E-01
HEADER AL6063 --	2.04E+06	3.52E+05	7.16E+02	3.10E+02	3.33E+01	1.28E+01	3.47E-01	2.85E-01	2.85E-01	2.85E-01

1ST WALL: First wall
OBLANKET: Outboard blanket
IBLK-JKT: Inboard blanket jacket
HEADER: Coolant manifold header
IBLANKET: Inboard blanket
REFLECTR: Neutron reflector
OBLK-JKT: Outboard blanket jacket

APPENDIX C

Summary of Activation Analyses for Toroidal-Field Magnet Designs

This appendix presents the nucleonic data for the radwaste management study of the STARFIRE TF-magnet system. A cross-sectional view of the magnet system analyzed is shown in Fig. C.1. Note that the superconductor zones [(9-11) Tesla Nb_3Sn and (0-9) Tesla NbTi zones] have been computationally divided into subzones in order to account for the spatial gradient across these components. The top, bottom, and outboard magnet portions are all categorized into the "OUTBOARD" magnet and distinguished from the "INBOARD" magnet section.

The activation information is provided in terms of:

Radioactivity concentration:	(MCi/m^3); (Table C.1)
Decay afterheat:	(MW/m^3); (Table C.2)
Contact biological dose:	(rem/h); (Table C.3)
Biological hazard potential in air:	(km^3-air/cc); (Table C.4)
Biological hazard potential in water:	(km^3-water/cc); (Table C.5)

The decay afterheat calculation mentioned above assumes that both beta- and gamma-ray energies are locally deposited at the source point, without transport.

The absorbed nuclear dose in the epoxy-base insulator (G-10) is shown in Fig. C.2, assuming an integral neutron wall load of 108 $MW\text{-}y/m^2$ (i.e., 3.6 MW/m^2 × 40 y × 0.75 availability).

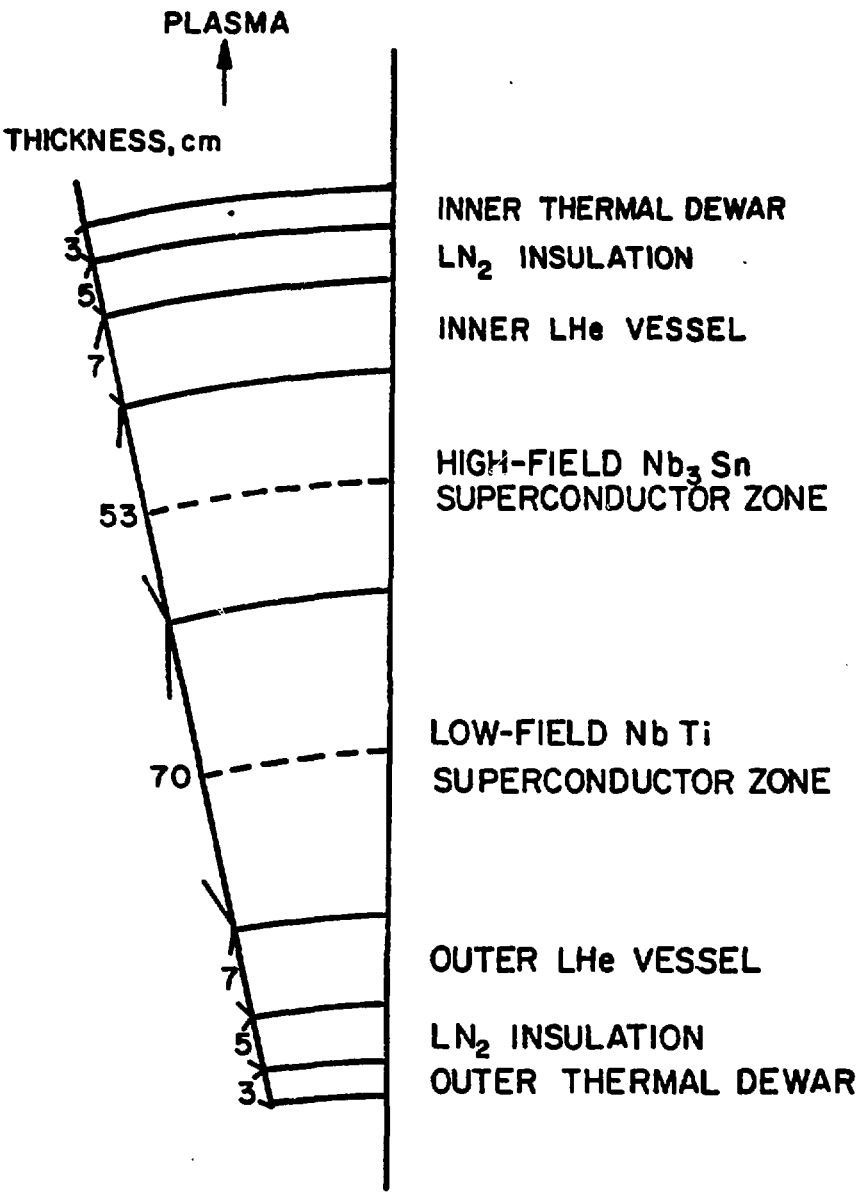

Fig. C.1. Cross-sectional view of the magnet system.

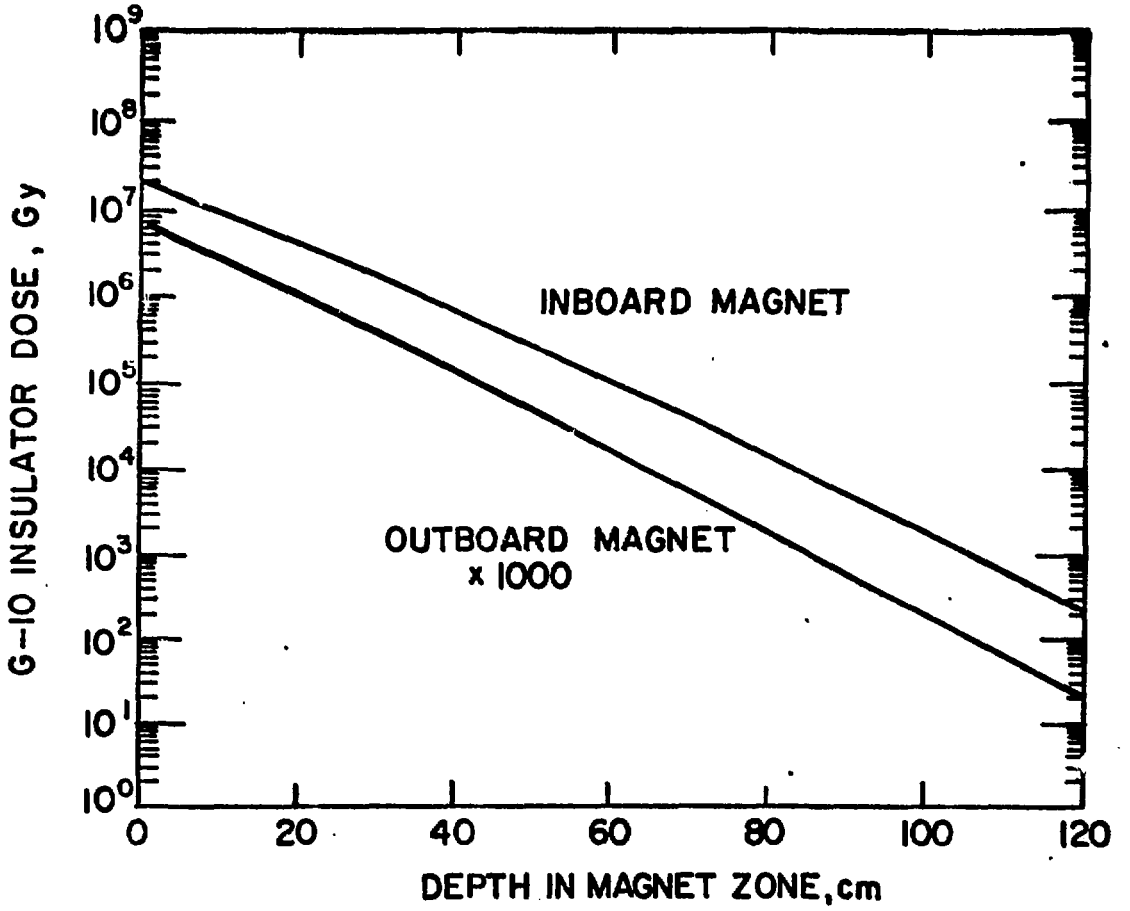

Fig. C.2. Absorbed nuclear dose in the epoxy-base insulators, G-10.

Table C.1. Radwaste Management for the STARFIRE TF-Magnet Design

Radioactivity Concentration of Magnet Components (MCi/m^3)

Magnet Component		Time After Reactor Shutdown									
		0	1 d	1 mo	1 y	5 y	10 y	50 y	100 y	500 y	1000 y
I-DEWAR1	FE1422 --	2.46E-04	6.83E-05	6.36E-05	4.02E-05	1.05E-05	2.70E-06	3.10E-09	1.96E-09	1.61E-10	6.68E-11
I-HEVSL1	304SS --	6.28E-05	3.20E-05	2.56E-05	1.39E-05	4.31E-06	1.19E-06	2.71E-08	1.97E-08	4.31E-09	2.55E-09
I-HFMAG1	304SS --	2.06E-05	8.84E-06	6.49E-06	3.25E-06	1.06E-06	3.13E-07	2.91E-08	2.04E-08	2.19E-09	9.48E-10
	COPPER --	2.70E-04	7.05E-05	3.98E-07	3.71E-07	2.85E-07	2.23E-07	1.21E-07	8.30E-08	4.06E-09	9.35E-11
	NB3SN --	9.67E-05	1.41E-05	5.84E-06	3.98E-06	1.94E-06	1.04E-06	1.14E-07	2.20E-08	1.40E-08	1.37E-08
	G10 --	5.49E-08	4.93E-14	4.93E-14	4.92E-14	4.92E-14	4.92E-14	4.90E-14	4.87E-14	4.64E-14	4.36E-14
I-HFMAG2	304SS --	2.67E-06	1.03E-06	6.94E-07	3.18E-07	1.11E-07	3.51E-08	5.67E-09	3.95E-09	3.33E-10	1.14E-10
	COPPER --	4.06E-05	1.04E-05	1.76E-08	1.64E-08	1.26E-08	9.85E-09	5.32E-09	3.64E-09	1.78E-10	9.10E-12
	N33SN --	1.29E-05	1.64E-06	7.53E-07	5.41E-07	2.42E-07	1.14E-07	1.12E-08	2.64E-09	1.90E-09	1.86E-09
	G10 --	2.48E-09	9.79E-15	9.79E-15	9.79E-15	9.79E-15	9.78E-15	9.73E-15	9.68E-15	9.22E-15	8.68E-15
I-LFMAG1	304SS --	2.11E-07	7.68E-08	5.03E-08	2.24E-08	8.04E-09	2.60E-09	4.87E-10	3.38E-10	2.63E-11	8.11E-12
	COPPER --	3.32E-06	8.45E-07	5.93E-10	5.54E-10	4.25E-10	3.31E-10	1.79E-10	1.22E-10	5.99E-12	1.38E-13
	NBTI --	5.91E-07	9.91E-09	6.26E-09	5.23E-09	4.24E-09	3.31E-09	5.28E-10	1.44E-10	1.10E-10	1.03E-10
	G10 --	8.33E-11	8.52E-16	8.52E-16	8.52E-16	8.51E-16	8.51E-16	8.46E-16	8.41E-16	8.02E-16	7.55E-16
I-LFMAG2	304SS --	7.24E-09	2.62E-09	1.70E-09	7.48E-10	2.72E-10	8.92E-11	1.77E-11	1.23E-11	9.03E-13	2.54E-13
	COPPER --	1.14E-07	2.83E-08	8.36E-12	7.80E-12	5.98E-12	4.67E-12	2.52E-12	1.72E-12	8.44E-14	1.94E-15
	NBTI --	1.93E-08	2.08E-10	1.56E-10	1.38E-10	1.13E-10	8.82E-11	1.47E-11	4.52E-12	3.61E-12	3.55E-12
	G10 --	1.17E-12	3.12E-17	3.12E-17	3.12E-17	3.12E-17	3.11E-17	3.10E-17	3.03E-17	2.93E-17	2.76E-17
I-HEVSL2	304SS --	4.26E-10	1.14E-10	7.03E-11	3.21E-11	1.17E-11	3.85E-12	7.76E-13	5.41E-13	4.64E-14	1.62E-14
I-DEWAR2	FE1422 --	8.15E-10	1.32E-11	1.09E-11	7.63E-12	2.57E-12	7.07E-13	3.11E-14	2.14E-14	1.22E-15	2.04E-16
O-DEWAR1	FE1422 --	1.61E-07	2.60E-09	2.09E-09	1.32E-09	3.91E-10	1.04E-10	2.81E-12	1.93E-12	1.25E-13	3.23E-14
O-HEVSL1	304SS --	1.99E-08	4.78E-09	2.56E-09	9.57E-10	3.36E-10	1.08E-10	1.95E-11	1.42E-11	2.58E-12	1.46E-12
O-HFMAG1	304SS --	8.54E-09	2.75E-09	1.72E-09	7.18E-10	2.61E-10	8.58E-11	1.73E-11	1.20E-11	1.08E-12	3.99E-13
	COPPER --	1.51E-07	3.93E-08	1.02E-11	9.54E-12	7.42E-12	5.87E-12	3.26E-12	2.23E-12	1.09E-13	2.51E-15
	NB3SN --	4.73E-08	5.76E-09	2.66E-09	1.94E-09	8.27E-10	3.64E-10	3.32E-11	9.09E-12	6.95E-12	6.83E-12
	G10 --	1.19E-12	3.04E-17	3.04E-17	3.04E-17	3.04E-17	3.04E-17	3.03E-17	3.01E-17	2.86E-17	2.70E-17
O-HFMAG2	304SS --	8.44E-10	3.11E-10	2.00E-10	8.65E-11	3.16E-11	1.04E-11	2.13E-12	1.48E-12	1.07E-13	2.97E-14
	COPPER --	1.34E-08	3.39E-09	4.40E-13	4.11E-13	3.17E-13	2.49E-13	1.35E-13	9.33E-14	4.56E-15	1.05E-16
	NB3SN --	3.87E-09	4.66E-10	2.25E-10	1.64E-10	6.66E-11	2.65E-11	2.12E-12	6.96E-13	5.68E-13	5.58E-13
	G10 --	5.39E-14	3.72E-18	3.72E-18	3.72E-18	3.72E-18	3.71E-18	3.70E-18	3.67E-18	3.50E-18	3.29E-18
O-LFMAG1	304SS --	4.45E-11	1.62E-11	1.05E-11	4.57E-12	1.67E-12	5.53E-13	1.13E-13	7.84E-14	5.50E-15	1.42E-15
	COPPER --	6.97E-10	1.76E-10	1.44E-14	1.35E-14	1.04E-14	8.13E-15	4.44E-15	3.03E-15	1.48E-16	3.42E-18
	NBTI --	1.15E-10	7.77E-13	6.90E-13	6.40E-13	5.24E-13	4.11E-13	7.25E-14	2.53E-14	2.15E-14	2.11E-14
	G10 --	1.81E-15	1.99E-19	1.99E-19	1.99E-19	1.99E-19	1.99E-19	1.98E-19	1.97E-19	1.87E-19	1.76E-19
O-LFMAG2	304SS --	1.01E-12	3.70E-13	2.39E-13	1.05E-13	3.85E-14	1.27E-14	2.62E-15	1.81E-15	1.24E-16	3.06E-17
	COPPER --	1.56E-11	3.92E-12	1.97E-16	1.84E-16	1.42E-16	1.11E-16	6.04E-17	4.13E-17	2.02E-18	4.65E-20
	NBTI --	2.51E-12	1.48E-14	1.36E-14	1.27E-14	1.04E-14	8.15E-15	1.48E-15	5.56E-16	4.71E-16	4.63E-16
	G10 --	2.51E-17	4.60E-21	4.60E-21	4.60E-21	4.60E-21	4.60E-21	4.57E-21	4.55E-21	4.33E-21	4.05E-21
O-HEVSL2	304SS --	4.61E-14	1.25E-14	7.70E-15	3.53E-15	1.29E-15	4.29E-16	8.86E-17	6.16E-17	4.86E-18	1.53E-18
O-DEWAR2	FE1422 --	9.14E-14	1.33E-15	1.09E-15	7.75E-16	2.68E-16	7.40E-17	3.50E-18	2.41E-18	1.37E-19	2.17E-20

I- Inboard
DEWAR1: Inner thermal dewar
HEVSL1: Inner liquid helium vessel
HFMAG1 1st 26.5 cm NbSn magnet zone
LFMAG1: 1st 35.0 cm NbTI magnet zone

O- Outboard/top/bottom
DEWAR2: Outer Thermal Dewar
HEVSL2: Outer liquid helium vessel
HFMAG2: 2nd 26.5 cm Nb_3Sn magnet zone
LFMAG2: 2nd 35.0 cm NbTi magnet zone

Table C.2. Radwaste Management for the STARFIRE TF-Magnet Design

Decay Afterheat of Magnet Components (MW/m^3)

Magnet Component			Time After Reactor Shutdown								
			0	1 d	1 mo	1 y	5 y	10 y	50 y	100 y	500 y	1000 y
I-DEWAR1	FE1422	--	2.81E-06	1.58E-07	1.42E-07	6.75E-08	7.20E-09	1.75E-09	3.53E-12	2.55E-13	3.69E-14	2.51E-14
I-HEVSL1	304SS	--	4.98E-07	6.03E-08	4.81E-08	1.72E-08	4.52E-09	1.79E-09	9.93E-12	2.35E-12	5.25E-13	3.33E-13
I-HFMAG1	304SS	--	1.81E-07	1.17E-08	8.73E-09	3.23E-09	8.98E-10	3.43E-10	4.64E-12	2.46E-12	3.07E-13	1.63E-13
	COPPER	--	5.34E-07	1.28E-07	3.44E-09	3.05E-09	1.80E-09	9.40E-10	1.90E-11	9.85E-12	4.82E-13	1.11E-14
	NB3SN	--	2.38E-08	5.25E-09	8.13E-10	1.71E-10	1.67E-10	1.63E-10	1.51E-10	1.49E-10	1.47E-10	1.44E-10
	G10	--	3.00E-09	1.37E-17	1.37E-17	1.37E-17	1.37E-17	1.37E-17	1.36E-17	1.36E-17	1.29E-17	1.22E-17
I-HFMAG2	304SS	--	2.43E-08	8.52E-10	5.58E-10	2.19E-10	6.74E-11	2.37E-11	7.41E-13	4.78E-13	5.00E-14	2.45E-14
	COPPER	--	8.32E-08	1.85E-08	1.54E-10	1.36E-10	8.06E-11	4.20E-11	8.37E-13	4.32E-13	2.11E-14	4.86E-16
	NB3SN	--	2.74E-09	2.51E-10	5.13E-11	2.23E-11	2.19E-11	2.15E-11	2.04E-11	2.02E-11	1.99E-11	1.96E-11
	G10	--	1.35E-10	2.73E-18	2.73E-18	2.73E-18	2.73E-18	2.73E-18	2.71E-18	2.70E-18	2.57E-18	2.42E-18
I-LFMAG1	304SS	--	1.98E-09	5.10E-11	3.02E-11	1.24E-11	4.08E-12	1.35E-12	6.10E-14	4.09E-14	4.05E-15	1.93E-15
	COPPER	--	6.84E-09	1.50E-09	5.18E-12	4.59E-12	2.72E-12	1.42E-12	2.81E-14	1.45E-14	7.10E-16	1.63E-17
	NBTI	--	1.67E-10	1.93E-11	5.00E-12	1.47E-12	1.25E-12	1.23E-12	1.18E-12	1.17E-12	1.15E-12	1.14E-12
	G10	--	4.55E-12	2.37E-19	2.37E-19	2.37E-19	2.37E-19	2.37E-19	2.36E-19	2.34E-19	2.23E-19	2.10E-19
I-LFMAG2	304SS	--	6.80E-11	1.52E-12	8.44E-13	3.58E-13	1.23E-13	3.89E-14	2.19E-15	1.49E-15	1.42E-16	6.60E-17
	COPPER	--	2.37E-10	5.10E-11	7.30E-14	6.47E-14	3.83E-14	2.00E-14	3.97E-16	2.05E-16	1.00E-17	2.30E-19
	NBTI	--	5.06E-12	2.97E-13	9.39E-14	4.40E-14	4.06E-14	4.01E-14	3.88E-14	3.85E-14	3.80E-14	3.73E-14
	G10	--	6.38E-14	8.69E-21	8.69E-21	8.68E-21	8.68E-21	8.68E-21	8.63E-21	8.58E-21	8.18E-21	7.70E-21
I-HEVSL2	304SS	--	4.54E-12	7.49E-14	3.58E-14	1.56E-14	5.53E-15	1.79E-15	9.60E-17	6.54E-17	6.93E-18	3.42E-18
I-DEWAR2	FE1422	--	1.21E-11	2.89E-14	8.83E-15	4.38E-15	1.12E-15	2.96E-16	3.85E-18	2.62E-18	2.30E-19	1.07E-19
O-DEWAR1	FE1422	--	2.38E-09	7.36E-12	3.33E-12	1.56E-12	2.16E-13	5.41E-14	4.03E-16	2.40E-16	2.48E-17	1.36E-17
O-HEVSL1	304SS	--	2.20E-10	4.29E-12	1.97E-12	7.66E-13	2.59E-13	1.01E-13	2.65E-15	1.69E-15	3.20E-16	1.95E-16
O-HFMAG1	304SS	--	8.49E-11	1.72E-12	8.65E-13	3.61E-13	1.27E-13	4.16E-14	2.14E-15	1.46E-15	1.59E-16	7.96E-17
	COPPER	--	3.01E-10	6.94E-11	8.50E-14	7.53E-14	4.46E-14	2.33E-14	5.00E-16	2.64E-16	1.29E-17	2.97E-19
	NB3SN	--	9.24E-12	1.93E-13	9.45E-14	8.00E-14	7.90E-14	7.79E-14	7.47E-14	7.41E-14	7.31E-14	7.18E-14
	G10	--	6.48E-14	8.48E-21	8.48E-21	8.48E-21	8.47E-21	8.47E-21	8.43E-21	8.38E-21	7.98E-21	7.51E-21
O-HFMAG2	304SS	--	7.83E-12	1.69E-13	9.05E-14	3.88E-14	1.37E-14	4.22E-15	2.61E-16	1.79E-16	1.69E-17	7.84E-18
	COPPER	--	2.81E-11	6.00E-12	3.75E-15	3.33E-15	1.97E-15	1.03E-15	2.12E-17	1.11E-17	5.41E-19	1.25E-20
	NB3SN	--	7.50E-13	1.15E-14	7.07E-15	6.41E-15	6.34E-15	6.28E-15	6.09E-15	6.05E-15	5.97E-15	5.87E-15
	G10	--	2.95E-15	1.04E-21	1.04E-21	1.04E-21	1.04E-21	1.03E-21	1.03E-21	1.02E-21	9.75E-22	9.18E-22
O-LFMAG1	304SS	--	4.16E-13	8.64E-15	4.63E-15	2.00E-15	7.09E-16	2.16E-16	1.38E-17	9.52E-18	8.80E-19	4.01E-19
	COPPER	--	1.46E-12	3.11E-13	1.24E-16	1.10E-16	6.50E-17	3.39E-17	6.92E-19	3.60E-19	1.76E-20	4.05E-22
	NBTI	--	2.83E-14	6.74E-16	3.32E-16	2.46E-16	2.39E-16	2.37E-16	2.31E-16	2.29E-16	2.26E-16	2.22E-16
	G10	--	9.87E-17	5.54E-23	5.54E-23	5.54E-23	5.54E-23	5.54E-23	5.51E-23	5.48E-23	5.22E-23	4.91E-23
O-LFMAG2	304SS	--	9.38E-15	1.94E-16	1.04E-16	4.52E-17	1.61E-17	4.84E-18	3.19E-19	2.20E-19	2.00E-20	9.02E-21
	COPPER	--	3.28E-14	6.93E-15	1.70E-18	1.51E-18	8.93E-19	4.65E-19	9.44E-21	4.90E-21	2.40E-22	5.51E-24
	NBTI	--	6.26E-16	1.14E-17	6.53E-18	5.34E-18	5.22E-18	5.18E-18	5.05E-18	5.03E-18	4.96E-18	4.87E-18
	G10	--	1.37E-18	1.28E-24	1.28E-24	1.28E-24	1.28E-24	1.28E-24	1.27E-24	1.27E-24	1.21E-24	1.14E-24
O-HEVSL2	304SS	--	4.90E-16	7.60E-18	3.51E-18	1.57E-18	5.67E-19	1.77E-19	1.09E-20	7.46E-21	7.47E-22	3.57E-22
O-DEWAR2	FE1422	--	1.35E-15	2.91E-18	6.86E-19	3.47E-19	1.11E-19	2.97E-20	4.27E-22	2.95E-22	2.55E-23	1.17E-23

Table C.3. Radwaste Management for the STARFIRE TF-Magnet Design

Contact Biological Dose of Magnet Components (rem/h)

Magnet Component			Time After Reactor Shutdown									
			0	1 d	1 mo	1 y	5 y	10 y	50 y	100 y	500 y	1000 y
I-DEWAR1	FE1422	--	5.50E+01	4.08E+00	3.65E+00	1.59E+00	9.04E-02	2.05E-02	9.96E-05	1.34E-07	1.41E-30	2.69E-59
I-HEVSL1	304SS	--	1.04E+01	1.61E+00	1.28E+00	3.72E-01	9.05E-02	4.31E-02	2.17E-04	3.36E-07	4.46E-08	4.38E-08
I-HFMAG1	304SS	--	3.60E+00	2.87E-01	2.20E-01	6.14E-02	1.55E-02	7.40E-03	3.72E-05	5.74E-08	7.34E-09	7.22E-09
	COPPER	--	9.88E-02	9.88E-02	9.77E-02	8.66E-02	5.10E-02	2.63E-02	1.33E-04	1.78E-07	1.88E-30	3.59E-59
	NB3SN	--	3.70E-01	3.46E-01	4.94E-02	3.39E-03	3.39E-03	3.39E-03	3.33E-03	3.33E-03	3.33E-03	3.27E-03
	G10	--	6.18E-02	0.0	0.0	0.0	0.0	0.0	0.0	0.0	0.0	0.0
I-HFMAG2	304SS	--	4.73E-01	1.77E-02	1.21E-02	2.89E-03	7.79E-04	3.77E-04	1.90E-06	2.89E-09	3.35E-10	3.29E-10
	COPPER	--	4.42E-03	4.42E-03	4.37E-03	3.87E-03	2.28E-03	1.18E-03	5.93E-06	7.97E-09	8.42E-32	1.61E-60
	NB3SN	--	1.70E-02	1.59E-02	2.54E-03	4.60E-04	4.60E-04	4.60E-04	4.59E-04	4.58E-04	4.52E-04	4.44E-04
	G10	--	2.79E-03	0.0	0.0	0.0	0.0	0.0	0.0	0.0	0.0	0.0
I-LFMAG1	304SS	--	3.82E-02	9.31E-04	5.68E-04	1.06E-04	3.11E-05	1.52E-05	7.64E-08	1.14E-10	1.15E-11	1.13E-11
	COPPER	--	1.49E-04	1.49E-04	1.47E-04	1.30E-04	7.69E-05	3.97E-05	2.00E-07	2.68E-10	2.84E-33	5.41E-62
	NBTI	--	6.43E-04	5.42E-04	1.16E-04	2.30E-05	1.93E-05	1.93E-05	1.92E-05	1.92E-05	1.89E-05	1.86E-05
	G10	--	9.38E-05	0.0	0.0	0.0	0.0	0.0	0.0	0.0	0.0	0.0
I-LFMAG2	304SS	--	1.31E-03	2.52E-05	1.38E-05	1.78E-06	5.92E-07	2.93E-07	1.48E-09	2.16E-12	1.72E-13	1.69E-13
	COPPER	--	2.10E-06	2.10E-06	2.08E-06	1.84E-06	1.03E-06	5.59E-07	2.82E-09	3.79E-12	4.00E-35	7.63E-64
	NBTI	--	9.44E-06	7.99E-06	1.99E-06	6.87E-07	6.34E-07	6.33E-07	6.33E-07	6.31E-07	6.23E-07	6.12E-07
	G10	--	1.31E-06	0.0	0.0	0.0	0.0	0.0	0.0	0.0	0.0	0.0
I-HEVSL2	304SS	--	8.77E-05	1.20E-06	5.83E-07	8.56E-08	3.28E-08	1.65E-08	8.29E-11	1.18E-13	6.99E-15	6.87E-15
I-DEWAR2	FE1422	--	2.31E-04	5.48E-07	1.47E-07	3.84E-08	2.13E-09	4.74E-10	2.30E-12	3.08E-15	3.26E-38	6.22E-67
O-DEWAR1	FE1422	--	4.56E-02	1.61E-04	7.95E-05	3.18E-05	1.75E-06	3.85E-07	1.86E-09	2.50E-12	2.64E-35	5.04E-64
O-HEVSL1	304SS	--	4.26E-03	7.98E-05	4.52E-05	1.23E-05	4.20E-06	2.09E-06	1.05E-08	1.52E-11	1.05E-12	1.03E-12
O-HFMAG1	304SS	--	1.63E-03	2.80E-05	1.49E-05	2.31E-06	8.44E-07	4.22E-07	2.12E-09	3.04E-12	1.87E-13	1.83E-13
	COPPER	--	2.44E-06	2.44E-06	2.41E-06	2.14E-06	1.26E-06	6.50E-07	3.28E-09	4.40E-12	4.65E-35	8.87E-64
	NB3SN	--	9.84E-06	9.30E-06	2.71E-06	1.68E-06	1.68E-06	1.68E-06	1.68E-06	1.68E-06	1.66E-06	1.63E-06
	G10	--	1.34E-06	0.0	0.0	0.0	0.0	0.0	0.0	0.0	0.0	0.0
O-HFMAG2	304SS	--	1.50E-04	2.66E-06	1.37E-06	1.23E-07	4.80E-08	2.42E-08	1.22E-10	1.73E-13	9.23E-15	9.07E-15
	COPPER	--	1.08E-07	1.08E-07	1.07E-07	9.44E-08	5.56E-08	2.87E-08	1.45E-10	1.94E-13	2.05E-36	3.92E-65
	NB3SN	--	5.06E-07	4.82E-07	1.84E-07	1.38E-07	1.38E-07	1.38E-07	1.37E-07	1.37E-07	1.35E-07	1.33E-07
	G10	--	6.07E-08	0.0	0.0	0.0	0.0	0.0	0.0	0.0	0.0	0.0
O-LFMAG1	304SS	--	7.98E-06	1.34E-07	6.78E-08	4.92E-09	2.02E-09	1.02E-09	5.16E-12	7.27E-15	3.40E-16	3.34E-16
	COPPER	--	3.56E-09	3.56E-09	3.52E-09	3.12E-09	1.84E-09	9.49E-10	4.78E-12	6.42E-15	6.79E-38	1.29E-66
	NBTI	--	1.84E-08	1.58E-08	6.02E-09	3.87E-09	3.77E-09	3.77E-09	3.77E-09	3.76E-09	3.71E-09	3.65E-09
	G10	--	2.04E-09	0.0	0.0	0.0	0.0	0.0	0.0	0.0	0.0	0.0
O-LFMAG2	304SS	--	1.80E-07	2.99E-09	1.49E-09	8.92E-11	3.90E-11	1.99E-11	1.00E-13	1.40E-16	5.51E-18	5.41E-18
	COPPER	--	4.89E-11	4.89E-11	4.84E-11	4.28E-11	2.52E-11	1.30E-11	6.57E-14	8.82E-17	9.32E-40	0.0
	NBTI	--	2.89E-10	2.52E-10	1.14E-10	8.39E-11	8.27E-11	8.27E-11	8.25E-11	8.24E-11	8.13E-11	7.99E-11
	G10	--	2.83E-11	0.0	0.0	0.0	0.0	0.0	0.0	0.0	0.0	0.0
O-HEVSL2	304SS	--	9.46E-09	1.15E-10	5.07E-11	4.56E-12	2.18E-12	1.12E-12	5.62E-15	7.79E-18	2.45E-19	2.40E-19
O-DEWAR2	FE1422	--	2.60E-08	5.28E-11	8.65E-12	8.57E-13	4.73E-14	1.10E-14	5.35E-17	7.19E-20	7.60E-43	0.0

Table C.4. Radwaste Management for the STARFIRE TF-Magnet Design

BHP of Air of Magnet Components (km^3 of air/cm^3)

Magnet Component			Time After Reactor Shutdown									
			0	1 d	1 mo	1 y	5 y	10 y	50 y	100 y	500 y	1000 y
I-DEWAR1	FE1422	--	3.73E-05	2.83E-05	2.60E-05	1.23E-05	9.68E-07	2.30E-07	2.08E-09	9.66E-10	6.51E-11	1.98E-11
I-HEVSL1	304SS	--	1.06E-05	8.69E-06	6.97E-06	3.08E-06	7.64E-07	3.41E-07	1.30E-08	8.07E-09	7.85E-10	3.07E-10
I-HFMAG1	304SS	--	2.19E-06	1.55E-06	1.22E-06	5.56E-07	1.57E-07	7.70E-08	1.41E-08	9.56E-09	6.00E-10	1.11E-10
	COPPER	--	7.27E-06	2.59E-06	8.26E-07	7.41E-07	4.70E-07	2.80E-07	6.15E-08	4.15E-08	2.03E-09	4.68E-11
	NB3SN	--	3.56E-07	3.50E-07	3.25E-07	3.09E-07	2.54E-07	1.98E-07	3.20E-08	9.03E-09	6.99E-09	6.87E-09
	G10	--	1.83E-09	4.93E-16	4.93E-16	4.92E-16	4.92E-16	4.92E-16	4.90E-16	4.87E-16	4.64E-16	4.36E-16
I-HFMAG2	304SS	--	1.76E-07	9.29E-08	7.09E-08	3.45E-08	1.25E-08	7.14E-09	2.77E-09	1.90E-09	1.08E-10	1.35E-11
	COPPER	--	9.89E-07	2.97E-07	3.68E-08	3.30E-08	2.09E-08	1.25E-08	2.70E-09	1.82E-09	8.91E-11	2.05E-12
	NB3SN	--	3.19E-08	3.16E-08	3.04E-08	2.90E-08	2.38E-08	1.87E-08	3.27E-09	1.14E-09	9.48E-10	9.32E-10
	G10	--	8.26E-11	9.79E-17	9.79E-17	9.79E-17	9.79E-17	9.78E-17	9.73E-17	9.68E-17	9.22E-17	8.68E-17
I-LFMAG1	304SS	--	1.14E-08	4.72E-09	3.49E-09	1.80E-09	7.86E-10	4.87E-10	2.38E-10	1.64E-10	9.02E-12	9.59E-13
	COPPER	--	7.87E-08	2.24E-08	1.24E-09	1.11E-09	7.05E-10	4.20E-10	9.07E-11	6.12E-11	2.99E-12	6.89E-14
	NBTI	--	2.09E-09	2.04E-09	1.83E-09	1.38E-09	1.09E-09	8.56E-10	1.60E-10	6.38E-11	5.49E-11	5.40E-11
	G10	--	2.78E-12	8.52E-18	8.52E-18	8.52E-18	8.51E-18	8.51E-18	8.46E-18	8.41E-18	8.02E-18	7.55E-18
I-LFMAG2	304SS	--	3.53E-10	1.24E-10	8.95E-11	4.89E-11	2.44E-11	1.59E-11	8.72E-12	5.99E-12	3.23E-13	3.01E-14
	COPPER	--	2.66E-09	7.37E-10	1.75E-11	1.57E-11	9.94E-12	5.92E-12	1.28E-12	8.62E-13	4.22E-14	9.71E-16
	NBTI	--	4.75E-11	4.68E-11	4.37E-11	3.62E-11	2.91E-11	2.30E-11	4.59E-12	2.05E-12	1.81E-12	1.77E-12
	G10	--	3.89E-14	3.12E-19	3.12E-19	3.12E-19	3.12E-19	3.11E-19	3.10E-19	3.08E-19	2.93E-19	2.76E-19
I-HEVSL2	304SS	--	2.10E-11	5.60E-12	3.84E-12	2.16E-12	1.10E-12	7.11E-13	3.78E-13	2.60E-13	1.49E-14	1.95E-15
I-DEWAR2	FE1422	--	4.14E-11	1.26E-12	1.05E-12	5.37E-13	1.21E-13	4.62E-14	1.54E-14	1.06E-14	5.21E-16	1.55E-17
O-DEWAR1	FE1422	--	8.53E-09	6.27E-10	5.57E-10	2.64E-10	2.68E-11	7.83E-12	1.40E-12	9.51E-13	4.73E-14	1.84E-15
O-HEVSL1	304SS	--	1.13E-09	3.74E-10	2.55E-10	1.28E-10	5.04E-11	2.82E-11	8.79E-12	6.08E-12	5.14E-13	1.72E-13
O-HFMAG1	304SS	--	4.23E-10	1.35E-10	9.37E-11	5.09E-11	2.52E-11	1.61E-11	8.37E-12	5.75E-12	3.35E-13	4.68E-14
	COPPER	--	3.62E-09	1.00E-09	2.06E-11	1.85E-11	1.18E-11	7.10E-12	1.65E-12	1.11E-12	5.45E-14	1.25E-15
	NB3SN	--	8.80E-11	8.77E-11	8.68E-11	8.30E-11	6.83E-11	5.38E-11	1.61E-11	4.03E-12	3.47E-12	3.42E-12
	G10	--	3.95E-14	3.04E-19	3.04E-19	3.04E-19	3.04E-19	3.04E-19	3.03E-19	3.01E-19	2.86E-19	2.70E-19
O-HFMAG2	304SS	--	3.92E-11	1.29E-11	9.12E-12	5.12E-12	2.74E-12	1.82E-12	1.05E-12	7.19E-13	3.87E-14	3.52E-15
	COPPER	--	3.12E-10	8.58E-11	9.03E-13	8.11E-13	5.15E-13	3.09E-13	6.91E-14	4.66E-14	2.28E-15	5.25E-17
	NB3SN	--	5.26E-12	5.24E-12	5.20E-12	4.97E-12	4.11E-12	3.25E-12	6.74E-13	3.18E-13	2.84E-13	2.79E-13
	G10	--	1.80E-15	3.72E-20	3.72E-20	3.72E-20	3.72E-20	3.71E-20	3.70E-20	3.67E-20	3.50E-20	3.29E-20
O-LFMAG1	304SS	--	2.04E-12	6.47E-13	4.58E-13	2.60E-13	1.42E-13	9.54E-14	5.58E-14	3.83E-14	2.04E-15	1.70E-16
	COPPER	--	1.62E-11	4.43E-12	2.98E-14	2.67E-14	1.70E-14	1.02E-14	2.25E-15	1.52E-15	7.42E-17	1.71E-18
	NBTI	--	1.95E-13	1.93E-13	1.87E-13	1.67E-13	1.36E-13	1.08E-13	2.36E-14	1.19E-14	1.03E-14	1.06E-14
	G10	--	6.02E-17	1.99E-21	1.99E-21	1.99E-21	1.99E-21	1.99E-21	1.98E-21	1.97E-21	1.87E-21	1.76E-21
O-LFMAG2	304SS	--	4.58E-14	1.44E-14	1.02E-14	5.83E-15	3.23E-15	2.18E-15	1.29E-15	8.86E-16	4.68E-17	3.65E-18
	COPPER	--	3.60E-13	9.84E-14	4.09E-16	3.67E-16	2.33E-16	1.39E-16	3.06E-17	2.07E-17	1.01E-18	2.33E-20
	NBTI	--	3.79E-15	3.76E-15	3.66E-15	3.32E-15	2.72E-15	2.16E-15	4.89E-16	2.58E-16	2.36E-16	2.32E-16
	G10	--	8.37E-19	4.60E-23	4.60E-23	4.60E-23	4.60E-23	4.60E-23	4.57E-23	4.55E-23	4.33E-23	4.03E-23
O-HEVSL2	304SS	--	2.18E-15	5.24E-16	3.52E-16	2.06E-16	1.14E-16	7.61E-17	4.33E-17	2.93E-17	1.66E-18	1.85E-19
O-DEWAR2	FE1422	--	4.58E-15	8.03E-17	6.20E-17	3.39E-17	1.15E-17	4.74E-18	1.74E-18	1.19E-18	5.87E-20	1.69E-21

Table C.5. Radwaste Management for the STARFIRE TF-Magnet Design

BHP of Water of Magnet Components (km^3 of water/cm^3)

Magnet Component			Time After Reactor Shutdown									
			0	1 d	1 mo	1 y	5 y	10 y	50 y	100 y	500 y	1000 y
I-DEWAR1	FE1422	--	2.09E-09	3.45E-10	3.06E-10	1.51E-10	1.91E-11	4.84E-12	9.95E-14	6.38E-14	3.78E-15	7.61E-16
I-HEVSL1	304SS	--	4.63E-10	1.79E-10	1.22E-10	5.17E-11	1.35E-11	6.10E-12	1.59E-12	1.32E-12	6.44E-13	4.39E-13
I-HFMAG1	304SS	--	1.50E-10	3.72E-11	2.38E-11	1.10E-11	3.92E-12	2.35E-12	1.20E-12	9.05E-13	2.43E-13	1.51E-13
	COPPER	--	1.30E-09	3.64E-10	1.33E-11	1.24E-11	9.51E-12	7.44E-12	4.05E-12	2.77E-12	1.35E-13	3.12E-15
	NB3SN	--	5.53E-09	3.98E-09	1.52E-09	9.27E-10	3.22E-10	9.42E-11	4.93E-12	4.74E-12	4.66E-12	4.58E-12
	G10	--	6.18E-20	6.16E-20	6.16E-20	6.16E-20	6.15E-20	6.15E-20	6.12E-20	6.08E-20	5.80E-20	5.45E-20
I-HFMAG2	304SS	--	1.83E-11	3.01E-12	1.77E-12	9.35E-13	4.72E-13	3.39E-13	2.15E-13	1.56E-13	2.98E-14	1.69E-14
	COPPER	--	1.91E-10	5.25E-11	5.88E-13	5.48E-13	4.21E-13	3.28E-13	1.77E-13	1.21E-13	5.94E-15	1.37E-16
	NB3SN	--	6.68E-10	4.64E-10	2.12E-10	1.43E-10	5.03E-11	1.46E-11	6.65E-13	6.43E-13	6.32E-13	6.21E-13
	G10	--	1.22E-20	1.22E-20	1.22E-20	1.22E-20	1.22E-20	1.22E-20	1.22E-20	1.21E-20	1.15E-20	1.08E-20
I-LFMAG1	304SS	--	1.49E-12	1.91E-13	1.07E-13	6.12E-14	3.57E-14	2.70E-14	1.80E-14	1.29E-14	2.14E-15	1.15E-15
	COPPER	--	1.55E-11	4.25E-12	1.98E-14	1.84E-14	1.41E-14	1.10E-14	5.96E-15	4.08E-15	2.00E-16	4.59E-18
	NBTI	--	1.30E-12	1.21E-12	2.23E-13	5.45E-14	4.76E-14	4.52E-14	3.82E-14	3.72E-14	3.66E-14	3.60E-14
	G10	--	1.06E-21	1.06E-21	1.06E-21	1.06E-21	1.06E-21	1.06E-21	1.06E-21	1.05E-21	1.00E-21	9.43E-22
I-LFMAG2	304SS	--	5.07E-14	5.90E-15	3.26E-15	1.95E-15	1.23E-15	9.50E-16	6.44E-16	4.60E-16	6.77E-17	3.46E-17
	COPPER	--	5.28E-13	1.44E-13	2.79E-16	2.60E-16	1.99E-16	1.56E-16	8.40E-17	5.75E-17	2.81E-18	6.47E-20
	NBTI	--	1.92E-14	1.79E-14	4.05E-15	1.64E-15	1.50E-15	1.44E-15	1.25E-15	1.22E-15	1.20E-15	1.18E-15
	G10	--	3.90E-23	3.90E-23	3.90E-23	3.90E-23	3.89E-23	3.89E-23	3.87E-23	3.85E-23	3.67E-23	3.45E-23
I-HEVSL2	304SS	--	3.31E-15	3.02E-16	1.41E-16	8.63E-17	5.53E-17	4.31E-17	2.96E-17	2.16E-17	4.25E-18	2.44E-18
I-DEWAR2	FE1422	--	8.06E-15	4.12E-17	2.44E-17	1.34E-17	4.74E-18	2.25E-18	1.03E-18	7.06E-19	3.49E-20	1.16E-21
O-DEWAR1	FE1422	--	1.59E-12	1.12E-14	7.60E-15	3.79E-15	7.27E-16	2.76E-16	9.26E-17	6.34E-17	3.16E-18	1.32E-19
O-HEVSL1	304SS	--	1.63E-13	1.72E-14	6.34E-15	3.42E-15	1.95E-15	1.49E-15	1.04E-15	8.46E-16	3.68E-16	2.48E-16
O-HFMAG1	304SS	--	6.31E-14	6.91E-15	3.30E-15	1.96E-15	1.25E-15	9.72E-16	6.69E-16	4.91E-16	1.04E-16	6.08E-17
	COPPER	--	7.20E-13	1.97E-13	3.40E-16	3.18E-16	2.47E-16	1.96E-16	1.09E-16	7.43E-17	3.63E-18	8.36E-20
	NB3SN	--	2.44E-12	1.65E-12	7.76E-13	5.41E-13	1.90E-13	5.49E-14	2.42E-15	2.35E-15	2.32E-15	2.28E-15
	G10	--	3.80E-23	3.80E-23	3.80E-23	3.80E-23	3.80E-23	3.80E-23	3.78E-23	3.76E-23	3.58E-23	3.37E-23
O-HFMAG2	304SS	--	5.83E-15	6.68E-16	3.63E-16	2.22E-16	1.44E-16	1.13E-16	7.71E-17	5.50E-17	7.93E-18	4.01E-18
	COPPER	--	6.22E-14	1.70E-14	1.46E-17	1.37E-17	1.06E-17	8.30E-18	4.54E-18	3.11E-18	1.52E-19	3.50E-21
	NB3SN	--	1.96E-13	1.34E-13	6.85E-14	4.86E-14	1.71E-14	4.92E-15	1.96E-16	1.92E-16	1.89E-16	1.86E-16
	G10	--	4.65E-24	4.65E-24	4.65E-24	4.65E-24	4.64E-24	4.64E-24	4.62E-24	4.59E-24	4.37E-24	4.12E-24
O-LFMAG1	304SS	--	3.09E-16	3.42E-17	1.88E-17	1.16E-17	7.59E-18	5.94E-18	4.06E-18	2.88E-18	3.83E-19	1.86E-19
	COPPER	--	3.23E-15	8.81E-16	4.81E-19	4.49E-19	3.46E-19	2.71E-19	1.48E-19	1.01E-19	4.95E-21	1.14E-22
	NBTI	--	3.73E-17	3.51E-17	1.32E-17	9.05E-18	8.55E-18	8.27E-18	7.41E-18	7.28E-18	7.17E-18	7.05E-18
	G10	--	2.49E-25	2.49E-25	2.49E-25	2.49E-25	2.49E-25	2.48E-25	2.47E-25	2.46E-25	2.34E-25	2.20E-25
O-LFMAG2	304SS	--	6.96E-18	7.67E-19	4.28E-19	2.65E-19	1.74E-19	1.36E-19	9.30E-20	6.53E-20	8.28E-21	3.89E-21
	COPPER	--	7.19E-17	1.96E-17	6.57E-21	6.14E-21	4.72E-21	3.70E-21	2.01E-21	1.38E-21	6.74E-23	1.55E-24
	NBTI	--	5.92E-19	5.60E-19	2.55E-19	1.94E-19	1.85E-19	1.79E-19	1.62E-19	1.59E-19	1.57E-19	1.54E-19
	G10	--	5.75E-27	5.75E-27	5.75E-27	5.75E-27	5.75E-27	5.74E-27	5.72E-27	5.68E-27	5.41E-27	5.10E-27
O-HEVSL2	304SS	--	3.55E-19	3.12E-20	1.45E-20	9.17E-21	6.07E-21	4.77E-21	3.29E-21	2.37E-21	4.05E-22	2.21E-22
O-DEWAR2	FE1422	--	9.04E-19	3.89E-21	2.08E-21	1.18E-21	4.95E-22	2.44E-22	1.15E-22	7.95E-23	3.93E-24	1.28E-25

APPENDIX D

Standards for Radioactive Waste Disposal

(Hazards Indices)

1. Introduction

The Environmental Protection Agency (EPA) has the primary responsibility for establishing standards for the management and disposal of radioactive materials. The agency plans to publish a rule for managing high level wastes "Environmental Standards and Federal Radiation Protection Guidance for Management and Disposal of Spent Nuclear Fuel, High-Level and Transuranic Radioactive Wastes," 40 CFR 191. Also being prepared are standards for disposing of less radioactive wastes.

Federal standards limit the radiation dose to individuals in the general population to less than 500 mrem per year [10 CFR 20].

Disposal systems shall be designed to comply with projected performance requirements which should provide a reasonable expectation that for 10,000 years after disposal, reasonably foreseeable releases of waste to the accessible environment (aquifer) are projected to be less than the stated amounts given in the rule. These quantities are the "cumulative releases to the accessible environment for 10,000 years after disposal."

The EPA standards limit the amount of materials to appear in the aquifer. The NRC standards, however, place the limits for shallow land burial on the concentration of the individual radionuclides acceptable for such disposal.

2. Rationale for Standards

In considering disposition of wastes from nuclear facilities, there are three categories that may be used.

1. Non-radioactive waste that can be discharged directly to the biosphere.

2. Waste that has to be confined for a period of time in a controlled manner with a predictably low level of release.
3. Waste that has to be isolated from the biosphere, thus minimizing release into the biosphere and inadvertent contact with man.

In such a system for classifying wastes, the method controlling disposal is based primarily on the hazard potential of the material and is expressed in terms of radioactivity per unit volume at the time of disposal.

It is necessary to compare the possible exposure to the public with the guidelines for acceptable doses to ascertain the acceptability of the disposal mode. This calls for identifying a set of reasonably conservative exposure events; describing the transport of the radioactivity through the environment to man or man's encounter into the waste; then calculating the concentrations or inventories of radioactivities in the wastes that will assure that doses to the population do not exceed the dose guidelines.

Calculations were made for typical transport events that would bring radioactive nuclides to man's proximity and thus provide a dose of radioactivity. From a comparison of the calculated dose with the acceptable dose, the limits for burial of that particular radionuclide can be established [ADAM]. In evaluating migration of radionuclides via groundwater, the following points were recognized; decay constant of the radionuclide in question, leaching constant for the radionuclide and its subsequent sorption upon soils in groundwater pathway.

From analyses similar to those mentioned previously, a table of limiting concentrations for shallow land burial was derived for the proposed "Land Disposal of Low-Level Radioactive Waste" [10 CFR 61]. The preliminary values and the rule were published for comment and as a result the table of limiting values was modified to yield the data in Table D-1.

Table D-1. Concentrations of Radionuclides for Establishing Waste Classification

Radionuclide	Concentration (Ci/m^3)		
^{14}C	8		
^{14}C in activated metal	80		
^{59}Ni in activated metal	220		
^{94}Nb in activated metal	0.2		
	Class A	Class B	Class C
Total of all nuclides with less than 5 year half-life	700	*	*
^{3}H	40	*	*
^{60}Co	700	*	*
^{63}Ni	3.5	70	700
^{63}Ni in activated metal	35	700	7000

*There are no limits established for these radionuclides in Class B or C wastes. Practical considerations such as the effects of external radiation and internal heat generation on transportation, handling, and disposal will limit the concentrations for these wastes.

For fusion reactors only three long-lived radionuclides are important for waste disposal, ^{14}C, ^{59}Ni, and ^{94}Nb. As long as the limits given in Table D-1 are not exceeded, the waste is acceptable for shallow land burial. If the concentration does not exceed 0.1 times the value in Table D-1, the waste is Class A, if it does exceed 0.1 times the value in Table D-1, the waste is Class C. The short-lived isotopes of importance for waste disposal are ^{3}H, ^{60}Co, and ^{63}Ni and if the limits for these nuclides given in Table D-1 are not exceeded the waste is suitable for shallow land burial.

If the radioactive waste does not contain any long-lived isotopes in Table D-1, classification is determined based on the concentrations of the short-lived isotopes in Table D-1. If a nuclide is not listed in Table D-1, it does not need to be considered in determining the waste class. If the radioactive waste does not contain any nuclides in Table D-1, it is Class A waste.

For the V15Cr5Ti after removal from the reactor and after 50 years decay, the residual activities of interest are

^{14}C	67 Ci/m^3
^{94}Nb	0.7 Ci/m^3
^{63}Ni	1.8 Ci/m^3

From Table D-1, the ^{14}C and ^{63}Ni are within acceptable limits for shallow land burial. The ^{94}Nb is 3.5 times too high. However, if 2 ft^3 of waste were placed in a 55 gal drum (7.5 ft^3) the overall concentration would be within acceptable limits.

For the PCA after 50 years cooling, the data of Table 2.14 show the ^{63}Ni to be approximately 20 times higher than the limit and ^{94}Nb to be approximately 65 times higher than the limit acceptable for shallow land burial.

3. Hazard Potential

In attempting to assess the hazard or safety of a system or a radionuclide, indices have been devised to reflect such a measure. Many factors have been suggested for inclusion in the estimation of safety indices. A review has been made of the many safety indices that have been proposed and five were selected as being adequate [VOSS]. The simplest index is merely the measure of the total curies involved. Total curies is not a good measure because it does not consider biological consequences. This can be corrected by introducing the maximum permissible concentration (in water or air) for the individual nuclides. This second measure, a hazards measure (HM) or biological hazard potential (BHP) is given by the following relation.

$$HM = \frac{Q(Ci)}{MPC\ (Ci/m^3)}$$

MPC = maximum permissible concentration

Introduction of the MPC takes into account the radioactive decay rate of the individual nuclids, the radiation energy level and the biological lifetime.

Neither of the indices mentioned reflect the rate of release of nuclides to the environment. This is accomplished with the following relation.

$$HM2 = \sum_{i=1}^{n} Q_i \left[\frac{a_i}{MPI_{wi}} + \frac{b_i}{MPI_{wi}} \right]$$

a_i, b_i = fraction of Q_i released in water and air respectively.

MPI = maximum permissible intake, defined as the nuclide concentration limits in air or water as specific in 10 CFR 20 times the average annual fluid intake in man.

The hazard index, HI is a relative quantity and is given by the equations below.

$$HI_i = \frac{HM_i}{V} = \frac{Q_i/V}{MPC}$$

Such a measure of the concentration of radionuclides in a waste form of given volume (V) divided by the MPC indicates the number of times the nuclides would have to be diluted to yield the MPC.

Another index is the relative toxicity index (RTI) and may be defined as the ratio of the amount of water required to dilute a quantity of waste to MPC levels with the amount of water required to dilute the amount of uranium mined to generate the waste quantity

$$RTI = \frac{\Sigma_i \ (Q_i/MPC_i) \text{ waste}}{\Sigma_j \ (Q_j/MPC_j) \text{ equiv. uranium ore}}$$

In utilizing these indices caution must be exercised. The basic hazard measure compares the amount of radioactivity with the maximum permissible concentration. Such a measure would be suitable for bare waste packages. When these packages are buried then release pathways to air and water must be considered. Basically all of the indices compare the radionuclide amount or concentration against the MPC for that radionuclide.

However, the most widely used safety index, the biological hazard potential (BHP) is similar to the hazard index HI and assumes total release of the radioactivity to the aquifer and complete dissolution of the radionuclides. Thus such a measure yields an upper limit to the hazard potential. A more recent analysis [PIGFORD] of radionuclide migration through soil and rock indicates that rate of water movement, solubility of radionuclides in water, and absorption and desorption of radionuclides on soils are important. When these factors are considered, the calculated hazard potential is much less than the BHP values.

In comparing fission and fusion wastes caution must be exercised. One difference that is immediately apparent is the presence of actinide elements in the fission wastes. Using the hazard measure (or biological hazard potential) comparison of fission and fusion wastes indicates that after one year, the fusion wastes are approximately 15 times less hazardous for inhalation than are the fission wastes. The gap is further widened after 100 years after shutdown to approximately 10,000 times less hazard for fusion wastes over fission wastes [KESSLER].

APPENDIX E
Materials Recycle

1. Introduction

Fusion reactors contain large amounts of material in their structure, approximately 25,000 Mg (tonnes). This material may be separated into two broad categories, that material part which is removed regularly and the material that will last through the reactor lifetime. In the first category is the first wall/blanket structure, containing approximately 1550 Mg (in the case of STARFIRE), 1/6 of which is removed annually. The bulk of the material in the second category, ∿17,200 Mg, is represented by the structural material of the shield and magnets, e.g., Fe 1422 (Fe 14 Mn 2 Ni 2 Cr) and 304 SS.

2. Recycle Candidates

Of the material removed from the fusion reactor annually the $LiAlO_2$ enriched in ^6Li (from a STARFIRE) or the vanadium (from a STARFIRE design using metallic lithium as the coolant) are the most likely candidates for recycle. However, both contain sufficient residual radioactivity even after reasonable decay times that direct handling is not acceptable. In the case of the $LiAlO_2$, within one year after removal from the reactor the residual activity is 2.4×10^{-6} Ci/cm^3 due primarily to ^{26}Al that decays with a 1.8 MeV gamma. This residual activity yields a surface dose rate of 2.8 rem/hr for a one meter sphere. For the vanadium alloy, the residual activity after ten years is 5.6×10^{-3} Ci/cm^3 yielding a contact dose rate of approximately 100 rem/hr for a one meter sphere. After 50 years, the residual activity is 9.3×10^{-5} Ci/cm^3 producing a contact dose rate of approximately 0.3 rem/hr. This contact dose rate is further reduced to 0.06 rem/hr if the residual ^{94}Nb can be removed. Under these conditions limited direct operation would be possible.

3. Recycle

The design of the STARFIRE reactor allows the blanket sectors to be removed remotely, using specially designed machines. These sectors will be removed from the reactor hall and delivered to a storage area for an

appropriate decay period before disassembly and processing is undertaken in a shielded cell. All of the functions carried out in the shielded cells will use specially designed equipment. There appears to be little question that the sectors can be disassembled remotely. A problem of importance is that reuse of the material in the refabrication of the blanket sectors may involve tasks, e.g., welding in small spaces, that are difficult to carry and using remote operation techniques. Use of long decay times (>50 y) to lower the dose rate levels may prove to be impractical from several points of view, e.g., inventory accumulation and degeneration of materials in storage.

4. Remote Operations in the Nuclear Field

Remote operations, of necessity, have been required in the nuclear operations starting with the first reactors and heavy metal recovery plants. More recently, mixed-oxide fuel fabrication plants have been built using glove box techniques for some handling operations. Based on experience with such plants a completely remotely operated fabrication plant for U-Pu mixed oxide fuels was designed, but was not built because of U.S. moratorium on reprocessing spent nuclear fuels. This work is being continued leading to a remote control fuel fabrication process for breeder reactor fuel [GERBER].

There is a large body of literature on remote control and operations techniques, usually reported in the annual proceedings of the Conference on Remote Systems Technology that is normally held in conjunction with American Nuclear Society Meetings. There are two general types of manipulative operations; first, processing and examination of irradiated materials and second, physical property measurements of irradiated materials. In addition, the body of experience on remote operations such as welding is increasing rapidly as power reactor operators find the activated corrosion products produce radiation fields that allow only very short working times in certain areas.

There are many pieces of equipment that have been used in a remote environment, e.g., motorized cranes, master slave manipulators, pneumatically operated end mill, horizontal drill, horizontal circular mill,

tape controlled mill, pneumatic impact wrenches, tool positioning tables. More recently, slave manipulators have been decoupled from the direct control of the master units. In the one case, the slave arms were mounted on a motor operated vehicle which could move about freely. The slave arms could be operated by computer assist, computer control, or programmed by magnetic recording [VERTUT]. An additional improvement lead to the design of a system with remote handling with master slave manipulators in the hot cell, but with the operator working in a distant control room [PEAGRAM].

There has been concern about designing remotely operated equipment for performing various maintenance functions around a reactor, in particular the various operations required for removing and replacing a sector from the STARFIRE [BAKER]. This has been an ongoing concern recognizing that servomanipulators were required for coping with the various normal and unpredicted tasks that might arise. Leak detection techniques and precise welding for vacuum tightness were demonstrated [RAIMONDI]. Other evaluations of the maintenance requirements for fusion reactors indicate that remote maintenance is feasible for all systems in the reactor hall [ZAHN] and that with careful attention to a "design for maintenance" plan, remote maintenance can be achieved [DOGGETT].

Finally, for the Fusion Materials Irradiation Test Facility a system is being designed to pump lithium to a target area for generation of a high energy neutron environment. The design will allow for remote maintenance of lithium system components such as the main lithium pump, heat exchanger, traps and valves [KELLY].

More recently at the International Machine Tool Show [IMTS] industrial robots were demonstrated by several manufacturers: Westinghouse, Bendix, General Electric, Cincinnati Milacron, etc. These robots usually were fixed in one position on the floor, but were able to move in three axes. The robot arms could be compared to the human arm, with shoulder, elbow and wrist movement. On a typical robot, the wrist attached to the forearm is capable of 180 degree bend and a 360 degree twist. These units are usually computer controlled and one unit offered accuracy of

location of $\pm$ 0.02" and repeatability of $\pm$ 0.005". Robots were demonstrated for moving an object from one position to another, which is the simplest task. However, from the state-of-the-art today, more intricate tasks should be capable of being performed by robots in the future.

Based on developments in remote operations in hot cells, the studies of remote operations for fusion systems, and the development of industrial robots, it appears likely that remote refabrication of blanket sectors can be accomplished, especially if such remote fabrication requirements were factored into the original design. Further studies in the area of materials recycle can assume that both fabrication and reassembly of fusion reactor components will be feasible by remote means.

APPENDIX F

Comments on Isotopic Tailoring

When the stainless steel structural material is irradiated in a fusion reactor, large amounts of ^{63}Ni and ^{93}Mo are produced by neutron interaction. The long half-lives of these nuclides results in long-lived radioactivity.

In the activation of the stainless steel, the ^{93}Mo is formed from the ^{92}Mo (n,γ) ^{93}Mo and ^{94}Mo $(n,2n)$ ^{93}Mo reactions. The two isotopes of ^{92}Mo (14.8% natural abundance) and ^{94}Mo (9.3%) cause more than 99% of the total ^{93}Mo activation due to the above reactions. It has been suggested [CONN] that this problem might be ameliorated by removing these isotopes from the molybdenum. It is further suggested that the molybdenum be constituted to contain 100% ^{97}Mo (9.6% natural abundance), the isotope least likely to pose the activation problem among the number of stable, molybdenum isotopes.

In a similar fashion, nickel isotopes ^{62}Ni (3.59% natural abundance) and ^{64}Ni (0.91%) react with neutrons to yield ^{63}Ni ($T_{1/2} \sim 100$ y) which decays by beta emission with no gamma. It has also been suggested that the nickel for the PCA be 100% ^{61}Ni (1.25% in natural abundance). However, the nitrogen content in the metal must also be minimized to limit the concentration of ^{14}C by the ^{14}N (n,p) ^{14}C. The ^{14}C has a 5730 y half-life and decays by beta emission.

The chemistry and properties of MoF_6 are very similar to those of UF_6 and hence it is expected that isotope separation by gaseous diffusion and gas centrifuge systems should be feasible. Separations methods based on diffusion would seek to isolate $^{97}MoF_6$ from $^{92}MoF_6$ and $^{94}MoF_6$. The theoretical separation factor based on the square root of the ratio of molecular weights ($\alpha = \sqrt{M_1/M_2}$) for ^{97}Mo and ^{94}Mo is 1.0158, somewhat larger than the 1.0064 for ^{238}U and ^{235}U. Other diffusional methods would be possible, e.g., thermal diffusion, but the value of α is the same. Centrifuge methods are less simply described but the separation varies as $(M_2-M_1)^2$. Hence, for a mass difference of 3 AMU separations should be comparable to the UF_6 system if all other parameters, i.e.,

density, diffusion coefficient, velocity of the rotor, length of the machine, are the same. Photoexcitation methods are even more complex and in the absence of spectral data no conclusions on their potential can be made although [FREUND] has reported favorable results. Magnetic methods, i.e., calutron mass spectrometry, are based on relatively simple principles of magnetic separation of, for example, $^{94}MoF_x^+$ and $^{97}MoF_x^+$. The theoretical factors are very large. Finally, chemical separation of isotopes takes advantage of isotope-related differences in equilibrium constants in solvent extraction or ion exchange systems. Calculations of theoretical separation factors are complex. The latter two methods are applicable to elements that do not form volatile compounds (fluorides) such as nickel. In the case of nickel, separation of adjacent nuclides reduces the theoretical separation factors owing to the small mass difference. Volatile compounds of metals such as $Ni(CO)_6$, acetyl acetonates and nickelocene, $(C_5H_5)_2Ni$, are not generally suitable since the adjunct molecules, i.e., CO, C_5H_5, are not monoisotopic and thus confound the separations based on mass effects. Such volatile compounds would be useful for photoexcitation processes that can yield high separations.

One such reported experiment with a CO_2 laser did yield a separation but not very efficiently [FREUND]. The attempt was to separate the molybdenum isotopes using MoF_6 as the gas. The experiment was a static experiment in which the isotopic distribution was measured before and after irradiation by the laser beam. In these experiments an enrichment ratio of 1.03 was achieved for ^{97}Mo, the isotope of interest. The maximum enrichment ratio was 1.14 for ^{92}Mo. These were room temperature experiments and it was suggested by Freund that cooling would provide for better resolution and hence, better isotope separation. These were crude experiments to provide proof of principle. For effective isotope separation better conditions must be sought.

Isotopic separations techniques are well enough documented to allow rough comparisons to be made between advantages and costs. It is likely that only the use of existing technology could be justified but additional information needs to be assembled before future directions will become evident.

One such reported experiment with a CO_2 laser did yield a separation but not very efficiently [FREUND]. The attempt was to separate the molybdenum isotopes using MoF_6 as the gas. The experiment was a static experiment in which the isotopic distribution was measured before and after irradiation by the laser beam. In these experiments an enrichment ratio of 1.03 was achieved for ^{97}Mo, the isotope of interest. The maximum enrichment ratio was 1.14 for ^{92}Mo. These were room temperature experiments and it was suggested by Freund that cooling would provide for better resolution and hence, better isotope separation. These were crude experiments to provide proof of principle. For effective isotope separation better conditions must be sought.

Isotopic separations techniques are well enough documented to allow rough comparisons to be made between advantages and costs. It is likely that only the use of existing technology could be justified but additional information needs to be assembled before future directions will become evident.

One such reported experiment with a CO_2 laser did yield a separation but not very efficiently [FREUND]. The attempt was to separate the molybdenum isotopes using MoF_6 as the gas. The experiment was a static experiment in which the isotopic distribution was measured before and after irradiation by the laser beam. In these experiments an enrichment ratio of 1.03 was achieved for ^{97}Mo, the isotope of interest. The maximum enrichment ratio was 1.14 for ^{92}Mo. These were room temperature experiments and it was suggested by Freund that cooling would provide for better resolution and hence, better isotope separation. These were crude experiments to provide proof of principle. For effective isotope separation better conditions must be sought.

Isotopic separations techniques are well enough documented to allow rough comparisons to be made between advantages and costs. It is likely that only the use of existing technology could be justified but additional information needs to be assembled before future directions will become evident.

APPENDIX G

Dismantling of the Magnet Structure

1. Remote Dismantling

Before dismantling begins and any cutting operation occurs, a large plastic curtain will be placed entirely around the assembly so that dust and fragments from the cutting can be contained. In addition to the curtain, all cutting tools will be equipped with a vacuum suction. These precautionary measures will greatly simplify cleanup. In the discussion that follows, reference is made to Section 3.1 for a description of the TF magnet and the nomenclature used.

The magnet dismantling operation begins after first separating the toroidal field coil/helium vessel assembly from the rest of the reactor by remotely removing related reactor elements such as the CF and EF coils, intercoil shear panels, and blanket and shield. Next, the individual TF coil/helium vessel magnets are disjoined by vertically cutting the common inner vacuum vessel between each magnet with a plasma torch. A plasma torch is preferable to a carbide saw because it can cut the 3 cm sections more quickly and thus less expensively [HAGER]. First, section I-DEWAR1 (see Section 3.1 for description of nomenclature) is cut using the Reactor Overhead Electro-Mechanical Manipulator [BAKER] to maneuver the torch. Then, section I-DEWAR2 is cut and the mechanical attachment to the centerpost is removed through the top of the centerpost vacuum opening. This frees section I-DEWAR2 and it is removed from the centerpost.

After disjoining the first magnet, it is positioned next to a large mounting fixture using the 600-Tonne Reactor Building Bridge Crane. Once positioned, the assembly is fastened to the mounting fixture using the Reactor Overhead Electro-Mechanical Manipulator to hold the assembly and the impact wrench of the Support System Module Electro-Mechanical Manipulator [BAKER] to attach the assembly to the mounting fixture. The assembly is now in place for remote stand-up cutting. A mounting fixture is preferable to a lay-down fixture because it does not require the inversion of the very large and heavy TF coil/helium vessel magnets and enables cutting on each side of the magnet [HAGER].

Once the magnet is attached to the mounting fixture, the portions of the TF coil/helium vessel assembly that have accumulated unacceptably high activity levels will be removed so that hands-on operations are possible. For purposes of this report, a contact biological dose rate of greater than 2.5 mrem/h is considered unacceptably high. This is the dose rate which would permit continuous 40-hour occupational exposure within 10 CFR 20 quarterly regulatory limits and which is used by most industries as the occupational worker radiation limit. The nucleonics data show that sections I-DEWAR1, I-HEVSL1, I-HFMAG1, and I-HFMAG2 must be removed (see Fig. 3.1). These sections are removed using an automated numerically-controlled milling machine to control the location and depth of the cuts. Owing to the large size of the assembly, there will be no problem in maneuvering the cutting tool of the milling machine and a milling cutter will not be necessary. Instead, a carbide saw, which cuts more quickly, will be used. Once again, a curtain is placed around the stand-up mounting fixture and magnet to simplify cleanup. A plasma torch cannot be used in this application because it is very difficult to control the depth of its cuts [HAGER]. Too deep a cut will segment the NbTi conductor windings which, because they have acceptable activity levels and current-carrying capacity, will be reused in the refabrication of the new magnet.

The milling machine will cut a series of trapezoidal grooves through and around each side of each component of the high activity portion of the magnet, as shown in Fig. G.1. First the vacuum vessel is cut, then the helium vessel, and finally the Nb_3Sn conductor. Because the conductor is pretensioned, it will be secured and cut very slowly so that the frictional overburden provided by the uncut windings will prevent sudden slippage and large shear loads between layers. The Reactor Overhead Electro-Mechanical Manipulator, which will be clamped to the high activity portion for support during cutting, will be used to successively remove and isolate each component.

If the above cutting operation were to be done only once, the automated milling machine would be much more expensive than a simple cutting tool attached to the end of a manipulator [HAGER]. However,

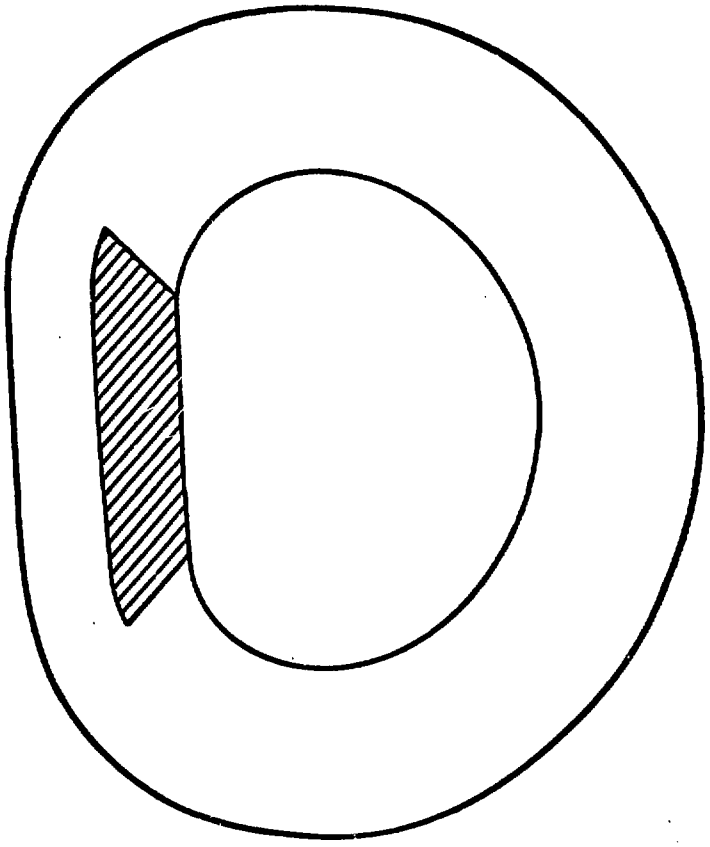

Fig. G.1. TF coil/helium vessel showing high activity portion (shaded) to be cut away by milling machine.

because STARFIRE is assumed to be the tenth commercial plant constructed from a standardized design and would, therefore, be only one of many fusion reactors being decommissioned, the increased capital cost of specialized equipment such as the milling machine is justified owing to savings resulting from an economy of scale operation. For this same reason, a carbide saw blade is used to make the cuts instead of a less expensive, but less durable, grinding wheel.

After isolating the high- and low-activity portions, the high-activity portions will be remotely cut into pieces of appropriate size for shipping using the Reactor Overhead Electro-Mechanical Manipulator with an attached plasma torch. Once the high-activity pieces are cut, they are placed in canisters using the manipulator and shipped to a storage site.

After the high-activity pieces are removed from the reactor building, the fragments and dust from the high-activity portion which have contaminated the low-activity portion are removed using a vacuum attached to a manipulator. After vacuuming, hands-on dismantling operations, which will reduce the difficulty and time required for the various tasks, are possible. The low-activity portion of the magnet is then removed from the mounting fixture, and transported to an adjacent refabrication area using the 600-Tonne Reactor Building Bridge Crane.

2. Hands-On Dismantling

At the refabrication area, the magnet is placed onto a large lay-down fixture which is specially designed to dismantle the TF coil/helium vessel magnets. The lay-down fixture, shown in Fig. G.2, has three large discontinuities which allow work to be done on the face-down side of the magnet. Within each of these discontinuities are mounts to secure an externally-controlled carbide drill, and a hydraulically-adjustable support which can be lowered and raised from the facility's floor.

Because the helium vessel is suspended within the center of the dewar by tiebars, before the vacuum vessel is removed, the helium vessel must be properly supported by supports which extend through the bottom of the dewar. The movable externally-controlled carbide drill is secured to one of the mounts within the lay-down fixture discontinuities. The drill bit is raised and a hole is drilled in the face-down side of the dewar. The drill is moved to the next discontinuity until all three holes are drilled. The use of a drill is preferable to using either a plasma torch or milling cutter for cutting holes because it is faster and offers more depth control [HAGER].

Next, the three hydraulically-adjustable supports are raised out of the refabrication facility's floor until they contact the helium vessel. In combination, the three supports sustain the helium vessel. The three-support triangular structure is used because it is the most structurally stable configuration to protect against wobbling. The dismantling steps

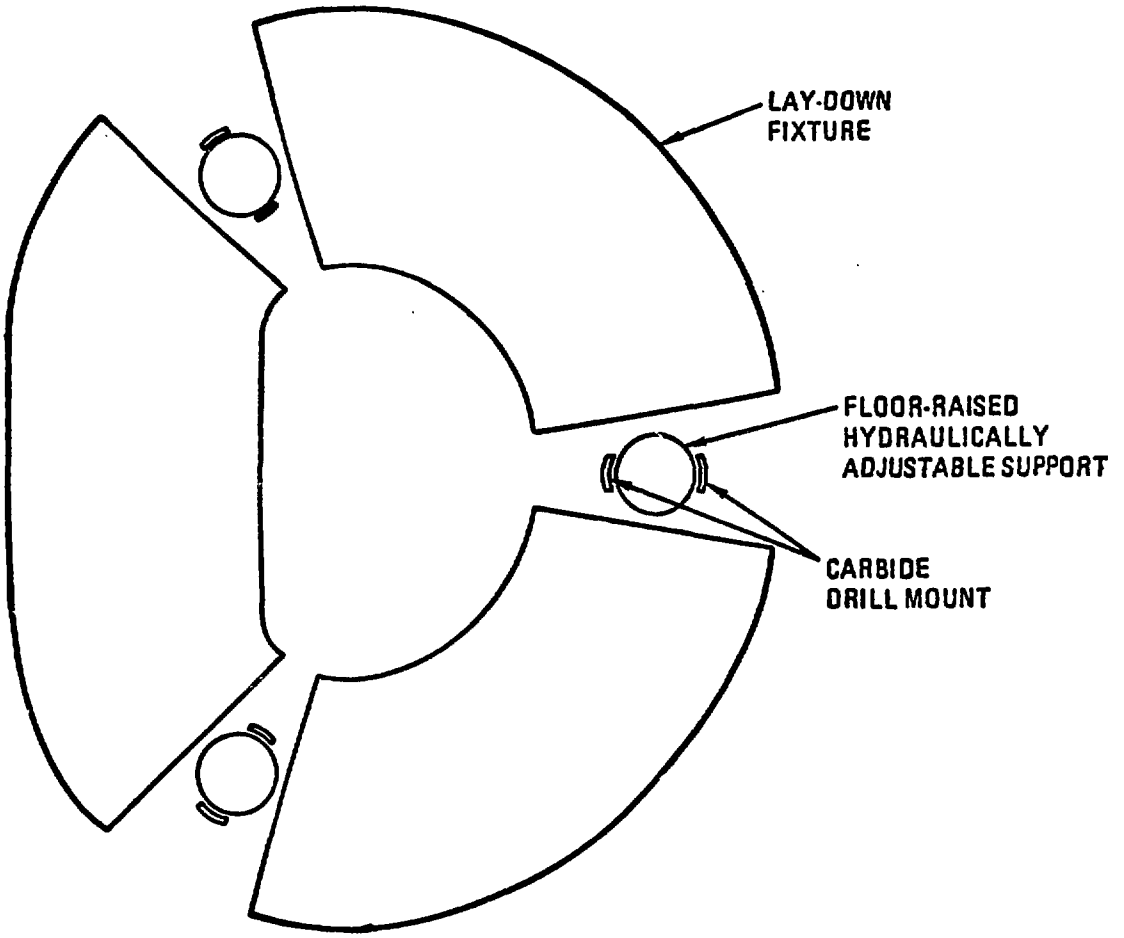

Fig. G.2. Discontinuous lay-down fixture showing carbide drill mounts and floor-raised hydraulically adjustable support.

that occur while the magnet is on the lay-down fixture are sequentially pictured in Fig. G.3, which shows a cross-section of the magnet outboard region.

After supporting the helium vessel, the remaining parts of the vacuum vessel, aluminum thermal radiation shield, and helium vessel are cut in two just above the central radial spine of the helium vessel. To control the depth of the cuts, the cuts are again made using a carbide saw which is guided by a clamp fixture that is attached to the lay-down fixture. The saw cuts entirely around the outside perimeter (the center-post dewar section I-DEWAR2 has already been removed), and then around the low-activity inside perimeter of the vacuum vessel (the high-activity inside portion has also already been removed). The upper portion of the vacuum vessel is then removed with the 600-Tonne Crane [Fig. G.3(B)]. Then the upper sections of the aluminum thermal radiation shield and helium vessel are removed [Fig. G.3(C)].

The upper set of pancake coils are now exposed. The Nb_3Sn coils from the outboard region of the assembly are removed first. Because the high-activity portion Nb_3Sn coil has been removed, the coil is not continuous and must be removed in sections. However, the NbTi coil is intact and is removed in whole using the 600-Tonne Crane [Fig. G.3(D)].

Before the lower set of coils can be removed, the central radial spine of the helium vessel must be detached. Once again, a carbide saw is used to cut out the spine using the lower portion of the helium vessel as a guide [Fig. G.3(E)]. The lower set of coils is then removed following the same procedure used for the upper set [Fig. G.3(F)].

Next, the lower portion of the helium vessel is removed from the inside of the dewar using the 600-Tonne Crane [Fig. G.3(G)]. The hydraulic supports are lowered and the vacuum vessel is also removed with an overhead crane. After removing the two helium vessel portions, the outermost section of each that faces the outside of the magnet is removed with a plasma torch. This readies the helium vessel for coil winding during refabrication.

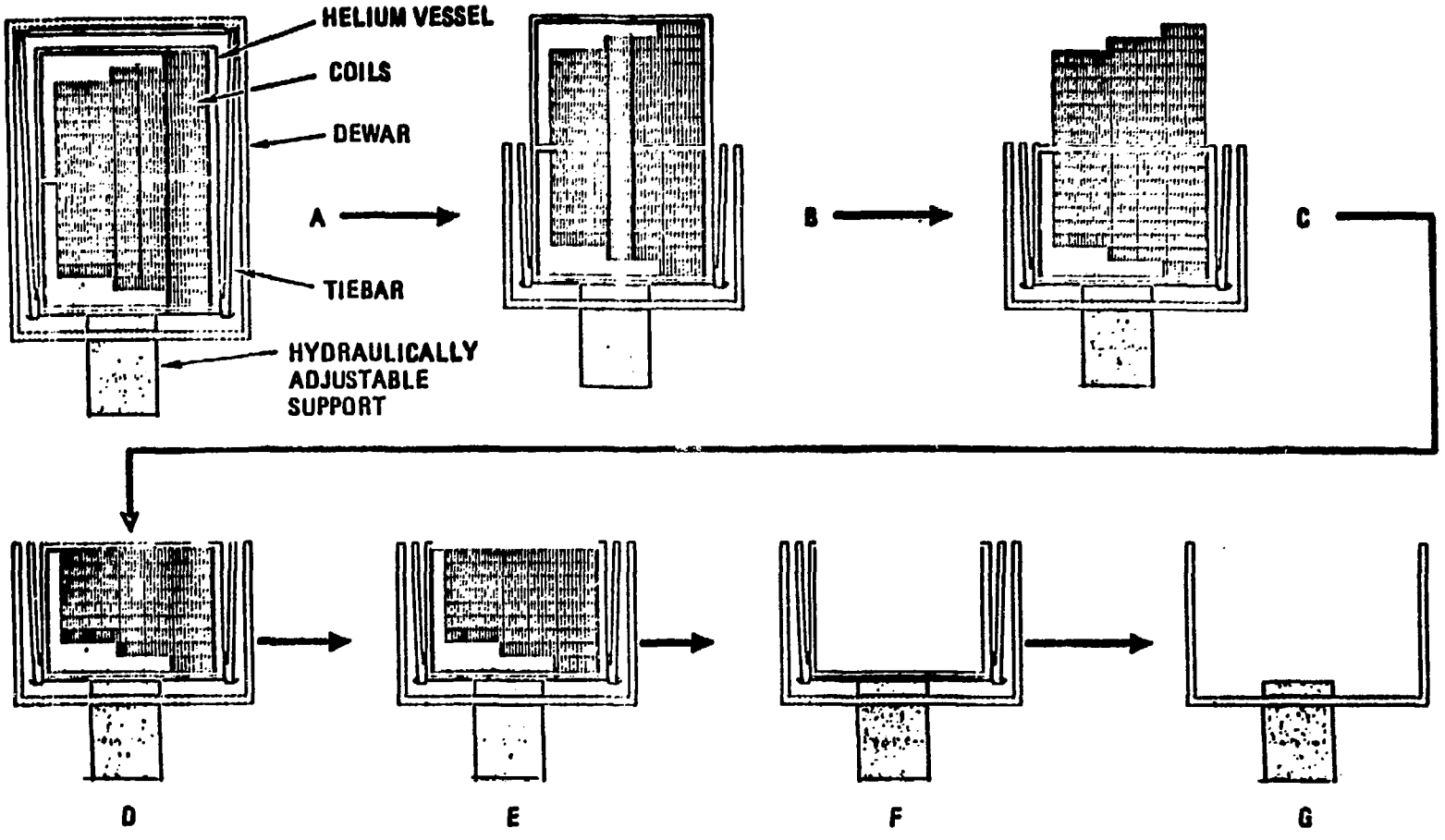

Fig. G.3. Dismantling steps in magnet outboard region.

The welds of the NbTi superconductor are ground open and the coil is unwound on a large, turntable. The same turntable is reused during winding. The G-10CR insulation and tiebars, as well as the aluminized Mylar thermal insulation, are discarded. The low activity Nb_3Sn superconductor is reprocessed as explained in Section 3. And, finally, the low-activity 316 LN and 14Mn-2Ni-2Cr austenitic stainless steel from the helium vessel and vacuum vessel, stainless steel from the coil support modules, and aluminum thermal radiation shield are saved for reuse during refabrication.

APPENDIX H

Estimate of Labor and Material Costs

Table H.1 presents a ROM* estimate of the number of man-hours required to perform each task in the refabrication of each TF coil/helium vessel magnet. It is assumed that the average labor rate of employees used in the refabrication task is $80K per man-year, or $38.50 per man-hour. The cost of materials used in each task is also listed. The cost of equipment, such as saw blades and grinders which will require replacement owing to wear but will not necessarily need to be replaced for each magnet, is listed as an average cost per magnet.

Table H.2 lists equipment required for the dismantling and refabrication tasks and shows which of this equipment already exists at the reactor site and which must be supplied by an outside contractor. The contractor's equipment is estimated to cost $15 million based upon the cost of comparably-sized, one-of-a-kind equipment. Assuming an 18% fixed charge rate, the annualized cost of this equipment is $2.7 million. Since this equipment will be used to dismantle and refabricate the TF coils/helium vessel assemblies from one STARFIRE reactor per year, this is also the cost-per-assembly.

*Rough-Order-of-Magnitude.

Table H.1. ROM Labor and Material Costs

Task	Man-Hours	Fabricated Material Cost ($K)
1. Set-up dismantling and refabrication equipment	650	15 (miscellaneous)
2. Place plastic curtain around assembly.	10	1 (curtain)
3. Cut inner vacuum vessel and remove mechanical attachment to centerpost vacuum opening.	130	—
4. Remove inner vacuum vessel section.	20	—
5. Position and attach assembly to mounting fixture.	30	—
6. Cut high-activity portion out with milling machine.	220	6 (saw blades)
7. Cut and prepare high-activity portion for shipment to storage site.	150	—
8. Vacuum fragments and dust left over from high activity portion.	50	—
9. Move magnet to dismantling and refabrication area.	30	—
10. Place magnet on lay-down fixture.	50	—
11. Secure carbide drill and drill holes in dewar (three holes).	20	4 (drill bits)
12. Sustain helium vessel with hydraulically-adjustable support.	10	—
13. Cut the vacuum vessel, thermal radiation shield, and helium vessel with carbide saw (inside and outside perimeter cuts).	80	10 (saw blades)

Table H.1 (Cont'd)

Task	Man-Hours	Fabricated Material Cost ($K)
14. Remove upper vacuum vessel , thermal radiation shield, and helium vessel sections.	40	—
15. Remove upper Nb_3Sn and NbTi coils.	30	—
16. Cut and remove helium vessel central radial spine.	60	4 (saw blades)
17. Remove lower Nb_3Sn and NbTi coils.	30	—
18. Remove lower helium vessel and dewar sections.	30	—
19. Cut and remove outermost section of helium vessel.	60	—
20. Grind open welds and unwind the NbTi conductor.	300	5 (grinders)
21. Fabricate and install new Nb_3Sn conductor.	150	650 (superconductor, copper, and stainless steel)
22. Weld new centerpost section helium vessel bobbin.	40	100 (solder and 316 LN steel)
23. Weld central radial spine to bobbin.	90	5 (solder)
24. Wind coils and support modules.	1000	20 (G-10CR)
25. Weld upper and lower sections of the helium vessel.	180	10 (solder)
26. Weld thermal radiation shield.	60	5 (solder)

Table H.1 (Cont'd)

Task	Man-Hours	Fabricated Material Cost ($K)
27. Wrap helium vessel and thermal radiation shield with aluminized Mylar.	40	20 (aluminized Mylar)
28. Position thermal radiation shield.	20	—
29. Bolt tiebars to helium vessel.	200	5 (bolts)
30. Weld circular piece to holes in bottom of the vacuum vessel.	30	20 (solder and 14Mn-2Ni-2Cr steel)
31. Place helium vessel inside lower section of the vacuum vessel.	30	—
32. Weld upper and lower section of the vacuum vessel.	100	5 (solder)
33. Weld new centerpost section to vacuum vessel.	50	170 (solder and 14Mn-2Ni-2Cr steel)
34. Attach common inner vacuum vessel.	120	—
35. Perform verification tests.	700	10 (miscellaneous)
Total per magnet contingency (@ 100%)	4810	—
Cost per magnet (@ $0.0385K per man-hour)	$370 K	$1065 K
Total cost for 12 magnets	$4440 K	$12780 K

Table H.2. Dismantling and Refabrication Equipment

		At Reactor Site	Supplied by Outside Contractor
1.	Miscellaneous equipment used to set-up dismantling and refabrication equipment		X
2.	Plastic curtain to enclose magnet assembly		X
3.	600-tonne crane	X	
4.	Remote manipulator	X	
5.	Plasma torch with vacuum		X
6.	Stand-up fixture		X
7.	Plastic curtain to enclose stand-up fixture and magnet		X
8.	Carbide saw with vacuum		X
9.	Vacuum equipment		X
10.	3 discontinuity lay-down fixture		X
11.	Carbide drill with vacuum		X
12.	Hydraulically adjustable supports		X
13.	60-tonne crane	X	
14.	Grinding equipment		X
15.	Coil winding turntable		X
16.	Nb_3Sn coil fabrication equipment		X
17.	Soldering equipment		X
18.	Welding equipment		X
19.	Verification test equipment		X
20.	Temporary vacuum barrier and strongback		X

APPENDIX I

Calculations to Indicate Selection of Magnet Materials for Recovery

In choosing magnet materials of sufficiently low radioactivity levels for recovery, it was assumed that if the BHP of a material were less than about ten, the material was a candidate for recovery and recycle. Using this rule of thumb, the Fe 1422 in I-DEWAR1 (Table I.1) is considered too radioactive for recycle and is discarded. The other Fe 1422 materials are then blended for recovery. In this case, 123 m^3 out of a total of 132 m^3 (93%) is recoverable. Similar calculations were made for the other magnet materials and are also given in Table I.1.

Table I.1. Selection of Magnet Materials for Recovery

Number	Section	Material Volume (m^3)	BHP at 1 Year (m^3 water/m^3 mtl)	Dilution Required (m^3)
		Fe 1422		
1	I-DEWAR1	8.8	1.51 + 05	1.33 + 06
2	O-DEWAR1	61.5	3.79 + 00	233
3	O-DEWAR2	61.5	1.18 - 06	7.26 - 05
	Total	132		

$$\text{Average BHP over Volumes 2 and 3} = \frac{\sum_{2,3} m^3}{\sum_{2,3} m^3 \text{ mtl}} \quad \frac{233}{123} = 1.9.$$

Percent Recovery = 93%

		NbTi		
1	I-LFMAG1	0.469	5.41 + 01	25.5
2	I-LFMAG2	0.469	1.64 + 00	0.77
3	O-LFMAG1	3.95	9.05 - 03	0.36
4	O-LFMAG2	3.95	1.94 - 04	0.001
	Total	8.84		

$$\text{Average BHP over all volumes} = \frac{\sum_{1-4} m^3}{\sum_{1-4} m^3 \text{ mtl}} \quad \frac{26.6}{8.84} = 3.01.$$

Percent Recovery = 100%

Table I.1 (Cont'd)

Number	Section	Material Volume (m^3)	BHP at 1 Year (m^3 water/m^3 mtl)	Dilution Required (m^3)
		Copper		
1	I-HFMAG1	3.28	1.24 + 4	40,600
2	I-HFMAG2	3.28	5.48 + 2	1,800
3	I-LFMAG1	6.2	1.84 + 1	114
4	I-LFMAG2	6.2	2.60 - 1	1.61
5	O-HFMAG1	27.7	3.18 - 1	8.79
6	O-HFMAG2	27.7	1.37 - 2	0.379
7	O-LFMAG1	52.0	4.49 - 4	0.023
8	O-LFMAG2	52.0	6.14 - 6	0.0003
	Total	178		

$$\text{Average BHP over Volumes 3-8} = \frac{\sum_{3-8} m^3}{\sum_{3-8} m^3 \text{ mtl}} \quad \frac{125}{172} = 0.727.$$

Percent Recovery = 96.3%

$$\text{Average BHP over Volumes 2-8} = \frac{\sum_{2-8} m^3}{\sum_{2-8} m^3 \text{ mtl}} \quad \frac{1920}{175} = 11.0.$$

Percent Recovery = 98.2%

Table I.1 (Cont'd)

Number	Section	Material Volume (m^3)	BHP at 1 Year (m^3 water/m^3 mtl)	Dilution Required (m^3)
		Nb_3Sn		
1	I-HFMAG1	0.341	9.27 + 05	3.15 + 05
2	I-HFMAG2	0.432	1.43 + 05	4.89 + 04
3	O-HFMAG1	2.88	5.41 + 02	1.56 + 03
4	O-HFMAG2	2.88	4.86 + 01	1.40 + 02
	Total	6.44		

$$\text{Average BHP over Volumes 3 and 4} = \frac{\sum_{3,4} m^3}{\sum_{3,4} m^3 \text{ mtl}} \frac{1700}{5.76} = 295.$$

Percent Recovery = 89%

Table I.1 (Cont'd)

Number	Section	Material Volume (m^3)	BHP at 1 Year (m^3 water/m^3 mtl)	Dilution Required (m^3)
		340 SS		
1	I-HEVSL1	7.55	5.17 + 04	3.90 + 05
2	I-HFMAG1	2.83	1.10 + 04	3.11 + 04
3	I-HFMAG2	2.83	9.35 + 01	264
4	I-LFMAG1	12.7	6.12 + 01	777
5	I-LFMAG2	12.7	1.95 + 00	24.8
6	I-HEVSL2	7.55	8.63 - 02	0.65
7	O-HEVSL1	64	3.42 - 01	21.9
8	O-HFMAG1	23.8	1.96 + 00	46.6
9	O-HFMAG2	23.8	2.22 - 01	5.28
10	O-LFMAG1	107	1.16 - 02	1.24
11	O-LFMAG2	107	2.65 - 04	0.028
12	O-HEVSL2	64	9.17 - 06	5.87 - 04
	Total	436		

$$\text{Average BHP over Volumes 3-12} = \frac{\sum_{3-12} m^3}{\sum_{3-12} m^3 \text{ mtl}} \frac{1140}{425} = 2.68.$$

Percent Recovery = 97.6%

REFERENCES

ABDOU

M. A. Abdou, et al., Parametric Systems Analyses for Tokamak Power Plants, ANL/FPP/TM-97 (October 31, 1977).

ACKERMAN

J. P. Ackerman, K. Kinoshita, P. A. Finn, J. W. Sim and P. A. Nelson, Advanced Fuel Cell Development, Progress Report for October-December 1977, ANL 78-16 (March 1978).

ADAM

J. A. Adam and V. L. Rogers, A Classification System for Radioactive Waste Disposal--What Waste Goes Where, NUREG-0456 (June 1978).

ALCORN

J. A. Alcorn, GA Technologies, personal communication (1982).

ALLEN

G. C. Allen, S. H. Dupree, J. M. Freedman, and S. H. Sutherland, A Waste Transportation System Plan for Geologic Nuclear Fuel Cycle Waste Repositories, in the Proceedings of the Fifth International Symposium, Packaging and Transportation of Radioactive Materials, Las Vegas, NV, May 7-12, 1978.

ANISN-ORNL

Anisn, Multigroup One-Dimensionial Discrete Ordinates Transport Code with Anisotropic Scattering, RSIC/CCC-254, Oak Ridge National Laboratory (1973).

ALUMINUM ASSOCIATION

Aluminum Standard and Data, Aluminum Association, p. 93 (1978).

ARONS

R. M. Arons, R. B. Poeppel, M. Tetenbaum and C. E. Johnson, Preparation, Characterization, and Chemistry of Solid Ceramic Breeder Materials, J. Nucl. Matls., 103-104, 573-578 (1981).

BADGER

B. Badger, et al., NUWMAK: A Tomamak Reactor Design Study, UWFDM-30, University of Wisconsin (1979).

BAKER

C. C. Baker, et al., STARFIRE - A Commercial Tokamak Fusion Power Plant Study, ANL-FPP 80-1 (September 1980).

BARNWELL

Barnwell Low-Level Radioactive Waste Disposal Facility, Rate Schedule (January 1982).

BOTTS-1978A
T. E. Botts and J. E. Powell, Waste Management Procedures for Fusion-Based Central Power Stations, BNL-50697 (August 1977).

BOTTS-1978B
T. E. Botts and J. E. Powell, Effects of Waste Management on the Impact of Fusion Power, Third ANL Topical Meeting on the Technology of Controlled Nuclear Fusion, Santa Fe, NM (May 1978).

BUREAU OF MINES
U.S. Bureau of Mines, Commodity Data Summary (1976).

BURGOYNE
R. M. Burgoyne, GA Technologies, private communication (1982).

CLAIRBORNE
H. C. Clairborne and D. K. Trubey, Dose Rates in a Slab Phantom from Monoenergetic Gamma Rays, Nucl. Appl. Technol. 8 (5), 450 (1970).

CLARK
L. L. Clark and B. M. Cole, Analysis of the Cost of Mined Geologic Repositories in Alternative Media, PNL-3949 (February 1982).

CLEMMER
R. Clemmer, Argonne National Laboratory, private communication (1982).

CONN-1974
R. W. Conn, T. Y. Sung, and M. A. Abdou, Comparative Study of Radioactivity and Afterheat in Several Fusion Reactor Blanket Designs, Nucl. Technol. 26, 391 (1974).

CONN-1976
R. W. Conn, et al., UWMAK-III, A Non-Circular Tokamak Power Reactor Design, Electric Power Research Institute Report, ER-368 (1976).

CONN-1978
R. W. Conn, K. Okula, and A. W. Johnson, Minimizing Radioactivity and Other Features of Elemental and Isotopic Tailoring of Materials for Fusion Reactors, Nucl. Technol. 41, 389 (1978).

CRASE
A. Crase, U.S. Ecology, private communication (1982).

CROFF
A. Croff and C. W. Alexander, Decay Characteristics of Once-Through LWR and LMFBR Spent Fuels, High Level Wastes and Fuel Assembly Structural Material Wastes, ORNL-TM-7431 (November 1980).

DOGGETT
J. N. Doggett, C. C. Damon, and C. L. Hanson, The Tandem Mirror Next Step - Remote Maintenance, in Proceedings of the 28th Conference on Remote Systems Technology, Vol 2, Washington, DC (November 1980).

DUDZIAK

D. J. Dudziak and R. A. Krakowski, Radioactivity Induced in a Theta-Pinch Fusion Reactor, Nucl. Technol. 25, 32 (1975).

EAGLE-PICHER

Eagle-Picher Co., private communication, B. Tryon (March 1982).

EVANS

R. K. Evans, Lithium Reserves and Resources, Symposium. on Lithium Needs and Resources, Corning, NY, October 12-14, 1977.

FINN

P. A. Finn, S. R. Breon, and N. R. Chellew, Compatability Studies of Solid Ceramic Breeder Materials, presented at the 2nd Topical Meeting on Fusion Reactor Materials, Seattle, WA (August 1981).

FREUND

S. M. Freund and J. L. Lyman, Multiple-Photon Isotope Separation in MoF_6, Chemical Physics Letters 55, 435, No. 3, May 1, 1978.

GARKEN

D. Garken (compiler), ENDF/B Summary Documentation, BNL-17541, Brookhaven National Laboratory (1978).

GEAR

C. W. Gear, Numerical Initial Value Problems in Ordinary Differential Equations, Prentice-Hall, NJ (1971).

GERBER

E. W. Gerber, L. H. Rice, R. M. Horgos, T. T. Nagamoto, and R. A. Graham, Secure Automated Fabrication: Remote Fabrication of Breeder Reactor Fuel, presented in the Proceedings of the 29th Conference on Remote Systems Technology at Bal Harbour, FL (June 1981).

GORE

B. F. Gore, J. D. Kaser, and T. J. Kabele, Fusion Fuel Cycle Solid Radioactive Wastes, PNL-2719 (June 1978).

GRAHAM

W. C. Graham, GA Technologies, personal communication (1982).

GREGORY

E. Gregory, W. G. Marancik, and F. T. Ormand, Composite Conductors Containing Many Filaments of Nb_3Sn, paper presented at 1974 Applied Superconductivity Conference, Oakbrook, IL., AIRCO, Murray Hill, NJ (October 1974)

GROUBER

J. Grouber, Evaluation of the Activity Levels in Fusion Reactor Blankets, HMI-B 202, Hahn Meitner Institut fur Kernsforschung, Berlin (1977).

HAGER
E. R. Hager, GA Technologies, personal communication (1982).

HOPKINS-1974
G. R. Hopkins, Fusion Reactor Applications of Silicon Carbide and Carbon, Proceedings of the 1st Topical Meeting on The Technology of Controlled Nuclear Fusion, Vol II, CONF-740402-P2-USAEC, p. 437 (1974).

HOPKINS-1981
G. R. Hopkins, et al., The Prospects of Low Activation Fusion Reactor Design, Proceedings of the 9th Symposium on Engineering Problems of Fusion Research, IEEE Pub. No. 81CH1715-2-NPS, p. 1871 (1981).

IMTS
International Machine Tool Show, Chicago, IL, September 8-17, 1982.

INTOR
International Tokamak Reactor: Zero Phase, IAEA, Vienna, (1980).

JACOBI
J. S. Jacobi, Recovery of Metals from Secondary Sources, Advances in Extractive Metallurgy Symposium Proceedings, Institute of Mining and Metallurgy, p. 396-397, London, England (1968).

JEPSON
B. E. Jepson and G. A. Cairns, Lithium Isotope Effects in Chemical Exchange with 2,2,1 Cryptand, MLM-2622, June 8, 1979.

JUNG-1979
J. Jung, Theory and Use of the Radioactivity Code RACC, Argonne National Laboratory ANN/FPP/TM-122 (1979).

JUNG-1980A
J. Jung and M. Abdou, Radioactive Inventories and Material Recyclability in a Tokamak Reactor, Trans. Am. Nucl. Soc. 34, 645 (1980).

JUNG-1980B
J. Jung, A Comparative Study of Tritium Breeding Performance of Lithium, Li_2O and Li_7Pb_2 Blankets in a Tokamak Power Reactor, J. Nucl. Technol. 50, 60 (1980).

JUNG-1981
J. Jung and M. Abdou, Importance of Shield Design in Minimizing Radioactive Material Inventory in Tokamaks, Proceeding at the 4th ANS Topical Meeting on The Technology of Controlled Nuclear Fusion, CONF-801011, Vol I, p. 458 (1981).

KELLY
V. P. Kelly, P. J. Brackenberry, and J. A. Yount, Remote Maintenance Features of the Fusion Materials Irradiation Test Facility Lithium System, in Proceedings of the 29th Conference on Remote Systems Technology, Bal Harbour, FL (June 1981).

KERNOHAN
R. H. Kernohan, et al., Cryogenic Radiation Effects on Electric Insulators, Oak Ridge National Laboratory, J. Nucl Matls. 85 and 86, p. 379-383 (1979).

KIRK-OTHMER-1965
R. E. Kirk, D. F. Othmer, M. Grayson, D. Eckroth, Kirk-Othmer Encyclopedia of Chemical Technology, 2nd Ed., John Wiley and Sons, Inc., New York, NY (1965).

KIRK-OTHMER-1979
R. E. Kirk, D. F. Othmer, M. Grayson, D. Eckroth, Kirk-Othmer Encyclopedia of Chemical Technology, 3rd Ed., John Wiley and Sons, Inc., New York, NY (1979).

KUMMER
D. L. Kummer, Ed., Conference Proceedings on Low Activation Materials Assessment for Fusion Reactors, San Francisco, CA, EPRI ER-328-SR, February 19-20, 1976.

KUNASZ
I. A. Kunasz, Lithium Resources - Prospects for the Future, in Lithium Resources and Requirements by the Year 2000, J. D. Vine, Ed., U.S. Geological Survey Professional Paper 1006, pp. 26-30 (1976).

KURASAWA
T. Kurasawa, H. Takeshita, S. Muraoka, and S. Nasa, J. Nucl. Matls. 80, 48-56 (1980).

LEJUS
A. M. Lejus, Rev. Hautes Temp. Refract. 1, 72 (1964).

LITHCOA
Lithcoa, private communication, M. Touchek (April 1982).

MCP-1
Chromium; Mineral Commodity Profiles; U.S. Department of Interior MCP-1, May 1977 (1977).

MCP-10
Columbium; Mineral Commodity Profiles, U.S. Department of Interior MCP-10, January 1978 (1978).

MOORE
R. L. Moore, GA Technologies, personal communication (1982).

NORTON

J. J. Norton, Lithium, Cesium, Rubidium, in U.S. Mineral Resources, U.S. Geological Survey Professional Paper 820, D. A. Brobst and W. P. Pratt, Eds. (1973).

NUREG

Draft Environmental Impact Statement on 10 CFR Part 61 - Licensing Requirements for Land Disposal of Radioactive Waste, NUREG-0782 (1981).

PEAGRAM

G. W. Peagram and G. J. Bauer, A New Concept in Remote Handling, in Proceedings of the 28th Conference on Remote Systems Technology, Vol I, at Las Vegas, NV (June 1980).

PIGFORD

T. H. Pigford, Geological Disposal of Radioactive Waste, Chemical Engineering Progress (March 1982).

POWELL-1973

J. R. Powell, F. T. Miles, A. Aronson, and W. E. Winsche, Studies of Fusion Reactor Blankets with Minimum Radioactive Inventory and with Tritium Breeding in Solid Lithium Compounds, BNL-18236, Brookhaven National Laboratory (1973).

POWELL-1974

J. R. Powell, Ed., Preliminary Reference Design of a Fusion Reactor Blanket Exhibiting Very Low Residual Radioactivity, BNL-19565 (1974).

PROFIO

A. E. Profio, Radiation Shielding and Dosimetry, A Wiley-Interscience Publication, John Wiley & Sons, NY (1979).

RACCXLIB

The associated cross section library, RACCXLIB, and decay data library, RACCDLIB, have not been published. However, these two data libraries are included in an RSIC computer code collection of Oak Ridge National Laboratory as CCC-388/RACC (1980).

RAIMONDI

T. Raimondi, Remote Handling in Joint Europeon Torus, in Proceedings of the 24th Conference on Remote Systems Technology at the ANS Meeting, Washington, DC (November 1976).

RAPPAPORT

W. Rappaport, Rose Cooperage Company, Montebello, CA, private communication (September 1982).

RHINEHAMMER
T. B. Rhinehammer and L. J. Wittenberg, An Evaluation of Fuel Resources and Requirements for the Magnetic Fusion Energy Program, MLM-2419, Mound Laboratory (1978).

RHOADS
R. E. Rhoads and P. L. Peterson, Conceptual Design of a Shipping Cask for Rail Transport of Solidified High Level Waste, in the Proceedings of the 5th International Symposium, Packaging and Transportation of Radioactive Materials, Las Vegas, NV (May 1978).

ROUSSIN
R. W. Roussin, et al., VITAMIN-C: The CTR Processed Multigroup Cross Section Library for Neutronics Studies, ORNL/RSIC-37, Oak Ridge National Laboratory (1980).

SMITH-1978
R. I. Smith, G. J. Konzek and W. E. Kennedy, Jr., Technology, Safety and Costs of Decommissioning a Reference Pressurized Water Reactor Power Station, NUREG/CR-0130 (June 1978).

SMITH-1979
D. L. Smith, et al., Fusion Reactor Blanket/Shield Design Study, ANL/FPP-79-1 (July 1979).

SONDERS
M. Sonders and O. W. Eshback, Eds., Handbood of Engineering Fundamentals, 3rd Ed., p. 1375 (1974).

STACEY
W. M. Stacey, Jr., et al., U.S. INTOR: The U.S. Contribution to the International Tokamak Reactor Phase-I Workshop (1981).

STEINBERG
M. Steinberg and V. Dang, Preliminary Design and Analysis of a Process for the Extraction of Lithium from Seawater, in Lithium Resources and Requirements by the Year 2000, J. D. Vine, Ed., U.S. Geological Survey Professional Paper 1005, pp. 79-88 (1976).

STEINER-1970
D. Steiner, The Neutron-Induced Activity and Decay Power of the Niobium Structure of a D-T Fusion Reactor Blanket, ORNL-TM-3094, Oak Ridge National Laboratory (1970).

STEINER-1972
D. Steiner and A. P. Fraas, Preliminary Observations on the Radiological Implications of Fusion Power, Nuclear Safety 13, 353-362, No. 5 (September-October 1972).

STEINER-1974
D. Steiner, The Nuclear Performance of Vanadium as a Structural Material in Fusion Reactor Blankets, Nucl. Fusion 14 (1974).

STEVENS
H. C. Stevens, Argonne National Laboratory, private communication (January 1980).

SU
S. Su, GA Technologies, private communication (1982).

TAKAHASHI
T. Takahashi and T. Kikuchi, Sintering of Lithium Oxide (Li_2O), JAERI-M7518, Japan Atomic Energy Research Institute (1978).

TRUCK-TRAILER
Truck-Trailer Manufacturers Association, 2430 Pennsylvania Avenue, N.W., Washington, DC 20037 (February 1982).

VERTUT
J. Vertut, P. Marschal, G. Debrie, M. Petit, D. Francois, and P. Coiffet, The MA23 Bilateral Servomanipulator System, in the Proceedings of the 24th Conference on Remote Systems Technology at the ANS Meeting, Washington, DC (November 1976).

VINE
J. D. Vine, The Lithium-Resource Enigma, in Lithium Resources and Requirements by the Year 2000, J. D. Vine, Ed., U.S. Geological Survey Professional Paper 1005, pp. 35-37 (1976).

VOGELSANG
W. F. Vogelsang, G. L. Kulcinski, R. G. Lott, and T. Y. Sung, Transmutations, Radioactivity, and Afterheat in a Deuterium-Tritium Tokamak Fusion Reactor, Nucl. Technol. 22, 379 (1974).

VOSS
J. W. Voss, Safety Indices and Their Applications to Nuclear Waste Management Safety Assessment, PNL-2727 (April 1979).

WESTON
J. R. Weston, W. F. Calaway, R. M. Yonco, and V. A. Maroni, Recent Advances in Lithium Processing Technology at Argonne National Laboratory, 2nd International Conference on Liquid Metal Technology in Energy Production, Richland, WA, April 20-24, 1980.

WILKES
W. Wilkes, private communication, Mound Laboratory (October 1981).

WILLENBERG
H. J. Willenberg, T. J. Kabele, R. D. May, and C. E. Willingham, Materials Flow, Recycle and Disposal for Deuterium-Tritium Fusion, PNL-2830 (December 1978).

WILLIAMS

M. L. Williams, R. T. Santoro, and T. A. Gabrial, The Calculated Performance of Various Structural Materials in Fusion-Reactor Blankets, Nucl. Technol. 29, 384 (1976).

WISWALL

R. Wiswal, E. Wirsing, and K. C. Hong, The Removal of Bred Tritium from Solid Lithium Compounds in Fusion Reactor Systems, 14th Intersociety Energy Conversion Engineering Conference, Boston, MA, August 5-10, 1979.

YOUNG

J. R. Young, Fusion Reactor Wastes, BNWL-SA-5943, Proceedings of the Symposium on Waste Management, Tucson, AR, CONF-761020, October 3-6, 1976.

ZAHN

M. S. Zahn and C. T. Curtis, Remote Systems Requirements for Tandem Mirror Fusion Power Reactors, in Proceedings of the 28th Conference on Remote Systems Technology, Vol 2, Washington, DC (November 1980).

10 CFR 20

Standards for Protection Against Radiation, NRC 10 CFR 20, Appendix B.

10 CFR 61

Nuclear Regulatory Commission Draft, Licensing Requirements for Land Disposal of Radioactive Waste, 10 CFR 61 (May 1982).

40 CFR 191

Environmental Protection Agency, Draft Proposed Rule, Environmental Standards and Federal Radiation Protection Guidance for Management and Disposal of Spent Nuclear Fuel, High Level and Transuranic Radioactive Waste, 40 CFR 191, March 19, 1981.

49 CFR 173

U.S. Code of Federal Regulations, 49 CFR Part 173, Shippers - General Requirements for Shipment and Packaging, Sec. 173.392 (Low Specific Activity Materials) and Sec. 173.393 (General Packaging and Shipping Requirements) (1977).

Distribution for ANL/FPP/TM-163

Internal:

M. Abdou
C. Baker
E. Beckjord
C. Boley
J. Brooks
L. Burris
F. Cafasso
Y. Cha
R. Clemmer
D. Ehst
K. Evans
P. Finn
Y. Gohar
L. Greenwood
D. Gruen
A. Hassanein
C. Johnson
J. Jung (5)
M. Kaminsky
S. Kim
Y-K. Kim
J. H. Kittel
R. Kustom
R. Lari
L. LeSage
B. Loomis
S. Majumdar
V. Maroni
R. Mattas
B. Misra
J. Roberts
D. Smith
M. Steindler (5)
H. Stevens
L. Turner
S. Vogler (5)
ANL Patent Dept.
FP Program (25)
ANL Contract File
ANL Libraries (2)
TIS Files (6)

External:

DOE-TIC, for distribution per UC-20, -20d, -20e (137)
Manager, Chicago Operations Office, DOE
Special Committee for the Fusion Program:
    S. Baron, Burns & Roe, Inc., Oradell, NJ
    H. K. Forsen, Exxon Nuclear Company, Inc., Bellevue, WA
    M. J. Lubin, Standard Oil Company of Ohio, Warrensville Heights, O
    G. H. Miley, University of Illinois, Urbana
    P. J. Reardon, Princeton University
    D. Steiner, Rensselaer Polytechnic Institute
    K. R. Symon, University of Wisconsin-Madison
    K. Thomassen, Lawrence Livermore National Laboratory
Review Committee for the Chemical Technology Division:
    B. C. Alcock, University of Toronto
    T. Cole, Jet Propulsion Laboratory, Pasadena, CA
    N. Delgass, Purdue University
    H. Perry, Resources for the Future, Washington, DC
    W. Worrell, University of Pennsylvania
Director, Science Applications, Inc.
R. Aamodt, Science Applications, Inc.
R. Alsmiller, Oak Ridge National Laboratory
D. Anthony, General Electric Company
R. Balzheizer, Electric Power Research Institute
D. Beard, DOE/Office of Fusion Energy
C. Blattner, McDonnell Douglas Astronautics Company
K. Blurton, Institute of Gas Technology
S. L. Bogart, Science Applications, Inc.
S. Buchsbaum, Bell Telephone Laboratories, Inc.
S. Burnett, GA Technologies
J. Butterworth, Culham Laboratory. UKAEA, England
G. Casini, Joint Research Centre, Ispra Establishment, Italy
R. Challender, UKAEA, Risley, England
C-H. Chen, Institute of Plasma Physics, People's Republic of China

F. Chen, University of California
S. Cohen, Princeton University
R. Davidson, MIT Plasma Fusion Center
N. A. Davies, DOE/Office of Fusion Energy
J. Decker, DOE/Office of Fusion Energy
W. Dove, DOE/Office of Fusion Energy
H. Dreicer, Los Alamos National Laboratory
W. Drummon, University of Texas-Austin
A. Dupas, Centre d'Etudes Nucleaires de Grenoble, France
W. Ellis, DOE/Office of Fusion Energy
R. Endicott, Public Service Electric and Gas Research Corporation
C. Finfgeld, DOE/Office of Fusion Energy
J. Foster, Jr., TRW, Inc.
T. Fowler, Lawrence Livermore National Laboratory
H. Furth, Princeton University
J. Gammel, St. Louis University
K. Gentle, University of Texas-Austin
J. Gilligan, University of Illinois
J. Gordon, TRW, Inc.
S. Gralnick, Grumman Aerospace Corporation
D. Graumann, GA Technologies
E. Greenspan, NRCN, Israel
B. Hall, Westinghouse R&D Center
R. Hancox, Culham Laboratory, UKAEA, England
A. Haught, United Technologies Research Center
I. Hedrick, Grumman Aerospace
T. Hiraeoka, Japan Atomic Energy Research Institute, Japan
R. Hirsch, Exxon Research and Engineering Company
H. Horwitz, General Electric Company
R. Huse, Public Service Electric and Gas Company
A. Husseiny, Iowa State University
T. Jernigan, Oak Ridge National Laboratory
R. Johnson, General Dynamics - Convair
T. Kammash, University of Michigan
D. Klein, Westinghouse Electric Corporation
I. Knoblock, Max Planck Institute für Plasmaphysik, West Germany
J. Kokoszenski, Ralph M. Parsons Company
A. Kolb, Maxwell Laboratories
H. Kouts, Brookhaven National Laboratory
R. Langley, Sandia Laboratories
T. Latham, United Technologies Research Center
D. Leger, CEA-Saclay, Service DCAEA/SECF., France
R. Lengye, Max Plack Institute für Plasmaphysik, West Germany
H. Levin, GA Technologies
L. Lidsky, Massachusetts Institute of Technology
I. Maya, GA Technologies
R. Mills, Princeton University
O. Morgan, Oak Ridge National Laboratory
G. Moses, University of Wisconsin-Madison
L. Muhlestein, Hanford Engineering Development Laboratory
T. Nakakita, Toshiba Corporation, Japan
S. Naymark, Nuclear Services Corporation
D. Nelson, DOE/Office of Fusion Energy
T. Ohkawa, GA Technologies

E. Oktay, DOE/Office of Fusion Energy
D. Peterman, GA Technologies
R. Post, Lawrence Livermore National Laboratory
R. Pyle, University of California
M. Roberts, DOE/Office of Fusion Energy
A. Robson, Naval Research Laboratory
J. Rogers, Los Alamos National Laboratory
D. Rose, Massachusetts Institute of Technology
M. Rosenthal, Oak Ridge National Laboratory
R. Santoro, Oak Ridge National Laboratory
M. Sawan, University of Wisconsin
G. Sawyer, Los Alamos National Laboratory
P. Schmitter, Max Planck Institute fur Plasmaphysik, West Germany
K. Schultz, GA Technologies
R. Seale, University of Arizona
G. Shatalov, I. V. Kurchatov Institute of Atomic Energy, Moscow
M. Stauber, Grumman Aerospace Corporation
L. Stewart, Princeton University
P. Stone, DOE/Office of Fusion Energy
S. Strausburg, GA Technologies
R. Werner, Lawrence Livermore National Laboratory
L. Wittenberg, Monsanto Research Corporation
G. Woodruff, University of Washington
D. Young, Jr., University of Texas-Austin
M. Youssef, University of California-Los Angeles
Library, Centre de Etudes Nucleaires de Fontenay, France
Library, Centre de Etudes Nucleaires de Grenoble, France
Library, Centre de Etudes Nucleaires de Saclay, France
Library, Centre de Recherches en Physique des Plasma, Lausanne, Switzerland
Library, FOM-Institute voor Plasma-Fysika, Jutphaas. The Netherlands
Library, Comitato Nazionale per l'Energia Nucleare, Rome, Italy
Library, Joint Research Centre, Ispra, Italy
Library, Japan Atomic Energy Research Institute, Ibaraki, Japan
Library, Max Planck Institute fur Plasmaphytsik, Garching, West Germany
Library, Culham Laboratory, UKAEA, Abingdon, England
Library, Laboratorio Gas Ionizati, Frascatti, Italy